Anti-epileptic effect of cannabidiol mediated by modulation of mitochondrial function

Thesis submitted for the degree of Doctor of Philosophy

Clementino Ibeas Bih

University of Reading

Reading School of Pharmacy

Submitted: August 2018

Accepted: April 2019

Supervisors:

Dr Alister J. McNeish – Reading School of Pharmacy

Dr Graeme S. Cottrell – Reading School of Pharmacy

The end of a matter is better than its beginning, and patience is better than pride.

Do not be quickly provoked in your spirit, for anger resides in the lap of fools.

Do not say, "Why were the old days better than these?" For it is not wise to ask such questions.

Wisdom, like an inheritance, is a good thing and benefits those who see the sun.

Ecclesiastes 7:8-11 (NIV)

Declaration of original authorship

I *Clementino Ibeas Bih* confirm that this thesis is entirely with my own work except for portions acknowledged otherwise. Other sources cited in this work were appropriately acknowledged and presented in the reference section of this thesis.

Signature:

Mr Clementino Ibeas Bih

Dedication

To my mum Emilia Bih.

Acknowledgement

I would like to address my special thanks to my supervisors, Dr Alister McNeish and Dr Graeme Cottrell for their involvement, support and guidance since the departure of my original supervisors (Prof. Benjamin Whalley and Dr Alistair Nunn). Although joining this project mid-way, they taught me how to become an independent scientist.

I would like to address my thanks to Prof. Benjamin Whalley and Dr Alistair Nunn for offering me this position. Without them, I would not be in Reading. During their time here at the University of Reading they provided me with foundational knowledge which allowed me to face my future challenges.

I greatly appreciate the materials and the financial support provided to me by GW pharma. Dr Michael Bazelot from GW pharma also taught me how to perform patch clamp on neurons of brain slices.

I thank the friends in Reading for their support. Dr Marcus Haag, Dr Wouter Eilers, Dr Jonathan Sheard, Roshan Limbu (my colleague), Pabitra Patra (my colleague), Samuel Joseph, Mark Shinn, Dr Matt Young and Dr Hannah Young, Henry Skinner, Josh Lau, Hamid Oudi, Shahab Karimi, Mariam Karimi, Dr Setareh Tabatabaee and Raouf Heidari.

Here is a non-exhaustive list of people who played a critical role for me to get here. My parents (Fernando Ibeas Riuz and Emilia Bih), my siblings, the Diaz family, Gaston Ebua, Juan Purcalla, Amanda Coe, Carmen Becker, teachers at the FG-Berlin, the Beyeart family, Jan-Gerald Krauser, the Posalski family, the Eboue family, the Moudiki family, members of the ADD (Nancy and Lyon), the Mourier family, the Fulgencio family and the Cattuto family.

Publication, poster and conferences

- **C. Ibeas Bih,** T. Chen, AVW. Nunn, M. Bazelot, M. Dallas, BJ. Whalley. Molecular Targets of Cannabidiol in Neurological Disorders. *The Journal of the American Society for Experimental Neurotherapeutics* (2015)
- **C. Ibeas Bih**, M. Bazelot, AJ. McNeish, BJ. Whalley. Effect of cannabidiol on mitochondrial function in epileptic adult rats induced by means of lithium/pilocarpine. *MITOX conference – Oxford* (2016).
- **C. Ibeas Bih**, GS. Cottrell, M. Bazelot, AVW. Nunn, BJ. Whalley, AJ. McNeish. Effect of cannabidiol on mitochondrial function in rats exhibiting spontaneous recurrent seizures following reduced-intensity *status epilepticus*. In preparation.

ABBREVIATIONS

5-HT	5-hydroxytryptamine
AA	Arachidonic acid
ADP^{3-} or ADP	Adenosine diphosphate
AED	Anti-epileptic drug
AMP^{2-} or AMP	Adenosine monophosphate
AMPA	α-amino-3-hydroxy-5-methyl-4-isoxazolepropionic acid
AR	Adenosine receptor
ATP^{4-} or ATP	Adenosine triphosphate
BB1	Blocking buffer 1 (for western blot)
BB2	Blocking buffer 2 (for immunocytochemistry)
BBB	Blood brain barrier
beta-m	β-mercaptoethanol
BKY	Benjamini, Krieger and Yekutieli pairwise comparisons
BSA	Bovine serum albumin
BSRL	Bilateral seizures followed by rearing and loss of balance
CBs	Cannabinoid receptors
CBD	Cannabidiol
CBDV	Cannabidivarin
CCCP	Carbonyl cyanide m-chlorophenyl hydrazone
COX	Cyclooxygenase

COX-IV	Cytochrome c oxidase IV
$cPLA_2$	Ca^{2+}-dependent phospholipase A2
CsA	Cyclosporin A
CypD	Cyclophilin D
Cyt C	Cytochrome C
cDNA	Complementary DNA
EGTA	Ethylene glycol-bis(β-aminoethyl ether)-N,N,N',N'-tetraacetic acid
ENT1	Equilibrative nucleoside transporter 1
EP	Epileptic
Δ9-THC	Δ9-Tetrahydrocannabinol
DDW	Distilled deionised water
DHA	Docosahexaenoic acid
DIDS	4,4'-diisothiocyanatostilbene-2,2'-disulphonate
DMEM-H	Dulbecco's modified eagle medium with high glucose (4.5 g/l) and 10% foetal bovine serum, but without L-glutamine
DMSO	Dimethyl sulphoxide
E. coli	*Escherichia coli*
EPSP	Excitatory post-synaptic potential
$FADH_2$	Reduced flavin-adenine dinucleotide
FAD	Oxidised Flavin-adenine dinucleotide
FBS	Foetal bovine serum
fEPSP	Field excitatory post-synaptic potential

Fe-S	Iron-sulphur centres
FLP-HEK293	Flp-In^{TM} human embryonic kidney cells 293
FRT	Flippase recognition target
GABA	γ-aminobutyric acid
GAT1	GABA transporter 1
GPCR	7-transmembrane G protein-coupled receptor
GlyR	Glycine receptor
HA	Human influenza hemagglutinin
HE	Healthy
HEK293	Human embryonic kidney cells 293
HEPES	4-(2-hydroxyethyl)-1-piperazineethanesulfonic acid
HRP	Horseradish peroxidase
IB	Isolation buffer
ICAM-1	Intercellular adhesion molecule-1
Igκ	Secretory peptide signal of the light chain of immunoglobulin kappa
IκB	Inhibitor of NF-κB
IKK	IκB kinase
IL-1β	Interleukin-1β
IL-1R1	Interleukin-1 receptor 1
I-V relationship	Current-voltage relationship
KA	Kainic acid

K-ADP	Potassium-ADP
KCC2	K^+/Cl^- co-transporter
LETM1	Leucine zipper EF Hand-containing transmembrane protein 1
LEV	Levitiracetam
Li-pilo	Lithium/pilocarpine-induced *SE*
LOX	Lipoxygenase
LTP	Long term potentiation
MCP1	Monocyte chemoattractant protein 1
MDR	Multidrug resistance transporter
MEA	Multi-electrode array
mEPSP	Miniature excitatory post-synaptic potential
MIP-2	Type-2 macrophage inflammatory protein
mPT	Mitochondrial permeability transition
mPTP	Mitochondrial permeability transition pore
MRP	Multidrug resistance-associated protein
NADH, H^+	Reduced nicotinamide-adenine dinucleotide
NAD^+	Oxidised nicotinamide-adenine dinucleotide
NCX	Na^+/Ca^{2+} exchanger
ND4	NADH-ubiquinone oxidoreductase chain 4
NDUFS1	NADH-ubiquinone oxidoreductase core subunit S1
NF-κB	Nuclear factor kappa-light-chain-enhancer of activated B cells

NHX	Na^+/H^+ exchanger
NMDA	N-methyl-D-aspartate
N-Smase	Neutral sphingomyelinase
NS-mito	Hippocampal non-synaptic mitochondria from rat
$NS\text{-}mito_{EP}$	Hippocampal non-synaptic mitochondria from epileptic rat
$NS\text{-}mito_{HE}$	Hippocampal non-synaptic mitochondria from healthy rat
NT	Non-treated
$O_2^-\bullet$	Superoxide anion
Om	Oligomycin A
ORF	Open reading frame
OXPHOS	Oxidative phosphorylation
P2X or P2XR	P2 purine receptor X
P2Y or P2YR	P2 purine receptor Y
PANX1	Pannexin 1
PBS	Phosphate-buffered saline
PBST	PBS with 0.1% $Tween^{20}$
PCR	Polymerisation chain reaction
PG	Prostaglandin
PGE2	Prostaglandin E2
Pi^{3-} or Pi	Inorganic phosphate
PiC	Phosphate carrier

POL	Phosphorothioate oligonucleotides
P:O ratio	Phosphate/Oxygen ratio
PSBB	Post-seizures behavioural battery
PTZ	Pentylenetetrazole
PVDF	Polyvinylidene
RB	Respiration buffer
RC	Respiratory chain
RCR	Respiratory control ratio
RIPA buffer	Radioimmunoprecipitation assay buffer
RISE	Reduced-intensity induced *status epilepticus*
ROS	Reactive oxygen species
RT	Reverse transcription
rVDAC2	Rat VDAC2
S18	S18-randomer
SB	Swelling buffer
SDS	Sodium dodecyl sulphate
SE	*Status epilepticus*
SEM	*Standard error of the mean*
S-mito	synaptic mitochondria
SOB	Super optimal broth
SRS	Spontaneous recurrent seizures

SUC	Na_2-succinate (5 mM)
SUDEP	Sudden unexpected death in epilepsy
SYN	Synaptosomes
TB	Transfer buffer
TBI	Traumatic brain injury
TLE	Temporal lobe epilepsy
TNFα	Tumour necrosis factor α
TRP	Transient receptor potential
Ub	Oxidised ubiquinone
UbH_2	Reduced ubiquinone
UCP	Uncoupling protein
Veh	Vehicle (dilution of medium in 3.19% DMSO)
Veh1	Vehicle 1 (0.03% DMSO in RB) (see chapter 3)
Veh2	Vehicle 2 (0.03% DMSO in SB) (see chapter 4)
Veh3	Vehicle 3 (0.03% DMSO in extracellular solution) (see chapter 5)
VDAC	Voltage-dependent anion-selective channel
VGCC	Voltage-gated Ca^{2+} channel
VGSC	Voltage-gated Na^+ channel
WHS	Wolf-Hirschhorn syndrome

TABLE OF CONTENTS

LIST OF TABLES

LIST OF FIGURES

ABSTRACT

Background and objectives:

Cannabidiol (CBD) is a non-psychoactive phytocannabinoid which exerts anti-convulsant effects in both rodents and humans. Although CBD appears to target a wide range of non-mitochondrial and mitochondrial proteins, the molecular mechanism underlying its anti-epileptic effect remains undetermined. In 2013, Rimmerman et al. demonstrated that CBD binds and inhibits the conductance of voltage-dependent anion-selective channel (VDAC) reconstituted in an artificial bilayer membrane. In the mitochondrion, VDAC is essentially expressed in the outer-membrane. Taken together, this led to the hypothesis that CBD may exert its anti-convulsant effect by altering mitochondrial function in a manner which is consistent with that of other VDAC inhibitors. To test this hypothesis, I assessed the effect of CBD on oxidative phosphorylation, Ca^{2+}-induced mitochondrial swelling and cytochrome C release of non-synaptic mitochondria isolated from hippocampi of healthy rats and of rats that have been rendered epileptic following *status epilepticus* induced chemically with lithium-pilocarpine. Furthermore, the effect of CBD on mitochondrial function was compared to that of a VDAC blocker (namely S18 randomer). Finally, I investigated the effect of CBD on the electrophysiological proprieties of HEK293 cells overexpressing an isoform of VDAC (namely VDAC2).

Results:

CBD (10 µM) increased mitochondrial swelling and state 4 respiration in non-synaptic mitochondria from epileptic rats, while it exhibited no effect in non-synaptic mitochondria from healthy rats. I showed that CBD does not target complexes II, III and IV or the ATP^{4-}

synthase. The direct effect of CBD on mitochondrial swelling and oxidative phosphorylation differed from that of S18 randomer. While S18 randomer dramatically increased Ca^{2+}-induced cytochrome C release, CBD did not exhibit any effect on the latter.

Conclusion:

CBD induces weak uncoupling and increases Ca^{2+}-induced mitochondrial swelling in non-synaptic mitochondria, suggesting that CBD may activate H^{+} uptake in these mitochondria. As the effects of CBD were inconsistent with that of S18 randomer, it is very likely that the mechanism of action of CBD is independent from VDAC.

CHAPTER 1 – LITERATURE REVIEW

1 LITERATURE REVIEW

1.1 EPILEPSY AND DRUG TREATMENT

1.1.1 DEFINITION, EPIDEMIOLOGY AND STIGMA

Epilepsy refers to a neurological disease characterised by the manifestation of spontaneous repeated seizures (SRS) caused by hyperexcitable neuronal networks. Comorbidities associated with epilepsy include gradual impairment of learning, memory and attention (Keezer et al., 2016; Stretton and Thompson, 2012). Furthermore, epilepsy increases the risk of mortality of which trauma, suicide, pneumonia, *status epilepticus* (SE) and sudden unexpected death (SUDEP) (Duncan et al., 2006). Epidemiological analyses suggest that epilepsy is relatively frequent. The number of individuals affected by this condition is around 500,000 individuals in the UK and 500 people die each year of SUDEP (Duncan et al., 2006). According the World Health Organisation, epilepsy is as common as dementia (WHO, 2017, 2018). About 50 million worldwide are thought to be affected by this condition. In some countries, epileptic patients suffer a great deal of stigma and marginalisation because of misconceptions, myths and misinformation surrounding the disease (ILAE, 2003; Jacoby and Austin, 2007). Due to socio-economic difficulties surrounding epilepsy, its high prevalence in many European countries, and its deleterious impact on health, the European Union has recently declared epilepsy as a medical priority (Baulac et al., 2015).

1.1.2 PATHOPHYSIOLOGY OF EPILEPSY

Environmental factors that cause brain insults (e.g. brain trauma, infection, SE, stroke or tumour) increase the risk of epilepsy (Conrad et al., 2013; Fountain, 2000; Maschio, 2012;

Shorvon, 2011). For example, seizures began to manifest in patient HM (who exhibited severe memory impairment caused by a surgical procedure aimed to control his pharmacoresistant epilepsy) at age 10 after been knocked down by a bicycle at age 7 or 9 (depending on the report) (Squire, 2009). Following epileptogenic brain insults, it usually requires several years for epileptic seizures to manifest recurrently in humans, while this takes only few weeks in rodents (Aroniadou-Anderjaska et al., 2008; Löscher, 2011). The asymptomatic phase between brain insults and the manifestation of the disease is called epileptogenesis. Epilepsy can also occur as a result of a genetic defects (e.g. *SCN1A* mutation in Dravet syndrome) (Finsterer and Zarrouk Mahjoub, 2012; Gil Borlado et al., 2010; Hart et al., 2014; Kaplan et al., 2017; Parihar and Ganesh, 2013).

1.1.3 Drug treatment for epilepsy

1.1.3.1 Origin of pharmacotherapy

Presently, there is no cure for epilepsy, and the most common method used to treat epilepsy is through pharmacotherapy. Modern pharmacotherapy of epilepsy is thought to have begun in the 19th century, approximately the same time as the birth of genetics (by Gregor Mendel) and Darwin's theory of evolution (Brodie, 2010). The first anti-epileptic drug (AED) was discovered by Dr Edward Sieveking who discussed in his paper published in 1857 the benefits of potassium bromide use in young women with epilepsy (Brodie, 2010). Thereafter, a number of established AEDs as well as new generation of AEDs were designed essentially to target the neurotransmission of excitatory neurons (releasing glutamate) or/and inhibitory neurons (releasing γ-aminobutyric acid (GABA)) (Brodie, 2010).

1.1.3.2 Mechanism of action of current pharmacotherapy

1.1.3.2.1 GABA transmission

AEDs that are presently available in the market can be classified into four categories based on their respective mechanism of action. AEDs such as benzodiazepines or phenobarbital increase GABAergic transmission by targeting $GABA_A$ receptors (Rogawski and Löscher, 2004). Conversely, other AEDs like vigabatrin or tiagabine were designed to increase the level of GABA by either inhibiting its degradation (mediated by GABA-transaminase) or its reuptake (mediated by GABA transporter 1(GAT1)), respectively (Rogawski and Löscher, 2004).

1.1.3.2.2 Glutamate transmission

Glutamate is the main excitatory neurotransmitter is the brain. Excessive activation of glutaminergic neurons can induce excitotoxity upon postsynaptic neurons (Hardingham and Bading, 2010). Glutamate release can be controlled by levetiracetam (LEV), thus reducing activation of α-amino-3-hydroxy-5-methyl-4-isoxazolepropionic acid (AMPA) and N-methyl-D-aspartate (NMDA) receptors (Lee et al., 2009). LEV reduces glutamate transmission by directly modulating pre-synaptic P/Q-type voltage-dependent Ca^{2+} channels (Lee et al., 2009). Furthermore, other drugs with multiple targets (e.g. voltage-gated Na^+ channels, Ca^+ channels and promote GABA transmission) such as topiramate also inhibit excitatory transmission (Brodie, 2010; Patsalos, 1999).

1.1.3.2.3 Voltage-gated Na^+ channels

Firing of neurons requires influx of Na^+ through voltage-gated Na^+ channels (VGSCs). Genetic changes causing a persistent Na^+ current leak in VGSCs and can result in epileptiform activity (Patel et al., 2016; Rogawski and Löscher, 2004). First-generation AEDs like

carbamazepine or phenytoin block Na^+ channels (Rogawski and Löscher, 2004). Given the mode of action of these AEDs, it is plausible that they may inhibit both GABAergic and glutamatergic neurons.

1.1.3.2.4 Ca^{2+} CHANNELS

Many AEDs have been designed to target Ca^{2+} channels, but they exert different effects on synaptic transmission (Brodie, 2010). Ethosuximide blocks a T-type Ca^{2+} channel and the inward rectifier K^+ channels (Huang and Kuo, 2015; Tian et al., 2018). Furthermore, it has been shown that ethosuximide can promote neurogenesis of GABAergic neurons in the forebrain cortex of infant rats (Sondossi et al., 2014). Conversely, topiramate decreases glutamatergic transmission while it increases GABAergic transmission (Brodie, 2010). LEV's effects are reported above (see section 1.1.3.2.2).

1.1.3.3 LIMITATIONS OF CURRENT PHARMACOTHERAPY IN EPILEPSY

1.1.3.3.1 TOLERANCE AND AEDS

In addition to the undesired effects associated with AEDs treatment (e.g. dizziness, cognitive disfunction or sleep disturbance), prolonged use of these drugs can result in loss of efficacy, this phenomenon is referred to as tolerance (Gilliam, 2002; Löscher and Schmidt, 2006). Preclinical studies in multiple rodent models of seizures have demonstrated a reduction in efficacy following long term use of both first and second-generation AEDs. This data is consistent with the clinical evidence summarised in Löscher and Schmidt's review (Löscher and Schmidt, 2006). For example, in a study performed on 167 children with epilepsy, 38% were seizure free after 6 months of AED monotherapy, however this percentage was reduced to 20% of seizure free children after 36 months of monotherapy (de Silva et al., 1996). Furthermore, long term use of a given AED (inducing tolerance) can render

the use of another AED of a similar category, ineffective (Löscher and Schmidt, 2006). This phenomenon referred to as cross-tolerance and has been observed in preclinical rodent model of seizures, particularly among AEDs targeting $GABA_A$ receptors (Gent et al., 1986; Löscher and Schmidt, 2006).

1.1.3.3.2 PHARMACORESISTANCE IN EPILEPSY

Despite over 160 years of AED development, including the release of new generation of AEDs in the market, approximately 30% of people with epilepsy continue to suffer from seizures attacks (Brodie, 2010; Schmidt and Schachter, 2014). This proportion of pharmacoresistant patients has not substantially changed despite the use of polytherapy. In fact, most pharmacoresistant patients take 2 to 4 AEDs (Brodie and Sills, 2011). When pharmacotherapy is proven to be ineffective in patients with epilepsy, surgery is their last resort (Steinhoff and Staack, 2018). Surgical intervention can be indicated in focal epilepsy (particularly in patients with complex partial seizures) or in cases of patients with generalised tonic-clonic seizures induced by focal seizures (Dwivedi et al., 2017). This surgery consists of excising the focal origin of seizures from the brain, previously determined using video electroencephalographic monitoring or other brain imaging methods (e.g. positron-emission tomography scan (Dwivedi et al., 2017; Engel et al., 2012). A relatively high percentage of pharmacoresistant patients become free from seizures (58-77%) after undergoing this surgery (Choi et al., 2008; Dwivedi et al., 2017; Engel et al., 2012; Wiebe et al., 2001). While this procedure may have little mortality risk (0.1 to 0.5%) (Choi et al., 2008; Dwivedi et al., 2017; Engel et al., 2012; Jobst and Cascino, 2015), it has been demonstrated that some of the patients experience alterations of cognitive function such as memory decline (approximately 40%) (Engel et al., 2012; Jobst and Cascino, 2015).

1.1.3.3.3 Comorbidities and AEDs

Seizure recurrence is not the only disorder affecting the quality of life of patients with epilepsy (Baca et al., 2011; Keezer et al., 2016; Modi et al., 2009). Comorbidities associated with epilepsy can include depression, anxiety disorders, psychosis, decline of cognitive function or migraine (Boro and Haut, 2003; Keezer et al., 2016; Stretton and Thompson, 2012). In addition to numerous adverse effects caused by anti-epileptic pharmacotherapy (see section 1.1.4.3.1), most comorbidities are not controlled by AEDs (Gower et al., 2003; Mula, 2016). Healthy humans treated with carbamazepine, phenytoin, gabapentin or lamotrigine exhibit a reduced memory recall of approximately 15% in comparison to non-AED-treated group (Motamedi and Meador, 2004). More examples of AEDs and their impact on cognition have been reviewed by Meador (Meador, 2006).

1.1.3.4 Potential causes of current AEDs limitations

1.1.3.4.1 Animals model used in epilepsy research

The discovery of numerous AEDs in recent years has depended heavily on preclinical rodent models. To date, models of seizures, such as the pentylenetetrazol (PTZ) or maximal electroshock, have preferentially been used to model epilepsy (e.g. SE-induced temporal lobe epilepsy (TLE) model) for AED discovery (Löscher, 2011). This may be due to the fact that these models of seizures allow the assessment of a wide range of compounds for anti-convulsant effect within a relatively short period of time. For example, the testing of 5-10 compounds for anti-convulsant effects in model of seizures can be performed in a single day, while the assessment of the same number of compounds for anti-convulsant effects would require several days to several months in models of epilepsy. Despite the advantage of fast screening, these models of seizures do not exhibit pathophysiological changes occurring in epilepsy (Löscher, 2011). Furthermore, high doses of PTZ (>80 mg/kg) induce seizures that are lethal

after a certain period (Hill et al., 2012). Increasing evidence suggests that some genetic models and rodent models of acquired epilepsy exhibit molecular and cellular changes also observed in human epilepsy (Curia et al., 2008; Kaplan et al., 2017; Löscher, 2011; Parihar and Ganesh, 2013).

1.1.3.4.2 Mechanisms underlying pharmacoresistance to AEDs

As previously described (in section 1.1.3.2), AEDs have been designed to control seizures by targeting factors involved directly in neurotransmission. During the last two decades, brain tissues resected from patients with pharmacoresistant epilepsy (particularly TLE) and rodent models of epilepsy have been used to determine mechanisms underlying the complexity of the pathophysiology of epilepsy. Currently, there are two mechanisms that have been identified to potentially contribute to pharmacoresistance in epilepsy.

(1) AEDs may not reach therapeutic concentrations in epileptic brain tissue. There is growing evidence from studies performed on human tissue resected from pharmacoresistant patients with epilepsy which shows that the expression of multidrug transporters (MDRs) (e.g. P-glycoprotein) and multidrug resistance-associated proteins (MRPs) are increased in endothelial cells and astrocytes (Löscher and Potschka, 2002; Luna-Tortós et al., 2010). As MDRs and MRPs are plasma membrane proteins involved drug efflux (Borst et al., 2000; Janneh et al., 2007), it is plausible that the increase of their expression may contribute to prevent the diffusion of AEDs into epileptic brain tissue (or epileptogenic neuronal network).

(2) In both animal and human, seizures in epilepsy are caused by activity of hyperexcitable and hypersynchronous rearranged neuronal networks. Altered glutamatergic and GABAergic transmission as well as rearranged neuronal networks have been observed

in the hippocampi of rodents with TLE (Barker-Haliski and White, 2015; Bradford, 1995; Covolan et al., 2000; Deisz et al., 2011; Ma et al., 2012; Parent and Lowenstein, 2002). Cellular changes implicated in the formation of hyperexcitable networks in the hippocampi of rodents with TLE can include degeneration of GABAergic interneurons, increased neurogenesis of glutamatergic neurons and abnormal synaptogenesis (Barker-Haliski and White, 2015; Bradford, 1995; Covolan et al., 2000; Deisz et al., 2011; Ma et al., 2012; Parent and Lowenstein, 2002). Furthermore, it has been demonstrated that impairments of GABAergic transmission can be implicated in pharmacoresistant epilepsy. For example, in patients with pharmacoresistant TLE, $GABA_A$ receptor activation can induce neuronal depolarisation as a result of $GABA_A$ receptor-mediated Cl^- efflux (Deisz et al., 2011; Huberfeld et al., 2007). Under normal conditions, $GABA_A$ receptor mediates hyperpolarisation because intracellular Cl^- is maintained at low concentration in neurons by a Cl^- efflux transporter, K^+/Cl^- co-transporter (KCC2). Given that neuronal expression of KCC2 is reduced in patients with pharmacoresistant TLE, this causes neuronal accumulation of intracellular Cl^- as a result of decreased Cl^- efflux (Deisz et al., 2011). Taken together, these findings demonstrated that in some cases, benzodiazepines or other $GABA_A$ receptor agonists should not be indicated since they may mediate adverse effects.

1.1.4 Cellular and molecular basis of hyperexcitability in epileptic neuronal network

1.1.4.1 Epileptogenesis

Over the years, model of epilepsy induced by brain insults (model of acquired epilepsy) have been used to study the pathogenesis of epilepsy. Epileptogenesis is defined as the asymptomatic period (no seizures are exhibited) during which hyperexcitable neuronal networks are formed in the brain.

1.1.4.2 CELLULAR AND MOLECULAR MODIFICATION OF NEURONAL NETWORK IN EPILEPSY

Several findings indicate that seizure events cause neuroinflammation. Proinflammatory mediators such as interleukin-1β (IL-1β) or prostaglandin E2 (PGE2) have been shown to increase during seizure-like events in *in vitro* and *in vivo* studies (Pepicelli et al., 2002; Stark and Bazán, 2011; Vezzani and Granata, 2005). The work of Stark and Bazan demonstrated that excitatory glutamatergic NMDA receptors mediate inflammation *in vitro* by activating the production prostaglandins (PGs) (Stark and Bazán, 2011). This NMDA receptor-induced prostaglandins synthesis may result from activation of cyclooxygenase-2 (COX2) upregulation induced by nuclear factor kappa-light-chain-enhancer of activated B cells (NF-κB) (Lee et al., 2004). A similar observation was made *in vivo* (Pepicelli et al., 2002). Also, the work of Balosso et al., showed an increase of IL-1β and its receptor (interleukin-1 receptor 1 (IL-1R1)) in mouse hippocampi after kainic acid (KA)-induced seizures (Balosso et al., 2008). Conversely, IL-1β potentiates NMDA receptors activation, suggesting that inflammation can promote seizure events (Balosso et al., 2008; Viviani et al., 2003). Moreover, the inhibition of IL-1β pathways reduces seizure events (Balosso et al., 2008). Consequently, these results also indicate that Ca^{2+} can act as at least one mediator of neuroinflammation since NMDA receptors are Ca^{2+} channels. Interestingly, the anti-convulsant drug LEV which targets Ca^{2+} channels can also reduce the rise of intracellular Ca^{2+} in neurons during epileptiform activity (Pisani et al., 2004).

Mitochondria play a key role in the homeostasis of intracellular Ca^{2+} (for review see (Williams et al., 2013)). Impairment of this function can promote epileptogenesis. For example, haploinsufficiency of the mitochondrial inner membrane Ca^{2+} regulator leucine Zipper EF Hand-containing transmembrane protein 1 (LETM1) causes the Wolf-Hirschhorn syndrome (WHS) (Hart et al., 2014). Patients suffering from WHS manifest epileptic seizures

at early age (Hart et al., 2014). This is consistent with the findings of Zang et al., who showed a downregulation of LETM1 in a model of epilepsy and an onset of epileptic seizures at earlier age which correlates with the inhibition of LETM1 in the same model (Zhang et al., 2014).

1.2 Central role of neuroinflammation in metabolic pathways involved in epilepsy

Presently, there is a need to develop AEDs that could control epileptogenesis, cellular and molecular changes during epilepsy (e.g. alteration of intracellular chloride concentration affecting $GABA_A$ receptor neurotransmission), comorbidities of epilepsy and drug-resistant seizures in epilepsy. Growing evidence in recent years demonstrates that inflammation may play a key role in epileptogenesis and pharmacoresistance in epilepsy. Furthermore, seizures are known to induce neuroinflammation, which in turn could render the brain tissue more susceptible to seizures. Here, I will be discussing the role of neuroinflammation in epileptogenesis, how it renders the brain more susceptible to epileptic seizures (including seizures in pharmacoresistant epilepsy) and how it may play a role in the progression of neuronal network remodelling in epilepsy by describing signalling pathways implicated both in brain inflammation and neuronal network remodelling.

1.2.1 Definition of Inflammation

Inflammation is an immune reaction consisting of detecting and eliminating a threat; this includes lesions, foreign bodies (e.g. pathogens) and tumours. As described in textbooks on immunology, an inflammatory reaction involves both cellular and molecular effectors. For example, during injury, resident cells in the tissue (e.g. microglia cells, fibroblasts, epithelial cells) simultaneously release cytokines (e.g. IL-1β) and chemoattractant molecules such as PGE2 or monocyte chemoattractant protein 1 (MCP1)) that activate and attract macrophages

to the site of damage (Chatenoud and Bach, 2012). Moreover, activated-macrophages "amplify" the signal of tissue damage by releasing metalloproteases which will modulate the extracellular matrix to allow a better diffusion of molecular factors. Furthermore, these activated-macrophages also release more cytokines (e.g. tumour necrosis factor α (TNFα), IL-1β or IL-6), chemoattractant molecules (e.g. MCP1, PGE2), and stimulate the expression of adhesion molecules (E-selectin, P-selectin and intercellular adhesion molecule-1 (ICAM-1)) at the plasma membrane of endothelial cells (Chatenoud and Bach, 2012; Dollery and Libby, 2006). This process allows the invasion of leukocytes (e.g. monocytes, neutrophils or/and lymphocytes) from the blood stream to the damage site (Fig. 1-1). Under normal physiological circumstances, inflammation resolves once the threat is eliminated (Chatenoud and Bach, 2012).

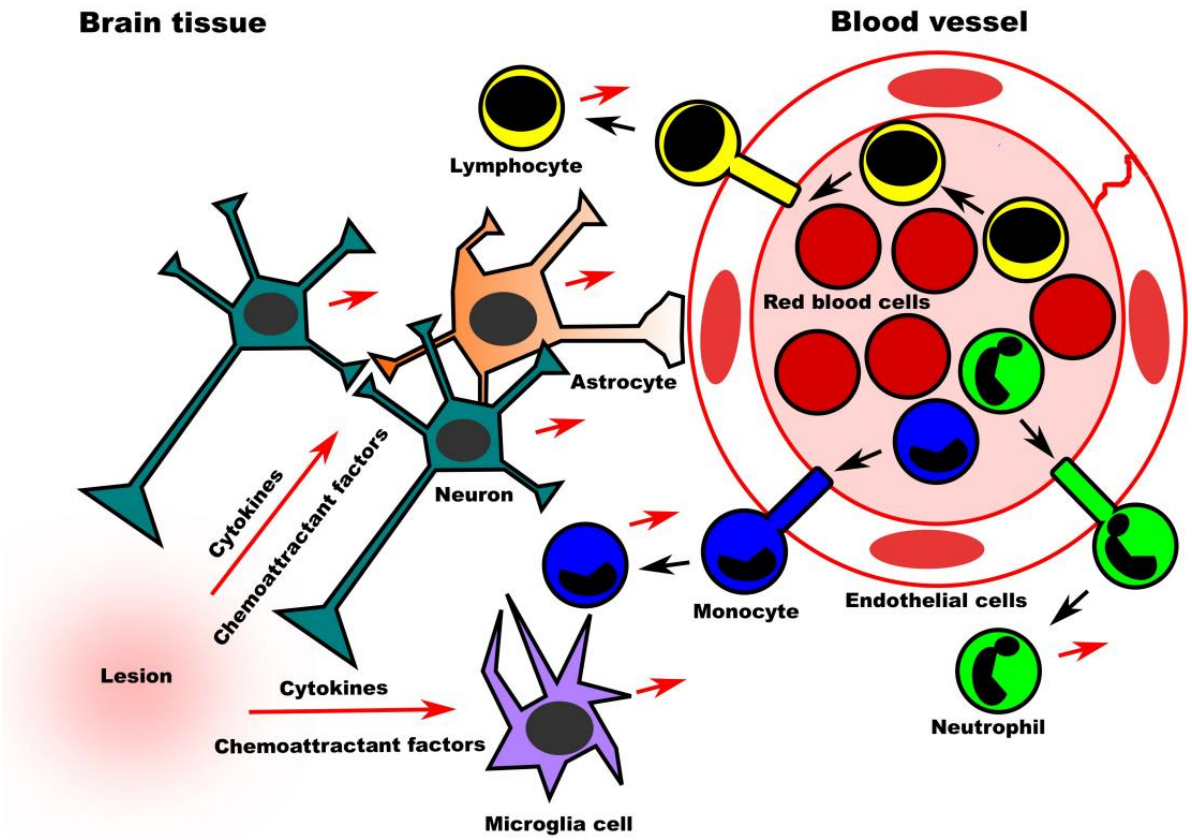

Figure 1-1. Diagram illustrating an example of inflammatory response. Brain lesion induce the production of both pro-inflammatory cytokines and chemoattractant factors (red arrow) in neurons, astrocytes, microglia cells, granulocytes (e.g. neutrophils), monocytes and lymphocytes. The release of pro-inflammatory cytokines (red arrow) into the brain parenchyma causes biochemical modifications in both endothelial cells (e.g. increase of adhesion molecules such as ICAM-1 at the surface of endothelial cells) and extracellular matrix (e.g. increase of metalloproteases release). Chemoattractant factors (red arrow) determine the destination of circulant leukocytes (granulocytes, monocytes and lymphocytes). Leukocytes infiltrate (black arrow) the brain parenchyma through adhesion to endothelial cells followed by transmigration.

Two investigators of the 19th century, Paul Ehrlich and Edwin Goldmann demonstrated that systemic administration of dyes such as alizarin blue-S or trypan blue left the brain unstained, while they were taken up into other organs (Ehrlich, 1885; Goldmann, 1913; Saunders et al., 2014). These findings established for the first time that the transport of molecules between the bloodstream and the brain is more selective compared to that between the bloodstream and other organs. As a result, this high selectivity between the blood stream and the brain was referred to as a barrier which led to the appellation blood-brain barrier (BBB). For many decades, it was thought that the brain was an immune-privileged organ, because it was perceived that the BBB was extremely selective and that cells presenting antigen in the brain such as microglial cells are very poor at expressing antigens to T-cells (Negi and Das, 2018). However, the growing understanding of neurological diseases in recent years has clearly showed that the brain is not free from immune responses. For example, in multiple sclerosis T-cell and B-cell have been shown to infiltrate the brain (Kaskow and Baecher-Allan, 2018; Severson and Hafler, 2010; Wekerle, 2017).

1.2.2 Brain inflammation in epileptogenesis and epilepsy

1.2.2.1 Inflammation in epileptogenesis

In recent years, the role of brain inflammation in epileptogenesis and epilepsy and have been extensively studied, particularly in *in vivo* and *in vitro* model of seizures and epilepsy.

Following induction of long-lasting seizures *SE* in an animal model, the expression of pro-inflammatory effectors such as cytokines (e.g. IL-1β or TNFα), chemoattractant molecules (e.g. PGE2 or chemokines), endothelial adhesion molecules (e.g. ICAM-1) or metalloproteases (e.g. MMP-9) have been shown to increase significantly in the hippocampus (Dubey et al.,

2017; Fabene et al., 2008; Foresti et al., 2009; Manley et al., 2007; Mizoguchi and Yamada, 2013; Mohd Sairazi et al., 2018; Takács et al., 2010). Furthermore, many studies have reported infiltration of leukocytes, such as monocytes and T-cells following SE (Zattoni et al., 2011). In a rodent model of traumatic brain injury (TBI), epileptogenesis is caused by a mechanical shock to the skull instead of *SE*. Inflammation has also been observed following brain trauma (Semple et al., 2017). Advancement in epilepsy research for the last two decades have shown that inflammation in not merely an epiphenomenon of brain insult. Using pharmacological methods, it has been demonstrated that at least some pathways involved inflammation are play a role in epileptogenesis. Using a TBI model, animals that have treated after brain trauma with an IL-1 receptor antagonist exhibit a reduce susceptibility to seizures (Semple et al., 2017). Similarly, anti-inflammatory drugs tend to exert anti-convulsant effects on SE. For example, minocycline, a drug that inhibits microglia activation, increases the time for young rodents to reach grade III seizures (according to Racine's scale) following KA-induced SE (Abraham et al., 2012; Racine, 1972). In a rodent model of kindling-induced epileptogenesis, treatment with docosahexaenoic acid (DHA) or neuroprotectin D1 reduced hippocampal hyperexcitability and seizures susceptibility (Musto et al., 2011).

1.2.2.2 Inflammation in epilepsy

Inflammation has been determined in patients with TLE. In resected hippocampal tissue from patients with pharmacoresistant TLE, cellular responses characteristic of inflammation such as microglial cell activation and tissue infiltration by T-cells has been observed (Beach et al., 1995; Zattoni et al., 2011).

1.2.2.2.1 Signalling pathways involved in brain inflammation

Although the mechanism underlying brain inflammation in epilepsy is not well understood, I will discuss how Ca^{2+} and mitochondria-dependent signalling pathways that may potentially contribute this process using biochemical and functional evidence from animal models (seizures and epilepsy) and patients with epilepsy.

1.2.2.2.1.1 Nuclear factor kappa-light-chain-enhancer of activated B cells

NF-κB is a heterodimer sequestrated in the cytosol by a protein called inhibitor of NF-κB (IκBα) (Jacobs and Harrison, 1998). However, IκBα can be phosphorylated by IκBα kinases (IKK) which induces nuclear translocation of NF-κB. In turn, once NF-κB is in the nucleus, it binds to its promoter and induces the expression of key genes involved in inflammation (e.g. IL-1β, COX2) (Karin, 1999; Yamamoto and Gaynor, 2004). Phosphorylation of the p65 subunit of NF-κB dramatically increases in the hippocampus at 2 and 14 days after induction of *SE* (Huang et al., 2017; Kim et al., 2013). This finding is consistent with the work of Chuang et al., which demonstrated that the p65 subunit of NF-κB is translocated into the nucleus soon after *SE* (30 min) (Chuang et al., 2010).

1.2.2.2.1.2 IL-1β/IL-1R and neutral sphingomyelinase pathway

A study published in 2008 by Balosso et al. demonstrated that inhibition of neutral sphingomyelinase reduced the pro-convulsive effect of IL-1β/IL-1R1 after KA-induced SE (Balosso et al., 2008). Consistent with this evidence, C2-cermanide (a ceramide analogue) exacerbate the duration of seizures and the number of seizures following KA-induced SE mice model (Balosso et al., 2008). Taken together, these findings suggest neutral sphingomyelinase is activated as a result of seizure activity, thus suggesting at least a transient increase of ceramide following *SE*. Metabolites of ceramides, such as ceramide-1-phosphate and

sphingosine-1-phosphate have been reported to activate both nuclear translocation of the p65 subunit of NF-κB and Ca^{2+}-dependent phospholipase A2 involved in the production of PGE2 pathway (Chalfant and Spiegel, 2005; Mattson and Camandola, 2001).

1.2.2.2.1.3 Intracellular Ca^{2+}

Pre-clinical models of TLE exhibit higher concentrations of intracellular Ca^{2+} subsequently to SE, throughout epileptogenesis and during the chronic phase of the disease characterised with SRS (Raza et al., 2001, 2004). Plasma membrane Ca^{2+} entry following SE as so far been demonstrated to require NMDA receptors and $P2X_7$ receptors ($P2X_7R$) (Deshpande et al., 2008; Kim et al., 2010; Raza et al., 2001, 2004; Sun et al., 2002; Vianna et al., 2002) (Fig. 1-2). This increase of intracellular Ca^{2+} following SE may play a critical role in epileptogenesis as well as cellular/molecular changes during epilepsy, given that Ca^{2+} activates numerous signalling pathways and is involved in neuronal hyperexcitability.

1.2.2.2.1.4 Purinergic signalling pathways

Signalling pathways mediated by adenosine-5'-triphosphate (ATP^{4-}) have been implicated in neuronal hyperexcitability, seizure susceptibility and epileptogenesis. ATP^{4-} is principally synthesised in mitochondria and can be metabolised into adenosine-5-diphosphophate (ADP^{3-}), adenosine-5-monophosphotate (AMP^{2-}), cyclic-AMP^{-} and adenosine. Extracellular levels of ATP^{4-}, ADP^{3-}, AMP^{2-} and adenosine are decreased in pilocarpine-induced epileptic model, although enzymes involved in the catabolism of ATP^{4-} (adenosine kinase and ecto-5'-nucleotidase) are increased in the hippocampi of both patients with TLE and preclinical model of TLE (Barros-Barbosa et al., 2016; Boison, 2012; Doná et al., 2016; Luan et al., 2017; Vianna et al., 2005). While adenosine targets adenosine receptors (ARs), ADP^{3-} and ATP^{4-} targets purinergic receptors, P2YRs and P2XRs (Kaebisch et al., 2015;

Rossi et al., 2012). ARs, P2YRs are 7-transmembrane G protein-coupled receptors (GPRs) whereas P2XRs are ATP-dependent Ca^{2+}-channels (Kaebisch et al., 2015; Rossi et al., 2012).

The expression of $P2Y_1R$ and $P2Y_2R$ are increased in patients with pharmacoresistant TLE, while P2Y13R was shown to decrease (Alves et al., 2017). In KA-induced SE model of epilepsy, $P2Y_1R$ and $P2Y_2R$ and $P2Y_{12}R$ are upregulated in the hippocampus (Alves et al., 2017). During SE in KA-treated mice, $P2Y_1R$ and $P2Y_4R$ increase in the hippocampus within 4 h by 2 and 4-fold, respectively (Alves et al., 2017). Given that among all P2YRs only changes in $P2Y_1R$ and $P2Y_2R$ are common across human and animal epilepsy, it is plausible that these receptors may promote neuronal hyperexcitability in epilepsy. To date, the role of $P2Y_1R$ and $P2Y_2R$ in brain inflammation remains unclear. However, their functions have been linked to inflammation in other organs such as in lungs (Le Duc et al., 2017). Adenosine exhibits both pro-convulsive and ant-convulsive effects depending on the AR it targets. In rodent model of seizures, activation of A1R repressed seizures while activation of $A2_AR$ exacerbate seizures (El Yacoubi et al., 2008, 2009; Fukuda et al., 2011; Namvar et al., 2008; Zeraati et al., 2006). Patients with pharmacoresistant TLE exhibit an increase of $A2_AR$ in glial cells in the hippocampus, particularly in activated astrocytes (astrogliosis). To date, there is clear link between targeting pharmacologically $A2_AR$ and seizures occurring in epilepsy. Conversely, in a pilocarpine-induced epileptic model, it has been demonstrated that blockade of A1R is proconvulsant, although its activation does not exhibit anti-convulsant proprieties (Amorim et al., 2016). The link between ARs and brain inflammation remains rather ambiguous. Activation of $A2_BR$ (expressed in astrocytes) in mouse striatum induced the expression and release of IL-6 (Vazquez et al., 2008), but in turn IL-6 can induce the synthesis of A1R (Biber et al., 2001, 2008). This finding is consistent with the work of Angelatou et al. who

demonstrated the upregulation of A1R in the cortex of patients with TLE (Angelatou et al., 1993). Furthermore, a biochemical study conducted in patients with Rasmussen encephalitis (exhibiting pharmacoresistant SRS) demonstrated a similar increase in A1R expression, particularly in cortical neurons (Luan et al., 2017). Although Biber et al. showed the involvement A1R in neuroprotection, its activation in cholinergic neurons inhibits adenylate cyclase (AC) while it activates nuclear translocation of NF-κB (Basheer et al., 2004; Biber et al., 2008). Taken together, it is plausible that acute activation of A1R may exhibit anti-convulsant effect, while chronic (or robust) activation may exhibit proinflammatory effect.

Prolong seizures leads to depletion of intracellular ATP^{4-} (Kovac et al., 2012). This intracellular ATP^{4-} decrease is partially due to ATP^{4-} efflux into the extracellular space, given that blockade of ATP^{4-} efflux through pannexin 1 (PANX1) exhibits anti-convulsant effect while its activation increases neuronal hyperexcitability (Santiago et al., 2011; Thompson et al., 2008). Investigations conducted on $P2X_7R$-deficient mice demonstrated that PANX1 mediates its action through $P2X_7R$ (Kim and Kang, 2011). In the TLE model of epilepsy, as well as in patients with TLE, $P2X_7R$ is upregulated (Jimenez-Pacheco et al., 2016; Vianna et al., 2002). Transient blockade of $P2X_7R$ causes a lasting suppression of seizures and astrogliosis as well as microgliosis in a rodent model of TLE (Jimenez-Pacheco et al., 2016). Additionally, $P2X_7R$ blockade was shown to reduced monocyte and neutrophil infiltration in the brain parenchyma following SE (Kim et al., 2010). This was further confirmed as this $P2X_7R$ blockade downregulates a chemokine such as the type-2 macrophage inflammatory protein (MIP-2), although $P2X_7R$ blockade has no effect on MCP1 expression (Kim et al., 2010).

1.2.2.2.1.5 Ca^{2+}-DEPENDENT PHOSPHOLIPASE A2

Although it has clearly been shown that prolonged seizures activate the Ca^{2+}-dependent phospholipase A2 ($cPLA_2$) pathway, the implication of this pathway in epilepsy is rather ambiguous (Bazán et al., 1982, 1983; Holtman et al., 2009, 2010; Rojas et al., 2014; Stark and Bazán, 2011) (Fig. 1-2). It has been demonstrated that the cPLA2 pathway is activated through activation of the NMDA receptor (Pepicelli et al., 2002; Stark and Bazán, 2011). Given that the $cPLA_2$ pathway may non-selectively activate release both anti-inflammatory omega-3 fatty acids (e.g. DHA) and pro-inflammatory omega-6 fatty acids (arachidonic acid (AA)) (Calder, 2010), it is plausible this pathway may play a compensatory role rather than a causative function in epilepsy. The downstream components of this $cPLA_2$ pathway includes cyclooxygenases (COXs) and lipoxygenases (LOXs) (Calder, 2010). With DHA as substrate, COXs and LOXs produced highly anti-inflammatory molecules such as D-series protectins and resolvins. Alternatively, when cPLA2 induce release of AA from phospholipid, COXs and LOXs metabolise AA into two highly pro-inflammatory molecules (2-series PGs and 4-series leukotrienes) (Calder, 2010). To date, pharmacotherapies targeting the pathway of COX/PGs exhibit inconsistent effect on seizures. Although some studies suggest that inhibition of the pathway of COX/PGs is anti-convulsant, others have demonstrated that its activation or inhibition is proconvulsant (Citraro et al., 2015; Holtman et al., 2009, 2010; Katyal et al., 2015; Kim et al., 2008; Oliveira et al., 2008; Salvadori et al., 2012).

1.2.2.2.1.6 REACTIVE OXYGEN SPECIES

Reactive oxygen species (ROS) are highly reactive molecules containing oxygen. The precursor of all ROS is the superoxide anion ($0_2^{\bullet}$), known to be produced by either nicotinamide adenine dinucleotide phosphate oxidase or complex I and complex III of mitochondrial respiratory chain (RC) (Dan Dunn et al., 2015; Murphy, 2009). In studies using

rodent models of prolonged seizures, it has been demonstrated that seizures cause a dramatic release of ROS from mitochondria (Qiu et al., 2013; Zhen et al., 2014). Since ROS activate the apoptosome complex as well as the nuclear translocation of NF-κB, it is likely that ROS is critical to promote neuroinflammation following seizures (Dan Dunn et al., 2015; Morgan and Liu, 2011; Siomek, 2012). This is consistent with the studies of Wake et al. and Morales-Aza et al. who demonstrated respectively the role of ROS and neuroinflammation in the downregulation of KCC2 in the hippocampus (Morales-Aza et al., 2004; Wake et al., 2007). The relevance of the downregulation of KCC2 in epilepsy has previously been discussed (see section 1.1.3.4.2).

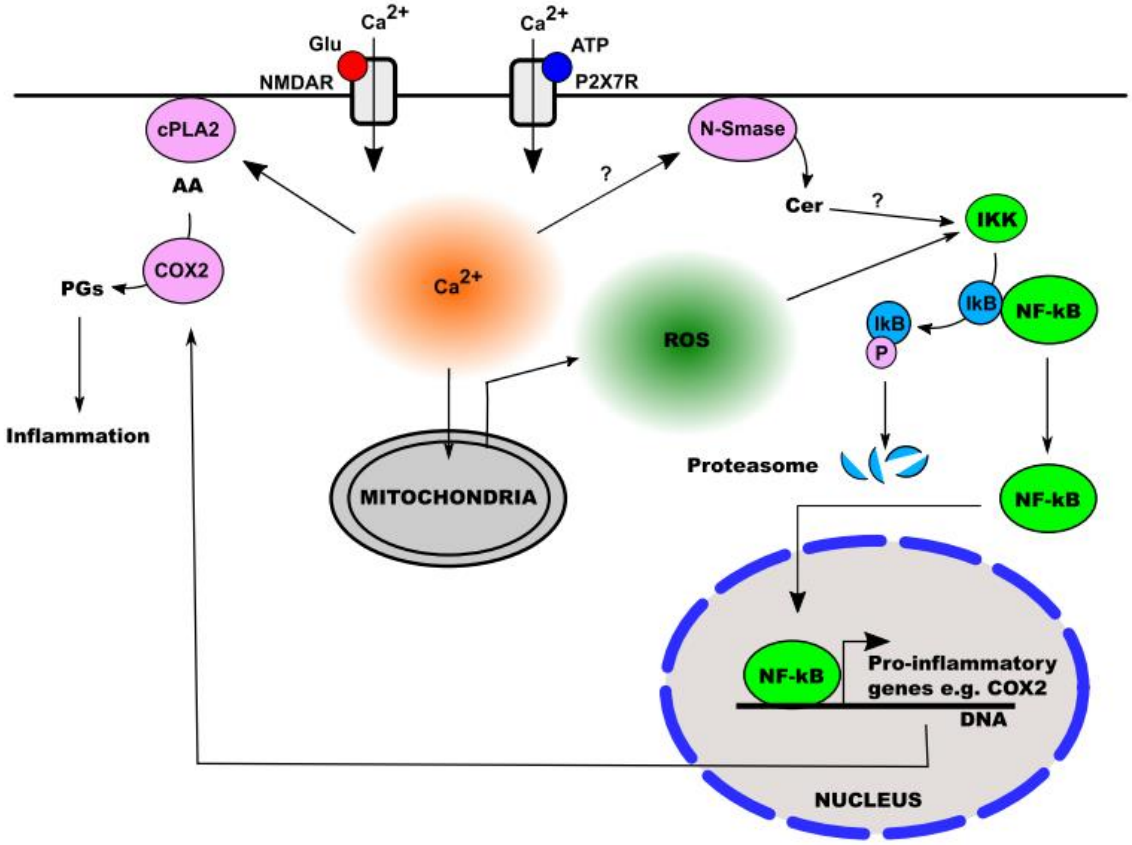

Figure 1-2. A simplified model of signalling pathway induced during seizures in epilepsy. Seizures cause Ca^{2+} influx through NMDAR and $P2X_7R$ in neurons which in turn increases intracellular levels of Ca^{2+}. Elevated intracellular Ca^{2+} can induce activation of cPLA2, mitochondrial reactive oxygen species (ROS) production and activation of neutral sphingomyelinase (N-Smase). Subsequently, both ROS and N-Smase can induce nuclear translocation of NF-κB through phosphorylation of IκBα with activated IKK. NF-κB binds to the promoter of genes (e.g. COX2) involved in inflammation. As cPLA2 is activated and that COX2 is upregulated, this results in the production of prostaglandins (PGs) which also contributes to promote inflammation.

1.3 CANNABIDIOL AND ITS ANTI-EPILEPTIC EFFECT

1.3.1 THERAPEUTIC EFFECT OF CANNABIDIOL IN ANIMAL MODELS AND IN HUMAN CLINICAL TRIALS

For centuries, *Cannabis sativa* extracts have been used for therapeutic purposes to treat neurological disorders including convulsions and pain (Brunner, 1973; Dark, 2000; Li, 1974; Manniche, 1989; Mathre, 1997; Mikuriya, 1969; Morningstar, 1985; Pollington, 2008; Touw, 1981). In modern days, this traditional use of the plant does not meet the criteria for clinical use. Cannabis *sativa* contains approximately 100 phytocannabinoids (Mehmedic et al., 2010). The plant's principal phytocannabinoid, Δ9-tetrahydrocannabinol (Δ9-THC) exhibits psychoactive effect and, its beneficial effect on epilepsy remains anecdotal and often ambiguous (Pertwee, 2014). Recently cannabidiol (CBD), another phytocannabinoid with non-psychoactive properties has been explored for therapeutic potential in animal models of seizures and epilepsy as well as in human clinical trial (see citations below). CBD exerts an anti-convulsant effect in many animal models of prolonged seizures (Consroe et al., 1982; Jones et al., 2010, 2012; Karler et al., 1973). A few clinical studies performed in the 1980's also demonstrated that CBD could control seizures in patients with TLE (Carlini and Cunha, 1981; Cunha et al., 1980). More recently the beneficial effect of this drug in two phase-3 clinical trials which included children with difficult to treat epilepsy such as Dravet syndrome and Lennox-Gastaut syndrome (GW Pharma, 2016). Furthermore, cannabidivarin (CBDV) a phytocannabinoid homolog to CBD, also exhibits anti-convulsant effect (Hill et al., 2012). In June 2018, the FDA approved the use of Epidiolex® (CBD) for Dravet syndrome and Lennox-Gastaut syndrome (Commissioner, 2018). The main concern about this drug is that the mechanism of action mediating its anti-epileptic effect is not clearly understood. A review published in 2015, attempted to narrow down possible targets of CBD with potential

relevance for its anti-epileptic effect (Ibeas Bih et al., 2015). In the sections below, I will review some of these targets.

1.3.2 Molecular targets of cannabidiol

Despite extensive progress in identifying molecular targets of CBD, the molecular mechanisms underlying its anti-epileptic effect remains undetermined. In 2015, a review was published summarising a total of 65 potential targets for CBD (Ibeas Bih et al., 2015). Since then, six novel targets have been identified, which include $GABA_A$ receptors, three G protein-coupled receptors (GPR3, GPR6, GPR12) and a mutant Nav1.6 sodium channel (Bakas et al., 2017; Laun and Song, 2017; Laun et al., 2018; Patel et al., 2016). Given the lack of evidence of CBD targeting type 1 (CB1) and type 2 (CB2) cannabinoid receptors (Ibeas Bih et al., 2015), other candidate targets with potential therapeutic implications will be discussed in section 1.3.2 (below). Targets of CBD with potential therapeutic effect in epilepsy were determined based on two criteria:

(1) The *in vitro* effect of CBD upon a given target should be observed within its *in vivo* concentration in the brain (<20 µM) (Deiana et al., 2012).
(2) The target has previously been shown to be implicated in epilepsy.

1.3.2.1 Receptors

1.3.2.1.1 G protein-coupled receptors

Growing evidence in recent years indicate that CBD does not act CB1 and CB2 receptors (Ibeas Bih et al., 2015). Alternatively, other GPRs, such as GPR3, GPR6, GPR12 and GPR55 are targeted by CBD (Laun and Song, 2017; Laun et al., 2018; Ryberg et al., 2007; Sylantyev et al., 2013; Whyte et al., 2009). For example, in a study conducted by Whyte et al. CBD inhibited the effect of CP55,940, an agonist of GPR55 with an IC_{50} of 445 nM (Whyte et

al., 2009). Further investigations performed in rat hippocampal slices demonstrated that CBD (1 µM) suppresses the constitutive activation of GPR55 which in turn prevents excitatory output of pyramidal neurons (Sylantyev et al., 2013). Alternatively, GPR55 activation (with lysophosphatidyl-inositol) triggers the release of Ca^{2+} from intracellular reserves that will facilitate synaptic transmission (Sylantyev et al., 2013). While GPR55 regulates neurotransmission, its role in hyperexcitability and epilepsy remains unknown and requires further investigation. As CBD act on GPR55 within its physiological concentration range (described in section 1.3.2) (Deiana et al., 2012), it is plausible that this target may be involved it the anti-epileptic effect of CBD.

1.3.2.1.2 Serotonin and Dopamine receptors

Serotonin (also referred as 5-hydroxytryptamine (5-HT)) receptors are implicated in autonomic control (Austgen and Kline, 2013). The serotoninergic axis in the brain is an essential target for anti-epileptic therapy, particularly because of its involvement in SUDEP (Richerson and Buchanan, 2011). The family of 5-HT receptors is diverse and is composed of ionotropic receptors (e.g. $5\text{-}HT_{3A}$ or $5\text{-}HT_{3B}$) as well as GPCRs (e.g. $5\text{-}HT_{1A}$ or $5\text{-}HT_{2A}$) (Amidfar et al., 2018). The $5\text{-}HT_{1A}$ coupled to $G\alpha_{i/o}$ protein and mediates inhibition of postsynaptic neuron (Saigal et al., 2013). CBD binds and activates $5\text{-}HT_{1A}$ receptors within a range of 8–32 µM (Russo et al., 2005). Alternatively, CBD may inhibit $5\text{-}HT_{2A}$ receptor with lesser potency (Russo et al., 2005). It is plausible that CBD's beneficial effect on Dravet syndrome may also involve targeting the serotoninergic axis, since drugs targeting serotoninergic neurotransmission like fenfluramine also exert anti-epileptic proprieties for Dravet syndrome (Ceulemans et al., 2012). While the involvement of 5-HT in the pathogenesis of Dravet syndrome remains undetermined, some 5-HT receptor subtypes may represent a valid therapeutic target (in epilepsy) for CBD (Ceulemans et al., 2012; Theodore et al., 2007).

Finally, it should be noted that CBD may also target the dopaminergic D4 receptor as its effect can be prevented with WAY-100635 (Soares et al., 2010). WAY-100635 is a potent agonist of D_4 receptor as well as an antagonist of 5-HT_{1A} receptor (Chemel et al., 2006; Fornal et al., 1996).

1.3.2.1.3 GLYCINE RECEPTORS

Glycine receptors (GlyR) are pentameric ionotropic receptors consist of a combination of α- and β-subunits (Dutertre et al., 2012; Lynch, 2004). The α-subunit is diverse because of its isoforms encoded by 4 different genes (α1 – α4) while there is only one gene coding for the β-subunit (Dutertre et al., 2012; Lynch, 2004). Since their activation lead to Cl^- uptake, they are involved in inhibiting postsynaptic neurons (Dutertre et al., 2012; Lynch, 2004). *In vivo*, CBD may not directly activate strychnine-sensitive α1 and α1β GlyRs but could act as a positive allosteric modulator of these GlyRs (Ahrens et al., 2009; Deiana et al., 2012; Ibeas Bih et al., 2015). In α1 and α1β GlyRs overexpressing HEK293 cells, CBD potentiate (with average EC_{50} < 20 μM) the effect glycine (Ahrens et al., 2009; Deiana et al., 2012; Ibeas Bih et al., 2015). The amplitude of glycine-induced current in HEK293 cells overexpressing the α3-subunit is increased by approximately 5-fold with CBD (1 μM) treatment (Xiong et al., 2012). Although GlyRs is predominantly expressed in neurons of the spinal cord and brainstem, there is evidence for GlyRs' presence in the hippocampus (Eichler et al., 2008). In recent years, growing evidence suggests the implication of altered GlyRs function and pharmacoresistant epilepsy (Eichler et al., 2008; Ude and Ambegaonkar, 2016; Wuerfel et al., 2014; Zuliani et al., 2014). Dysfunction of GlyRs signalling has been observed in patients with pharmacoresistant TLE (Eichler et al., 2008). Furthermore, patients with auto-antibodies directed against their GlyRs exhibit drug-resistant epilepsy (Ude and Ambegaonkar, 2016; Wuerfel et al., 2014;

Zuliani et al., 2014). Given the critical role of GlyRs impairment in the pathophysiology of epilepsy, it is very likely that CBD's anti-epileptic may be mediated by GlyRs.

1.3.2.1.4 $GABA_A$ RECEPTORS

AEDs targeting $GABA_A$ receptors have commonly been used to treat epilepsy (see section 1.1.4.2.1). Classical constituents of $GABA_A$ receptors are α-subunits (α1 – α6), β-subunits (β1 – β3) and γ-subunits (γ1 – γ3) (Uusi-Oukari and Korpi, 2010). Recently, Bakas et al. showed that CBD potentiates the effect of GABA in HEK293 cells overexpressing different subunits of $GABA_A$ receptors (e.g. α2β2γ2L or α2β3γ2L), thus suggesting that CBD is a positive allosteric modulator for $GABA_A$ receptors (Bakas et al., 2017). Furthermore, the authors demonstrated that CBD's effect on $GABA_A$ receptors does not require the γ2 subunit (Bakas et al., 2017). Although CBD exhibits high potency for α4β2γ2L (EC_{50} = 0.9 μM), α5β2γ2L (EC_{50} = 1.4 μM), α6β2γ2L (EC_{50} = 8.2 μM), α1β2γ2L (EC_{50} = 6.5 μM), α3β2γ2L (EC_{50} = 10 μM), its efficacy on these subtypes of $GABA_A$ receptors is significant lower compared with the α2β2γ2L (EC_{50} = 16.1 μM) subtype (Bakas et al., 2017). This suggests that CBD may have varying effect on different subtypes of $GABA_A$ receptors *in vivo*. In the hippocampi of animals with TLE, the expression of subunits of $GABA_A$ receptors were shown to be altered (Houser and Esclapez, 2003; Laurén et al., 2003; Rice et al., 1996; Schwarzer et al., 1997; Tsunashima et al., 1997). Other studies in patients with pharmacoresistant epilepsy have demonstrated impairment of $GABA_A$ receptors function (Baulac et al., 2015; Bradley et al., 2008; Deisz et al., 2011; Kumari et al., 2010; Wallace et al., 2001). However, the implication of $GABA_A$ receptors in the anti-epileptic mechanism of CBD requires more investigation, since the activation of $GABA_A$ receptors induces a depolarising effect (rather than an inhibitory effect) in postsynaptic pyramidal neurons of resected brain tissue from patients with pharmacoresistant TLE (Deisz et al., 2011).

1.3.2.1.5 Adenosine transporter: Equilibrative nucleoside transporter 1

Although the role of adenosine in epilepsy remains ambiguous, CBD has been shown to target the equilibrative nucleoside transporter 1 (ENT1) under *in vitro* conditions. ENT1 is a plasma membrane transporter implicated in adenosine uptake (Yamamoto et al., 2007). Both astrocyte and neurons express ENT1 (Governo et al., 2005; Peng et al., 2005). Using a competitive radiolabelled binding assay, Carrier et al. demonstrated that CBD displaced the radiolabelled blocker of ENT1 ([^{3}H] S-(4-nitrobenzyl)-6-thioinosine) with a dissociation constant of 237 nM (Carrier et al., 2006). This result is consistent with another finding demonstrating that CBD (ranging from 1 to 1000 nM) inhibits adenosine uptake in EOC20 microglia from rat (Carrier et al., 2006). Given that adenosine levels are diminished in TLE (see section 1.2.1.2.4), it is plausible that CBD increases adenosine concentration in the synaptic cleft under *in vivo* conditions. Currently, the implication of the effect of this possible extracellular adenosine increase in epilepsy remains unclear, as there are still inconsistencies on the role of either A_1R or A_2R in epilepsy (Ibeas Bih et al., 2015).

1.3.2.2 Ion channels

1.3.2.2.1 Transient receptor potential channels

In 2001, Bisogno et al. demonstrated for the first time that CBD act on transient receptor potential (TRP) ion channels (Bisogno et al., 2001) (Table 1-1). TRP channels are expressed at the plasma membrane of many cells types of different tissues and are permeable to cations such as Na^+, Ca^{2+} and Mg^{2+} (Billeter et al., 2014). Using HEK293 cells overexpressing human TRP vanilloid type 1 (hTRPV1), CBD (0.1 µM-10 µM) was demonstrated to act as a full agonist of hTRPV1 (Bisogno et al., 2001; De Petrocellis et al., 2011). However, the data regarding the effect of CBD on rat TRP vanilloid type 1 (rTRPV1) remains controversial. CBD

did not affect HEK293 cells overexpressing rTRPV1 in Qin et al. study, while the work of Iannotti et al. demonstrated otherwise (Iannotti et al., 2014; Qin et al., 2008). In the brain, TRP vanilloid type 2 (TRPV2) is expressed in neurons and astrocytes (Shibasaki et al., 2010, 2013). CBD exhibits a better potency for rTRPV2 (EC_{50} = 3.7 µM) compared to hTRPV2 (EC_{50} = 31.7 µM) (Qin et al., 2008) (Table 1-1). Furthermore, CBD has been shown to activate TRPV3, TRPV4, TRPA1 and while it exerts an antagonist effect on TRPM8 (De Petrocellis et al., 2008, 2011, 2012; Iannotti et al., 2014; Qin et al., 2008) (Table 1-1). The role of TRP channels in the pathophysiology of epilepsy is not clearly understood. However, changes in expression of some TRP channels have been reported in some preclinical rat model of seizures and epilepsy as well as in patients with epilepsy. For example, TRPV1 upregulation has been demonstrated in preclinical rodent model following prolong seizures as well as in models of epilepsy (Bhaskaran and Smith, 2010; Saffarzadeh et al., 2015, 2016). Furthermore, TRPV1 is increased in the hippocampus and temporal cortex of patients with mesial temporal lobe epilepsy (Sun et al., 2013). Since 2010, there have been growing evidence from preclinical studies suggesting that activation of TRPV1 is pro-convulsant while its inhibition exerts anti-convulsant effects (Bhaskaran and Smith, 2010; Gonzalez-Reyes et al., 2013; Huang et al., 2015; Manna and Umathe, 2012; Socała et al., 2015). Among other TRP channels targeted by CBD, only TRPA1 and TRPV4 were shown to have potential implications in the pathophysiology of epilepsy. TRPV4 expression is upregulated following induction of hyperthermia febrile seizures in larval zebrafish (Hunt et al., 2012). Whilst antagonising TRPV1 does not affect febrile seizures, inhibition of TRPV4 reduced febrile seizures in larval zebrafish (Hunt et al., 2012). Given that CBD activates both TRPV1 and TRPV4, it seems unlikely that its anti-epileptic proprieties are dependent on either of these channels.

Table 1-1. Effect of CBD on TRP channels.

Activation (+), inhibition (-), not determined (ND) and no significant change (NSC).

Type	Effects	EC_{50}/IC_{50} (μM)	Maximal response (%)/ Dose (μM)	System/Species	Reference
TRPV1	+	3.5±0.3	64.1+3.9/10	HEK293/ Human	(Bisogno et al., 2001)
	+	1.0±0.1	44.7±0.02/		(De Petrocellis et al., 2011)
	NSC	ND	ND	HEK293/ Rat	(Qin et al., 2008)
	+	Single dose	ND/ 30		(Iannotti et al., 2014)
TRPV2	+	31.7	ND	HEK293/ Human	(Qin et al., 2008)
	+	1.25±0.23	40.5± 1.6	HEK293/Rat	(De Petrocellis et al., 2011)
	+	3.7	160/100		(Qin et al., 2008)
	+	22.2	100/100	U87MG glioma cells/Rat	(Nabissi et al., 2013)
	+	Two doses	ND/ 10-30	HEK293/ Rat	(Iannotti et al., 2014)
TRPV3	+	3.7±1.6	50.1±4.8/100		(De Petrocellis et al., 2012)
TRPV4	+	0.8±0.3	16.7±1.0/100		(De Petrocellis et al., 2012)
TRPA1	+	81.4	100/100		(Qin et al., 2008)
	+	0.096±0.012	~84/10		(De Petrocellis et al., 2008)
	+	Two doses	ND/ 10-30		(Iannotti et al., 2014)
	+	0.11±0.05	115.9±4.6/100		(De Petrocellis et al., 2011)
TRPM8	-	0.08±0.01	0/~10		(De Petrocellis et al., 2008)
	-	0.06±0.01	ND/ND		(De Petrocellis et al., 2011)

1.3.2.2.2 VOLTAGE-GATED CA^{2+} CHANNELS

Voltage-gated Ca^{2+} channels (VGCCs) are a large family of Ca^{2+} channels. Constituents forming VGCCs are α1, α2, β, δ and γ subunits (Catterall, 2011) and N-, P/Q-, L- and T-type VGCCs are already established targets for AEDs such as gabapentin, lamotrigine and ethosuximide (Brodie, 2010; Oka et al., 2003; Rogawski and Löscher, 2004). Such drugs are particularly useful in the treatment of absence seizures, given that mutations in T-type VGCCs have been associated with the pathogenesis of some absence epilepsies (Bezençon et al., 2017; Cheong and Shin, 2013; Huguenard, 2004). CBD can block T-type currents of VGCCs in HEK293 overexpressing the human CaV3 gene family (Ross et al., 2008) (Table 1-2). Furthermore, it has been shown that CBD abolishes the conductance of CaV 3.1, 3.2 T-type channels with comparable potency, while it acts on CaV 3.3 with lower potency (Table 1-2). This finding was consistent with the inhibitory effect of CBD on native T-type conductance in mouse trigeminal ganglion neurons (Ross et al., 2008). Both the potency of CBD on these VGCCs and their implication in the pathophysiology of epilepsy make VGCCs as plausible targets for the underlying anti-epileptic mechanism of CBD. Interestingly, the effect of CBD on T-type channels may suggest that the drug blocks these channels in the opened or closed state (Ibeas Bih et al., 2015; Ross et al., 2008), while ethosuximide blocks T-type channels at their opened state (Gomora et al., 2001).

Table 1-2. Effect of CBD on VGCCs.

Activation (+), inhibition (-) and not determined (ND).

Type	Effects	EC_{50}/IC_{50} (μM)	Concentration range (μM)	System/ Species	Reference
CaV 3.1	–	0.82	10^{-2} – 10	HEK293/ Human	(Ross et al., 2008)
CaV 3.2	–	0.78	10^{-2} – 10		
CaV 3.3	–	3.7	10^{-2} – 30		

1.3.2.2.3 VOLTAGE-GATED NA^+ CHANNELS

The integrity of the function of VGSCs is critical for action potential firing. Different classes of neurons express different types of VGSCs. For example, $Na_v1.1$ is localised in GABAergic neurons (Cheah et al., 2012). Genetic mutations some of these VGSCs, particularly in $Na_v1.1$, can lead to a severe form of epilepsy like Dravet syndrome. The growing evidence in recent years, suggests that anti-convulsant effect of CBD is mediated not mediated through $Na_v1.1$. Although the work of Hill et al. performed *in vitro* showed an apparent block of the human $Na_V1.1$ ($hNa_V1.1$) with CBD, the effect of CBD does not follow a conventional concentration-dependent response relationship (Hill et al., 2014). Instead, CBD does not have any effect on this channel at concentrations lower that 10 μM, above which the activity of the channel suddenly drops to less than 25% activity (Hill et al., 2014). This response is suggestive of an artefactual nonspecific effect (e.g. disruption of the lipid membrane). The work is in agreement with the work of Patel et al. who showed that no effect of CBD on $Na_V1.1$ (Patel et al., 2016). While the effect of CBD on $hNa_V1.2$ and $hNa_V1.5$ are similar with that of $hNa_V1.1$,

it has been shown that CBD (1 µM) blocks the $hNa_V1.6$ and two mutated forms of $hNa_V1.6$ causing a severe epileptic encephalopathy at early age (Blanchard et al., 2015; Carvill et al., 2013; Hill et al., 2014; Ibeas Bih et al., 2015; O'Brien and Meisler, 2013; Veeramah et al., 2012). In summary, given the low concentration of CBD required to act upon $Na_V1.6$, it is likely that its anti-convulsant effect may involve $Na_V1.6$.

1.3.2.2.4 VOLTAGE-DEPENDENT ANION-SELECTIVE CHANNEL

1.3.2.2.4.1 FUNCTION OF VOLTAGE-DEPENDENT ANION-SELECTIVE CHANNEL

Investigations of mitochondrial porin, also known as voltage-dependent anion-selective channel (VDAC) began in the 1970's (Schein et al., 1976). Using VDAC isolated from paramecium aurelia reconstituted in a planar lipid bilayer, Schein et al. showed that VDAC is was more permeable to negatively monoatomic ions such as Cl^- compared to positively charged monoatomic ions like K^+ (Schein et al., 1976). The group further demonstrated that VDAC was impermeable to Ca^{2+} (Schein et al., 1976). After purification of VDAC from rat liver mitochondria in the early 1980's, other functions of VDAC began to be discovered (Colombini, 1983). VDAC was subsequently shown to transport both anions (ATP^{4-}, UTP^{4-}, GTP^{4-}, ADP^{3-}, $citrate^{3-}$, $succinate^{2-}$, Cl^-, HPO_4^{2-}, $H_2PO_4^-$) and cations (Na^+, K^+ and Ca^{2+}) depending on the membrane potential (Hodge and Colombini, 1997; Rostovtseva and Bezrukov, 1998; Rostovtseva and Colombini, 1996; Tan and Colombini, 2007; Tan et al., 2007a; Villinger et al., 2014). VDAC transports mainly anions during the opened state (from -20 mV to +20 mV) while cations are transported during the closed state (<-20 mV and >+20 mV) (Hodge and Colombini, 1997; Tan and Colombini, 2007). Further investigations using liver mitochondria and inhibitors of VDAC have demonstrated that VDAC can transport ROS (Tikunov et al., 2010).

1.3.2.2.4.2 ISOFORMS OF VDAC

VDAC is abundantly expressed in the outer membrane of mitochondria as well as at the plasma membrane (Bàthori et al., 1999; Báthori et al., 2000; Colombini, 1979; Forte et al., 1987; Mannella and Bonner, 1975; Mannella et al., 1983). There are three isoforms of VDAC encoded by different genes. Alignment of VDAC isoforms predicts that they have a highly similar protein structure (De Pinto et al., 2010; Messina et al., 2012; Sampson et al., 1997). However, individual VDAC isoforms (VDAC1, VDAC2 and VDAC3) have distinct biological functions (see chapter 3 and 4 for more details).

1.3.2.2.4.3 VDAC AS A POTENTIAL TARGET FOR EPILEPSY

CBD prevents and supresses intracellular Ca^{2+} oscillations induced by epileptiform activity in neurons from hippocampal cultured (Ryan et al., 2009). In neuronal mitochondria, carbonilcyanide-p-triflouromethoxyphenylhydrazone (a mitochondrial uncoupler) induces a rapid Ca^{2+} efflux, while CBD activates a slow rate Ca^{2+} efflux (Ryan et al., 2009). While CBD depletes mitochondrial Ca^{2+}, this subsequently allows a rapid Ca^{2+}uptake in mitochondria of neurons during NMDA receptors activation (Ryan et al., 2009). Under high extracellular K^+ conditions (50 mM), both mitochondrial and cytosolic Ca^{2+} increase (Ruiz et al., 2014; Sun et al., 2002). However in neurons and glia cells, the increase of cytosolic Ca^{2+} induced with high extracellular K^+ is reduced with CBD treatment (1 µM) (Ryan et al., 2009). Therefore, it seems that CBD activates slow mitochondrial Ca^{2+} efflux when cytosolic Ca^{2+} remains at resting state, whereas a rapid influx of mitochondrial Ca^{2+} is activated by CBD when the cytosolic Ca^{2+} is high. Given that VDAC may transport Ca^{2+} in a bidirectional manner and that the conductance of at least one of the isoform of VDAC (namely VDAC1) may be directly inhibited by CBD, it is plausible that its anti-epileptic effect is mediated through VDAC by activating the slow rate

efflux of Ca^{2+} (Ben-Hail and Shoshan-Barmatz, 2016; Rimmerman et al., 2013; Tan and Colombini, 2007).

1.3.2.3 ANTIPORTER: Na^+/Ca^{2+} EXCHANGER

In the initial work of Ryan et al., the authors concluded that CBD activates the inner-membrane mitochondrial Na^+/Ca^{2+} exchanger (NCX) to mobilise mitochondrial Ca^{2+} given that CGP37157, a blocker of NCX prevented the effect of CBD (Ryan et al., 2009). The action of CGP37157 may not be limited to mitochondrial NCX. Recently, a study by Ruiz et al. demonstrated that CGP37157 mediated its anti-excitotoxicity by blocking VGCCs in neurons from primary cell culture (Ruiz et al., 2014). Since the mode of action of CBD was investigated in cells (neurons and glia cells) (Ryan et al., 2009), this can allow the possibility of indirect or non-specific effects. While CBD induces a mitochondrial slow rate Ca^{2+} efflux and a rapid Ca^{2+} influx depending on the cytosolic concentration of Ca^{2+}, the target (or targets) involved in these processes remains undetermined. Moreover, the direct functional effect of CBD on isolated mitochondria remains yet to be examined.

1.3.2.4 A CAUTIONARY NOTE ON THE EFFECT OF CBD

As previously described, the effect of CBD on some signalling pathways is not entirely consistent with an anti-convulsant effect. For example, CBD is known to activate TRPV1, an effect which has been shown to be inconsistent with an anti-convulsant effect since the activation of TRPV1 promote seizures while its inhibition is anti-convulsant (Bhaskaran and Smith, 2010; Gonzalez-Reyes et al., 2013; Huang et al., 2015; Manna and Umathe, 2012; Socała et al., 2015) (Table 1-1). Furthermore, CBD could exhibit some mitochondrial toxicity as it inhibits complex I (Fišar et al., 2014). Some effects of CBD could be due to its action on the biophysical property of lipid bilayer membranes rather than a direct action on proteins

(Hillard et al., 1985). Taken together, the outcome of these unintended effects of CBD remain poorly understood thus require further investigation.

1.4 Role of mitochondrial dysfunction in epilepsy

1.4.1 Mammalian mitochondria inheritance

Under physiological conditions, mitochondria use metabolites from macronutrients (lipids, carbohydrates and proteins) to produced ATP^{4-}, the most abundant source of energy for metabolic reaction. These organelles possess their own genome with a unique genetic code (Barrell et al., 1979; Fearnley and Walker, 1987; Watanabe and Yokobori, 2011). In mammals, mitochondria are mainly inherited from the female but there are rare cases of paternal inheritance (Sato and Sato, 2013; Schwartz and Vissing, 2002). Mitochondrial DNA is circular, but length varies across mammalian species. For example, in humans the length of mitochondrial genome is 16,569 bp, while in rodents the size is ~16,300 bp. Mammalian mitochondrial DNA possesses genes encoding for 13 proteins involve in OXPHOS (Taanman, 1999). Among these 13 proteins, I will investigate the change of expression of NADH-ubiquinone oxidoreductase 4 (a component of complex I) in epilepsy (see chapter 4).

1.4.2 Krebs cycle

ATP^{4-} synthesis in mitochondria requires oxidation of reducing agents such as nicotinamide adenine dinucleotide (NADH, H+) and flavin adenine dinucleotide ($FADH_2$). After glucose or fatty acids are catabolised into acetyl-coenzyme A through glycolysis or β-oxidation respectively (Lodish et al., 2000; Murray et al., 2003), citrate synthase initiate the Krebs cycle by synthesising citrate from acetyl-coenzyme A and oxaloacetate (both present in mitochondrial matrix) (Fig. 1-3). A complete cascade of Krebs cycle reaction leads to the

production of NADH, H^+ and $FADH_2$, which will in turn serve as electron donors to the RC (Fig. 1-4).

1.4.3 TRANSFERS OF E^- THROUGH THE RESPIRATORY CHAIN AND ATP^{4-} SYNTHESIS

The ATP^{4-} synthesis from ADP^{3-} and Pi^{3-} requires free energy ($\Delta G°' = +7.3$ kcal/mol) (Lodish et al., 2000). Oxidation of the either reducing agents provides the necessary free energy required for ATP^{4-} synthesis. For example, the oxidation of NADH, H^+ by complex I yields a $\Delta G°' = -52.6$ kcal/mol while oxidation of $FADH_2$ by complex II produces a $\Delta G°' = -43.4$ kcal/mol (Lodish et al., 2000). Iron-sulphur centres (Fe-S) in complex I and II allow the transfer of two e^- to ubiquinone simultaneously (Lodish et al., 2000). Given that oxidoreduction couples in complex III and IV can only allow transfer of a single e^- at a time, the reduced ubiquinone (UbH_2) (which already contains two e^-) can transfers one e^- at a time to complex III (Fig. 1-5). The final oxidoreduction reaction occurring in the RC is the reduction of O_2 into H_2O.

H^+ translocation into the intermembrane space by complex I, III and IV is mediated oxidoreduction reactions occurring in each of these complexes (Fig. 1-5). As the concentration of H^+ rises in the intermembrane space, this creates a gradient of H^+ which in turn allows influx of H^+ in the mitochondrial matrix through the ATP^{4-} synthase (Fig. 1-4). This influx of H^+ through the ATP^{4-} synthase activates ATP^{4-} synthesis (Lodish et al., 2000).

1.4.4 RESPIRATORY CHAIN AND REACTIVE OXYGEN SPECIES

The main substrate of all ROS molecules is the superoxide anion ($O_2^-•$). $O_2^-•$ is a molecule of oxygen to which an e^- has been added. Given that $O_2^-•$ is enriched in e^-, this renders the ion highly reactive, and under some circumstances may even cause damage to molecules like membrane lipids or DNA (Murphy, 2009). In mitochondria, $O_2^-•$ can be

produced by either complex I or complex III (Murphy, 2009). The elimination of $O_2^{-}\bullet$ in mitochondria begins with the reduction of $O_2^{-}\bullet$ into H_2O_2 (Murphy, 2009). Subsequently, H_2O_2 is further reduced into H_2O with mitochondrial glutathione peroxidases or peroxiredoxins (Murphy, 2009).

Modified illustration of Murray et al. 2003

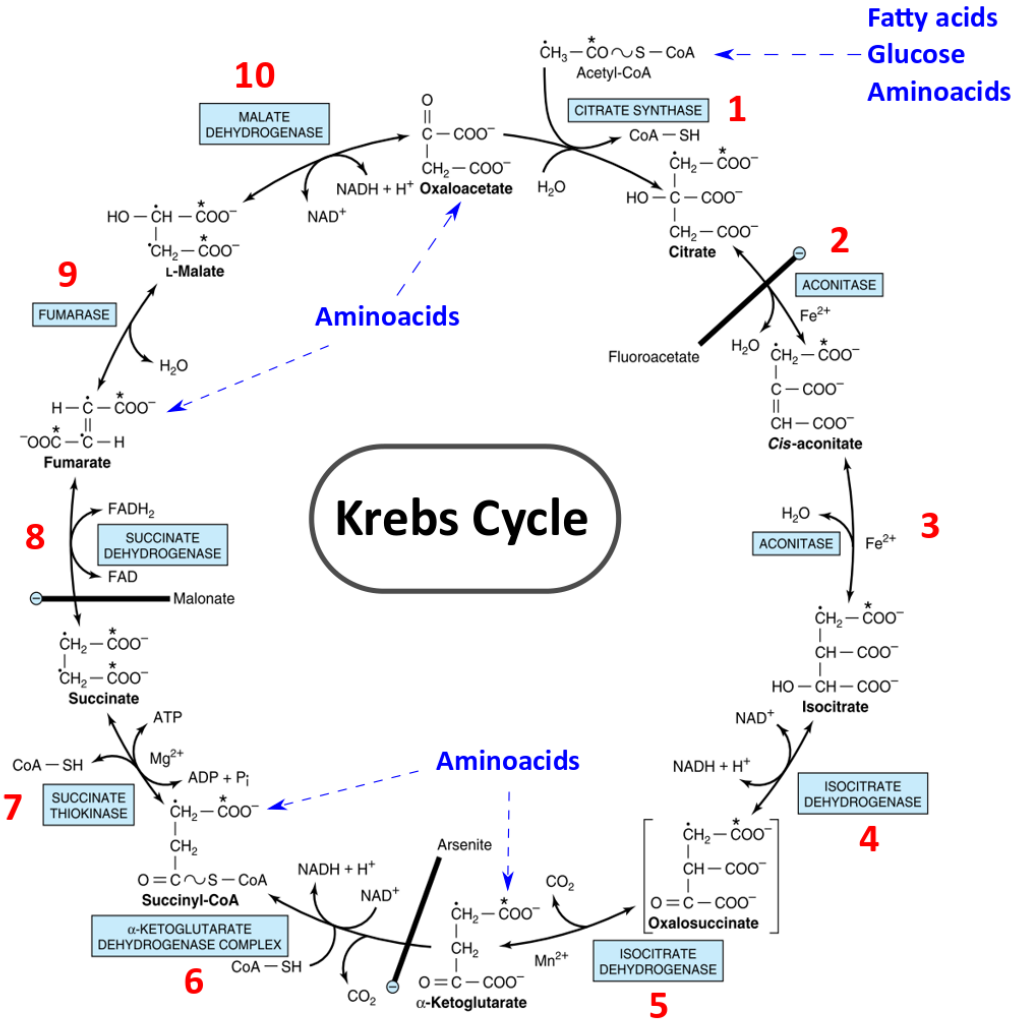

Figure 1-3. Krebs cycle metabolic reactions (Murray et al., 2003). The Krebs cycle entry point of fatty acids and glucose is acetyl-coenzyme A (Acetyl-coA), while amino acids have multiple entry points. A complete Krebs cycle reaction yields reducing agents such as NADH, H^+ and $FADH_2$ which will be oxidised by the complex I and II in the respiratory chain.

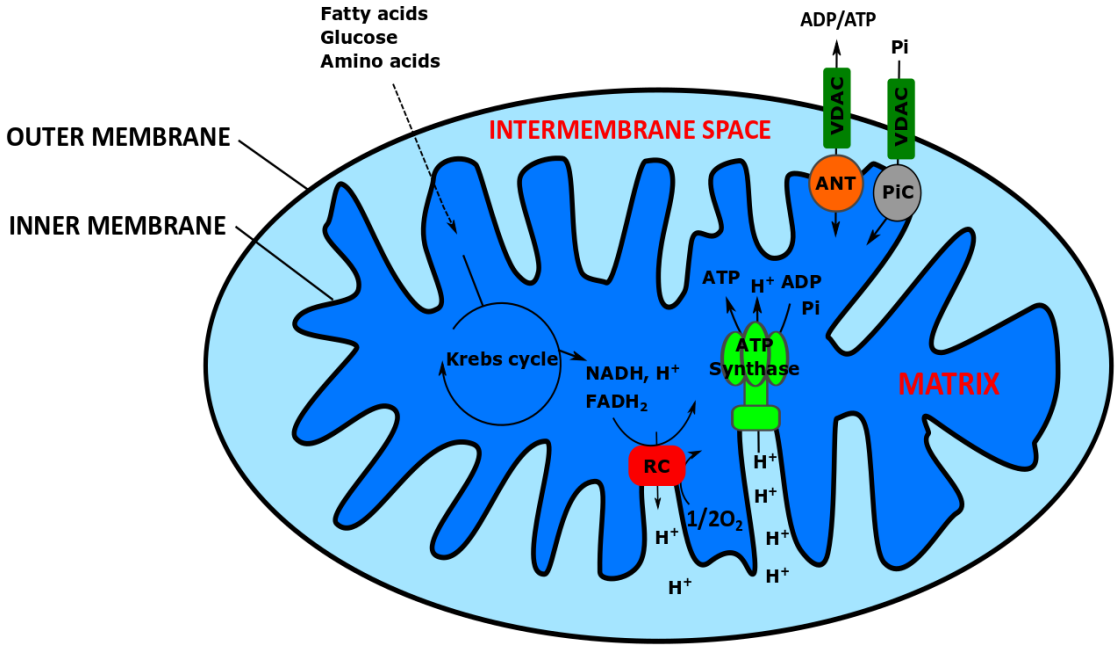

Figure 1-4. Overview of oxidative phosphorylation. Reducing agents generated in the Krebs cycle (NADH, H^+ and $FADH_2$) are subsequently oxidised by the respiratory chain (RC). Transfer of electrons through the RC causes H^+ released into the intermembrane space which in turn will activate the ATP^{4-} synthase, thus allowing ATP^{4-} production in the presence of ADP^{3-} and Pi^{3-}

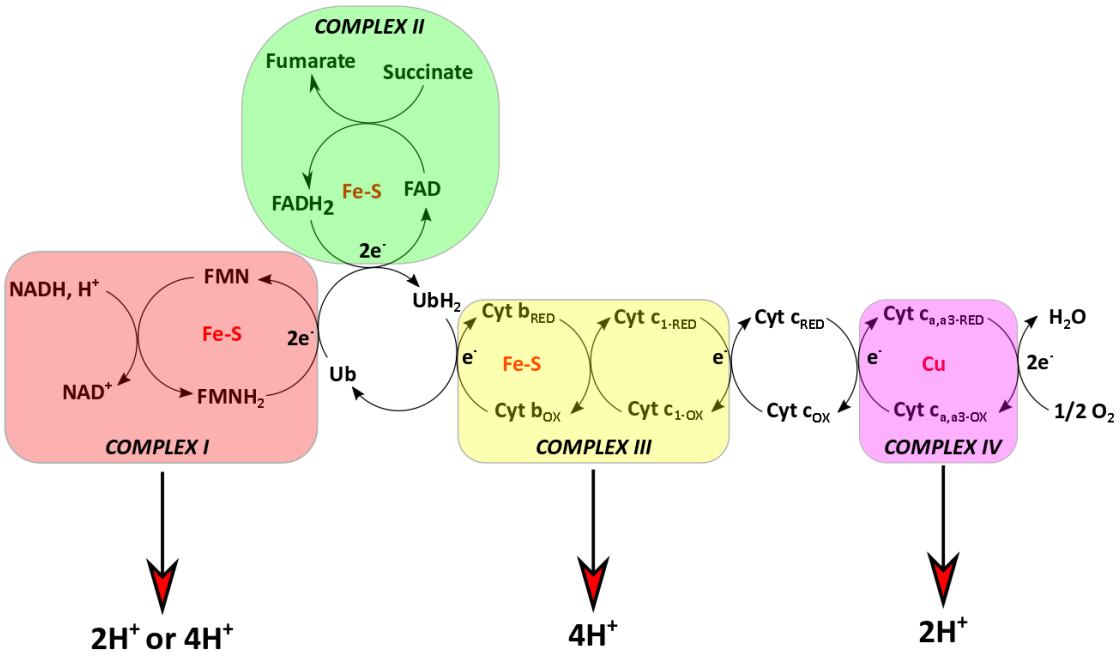

Figure 1-5. Oxidoreduction reactions occurring at the respiratory chain. Oxidation of NADH, H^+ produces 8 or 10 H^+ in the intermembrane space while oxidation of $FADH_2$ produces 6 H^+. Two oxidoreduction reactions occur in complex II. First, FAD is reduced by succinate then $FADH_2$, is oxidised by ubiquinone (Ub). Complex I, II and III are equipped with iron-sulphur (Fe-S) centres which allow electrons (e^-) transfer, while complex IV possesses a cooper (Cu) centre which mediates e^- transfer. FMN, flavin mononucleotide. Cyt b, cytochrome b. Cyt C_1, cytochrome c_1 Cyt C, cytochrome c. Cyt $c_{a,a3}$, cytochrome $c_{a,a3}$.

1.4.5 MITOCHONDRIA AND APOPTOSIS

The intrinsic pathway of apoptosis is regulated by mitochondria. Increase of the permeability of mitochondrial outer-membrane could lead to Cyt C release from the intermembrane space into the cytosol. This release of Cyt C could be triggered by activation of mitochondrial transition (mPT) or by means independent form mPT (e.g. Bcl-2-associated X protein (Bax)) (Jürgensmeier et al., 1998; Kobayashi et al., 2003). Once in the cytosol, Cyt C forms a complex (called apoptosome) with the apoptotic protease activating factor 1 and caspase-9 (Guo et al., 2002). This complex can then activate caspase-3, a mediator of apoptosis. Smac/Diablo protein released by mitochondria during activation of the intrinsic pathway of apoptosis (Adrain et al., 2001; Guo et al., 2002). These factor inhibits the inhibitors of apoptosis proteins to diminish their inhibitory effect on apoptosis (Adrain et al., 2001; Guo et al., 2002).

1.4.6 MITOCHONDRIAL MODULATION OF NEURONAL ACTIVITY: IMPLICATION OF ATP^{4-}, Ca^{2+} AND NEUROTRANSMITTERS

Growing evidence in recent years indicates that alterations of mitochondrial function or structure, directly affect neuronal activity (Cserép et al., 2018; Ryan et al., 2009; Whittaker et al., 2011). For example, fast-spiking interneurons mitochondria exhibit a different ultrastructure to that of regular-spiking interneurons mitochondria (Cserép et al., 2018). Furthermore, complex IV inhibition with potassium cyanide reduced the firing rate of hippocampal fast-spiking interneurons (Whittaker et al., 2011). This suggests that either ATP^{4-} depletion or mitochondrial ROS production (resulting from respiratory chain inhibition) could exert a detrimental effect on neuronal activity. Although mitochondria could regulate neuronal activity through ROS and ATP^{4-}, many studies (as reviewed by Kann and Richard

Kovac) have demonstrated the significant role of mitochondrial Ca^{2+} homeostasis neuronal activity (Kann and Kovács, 2007). In chemical synapses, neurotransmission require the release of neurotransmitter in the synaptic cleft which will activate or inhibit the post synaptic neuron. It appears that mitochondria are involved in many metabolic pathways controlling the synthesis of these neurotransmitters (e.g. glutamate).

1.5 HYPOTHESIS AND OBJECTIVES

As previously described, mitochondria regulate oxidative phosphorylation (OXPHOS), Ca^{2+} homeostasis, ROS production and apoptosis. Genetic mutations affecting their function can cause epilepsy (Finsterer and Zarrouk Mahjoub, 2012; Gil Borlado et al., 2010; Hart et al., 2014). Furthermore, alterations of mitochondrial structure and function have been reported in TLE (Chuang et al., 2004; Folbergrová and Kunz, 2012; Gao et al., 2007), suggesting a potential implication of mitochondrial impairment in the pathophysiology of TLE. Although the mechanism underlying the anti-epileptic effect of CBD remains uncertain, there is some evidence suggesting that it may modulate mitochondrial Ca^{2+} homeostasis in cells (see section 1.3.2.3 and section 1.3.2.4). In addition, CBD was shown to bind directly and inhibit VDAC (Rimmerman et al., 2013). Based on the current literature, it is plausible that the anti-epileptic effect of CBD could be mediated by its direct action on mitochondria. Given that it has not been established whether CBD mediates its anti-epileptic effect (e.g. mitochondrial Ca^{2+} homeostasis) by acting directly on mitochondria, the aim of this project is to investigate the effect of CBD on the function of mitochondria isolated from rat hippocampi. In this study, I tested the effect of CBD on non-synaptic mitochondria (from the soma of neurons and glia cells) isolated from hippocampi of healthy (NS-mito$_{HE}$) and/or epileptic (NS-mito$_{EP}$) rats. The model of epilepsy is a *status epilepticus* (*SE*) model of TLE. As with other refined-pilocarpine

model of SE, the model used here exhibited low mortality rate during SE induced with lithium/pilocarpine in juvenile rats (< 10%) (Curia et al., 2008; Modebadze et al., 2016).

(1) In this study, I determined some functional and biochemical alterations occurring in rats exhibiting SRS (epilepsy).

(2) To establish whether CBD directly acts on NS-mito$_{HE}$ and NS-mito$_{EP}$, I assessed the effect of the drug on oxidative phosphorylation, Ca^{2+}-induced swelling and Cyt C release of isolated mitochondria.

(3) The effect of CBD was also compared to that of cyclosporin A, VDAC inhibitors, and CBDV. Given that CBDV is a homolog of CBD with anti-convulsant proprieties, I determined whether its mechanism of action differs from that of CBD (Fig. 1-6).

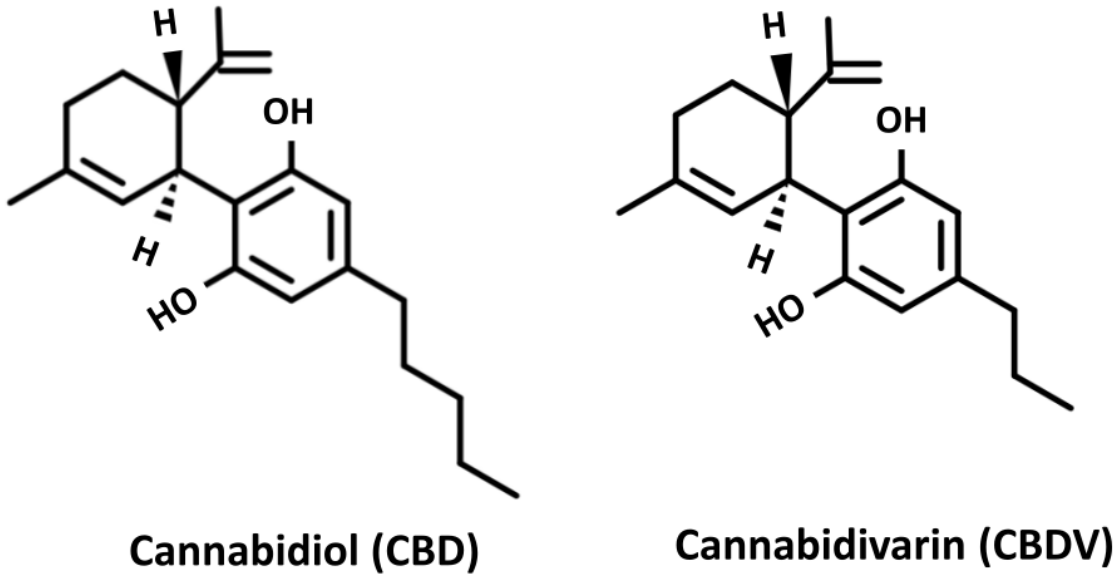

Figure 1-6. Chemical structure of cannabidiol and cannabidivarin. CBD possesses two carbons longer at its lateral aliphatic chain compared to CBDV.

CHAPTER 2 – MATERIALS AND METHODS

2 MATERIALS AND METHODS

2.1 ANIMALS AND MODEL OF EPILEPSY

2.1.1 ANIMALS AND TERMINATION PROCEDURE

This work was undertaken using male Wistar rats (Harlan Envigo-UK, 300-450 g) under a UK Home Office project licence (70/7672 – RO39) in accordance with the Animals Scientific Procedures Act, 1986. All animals were housed in a room at 22°C with a 12 h light/12 h dark cycle and were supplied with water and food ad libitum.

2.1.2 RAT MODEL OF EPILEPSY

Rats with temporal lobe epilepsy (TLE) used throughout this project, are rats with spontaneous recurrent seizures (SRS) that underwent a reduced-intensity induced *status epilepticus* (*SE*) (RISE-SRS) (Modebadze et al., 2016). Here, SE was induced in rats using lithium-pilocarpine (Li-pilo) (Curia et al., 2008). Upon arrival, healthy juvenile Wistar rats (Harlan Envigo, UK, 70-110 g) were left to recover for 3 days and *SE* was chemically induced using pilocarpine, at day-5 after arrival from the supplier. The protocol of *SE* induction began at day-4 after arrival when the rats were first treated with LiCl (127 mg/kg, s.c.) in other to potentiate the effect of low-dose pilocarpine, given that treatment of rodents with high-dose of pilocarpine increases the rate of mortality during *SE* (Curia et al., 2008). At day-5, these rats were pre-treated a second time 24 h post LiCl administration with methyl-scopolamine (1 mg/kg, s.c.), a non-penetrating blood brain barrier muscarinic receptor antagonist which prevents undesirable peripheral effects of pilocarpine. The first dose of the pilocarpine (25 mg/kg, s.c.) was administered 30 min after the methyl-scopolamine. Then, successive administrations of a second or third dose of pilocarpine (50 or 75 mg/kg) were performed

every 30 min upon absence of bilateral seizures followed by rearing and loss of balance (BSRL) (described as stage 5 seizures according to Racine's scale (Racine, 1972)) (see detailed scores of seizures in the appendix). Rat that did not exhibit bilateral seizures were excluded in this study, while rats that manifested BSRL were immediately injected with xylazine (2.5 mg/kg, i.m.) to prevent the lethal tonic state of the *SE*. Finally, the *SE* was terminated with a STOP mix (s.c.) containing MK-801 (0.1 mg/kg), diazepam (2.5 mg/kg) and 2-methyl-6-(phenylethylnyl)-pyridine (20 mg/kg) (Fig. 2-1). Subsequently, rats were left to recover from *SE* and were checked for weight loss and other alterations (e.g. skin lesions, rashes, any eye disease or symptom of pain) for 2 weeks. Rats exhibiting SRS following the third week onward, were considered as epileptic. Furthermore, as rats were discontinuously monitored for SRS, two post-seizures behavioural battery (PSBB) tests, consisting of touching and picking up the animal were performed twice a week, to assess for animals with SRS (Modebadze et al., 2016) (Table 2-1). Although the original PSBB tests consisted of four tests (Moser et al., 1988; Polascheck et al., 2010), both the approach-response test and the finger-snap test were dismissed in my study because the combination of both touch-response test and pick-up test is sensitive in detecting SRS rats (Modebadze et al., 2016). Responses to the touch and pick up tests were scored from 1 to 7 and from 1 to 6, respectively (Table 2-1). Scores resulting from both tests were then multiplied to each other. Any final calculated score of 10 or more was considered as high. To determine whether a rat is epileptic, this final score had to be high for 4 consecutive times within a period of two weeks. Video monitoring of seizures was also used to confirm the result of PSBB tests. In this model, the proportion of non-epileptic animals was low; and regarding animals that became epileptic, the asymptomatic period, could last about 3-13 weeks (Fig. 2-2).

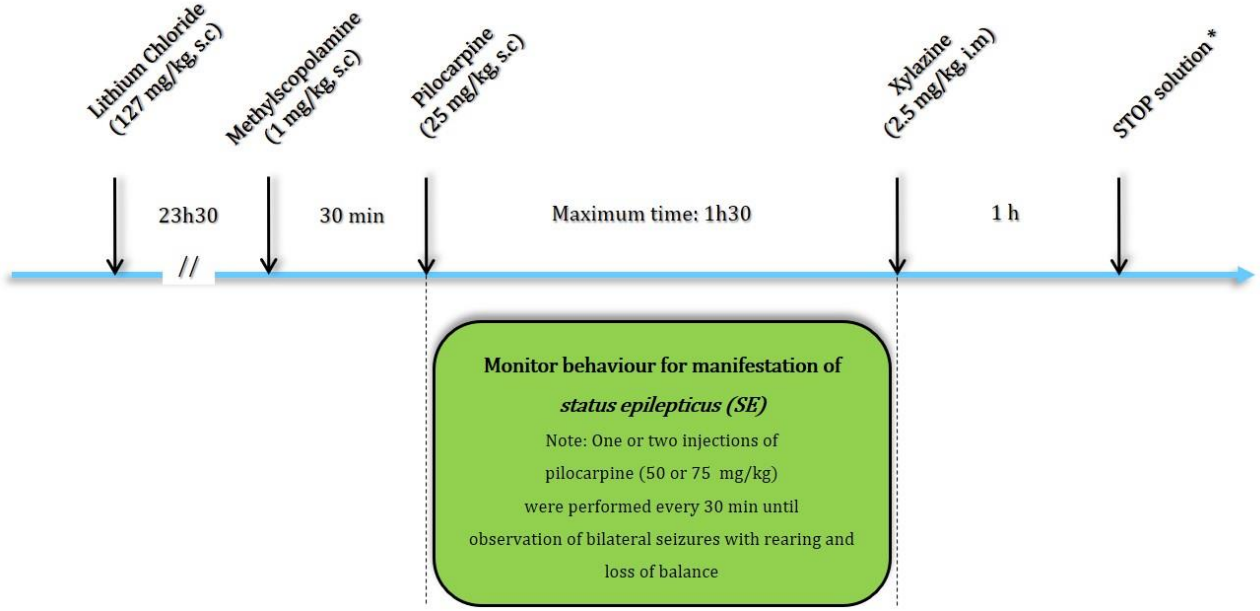

* **Stop solution**: MK-801 (0.1mg/kg), diazepam (2.5 mg/kg) and 2-methyl-6-(phenylethylnyl)-pyridine (20 mg/kg) diluted in ethanol

Figure 2-1. Chart illustrating protocol of induction and arrest of *status epilepticus* by lithium-pilocarpine.

Table 2-1. Post-seizure behavioural battery tests.			
Stimulus	**Description**	**Score**	**Behavioural response**
Touch	The animal is gently approached with a pen to touch the hip	1	Animal exhibits no reaction
		2	Animal turns toward the object, while been approached by the pen
		3	Animal moves away from the object, while been approached by the pen
		4	Animal freezes
		5	Animal exhibits no reaction while the pen is approaching, but moves towards the touch
		6	Animal exhibits no reaction while the pen is approaching, but moves away from the touch
		7	Animal jumps with or without vocalisation
Pick up	The animal is picked up by grasping around the body	1	Very easy
		2	Easy with vocalisation
		3	Some difficulties, as the animal rears and faces the hand
		4	Animal freezes
		5	Difficult, the rat moves away
		6	Very difficult, the rat behaves defensively and attacks the hand

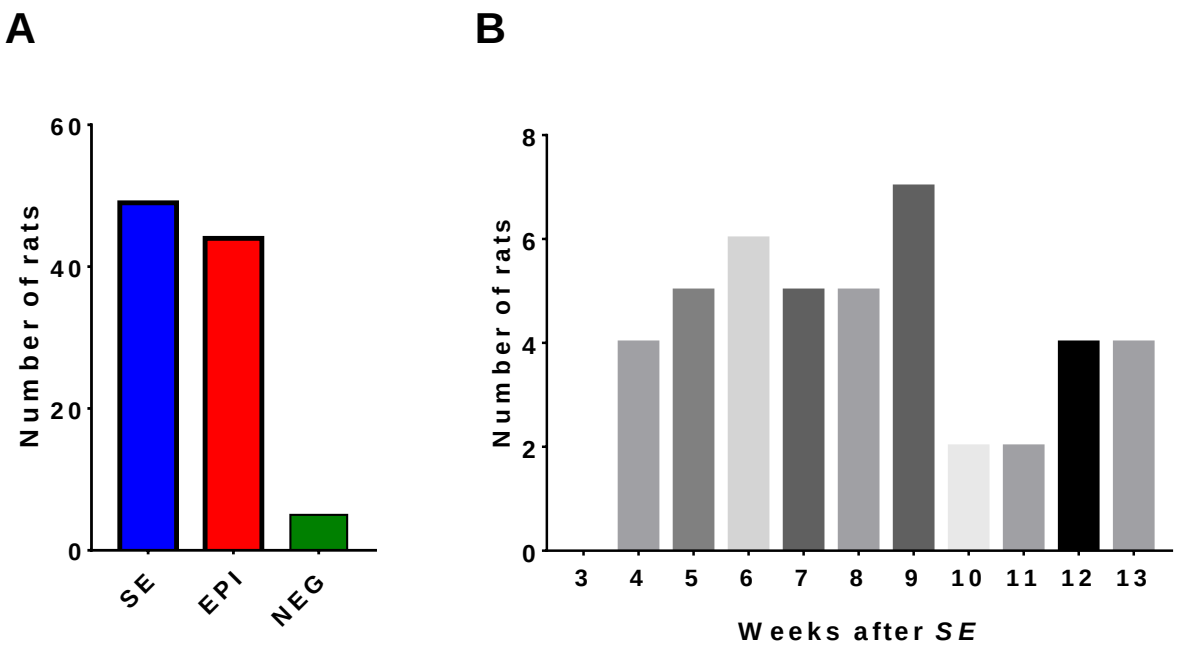

Figure 2-2. A high proportion of rats were confirmed epileptic particularly between week 4 and week 9 following *status epilepticus* (*SE*). (A) A high proportion of rats that underwent *SE* induction were confirmed epileptic (through PSBB and observable seizures). (B) Most rats were confirmed epileptic between the 4th and 9th week after *SE*.

2.2 PROCEDURES OF HIPPOCAMPAL DISSECTION

Isolation of rat brain was immediately performed (<80 s) *post-mortem*, as longer periods did not yield good quality mitochondria. Following termination, each animal was decapitated, then the skull was sagittally sectioned beginning at the foramen magnum. Furthermore, the vault of the skull was carefully removed using dental extracting forceps. Meninges were removed using straight fine tip tweezers to prevent alteration of the brain during extraction. A Chattaway spatula was used to remove the brain from the base of the skull and was transferred into a beaker filled with ice-cold isolation buffer (4°C). The brain was subsequently placed in a large petri dish filled with ice-cold isolation buffer (IB). The hindbrain and a third of the frontal lobe were cut off by two coronal sections. The brain was positioned in a manner that the caudal region faced the experimenter while the dorsal region faces upward. The remaining mesencephalon and diencephalon were removed, and the hippocampus was detached from the cortex using a spear-shaped dissection needle and straight dissection needle and was placed in ice-cold IB.

2.3 ISOLATION OF NON-SYNAPTIC MITOCHONDRIA

2.3.1 REAGENTS AND DRUGS

Non-synaptic mitochondria (NS-mito) were isolated in IB containing in mM: 220 mannitol, 70 sucrose, 5 HEPES (4-(2-hydroxyethyl)-1-piperazineethanesulfonic acid) and 1 EGTA (ethylene glycol-bis(β-aminoethyl ether)-N,N,N',N'-tetraacetic acid) diluted in distilled deionised water (DDW) and the pH was titrated to 7.4 with KOH.

A solution of bovine serum albumin (BSA) free from fatty acids was prepared by diluting 100 mg in 10 ml DDW. Various dilutions of Percoll were prepared and the pH was titrated at 7.4 with HCl:

- 40% Percoll: 20 ml of 100% Percoll added to 30 ml IB
- 23% Percoll: 11.5 ml of 40% Percoll added to 8.5 ml IB
- 15% Percoll: 7.5 ml of 40% Percoll with the addition of 12.5 ml IB

2.3.2 PROCEDURE

NS-mito were isolated in an ice-cold IB from hippocampal homogenate using a method adapted from Sims and Anderson protocol (Sims and Anderson, 2008). Following the dissection of hippocampus, the tissue was gently homogenised in 9 ml ice-cold IB using a Teflon homogeniser. The homogenate was transferred into a 10 ml polycarbonate tube and centrifuged at 1100 *g* for 3 min (4°C) using the SS-34 rotor (Thermofisher-UK) designed for Sorvall RC-5C Plus Centrifuge (UK). While the supernatant was transferred into a 50 ml tube, the pellet was resuspended in 10 ml ice-cold IB before being centrifuged a second time (1100 *g*, 3min, 4°C). The resulting supernatant was pooled with the one from the previous centrifugation then centrifuged at 20,800 *g* for 10 min (4°C). The pellet was resuspended in 15% Percoll (in IB; pH 7.4) and was gently poured on the top a two-layered Percoll density gradient with 23% Percoll (in IB; pH 7.4) at the top and 40% Percoll (in IB; 7.4) at the bottom. The discontinuous Percoll density gradient was centrifuged at 30,200 *g* for 8 min (4°C). As a result, three distinct white bands were formed. The top one consists mainly of myelin, whereas the middle and bottom are enriched with synaptosomes (SYN) (contains synaptic mitochondria) and NS-mito, respectively. The fraction enriched with NS-mito was carefully aspirated and transferred into a new tube using a plastic Pasteur pipet. To eliminate all traces

of Percoll, the NS-mito fraction was first washed by centrifugation at 16,600 *g* for 8 min (4°C) in 9 ml IB. Depending on whether mitochondrial swelling assay or biochemical experiments were being performed, the pellet of NS-mito was resuspended in either IB with BSA (1 mg/ml) free from fatty acids (5 ml) or in IB without EGTA (5 ml), respectively. The NS-mito suspension was then washed a second time at 6800 *g* for 8 min (4°C). Finally, the pellet was suspended again with media appropriate to the assay being performed as detailed below (see section 2.5.4, 2.6.4 & 2.8).

2.4 Determination of protein concentration

Protein concentration was determined spectrophotometrically using the colorimetric bicinchoninic acid (BCA) protein assay kit (Pierce, #23225, UK). A mixture of reagents A and B (1:1, v/v) of the BCA kit (200 µl) was added protein lysates (10 µl), then incubated for 25 min at 37°C. Optical density (OD) were measured (at 540 nm) using the E_{MAX} plate reader (Molecular Devices, USA). Concentrations of BSA ranging from 0 to 2 mg/ml (in DDW) were used as protein standard.

2.5 Oxygen consumption assay

2.5.1 Principle

Assessment of oxygen consumption in mitochondria dates back over six decades (Clark et al., 1953; Kreuzer, 1957; Sproule et al., 1957), and it remains the preferred method used to investigate OXPHOS. In the presence of reducing agents such as nicotinamide-adenine dinucleotide (NADH, H^+) or flavin-adenine dinucleotide ($FADH_2$), mitochondria increase their capacity of oxygen uptake as a result of complex IV activity. Furthermore, mitochondrial oxygen consumption increases further during adenosine triphosphate (ATP^{4-}) synthesis. In the

presence of adenosine diphosphate (ADP^{3-}), H^+ that are pumped by complexes I, III and IV into the intermembrane space during oxidation of reducing agents will influx through the ATP^{4-} synthase to drive ATP^{4-} synthesis (Fig. 2-3).

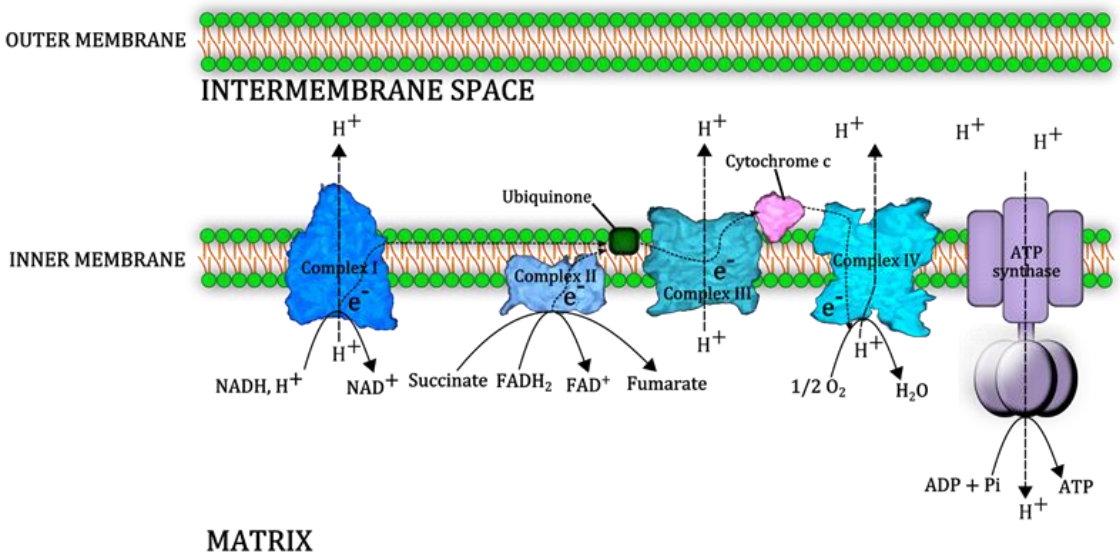

Figure 2-3. Schematic presentation of oxidative phosphorylation involving the respiratory chain and the ATP^{4-} synthase. The respiratory chain consists of four complexes, ubiquinone and cytochrome C (cyt C). Complex I and complex II respectively capture two electrons (e^-) from reduced nicotinamide adenine dinucleotide (NADH, H^+) and reduced flavin adenine dinucleotide ($FADH_2$). Complex III receive e^- from complex I and complex II via ubiquinone. Cyt C captures the e^- from complex III and transfer it to complex IV were it is finally used to reduce oxygen. Furthermore, complex I, III and IV release protons (H^+) in the intermembrane space membrane during passage of e^-. H^+ gradient through the ATP^{4-} synthase powers the multimeric enzyme to catalyse ATP^{4-} in the presence of Pi^{3-} and ADP^{3-}.

2.5.2 EQUIPMENT

The oxygen consumption assay was performed using the MT200 respirometer, which contains a respirometer cell, a 1302 electrode with a polypropylene membrane, an oxygen meter (Model 782) connected to monitoring software (Strathkelvin oxygen system software 782, version 4.1). The respiration chamber was heated with warm water (37°C) supplied with a mechanical pump. The volume of the respiration chamber was adjusted with a plunger to 110 µl and the substrates and drugs were delivered in the respiration chamber using a 1 µl Hamilton syringe. During the experiments mitochondrial suspensions were stirred with stainless-steel spin bars.

2.5.3 REAGENT, SUBSTRATES AND DRUGS

2.5.3.1 REAGENT

The assay was performed in a respiration buffer (RB) containing in mM: 125 KCl, 20 HEPES, 5 K_2HPO_4, 1 EGTA and BSA free fatty acid (0.1%, w/v) diluted in 1 l DDW, with pH titrated to 7.2 with KOH.

2.5.3.2 SUBSTRATES AND DRUGS

Both substrates and drugs were delivered in the respiration chamber at a volume of 1 µl. Drug stocks were stored at -20°C and were defrosted 30 min prior to when the experiment is conducted.

- A solution of Na_2SO_3 diluted in DDW (60 mM)
- Na_2-succinate: a stock of 550 mM (diluted in RB) was titrated with KOH to pH 7.2.
- Two stocks of potassium ADP^{3-} (9 mM and 30 mM) were diluted in DDW and the pH adjusted to 7.2.
- The stock of the vehicle (Veh) contains 2.3% DMSO diluted in RB.

- A stock of 345 µM of S18 randomer (S18) was diluted in the stock solution of the Veh.
- Cannabidivarin (CBDV) and Cannabidiol (CBD) were solubilised in 100% dimethyl sulfoxide (DMSO) (35.1 mM), then a second stock was prepared by diluting the first stock (with DMSO) in RB to make up a concentration of 1.14 mM.
- Oligomycin A (Om) was solubilised in 100% DMSO (25.1 mM) then was sequentially diluted in RB to make up 1.14 mM stock solution.

2.5.4 PROTOCOL

Following isolation, NS-Mito were suspended in ice-cold RB (approximately 1.4 mg protein/ml). Immediately before loading in the sample chamber, NS-Mito were diluted to a final concentration of 0.35 mg protein/ml in pre-warmed RB (37°C). After each experiment, the chamber was washed twice with 100% ethanol and 8 times with DDW.

NS-Mito were allowed to recover in the chamber for at least 2 min to allow the resting respiratory rate to stabilise prior to experimentation. As depicted in Fig. 2-4, 5 mM Na_2-succinate (SUC) was added 1 min after the beginning of the recording, followed by addition of drugs such as CBD (10 µM), CBDV (10 µM), S18 (3 µM) or Veh1 (with 0.03% DMSO, final concentration). Finally, ADP^{3-} (80 µM) or ADP^{3-} (268 µM) and Om (10 µM) were added to achieve state 3 and state 4, respectively.

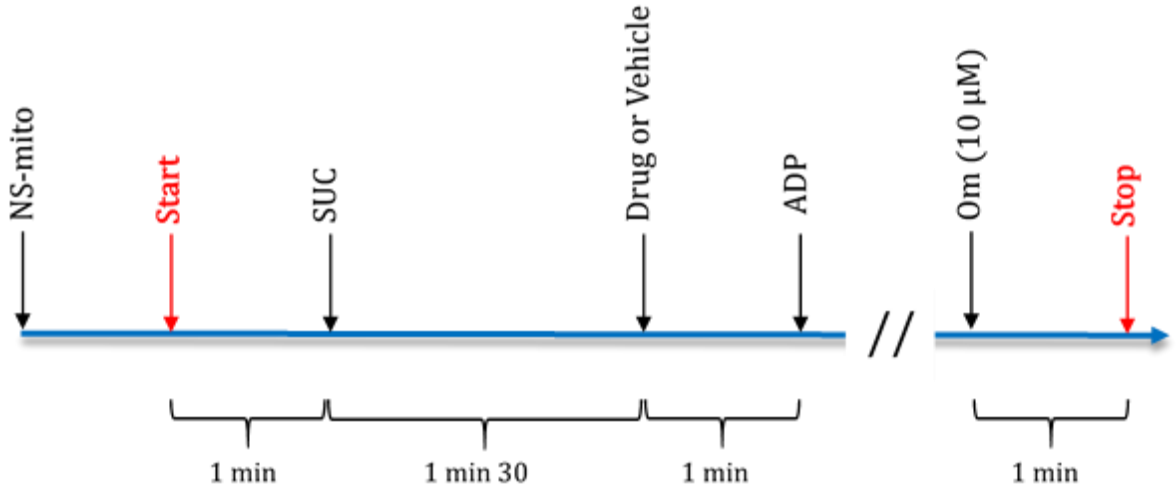

Figure 2-4. Experimental design aiming to assess the effect of S18 randomer (S18, 3 µM), cannabidiol (CBD, 10 µM) and cannabidivarin (CBDV, 10 µM) on oxidative phosphorylation of non-synaptic mitochondria from hippocampi (NS-mito) of healthy and epileptic rats. NS-mito were energised with 5 mM succinate (SUC). Prior to induction of state 3 respiration with ADP^{3-} (80 or 268 µM), drugs listed above were added and their individual effect was compared to vehicle 1 (Veh1) which consist of 0.03% DMSO. State 4 respiration was achieved with addition of oligomycin A (Om, 10 µM).

2.5.5 PARAMETERS OXPHOS IN RESPIROMETRY

The respirometry method allows the identification of compounds acting upon RC complexes, transport of ions (e.g. Ca^{2+}, HPO_4^{3-}, $citrate^{3-}$ or ADP^{3-}) and ATP^{4-} synthesis. Classical parameters determined by this technique are:

- Resting respiratory state: respiratory rate (nmol/min/mg protein) with no addition of substrates or drugs.
- State 3: ADP^{3-}-stimulated respiratory rate (nmol/min/mg protein) achieved with addition limited amount of ADP^{3-} (80 or 267 µM) to SUC-stimulated mitochondria.
- State 4: respiratory rate (nmol/min/mg protein) achieved with addition of Om (10 µM), an ATP^{4-} synthase inhibitor, to SUC-stimulated mitochondria.
- RCR: or State 3/State 4 ratio. This is used to determine the tightness of coupling between RC and ATP^{4-} synthase.
- P:O ratio: number of moles of ADP^{3-} metabolised into ATP^{4-} for each atom of oxygen consumed.
- Duration (or length) of state 3 respiration: time required for all molecules of ADP^{3-} to be metabolised into ATP^{4-}.

2.5.6 DATA ACQUISITION AND ANALYSIS

2.5.6.1 DATA ACQUISITION

Data was acquired using a Strathkelvin Instruments oxygen meter 782 that was controlled with the Strathkelvin oxygen system software 782 (version 4.1) configured to closed-cell respirometry mode, as this configuration is user friendly and allows calculation of respiratory rates normalised to the quantity of mitochondrial protein. Oxygen was detected

using a 1302 electrode securely sealed in a 1 M KCl-filled polypropylene pre-membraned jacket which is only permeable to gas (Fig. 2-5).

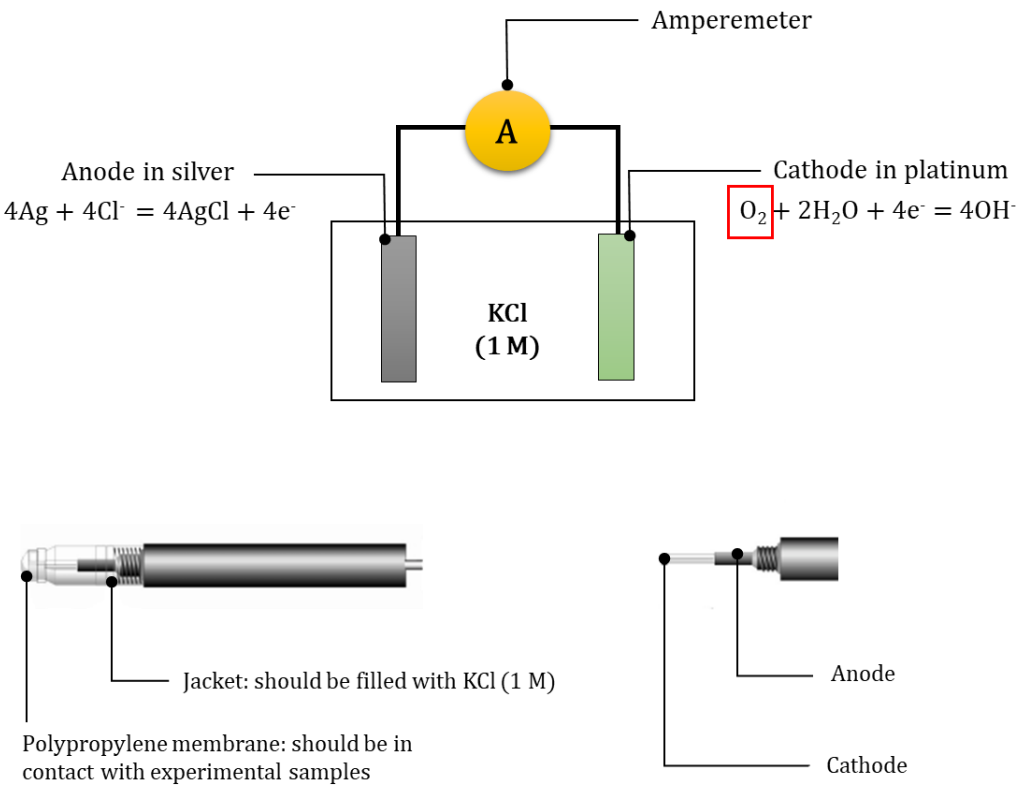

Note:

- KCl is essential to ensure a closed circuit, thus allowing electrons to move from the anode to the cathode, thus generating current.
- Scavenging oxygen (O_2) prevents the system from generating current

Figure 2-5. Chart showing principle and structure of 1302 oxygen electrode.

2.5.6.2 CALIBRATION OF THE ELECTRODE

Like the Clark electrode, the 1302 electrode generates current in the presence of oxygen. The sample chamber (110 µl) was calibrated for minimal oxygen level (0 µM) using Na_2SO_3 (60 mM). To eliminate all traces of Na_2SO_3, the chamber was rinsed 5 times with DDW. Finally, the maximal concentration of oxygen in the RB was calibrated to 222.5 µM using RB (37°C) perfused with air for 20 min.

2.5.6.3 DATA ANALYSIS

Parameters of OXPHOS such as SUC-induced respiration (achieved with addition of SUC), state 3 respiration (addition of ADP^{3-}), state 4 respiration (addition of Om), P:O ratio (number of moles of ADP^{3-} metabolised per number of moles of oxygen consumed) and RCR (state 3/state 4), were determined using the Strathkelvin oxygen system software (version 4.1).

2.6 MITOCHONDRIAL SWELLING ASSAY

2.6.1 PRINCIPLE

The change in absorbance in a mitochondrial suspension at 510 nm correlates with change in mitochondrial size (swelling or contraction) and this spectrophotometric method has extensively been used to monitor mitochondrial swelling. Dramatic changes in mitochondrial volume can be determined by measuring absorbance, whereas small changes of mitochondrial volume are determined by measuring angular light scattering (Gotterer et al., 1961). Given that angular light scattering measurements requires expensive and complex equipment, many laboratories still use the absorption method as the sensitivity of the angular scattering method is often unnecessary. Mitochondrial swelling occurs as a result of mitochondrial permeability transition (mPT). Compounds which inhibit mPT also prevent

mitochondrial swelling (Hunter et al., 1976). Therefore, methods used to assess mitochondrial swelling are understood as indirect measurements of mPT induction. MPT is induced by the opening of an inner membrane mega channel, referred to as the mitochondrial permeability transition pore (mPTP) (Wong et al., 2012) (Szabó et al., 1992).

2.6.2 Reagents

The swelling assay was performed in a buffer (SB) containing in mM: 200 sucrose, 1 K_2HPO_4, 0.02 EGTA, 20 HEPES, 5 SUC, 0.002 rotenone, with pH titrated to 7.4 using KOH.

2.6.3 Drug treatment

- The stock of vehicle (Veh) consisted of DMSO (with 3.19% DMSO) diluted in SB. However, the vehicle was referred as vehicle 2 (Veh 2), when added to mitochondrial suspension as the final concentration of DMSO became 0.03%.
- The stock of cyclosporin A (CsA), a known inhibitor of mitochondrial transition pore (mPTP) was prepared in 100% DMSO (35.1 mM) then diluted in SB to make a working stock for mitochondrial swelling assay at 1.06 mM. The final concentration of CsA was 9.5 µM.
- CBD was prepared in 100% DMSO (35.1 mM), then diluted with SB to make a stock of 1.12 mM. The final concentration of CBD was 10 µM.
- S18 randomer (S18), a known blocker of VDAC, was initially diluted in Veh to make stocks concentrations of 0.333 mM or 2.22 mM. This is to achieve respectively, final concentrations of 3 µM and 20 µM of S18 in the assay.

2.6.4 PROTOCOL

Mitochondria were suspended (0.70 mg protein/ml) in an ice-cold SB. This suspension (100 µl/well) was transferred into a clear 96-well microplate and was left for 5 min to warm to room temperature prior to absorbance recording. Furthermore, warm 98 µl SB (35℃) and 2 µl of drug or Veh2 were added to the mitochondrial suspension. The swelling assay was performed at 30℃ using FLUOstar OPTIMA (BMG Labtech, UK) by monitoring decrease of absorbance (at 544 nm) induced by $CaCl_2$ (200 µM).

2.7 WESTERN BLOT

2.7.1 LYSATE PREPARATION

Western blot was used to assess the expression of voltage-dependent anion-selective channel 1 (VDAC1) and proteins involved in OXPHOS like NADH-ubiquinone oxidoreductase chain 4 (ND4), NADH-ubiquinone oxidoreductase core subunit S1 (NDUFS1) and Cytochrome c oxidase IV (COX-IV). To prepare tissue lysate, whole hippocampi were homogenised in IB-without EGTA (60 mg of tissue/ml) then lysis buffer (LB) (containing 30 mM HEPES, 10% Glycerol, 1% Triton-X-100, 150 mM NaCl and a tablet of protease inhibitors mixture (EGTA free SIGMA) (pH titrated to 7.4 with KOH) was added (1:1, v/v). Regarding NS-mito lysates, following preparation both were washed twice in IB without EGTA (10 ml each times) by centrifugation at 6,800 *g* for 8 min (4°C) to eliminate traces of EGTA. Subsequently, LB was added to the pellet of NS-mito devoid of EGTA. Proteins were solubilised by incubating the samples in LB for 1 h on ice while they were vigorously vortexed every 20 min, stored overnight at -20°C, then thawed on ice. Insoluble debris was removed by centrifugation at 14,000 *g* for 10 min (4°C). Sample supernatant was transferred into a new microfuge tube. Protein concentration was determined as described in section 2.4. Finally, SYN resulting from

cell fractionation (see section 2.3.2) were washed, lysed and freed from insoluble debris in the same manner as NS-mito.

2.7.2 SDS- POLYACRYLAMIDE GEL ELECTROPHORESIS GEL

Prior to loading sample into the gel, proteins were reduced and denatured in a loading buffer containing 2% sodium dodecyl sulphate (SDS), 10% glycerol, 0.01% bromophenol blue, 250 mM Tris-base 2.5% β-mercaptoethanol (beta-m) (pH 7.4). In addition, samples were warmed at 95°C for 3 min (or 70°C for 10 min) and were allowed to cool at room temperature. The amount of protein loaded in each well was 20 µg for NS-mito lysate, 30 µg for SYN lysate and 50 µg for tissue lysates.

2.7.3 PROTEINS ELECTROPHORESIS AND TRANSFER

Proteins were subsequently separated by electrophoresis (at 20mA constant current per gel) using either 12% or 15% SDS-polyacrylamide gel electrophoresis. Following electrophoresis, gels were incubated for 10-15 min in a transfer buffer (TB) containing 25 mM Tris-base, 192 mM Glycine, 0.3% SDS and 20% methanol. Polyvinylidene fluoride (PVDF-plus; Santa Cruz) membranes were activated in 100% methanol for 30 s, then incubated in TB for 10 min. Proteins in the gel were transferred to PVDF-plus membrane for either 4 h (at 250 mA, 4°C) or 1 h (at 1 A, with dry ice) using a wet transfer system apparatus (Biorad).

2.7.4 IMMUNOBLOTTING

After transfer membranes were washed three times (5 min, each time) with PBS containing 0.1% Tween^{20} (PBST), then incubated at RT for 1 h in a blocking buffer (BB) containing 5% BSA or Milk in PBST to prevent non-specific binding of antibodies. Subsequently, membranes were incubated overnight with primary antibodies VDAC1 (1:2000), NDUFS1 (1:2000), ND4 (1:500) or COX-IV (1:500) (More details are described in the

appendix). Excess primary antibody was removed by washing the membrane 6 times (5 min, each time) with PBST at RT. Subsequently, membranes were incubated with secondary anti-IgG antibodies raised in goat and conjugated with horseradish peroxidase (HRP) directed against either mouse, rabbit or goat (all diluted at 1:10,000) primary antibodies. Membrane were washed another 6 times (5 min, each time) to remove excess of secondary antibodies. Immunoreactive proteins were visualised using ImageQuant™ LAS 4000 (GE Healthcare Life Sciences, UK) to detect chemiluminescence release by HRP in the presence of peroxidase substrate for enhanced chemiluminescence (BioRad, UK).

2.7.5 Densitometry of protein quantification

Intensities of immunoreactions were determined by densitometry using ImageQuant™ TL software (GE Healthcare Life Sciences, UK). Each protein of interest was normalised to NDUFS1. The Fisher's exact test was used to determine whether the variance of NDUFS1 and that of COX-IV were equal. My results showed that NDUFS1 is a more reliable loading control than COX-IV, as signals resulting from NDUFS1 immunoreaction exhibited less variability than that of COX-IV (Table 2-2 & Fig. 2-6).

Types of lysate	NDUFS1 *vs* COX-IV (N = number of animals per group)	Equal variance? (Fisher's F-test)
Tissue	100 ± 14.4 *vs* 100 ± 56.4 (N = 13)	No
NS-mito	100 ± 8.9 *vs* 100 ± 43.7 (N = 14)	No
SYN	100 ± 34 *vs* 100 ± 88.9 (N = 8)	No

Table 2-2. COX-IV showed greater variability than NDUFS1 across different types of lysate. Intensities of immunoreaction of COX-IV and NDUFS1 were normalised to mean of COX-IV and NDUFS1, respectively. Fisher's F-test was used to assess equal variance between NDUFS1 and COX-IV ($P>0.05$). Results are presented as mean ± SD. **Abbreviation: NS-mito** – Non-synaptic mitochondria isolated from rat hippocampus.

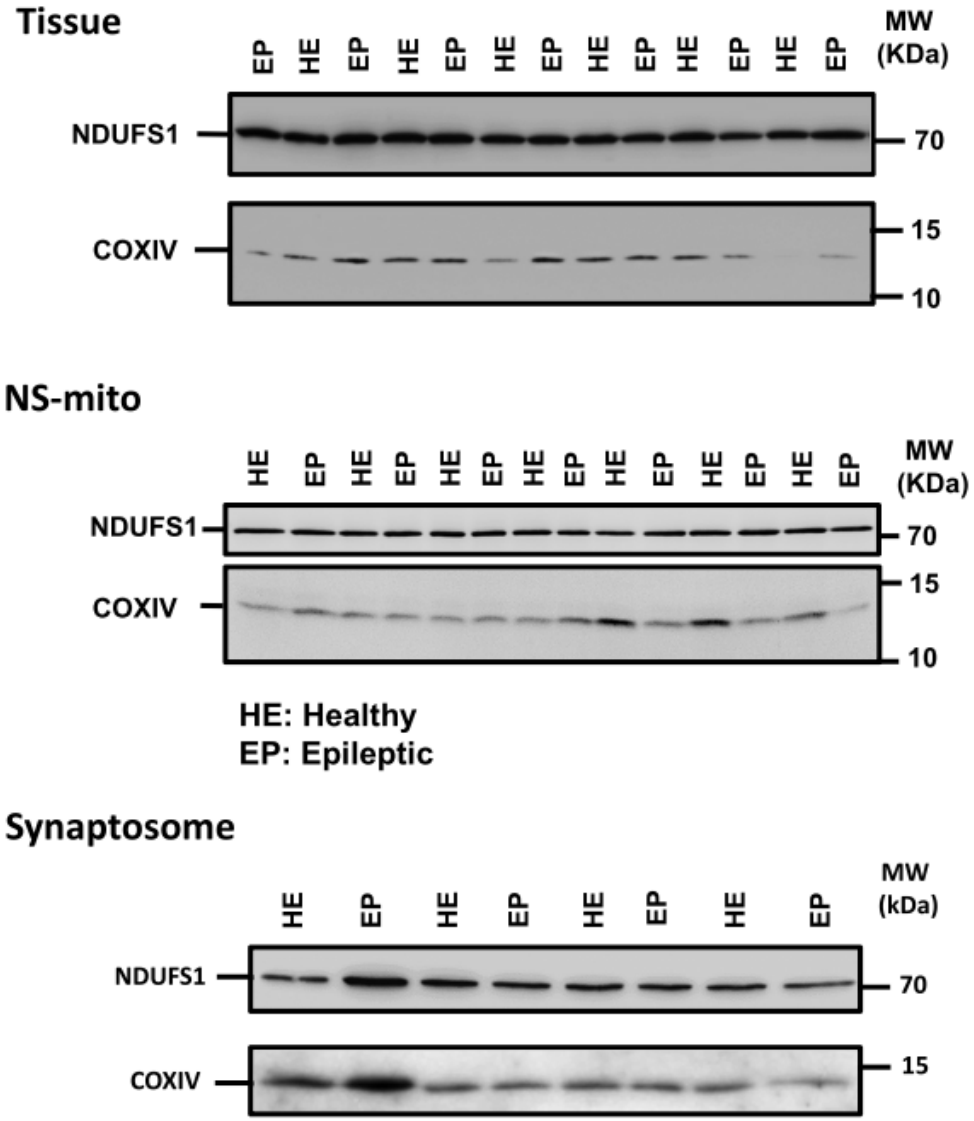

Figure 2-6. COX-IV showed greater variability than NDUFS1 across different types of lysate. Intensities of immunoreaction of COX-IV (14 kDa) and NDUFS1 (75 kDa) were normalised to mean of COX-IV and NDUFS1, respectively (as shown in Table 2-2). Fisher's F-test was used to assess equal variance between NDUFS1 and COX-IV ($P>0.05$). Densitometry results are presented in the appendix as mean ± SEM (Table 9-4). **Abbreviation: NS-mito** – Non-synaptic mitochondria isolated from rat hippocampus.

2.8 CYTOCHROME C RELEASE ASSAY

Western blot was used to determine cytochrome C (Cyt C) release from NS-mito from epileptic rats. Subsequently to mitochondrial isolation, NS-mito were resuspended in SB then treated for 10 min with Veh 2 (0.03% DMSO in SB), S18 (3 µM), CBD (10 µM) and CBDV (10 µM). $CaCl_2$ (200 µM) was added to treated mitochondrial suspension were incubated for another 10 min. The supernatant was separated from NS-$mito_{EP}$ by centrifugation (14,000 *g*, 10 min) at 4˚C. Collected supernatant (40 µl/well) were denatured and reduced at 95℃ for 3 min in SDS (2%) and β-mercaptoethanol (2.5%). Proteins were subsequently separated by electrophoresis in RB (at 20mA constant current per gel) using 15% SDS-PAGE. Proteins were transferred into a membrane and were probed for Cyt C detection (with mouse polyclonal anti-cyt C, 1:1000, Abcam) as described in section 2.7.

2.9 HUMAN EMBRYONIC KIDNEY CELLS: TRANSFECTION AND ELECTROPHYSIOLOGICAL RECORDINGS

2.9.1 CELL CULTURE

2.9.1.1 CELLS AND CULTURE CONDITIONS

Human embryonic kidney cells 293 possessing a flippase recognition target (FRT) and the gene of zeocin resistance (FLP-HEK293) were used in this study for transfection (Invitrogen, UK). Cell culture was performed at 37℃ under 0.5% CO_2 and 21% O_2 with relative humidity at 85-90%. Dulbecco's modified eagle medium without L-glutamine and containing high glucose (4.5 g/l) and 10% foetal bovine serum (DMEM-H) (Sigma, UK) was used for cell growth (Rajendra et al. 2012). This medium will be referred subsequently as DMEM-H. Depending on the cell type (antibiotics resistance) and the procedure performed with the

cells (e.g. transfection), zeocin or hygromycin B (both 100 µg/ml), were added to the medium as appropriate.

2.9.1.2 Cell culture following cryopreservation

Prior to transfection, cells (~ 3 X 10^6 cells in 1 ml) that have been stored in liquid nitrogen were immediately defrosted (to avoid formation ice crystals). To wash-out the 10% DMSO that was used for cryopreservation, these cells (in 1 ml medium) were resuspended in 9 ml DMEM-H with relevant antibiotic (100 µg/ml), then centrifuge at 100 *g* for 5 min at room temperature. The supernatant was discarded while the pellet of cells was resuspended in 10 ml DMEM-H with relevant antibiotic (100 µg/ml). These cells were subsequently transferred into a T75 flask and were allowed to grow under the conditions mentioned above (section 2.9.1.1). Every 2-3 days, the medium was renewed.

2.9.1.3 Culture passage

Once the cells have proliferated and reached ~ 90% confluency, the concentration of cells was diluted 5 times (~ 3 X 10^6 cells in 10 ml) for subsequent culture in a T75 flask. During this procedure, DMEM-H with relevant antibiotic was removed from confluent cells then PBS (without $CaCl_2$ and $MgCl_2$) was used to wash the cells. Adherent cells were trypsinised for 2 min at 37°C with 5 ml trypsin (0.25%). The activity of trypsin was arrested with 5 ml DMEM-H (with relevant antibiotic). Following centrifugation at 100 *g* for 5 min and at room temperature, the supernatant containing trypsin was discarded and the pellet resuspended with DMEM-H (with appropriate antibiotic).

2.9.2 Extraction of rat hippocampi RNA

2.9.2.1 Procedure

Total RNA was isolated from rat hippocampus using the miRNeasy Mini Kit (Qiagen, UK). Frozen hippocampi (~ 140 mg) were homogenised with a glass tissue grinder in QIAzol Lysis Reagent (700 µl). The resulting homogenate was transferred into a 1.5 ml microfuge tube and were left to incubate at room temperature for 5 min to allow the tissue to dissolve further in solution. To precipitate RNA, 140 µl chloroform was added to the mixture, and was vigorously vortexed for 15 s then left to incubate at room temperature for 3 min. To separate the aqueous phase from the organic phase, the mix was centrifuged at 12,000 *g* (4°C) for 15 min. The upper aqueous phase was transferred into a new collection tube and 100% ethanol (525 µl) was added and vortexed vigorously. The sample was then transferred into a RNeasy Mini column in a 2-ml tube and was centrifuged at 9000 *g* for 15 s (room temperature) to eliminate the flow-through. The column was washed with buffer RWT (700 µl), then rinsed twice with buffer RPE (500 µl) as recommended by the manufacturer. To elute the RNA, the column containing the RNA was transferred into a 1.5 ml microfuge tube and 75 µl of RNAase-free water was directly added into the RNeasy Mini column membrane then centrifuged at 9000 g for 1 min.

2.9.2.2 Determination of RNA concentration

The concentration of RNA extract and its purity was determined using a spectrophotometer (Nanodrop 2000/2000c, Thermofisher, UK). Absorbances of the samples were measured at 260 nm (to determine the concentration of nucleic acids), 280 nm (to detect protein) and 230 nm (to characterise phenol impurities). RNA samples were considered "pure" when the 260/280 ratio was greater than 1.8 and the 260/230 ratio was greater than 1.6.

2.9.3 Reverse transcription

Synthesis of complementary DNA (cDNA) from total RNA (150ng/µl) isolated from rat hippocampus was performed with a High-Capacity cDNA Reverse Transcription Kit (Applied Biosystems, UK). The reverse transcription (RT) reaction was performed at 37°C for 2 h in RT buffer also containing deoxynucleotides (2.5 mM) mix, MultiScribe® Reverse Transcriptase (2.5 U/µl), Oligo(dT) (25 ng/µl) and the reaction was diluted with diethyl pyrocarbonate treated distilled deionised water (DEPC-water) as recommended by the manufacturer.

2.9.4 Cloning of plasmids

2.9.4.1 Cloning of pcDNA5/FRT:rVDAC2

RT-polymerase chain reaction (PCR) was used to amplify the cDNA of rat VDAC2 (rVDAC2). Primer 1 and 3 were used to generate amplicons of rVDAC2 cDNA (Table 2-3), as both flank respectively, the upstream and downstream of its open reading frame (ORF). Resulting rVDAC2 cDNA fragments contained a restriction site for *BamHI* (GGATCC) and a Kozak sequence (CCACC) (to facilitate initiation of translation) at the 5' extremity of its ORF, while the 3' extremity of its ORF possessed a restriction site for *XhoI* (CTCGAG) (Table 2-3 and Fig. 2-7A). To potentiate activities of *BamHI* and *XhoI*, TATATA sequences were added to both upstream and downstream of the primers used to amplify the rVDAC2 PCR product. Digestion of both rVDAC2 and pcDNA5/FRT plasmid (300 ng) was performed separately with *BamHI* and *XhoI* in Cutsmart buffer (New England Biolabs, UK) containing BSA (0.1 mg/ml) at 37°C (overnight). To ensure the size of the digestion product, both DNA fragments (rVDAC2 and pcDNA5/FRT) were then separated using electrophoresis (80 V for 1 hour) in a 1% agarose gel buffered with TAE-buffer (Promega, UK) and stained with SYBR safe (2µl; Invitrogen, UK). Under blue light exposure, the fragments of interest were excised from the gel and transferred into a new tube. The DNA fragments were subsequently purified from the gel

using the QIAquick Gel Extraction Kit (Qiagen, UK). Finally, rVDAC2 (2 µl) was cloned into pcDNA5/FRT (0.5 µl) using the T4 ligase (New England, UK) at 14°C for 4 hours in a volume of 5 µl to generate pcDNA5/FRT:rVDAC2 (Fig. 2-7A).

2.9.4.2 Cloning of pcDNA/FRT/Igκ:HA-rVDAC2

To enable rVDAC2 detection in the possibility that anti-VDAC2 antibodies may not detect rVDAC2, a HA sequence was added at the upstream of the rVDAC2 (HA-rVDAC2) sequence using PCR and both primer 2 and 3. Furthermore, to allow plasma membrane expression of rVDAC2 once expressed in HEK293 cells, the HA-rVDAC2 DNA fragment was cloned into a plasmid construct which contains the secretory peptide signal of the light chain of immunoglobulin kappa (Igκ) (pcDNA5/FRT/Igκ) at the upstream of HA-rVDAC2 (Fig. 2-7B). PcDNA5/FRT/Igκ was generated from pcDNA3.1 (+) by Graeme Cottrell (Cottrell et al., 2004).

2.9.5 Polymerase chain reaction (PCR)

Amplification of rVDAC2 was generated from cDNA template (section 2.9.3) and was performed with primer 1 and primer 3 (Table 2-3). KOD high fidelity polymerase (Novagen, UK) was used instead of Taq DNA polymerase (Qiagen, UK) (which is more susceptible to introduce errors during cDNA amplification) or Q5 high fidelity DNA polymerase (New England, UK), since the latter did not amplify the sequence of interest. Regarding, reagents of the PCR, all is summarised below (Table 2-3). PCR conditions involved (1) activation of the polymerase (98°C, 5 min), (2) denaturation of the template (98°C, 30 s), (3) hybridisation of primers to the template (55°C, 30 s), (4) synthesis of a complementary sequence to the template also known as the extension step (72 C, 1 min). Steps (2) to (4) were repeated 25 times before a final 10 min extension step at 72°C. The PCR product was left to either cool at 10°C or on ice.

Table 2-3. Primers for rat VDAC2 cloning and colony PCR.		
Primer	**Position**	**Sequence**
Primer 1	Forward	5’-TATATAGGATCCACCATGGCTGAATGTTGTGTACCG-3’
Primer 2	Forward	5’-TACCCCTACGACGTGCCCGACTACGCCATGGCTGAATGTTGTGTACCG-3’
Primer 3	Reverse	5’-GCCTTGGAATTGGAGGCTTAACTCGAGTATATA-3’
Primer 4	Forward	5’-CGCAAATGGGCGGTAGGCGTG-3’

2.9.6 BACTERIAL TRANSFORMATION

Escherichia coli (*E. coli*) were rendered competent chemically (with a $CaCl_2$ (10 mM), KCl (150 mM), $MnCl_2$ (35 mM) and piperazine-1,2-bis[2-ethanesulfonic acid] (10 mM), pH adjusted at 6.7) (Inoue et al., 1990) and were stored in 50 µl aliquot at -80°C. Heat shock procedure was used to transform competent *E. coli* with the plasmids of interest. To perform this transformation, competent *E. coli* that were previously stored at -80°C were left to defrost on ice for 30 min. Subsequently, these bacteria were mixed with the plasmids (~ 50 ng) and were left to incubate for 30 min under ice-cold condition. Heat shock was performed by incubating the plasmid-bacteria mix at 42°C for 45 s. The mix was cooled for 5 min under ice-cold conditions before adding super optimal broth (SOB) medium (950 µl) supplemented with glucose (250 mM). The bacteria were allowed to proliferate in the medium for 1 h (at 37°C). Subsequently, these bacteria were transferred into a petri dish containing agar-SOB (1.5% agar diluted in SOB) treated with ampicillin (100 µg/ml) to select only transformed bacteria, as plasmids used in this study all express the ampicillin resistance gene. Colonies obtained after overnight growth (at 37°C) were tested for intact sequence (using PCR with primer 4 and primer 3 (table 2-3 & Fig. 2-7), restriction enzyme digest, or sequencing) or were used for small- and large-scale preparation of plasmid DNA.

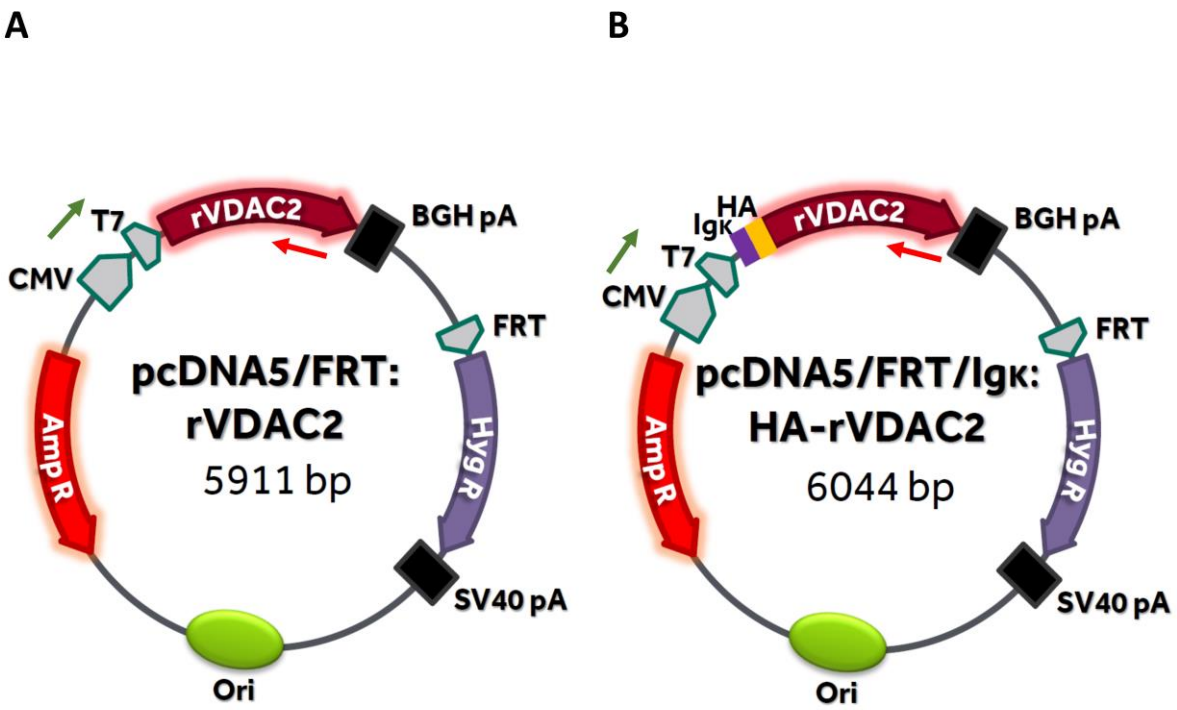

Figure 2-7. Cloning of rVDAC2 and HA-rVDAC2 in pcDNA5/FRT and pcDNA5/FRT/Igκ plasmid constructs. (A) Complementary DNA (cDNA) of rVDAC2 cloned in pcDNA5/FRT. The synthesis of fragment requires primer 1 and primer 3 (Table 2-3). (B) cDNA of HA-VDAC2 cloned in pcDNA5/FRT/Igκ. This fragment was synthesised using primer 2 and primer 3. The arrows indicate the binding sites of primers used in colony PCR. Green arrow, primer 4. Red arrow, primer 3.

2.9.7 Extraction of plasmid DNA from bacteria

2.9.7.1 Small-scale preparation of plasmid DNA

Isolation of plasmid DNA for quality control and storage purposes was performed with a miniprep kit of QIAgen (Qiagen, UK). Bacteria cultured overnight (section 2.9.6) were collected by centrifugation 3,500 *g* for 5 min (4°C). The pellet was suspended in ice-cold buffer P1 (250 µl) after discarding the supernatant. Lysis of bacteria was performed for less than 5 min with P2 (250 µl), which in turn was arrested with buffer N3 (350 µl). While the debris from lysate was removed by centrifugation at 17,000 *g* for 10 min, the supernatant was transferred into QIAprep 2.0 spin column, where the DNA was washed by successive flow though of buffer PB (500 µl) and buffer PE (750 µl) (both 17,000 *g*, 1 min). Finally, plasmid DNA was eluted (17,000 *g*, 1 min) with 50 µl DDW.

2.9.7.2 Large-scale preparation of plasmid DNA for FLP-HEK293 cells transformation

Extraction of highly purified plasmid DNA from bacteria was performed with an endoFree plasmid Maxikit (Qiagen, UK). First, E. coli bacteria were allowed to proliferate overnight (at 37°C) in 200 ml SOB medium supplemented with glucose (250 mM). The bacteria were then collected by centrifugation 3,500 *g* for 20 min (4°C). The supernatant was discarded, and the bacterial pellet was resuspended in buffer P1 (10 ml). P1 contained RNase and lyse blue reagent according to the manufacturer's recommendation. After bacterial lysis with buffer P2 (10 ml), chilled buffer P3 (10 ml) was added to neutralise the process. Resulting *E. coli* debris were then filtered of the lysate, as advised by the manufacturer. Plasmid DNA was purified from the filtered lysate by solid phase chromatography using QIAgen-tip 500 columns provided by the supplier. Following activation of the column with buffer QBT, the filtered lysate was flow through the column, thus allowing the plasmid to be trapped in the column. Impurities and solvents were washed out twice using buffer QC (30 ml/wash). Buffer

QN (15 ml) was used to elute the plasmid DNA into a 30-ml endotoxin-free tube. The plasmid DNA was precipitated in 40% isopropanol. The plasmid DNA was separated with the solvent by centrifugation at 4,800 *g* for 1 h 30 min (4°C). Subsequently to centrifugation, the supernatant was carefully removed and the plasmid DNA pellet was gently resuspended in 70% ethanol. Finally, ethanol was removed after centrifugation (at 4,800 *g* for 30 min at 4°C) and evaporation, then the pellet of DNA was dissolved in endotoxin-free buffer TE.

2.9.8 TRANSFECTION PROCEDURE

As previously mentioned (section 2.9.1.1), FLP-HEK293 cells contain the gene of resistance to zeocin and one integrated FRT site. In the presence of pcDNA5/FRT and pOG44 in FLP-HEK293 cells, pOG44, a plasmid expressing the FLP-recombinase catalysis the integration of pcDNA5/FRT into the genome of FLP-HEK293 through homologous recombination at the FRT site. The pcDNA5/FRT/Igκ:HA-rVDCA2 plasmid was transfected into FLP-HEK293 cells using lipofectamine® 2000 as transfecting reagent. First, using a 6-well plate, cells ($\sim$ 3 X 10^6 cells/well) were cultured overnight in a DMEM-H free from antibiotics. During the following day, the medium of the cells was renewed with 1.5 ml DMEM-H free from antibiotics. Lipofectamine® 2000 (8 µl/well) was then incubated for 20 min at room temperature with a mix of plasmids containing pcDNA5/FRT/Igκ:HA-rVDCA2 (0.3 µg/well) and pOG44 (2.7 µg/well; Invitrogen) which express a recombinase. The mix containing lipofectamine® 2000, pOG44 and pcDNA5/FRT/Igκ:HA-rVDCA2 was diluted in 250 µl/well Opti-MEM™ medium (Invitrogen) then added to the cell. After incubation of the cells with the transfection mix (48 hours at 37°C), the cells were detached in the absence of antibiotics with trypsin (according to the protocol mentioned in section 2.9.1.3). The cells were then pooled into a falcon tube (15 ml). To select cells expressing rVDAC2, the supernatant was discarded

following centrifugation (100 *g*, 5 min), then resuspended the cells in 10 ml of DMEM-H containing hygromycin B (100 µg/ml, Invitrogen). The cells were finally cultured at 37℃ in DMEM-H with hygromycin B (100 µg/ml) using a T75 flask while the medium was renewed every 2-3 days. Given that cells expressing Igκ:HA-rVDCA2 will also expressed the resistant gene for hygromycin B, non-transfected cells will be eliminated during this process. To characterise cells expressing Igκ:HA-rVDCA2 at the plasma membrane, a combination of three biochemical techniques were used (biotinylation assay to detect Igκ:HA-rVDCA2 in the plasma membrane protein, western blot to detect Igκ:HA-rVDCA2 in the cell lysate and immunocytochemistry to determine the localisation of Igκ:HA-rVDCA2 in the cell).

2.9.9 Biochemical characterisation of the HEK293 cells expressing Igκ:HA-rVDAC2

2.9.9.1 Biotinylation assay

HEK293 cells (~ 6 X 10^6 cells) were layered on poly-D-lysine treated petri dishes (with 12 cm diameter) and were incubated in DMEM-H containing hygromycin B overnight under sterile conditions at 37°C. After removing the cell medium, cells were rinse 3 times with ice-cold Dulbecco's PBS (with Ca^{2+} and Mg^{2+}). To allow only biotinylation of plasma membrane proteins, cells were incubated (at 4°C) for 1 h on a rocker with EZ™ Sulfo-NHS-SS-biotin (0.3 mg/ml; Invitrogen, UK) diluted in PBS (with Ca^{2+} and Mg^{2+}). Excess of biotin was subsequently removed by washing the cells 3 times with ice-cold PBS. Biotinylated cells were lysed with radioimmunoprecipitation assay (RIPA) (containing 50 mM Tris-HCl, 150 mM NaCl, 10 mM Na_4PO_2, 10 mM NaF, 0.1 mM $NaCO_4$, 1 mM EGTA, 0.5% NP40, 5 mM $MgCl_2$ and a cocktail of protease inhibitors, pH adjusted at 7.4). Pierce™ NeutrAvidin™ agarose (30 µl) was added to cell lysate then was left to mix overnight (at 4°C) on a rotating platform. Biotinylated proteins bound to neutravidin-agarose were collected by centrifugation at 12,000 *g* for 1 min. After the supernatant was removed, the pellet was washed 3 times in 1 ml RIPA buffer. To

dissociate plasma membrane proteins from neutravidin, the loading buffer was directly added (which contains beta-m and SDS) to the beads and the mix was subsequently boiled at 95°C for 5 min.

2.9.9.2 WESTERN BLOT

To detect the expression of Igκ:HA-rVDAC2 in plasma membrane or cell lysate, proteins were denatured and reduced in both preparations as described in section 2.7. For Igκ:HA-rVDAC2 detection, both anti-VDAC2 antibodies raised in either mouse or rabbit and an anti-HA antibody raised in mouse were used. The expression of Igκ:HA-rVDAC2 was normalised with that of β-actin (using anti-β-actin antibody; 1:1000) in whole cell lysate and with that of Na^+/K^+-ATPase (using anti-Na^+/K^+-ATPase antibody; 1:10,000) in plasma membrane protein. Under physiological conditions, β-actin is a housekeeping protein while Na^+/K^+-ATPase is a plasma membrane marker. Further details about these primary antibodies are listed in the appendix.

2.9.9.3 IMMUNOCYTOCHEMISTRY

For visualisation of Igκ:HA-VDAC2 on the stable transfected HEK293 cells, cells were plated (3 X 10^5 cells/well) on coverslips coated with poly-D-lysine in a 6-well plate and were left to incubate overnight at 37°C under sterile conditions. Following removal of cell media, these cells were rinsed 3 times with ice-cold Dulbecco's PBS (with Ca^{2+} and Mg^{2+}). Cells were then permeabilised for 20 min with 4% paraformaldehyde (in PBS). Permeabilisation was arrested by washing of PFA from cells 3 times (10 min each time) with chilled blocking buffer 2 (BB2) (1% normal horse serum and 0.1% saponin in PBS). Fixed and permeabilised cells were then incubated overnight at 4°C with either an anti-HA antibody or two other antibodies directed against VDAC 2 (see details in the appendix). All primary antibodies were diluted in

the BB2 (1:250). The day after, excess of primary antibodies was removed by washing cells 3 times (10 min each time) with BB2 and cells were incubated for 2 h with either mouse or rabbit anti-IgG antibodies raised in goat and conjugated with Alexa Fluor-488. Excess of secondary antibodies were washed out with BB2. Nuclei were stained with a Vectashield mounting medium for coverslip containing DAPI (Vectorlabs, UK).

2.9.10 Visualisation of immunofluorescently labeled cells

Subsequently to cell staining as described above (see section 2.9.9.3), a Nikon Eclipse Ti Laser-scanner confocal microscope was used to visualise and acquire pictures of fluorescently labeled proteins and nucleus. Images of cells were obtained with a 100 X/1.45 Oil DIC N2 objective. The setting of zoom adjustment was 2 units. Five focal planes were acquired from each cell at 0.5 µm interval. However, only a representative focal plane is presented in the result section (see chapter 5). Excitations of DAPI (on nuclei) and Alexa Fluor-488 (on immunofluorescently labeled protein) were performed with 405 nm (emission measured at 460 nm) and 488 nm (emission measured at 520 nm) laser lines, respectively. Images were initially processed with image J software to improve the signal-to-noise ratio by subtracting noise from the background. The same value of background noise was used consistently in all images. Finally, Adobe Photoshop software was used to create a photomontage comprising three images. The first image is a blue channel (with nuclei), the second is its corresponding green channel (with fluorescently labeled proteins) and the third is the merged image of both blue and green channels (see chapter 5).

2.9.11 SINGLE-CELL ELECTROPHYSIOLOGY

2.9.11.1 RECORDING CHAMBER

Intracellular patch clamp recordings were performed in both empty-vector-control-HEK293 (VC-HEK293) cells and Igκ:HA-VDAC2 expressing HEK293 cells. These cells were layered on poly-D-lysine treated coverslips (~ 60 000 cells/ml) and were allowed to proliferate overnight under sterile conditions at 37℃ in a 6-well plate filled with DMEM-H containing hygromycin B (100 µg/ml, 1.5 ml). Coverslips on which these cells are layered were then transferred into a recording chamber filled with extracellular solution containing (in mM): 135 NaCl, 10 HEPES, 2 $MgCl_2$, 10 Glucose and NaOH to titrate the pH at 7.4. All experiments were performed at room temperature.

2.9.11.2 RECORDING ELECTRODE

The patch electrode was formed by fitting a low resistance (3-8 MΩ) glass micropipette (filled with intracellular solution) to a Ag/AgCl electrode connected to the CV-7B head stage multi-clamp amplifier (Axon Instruments). The intracellular solution contains (in mM): 135 KCl, 1 EGTA, 2 $MgCl_2$, 10 HEPES and KOH to adjust the pH at 7.2. Using the model P-97 of Flaming/Brown micropipette puller (Sutter instrument Co., USA), these pipettes were made from borosilicate capillaries (30-0057, Harvard apparatus, USA) of 100 mm length, 1.5 mm outer diameter and 0.86 mm inner diameter.

2.9.11.3 PROTOCOL

The membrane potential of HEK293 cells was maintained at -60 mV in voltage-clamp mode. The effect of voltage-evoked currents was determined using either a voltage-steps protocol (-60 mV to +60 mV, with 5 mV increment lasting 500 ms, at 0.5 Hz) or a voltage-ramp

protocol (-70 mV to +80 mV lasting 500 ms, at 0.5 Hz). The capacitance of the cell was determined prior to each protocol.

2.9.11.4 Data acquisition and analysis

The data was acquired using pCLAMP software (version 10). During analysis of the data, the noise was removed from recorded traces with Clampfit software (version 10.4) using an 8-pole low-pass Butterworth filter (2.04 kHz) (Rostovtseva et al., 2002a). Each current output was normalised to the capacitance of the cell (current/capacitance).

2.10 Statistics

Results are expressed as mean ± SEM. N, represents number of animals. Outliers in the data were identified using a Cook distance method and were excluded from the study. Data were tested for normality using Lilliefors ($P<0.05$) and Shapiro-Wilk tests ($P<0.05$). Depending on the number of groups, comparisons amongst groups were performed with either student t-test ($P<0.05$), Mann-Whitney test ($P<0.05$; when a group fails the normality test and have unequal variance), Kruskal-Wallis ($P<0.05$; when all groups have unequal variance), one-way ANOVA ($P<0.05$) or two-way ANOVA ($P<0.05$). Upon significance with Kruskal-Wallis, one-way ANOVA or two-way ANOVA, pairwise comparisons were performed using either the Dunn's multiple comparisons test or the two-stage linear step-up procedure of Benjamini, Krieger and Yekutieli (BKY) (Benjamini et al., 2006). Statistical differences determined by the BKY are reported in the adjusted P-value called Q-value ($Q<0.05$).

CHAPTER 3 – EFFECT OF CANNABIDIOL ON OXIDATIVE PHOSPHORYLATION IN NON-SYNAPTIC MITOCHONDRIA ISOLATED FROM HEALTHY AND EPILEPTIC RAT HIPPOCAMPI

3 EFFECT OF CANNABIDIOL ON OXIDATIVE PHOSPHORYLATION IN NON-SYNAPTIC MITOCHONDRIA ISOLATED FROM HEALTHY AND EPILEPTIC RAT HIPPOCAMPI

3.1 INTRODUCTION

Epilepsy refers to a neurological disease characterized by manifestations of spontaneous recurrent seizures. Despite more than 160 years of anti-epileptic drug (AED) development (Brodie, 2010), 30-40% of patients with epilepsy remain refractory to drug treatment (Bialer and White, 2010; Löscher, 2011; Perucca et al., 2007; Picot et al., 2008). So far, AEDs have been designed to target directly actors of neurotransmission such as ion channels (e.g. carbamazepine targets sodium channels), receptors (e.g. benzodiazepines target aminobutyric acid ($GABA_A$ receptors) or enzymes involved in the metabolism of neurotransmitter (e.g. Vigabatrin inhibits GABA transaminase) (Brodie, 2010). In his review published in 2011, Löscher argues that AEDs with better efficacy (given the persistent proportion of pharmacoresistant patients) has not yet been discovered because of the lack of appropriate use of models of seizures or model of epilepsy in AEDs discovery (Löscher, 2011). Models of seizures (e.g. pentylenetetrazol mice model) are largely used for AEDs discovery although they do not undergo molecular and cellular changes which occur in the pathophysiology of epilepsy (Löscher, 2011). Therefore, to develop new AEDs with improved efficacy, it would be appropriate to use models of epilepsy (e.g. *status epilepticus*-induced model of temporal lobe epilepsy).

Cannabidiol (CBD) is a non-psychoactive cannabinoid which exerts anti-convulsant/anti-epileptic effects in a variety of preclinical models (Consroe et al., 1982; Jones et al., 2010, 2012; Karler et al., 1973) as well as in different clinical studies, particularly in patients with

difficult-to-treat epilepsy (Carlini and Cunha, 1981; GW Pharma, 2015). While there are many targets of CBD, the mechanisms which underly its therapeutic effect in epilepsy remain poorly understood (Ibeas Bih et al., 2015). In recent years, it has been demonstrated that CBD acts on oxidative phosphorylation (OXPHOS) (Fišar et al., 2014; Valvassori et al., 2013). For example, acute (a single bolus) and repeated (once per day, for 14 days) *in vivo* administration of CBD (60 mg/kg, i.p.) increased the activity of the respiratory chain (RC) in rat brain (Valvassori et al., 2013). In the hippocampus in particular, the activities of complex II, II/III and IV were increased following a single dose of CBD (60 mg/kg, i.p.), while the activity of complexes I and II was only elevated after repeated CBD treatment (60 mg/kg, i.p., once per day, for 14 days) (Valvassori et al., 2013). In contrast, Fišar et al. who investigated the direct effect of CBD on the complexes of the RC of mitochondria isolated from pig brain (*in vitro*), showed that CBD inhibits the activities of complex I (IC_{50} = 8.2 μM), II (IC_{50} = 19.2 μM), and IV (IC_{50} = 18.8 μM), while it does not exert any direct effect on complex II/III (Fišar et al., 2014). Furthermore, complex I is fully inhibited with approximately 40 μM of CBD treatment (Fišar et al., 2014). Conversely, complex II is completely inhibited only at high concentration of CBD (100 μM), while complex IV still retains 75% of its activity when treated with high concentration of CBD (100 μM) (Fišar et al., 2014). Taken together, it is plausible that *in vivo* administration of CBD may indirectly act though signalling pathways which upregulate genes involved in the synthesis of complexes of RC, while its direct effect on RC may be inhibitory. Although the direct effect of CBD on mitochondrial complexes was demonstrated to be inhibitory, it remains unclear whether these actions are physiologically relevant because Deiana et al. demonstrated (using a dose of 120 mg/kg (i.p.)) that CBD could not exceed a concentration ranging between 22-27 μM (determined from the C_{max} of rats and mice) in rat brain (Deiana et al., 2012). Given that the dose at which CBD exerts its anti-convulsant effect

is 100 mg/kg (i.p.) across rodent model of seizures and epilepsy (Jones et al., 2010, 2012; Kaplan et al., 2017), it could be argued that the therapeutic concentration of CBD in the brain may not exceed 22 μM. Therefore, I will assume that the concentration of CBD with physiological relevance is lower than 22 μM. As the potency of CBD on complex II and IV is low (Fišar et al., 2014), it seems unlikely that the inhibition of these complexes by CBD would occur *in vivo*. In contrast, it is plausible that CBD may exert its inhibitory effect on complex I *in vivo* at concentrations that are physiologically relevant due its low IC_{50} (Fišar et al., 2014). It is unlikely that the reduction of the activity of complex I induced by a direct action of CBD could account for its therapeutic effect since the activity of complex I is already deficient during seizures and epilepsy (Folbergrová et al., 2010; Kang et al., 2007; Kunz et al., 2000).

As CBD's direct effect on RC complexes does not explain its anti-epileptic effect, I hypothesise that the mechanisms underlying its anti-epileptic effect are dependent on a different mitochondrial target. The work of Rimmerman et al. published in 2013, demonstrated that CBD binds (using a thermophoretic method) and inhibits (with 20 μM CBD) an isoform of VDAC (VDAC1) (Rimmerman et al., 2013). VDAC is expressed in the outer-membrane of mitochondria (Colombini et al., 1996). Despite this, there is still no evidence demonstrating that CBD exhibits a direct functional effect upon OXPHOS through mitochondrial VDAC. In this study, will investigate whether CBD modulates OXPHOS in non-synaptic hippocampal mitochondria (NS-mito) through VDAC. CBD's effect on OXPHOS will be compared with that of S18 randomer (S18), a recently developed inhibitor of VDACs belonging to the family of phosphorothioate oligonucleotides (POL) (Tan et al., 2007b, 2007a). Previously, it has been shown that blockade of mitochondrial VDAC using G3139 (another type of POL) alters OXPHOS in liver mitochondria (Tan et al., 2007a). Therefore, I am expecting

S18 to alter OXPHOS in non-synaptic mitochondria from rat hippocampus (NS-mito). Furthermore, I will investigate whether the mechanisms underlying the anti-convulsant effect of cannabidivarin (CBDV) are mediated by similar mechanisms to CBD (Hill et al., 2012), since CBDV is structurally identical to CBD with the exception of its shorter lateral aliphatic chain (Fig. 1-6).

To assess the effect of CBD (10 µM), CBDV (10 µM) and S18 on OXPHOS in NS-mito from healthy (NS-mito$_{HE}$) and epileptic (NS-mito$_{EP}$) rats, I will be using a respirometry assay that was developed and optimised to measure oxygen consumption in isolated mitochondria.

3.2 RESULTS

3.2.1 CHARACTERISATION AND OPTIMISATION OF NS-MITO PREPARATION FOR RESPIROMETRY

3.2.1.1 FROZEN TISSUE MITOCHONDRIA AND FRESH HIPPOCAMPAL MITOCHONDRIA

Initially, I investigated whether NS-mito isolated from frozen rat hippocampi could be used in this study because it would prevent inconsistency related to the age of the animals at which hippocampi were harvested. Following brain dissection, hippocampi were immersed in isolation buffer (IB) containing EDTA or EGTA and were rapidly frozen in liquid nitrogen. For long term storage, the samples were kept at -80°C. Nevertheless, isolation of optimal functioning NS-mito from these tissues prove to be challenging as they exhibited uncoupled OXPHOS. While energised with succinate (SUC; 5 mM), addition of either ADP^{3-} (268 µM) or carbonyl cyanide m-chlorophenyl hydrazone (CCCP; 0.5 µM) failed to increase oxygen consumption in these mitochondria (Fig. 3-1A & 3-1B). Accordingly, subsequent experiments were performed on NS-mito harvested from healthy rats immediately after their termination. Addition of ADP^{3-} (80 or 533 µM) increased the respiratory rate from SUC-induced respiration

in NS-mito from rats immediately after death (Fig. 3-2A & 3-2B). Similarly, CCCP (0.5 μM) increased respiration under SUC-stimulated respiration (Fig. 3-2C).

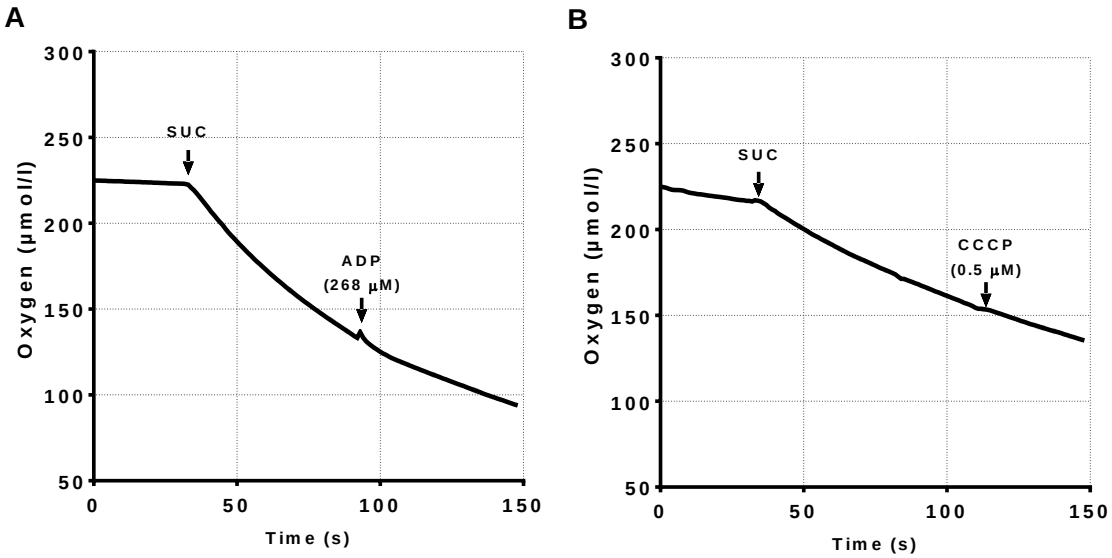

Figure 3-1. Traces showing no effect of ADP^{3-} (268 µM) and CCCP (0.5 µM) in NS-mito from frozen hippocampi of heathy rats. Oxygen consumption assay was performed on NS-mito suspended in respiration buffer containing KCl (135 mM), $MgCl_2$ (2 mM), K_2HPO_4 (5mM), HEPES (20 mM) and BSA free fatty acid (0.1%, w/v) with pH at 7.2, titrated with KOH. (A) No effect of ADP^{3-} (268 µM) on NS-mito (400 µg/ml protein) from frozen hippocampi following succinate-induced respiration. (B) No effect of CCCP (0.5 µM) on NS-mito (250 µg/ml protein) from frozen hippocampi following succinate-induced respiration.

3.2.1.2 JUSTIFICATION OF THE USE OF Ca^{2+} CHELATOR TO ISOLATE MITOCHONDRIA: EFFECT OF RESPIRATION BUFFER CONTAINING $MgCl_2$ OR EGTA ON OXPHOS OF NS-MITO

Isolation of mitochondria requires mechanical processes (homogenisation of the tissue) which causes the plasma membrane of cells to rupture. As a result, Ca^{2+} from the extracellular compartment diffuses freely by means of concentration gradient into the cytosol (Chapp et al., 2018; Liao and Lien, 2009). This increase of cytosolic Ca^{2+} can lead to overload of Ca^{2+} in mitochondria, which will inevitably cause uncoupling of their OXPHOS (Pandya et al., 2013). To prevent such phenomenon from occurring, chelating agents of Ca^{2+} such as EDTA or EGTA are generally added to IB. In this study, I included EGTA (1 mM) instead of EDTA in the IB, because EGTA exhibits greater selectivity for Ca^{2+} than EDTA, while the latter also binds Mg^{2+} with high affinity.

Whilst ADP^{3-} could stimulate state 3 respiration in NS-mito isolated from fresh hippocampi, it was apparent that this response was abnormally delayed by approximately 33 s with different concentrations of ADP^{3-} (Fig. 3-2A & 3-2B). In other to avoid this delay, I subsequently changed the composition of the respiration buffer (RB) in which NS-Mito were suspended during the respirometry assay. Thus, the oxygen consumption assay was performed in RB in the absence or presence of the Ca^{2+} chelator EGTA. RB without EGTA contained either $MgCl_2$ (2 mM) or was free from $MgCl_2$. The delay of mitochondrial response to ADP^{3-} was only observed using buffer containing less than 2 mM $MgCl_2$ (Fig. 3-3A). However, in the absence of $MgCl_2$, mitochondria were uncoupled, as ADP^{3-} did not significantly increase respiration under succinate-induced respiration (Fig. 3-3B). I demonstrated that only in the presence of EGTA (1 mM) that the delay in response to ADP^{3-} application was non-existent (Fig. 3-3C & 3-3D).

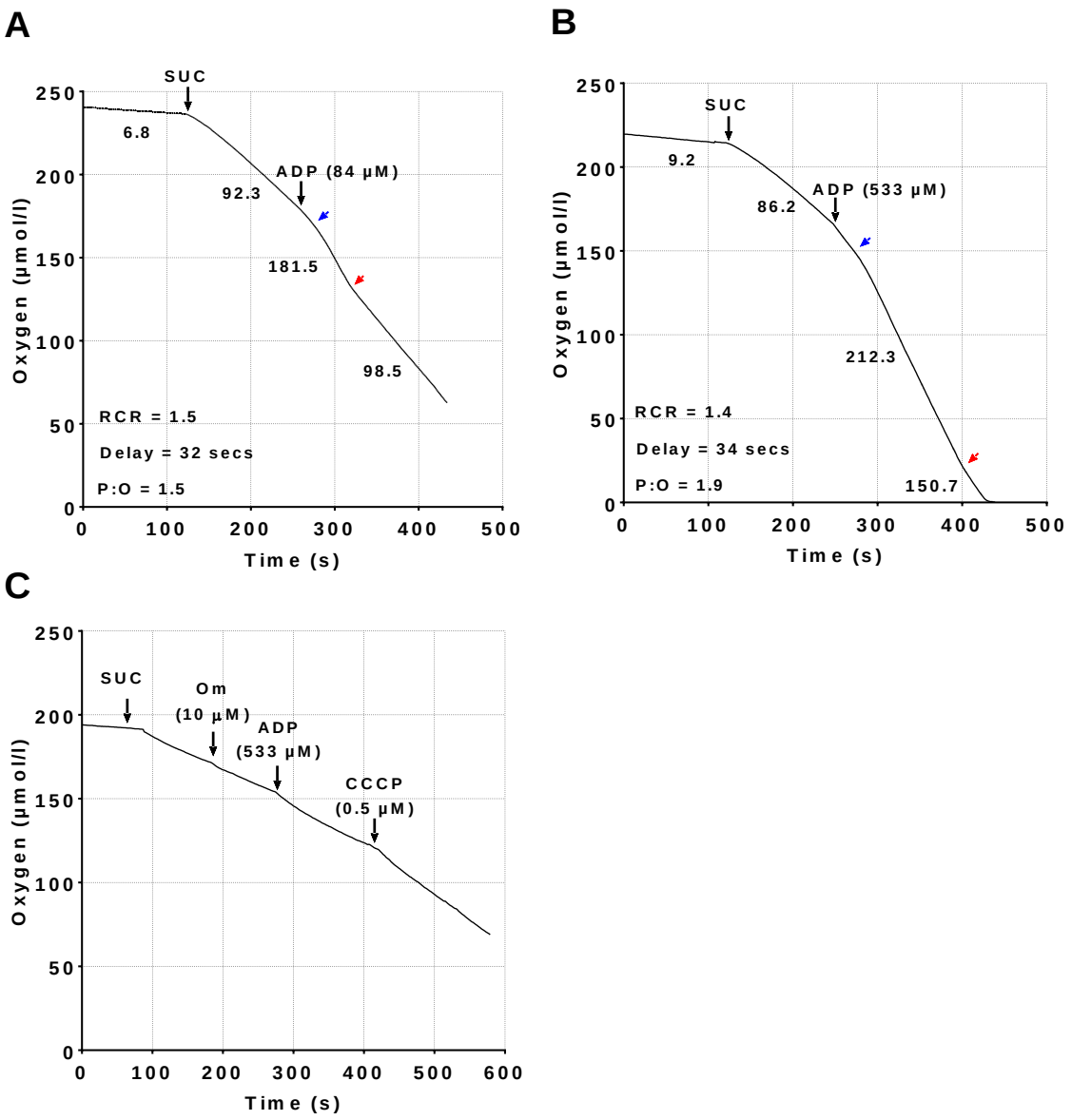

Figure 3-2. Traces showing increase of respiration as ADP^{3-} (80 or 533 µM) or CCCP (0.5 µM) is added on NS-mito isolated immediately after termination of the rat. Oxygen consumption assay performed on NS-mito (350 µg/ml protein) suspended in respiration buffer containing KCl (135 mM), $MgCl_2$ (2 mM), K_2HPO_4 (5mM), HEPES (20 mM) and BSA free fatty acid (0.1%, w/v) with pH at 7.2, titrated with KOH. Addition of ADP^{3-} at (A) low (80 µM), (B) high (268 µM) concentration or (C) CCCP (0.5 µM) following succinate-induced respiration (SUC: 5 mM). The blue arrow indicates the beginning of state 3 respiration while the red arrow indicates the point at which state 3 respiration changes into state 4 respiration.

3.2.2 OPTIMISATION OF THE RESPIRATORY CONTROL RATIO

The respiratory control ratio (RCR) is a parameter used to determine the tightness of the coupling of OXPHOS. For instance, drugs (e.g. CCCP) that causes particularly strong uncoupling of OXPHOS will increase state 4 respiration (see section 2.5.5 for definition) and reduce the RCR. Alternatively, drugs that induces mild uncoupling of OXPHOS may increase state 4 respiration but may not alter the RCR as state 3 respiration (see section 2.5.5 for definition), as the latter can be relatively variable. Various laboratories studying mitochondria isolated from brain tissue have reported different values of the RCR (Table 3-1). In this study, as respiration was induced with SUC, optimal RCR of NS-mito isolated from healthy rats (NS-mito$_{HE}$) ranged between 2.4 and 3.7. Importantly, maximal RCR was achieved with addition of oligomycin A (Om; 10 µM) following SUC-induced respiration to inhibit the ATP^{4-} synthase in NS-mito (Fig. 3-4A & 3-4B).

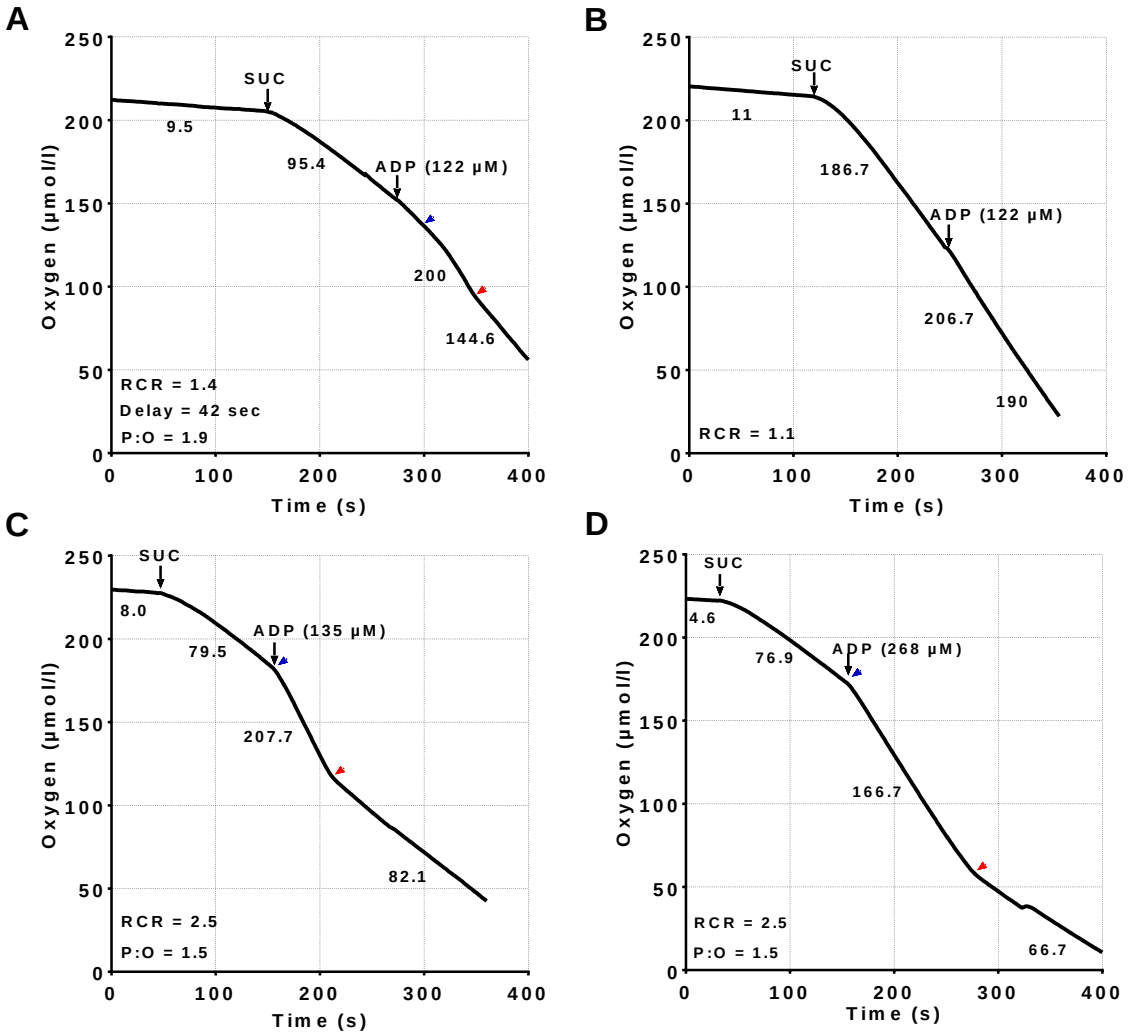

Figure 3-3. Traces showing suppression of delayed induction of state 3 respiration with EGTA (1mM) in NS-mito from healthy rats. (A) Oxygen consumption assay was performed on NS-mito (350 µg/ml protein) from healthy rats suspended in respiration buffer containing KCl (135 mM), $MgCl_2$ (2 mM), K_2HPO_4 (5mM), HEPES (20 mM) and BSA free fatty acid (0.1%, w/v) with pH at 7.2, titrated with KOH. (B) Oxygen consumption assay was performed on NS-mito (350 µg/ml protein) from healthy rats suspended in respiration buffer was free from $MgCl_2$. (C-D) Oxygen consumption assay was performed on NS-mito (350 µg/ml protein) suspended in respiration buffer containing EGTA (1 mM) instead of $MgCl_2$. Addition of ADP^{3-} was subsequent to succinate-induced respiration (SUC: 5 mM). The blue arrow shows the beginning of state 3 respiration while the red arrow indicates the point at which state 3 respiration changes into state 4 respiration. (B) Note the absence of arrows when NS-mito respiration is measured in a respiration buffer free from $MgCl_2$.

Table 3-1. Examples of RCR from brain mitochondria in the literature.						
Tissue	**Animal**	**Anaesthetic**	**O-Substrate**	**RCR**	**P:O**	**Reference**
Forebrain	Wistar 12 weeks rats	No	GM	23.6	-	(Batandier et al., 2014)
			S	6.7	-	
Cortical tissue	Fischer 344 rats	Isoflurane + CO_2 until flaccid	PM	6.5	-	(Gilmer et al., 2010)
Neocortex	129/Sv × C57BL/6J mice	No	S	1.8	-	(Lobão-Soares et al., 2005)
Entorhinal cortex	129/Sv × C57BL/6J mice	No	S	1.7	-	
Hippocampus	129/Sv × C57BL/6J mice	No	S	1.6	-	
Cerebellum	129/Sv × C57BL/6J mice	No	S	2	-	
Forebrain	Wistar 30-day-old rats	No	GM	23	2.8	(Tonin et al., 2010)
Forebrain	Wistar 30-days-old rats	No	S	5.2	1.7	
Cortex	Wistar rats (>270 g)	No	G	2	-	(Benani et al., 2009)
Hypothalamus	Wistar rats (>270 g)	No	G	2	-	
Olfactory bulb	Wistar rats (>270 g)	No	G	4	-	
Half brain	7-day-old Sprague Dawley rats	Halothane	GM	4.1	-	(Rajapakse et al., 2001)
Abbreviations: S: succinate; G: glutamate; PM: pyruvate + malate; GM: Glutamate + malate						

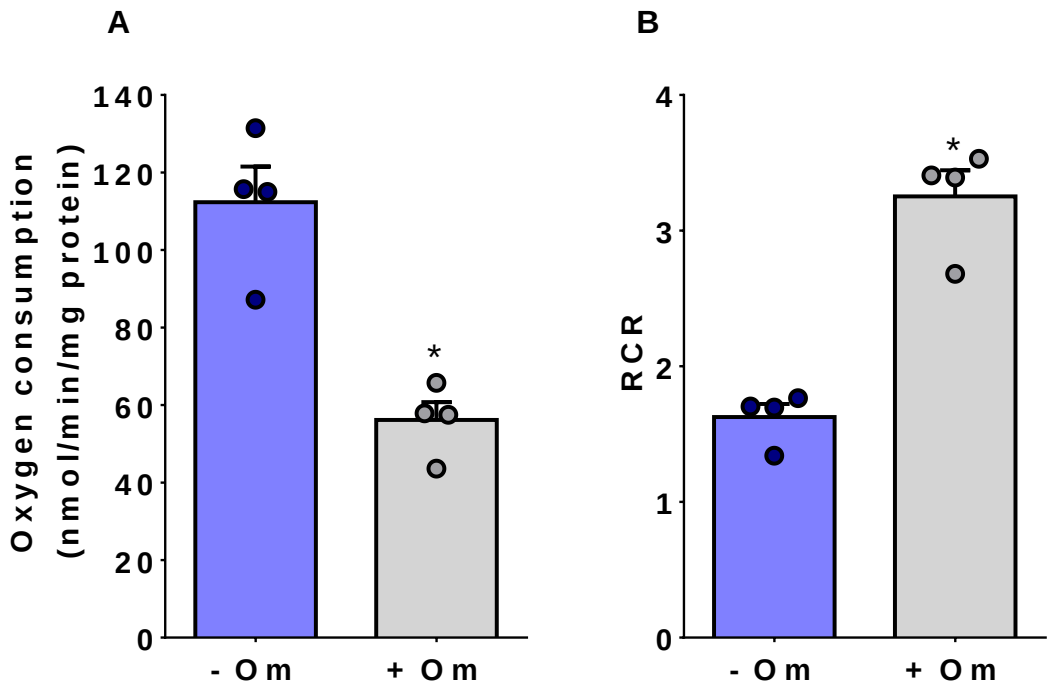

Figure 3-4. Oligomycin (Om; 10 µM) decreases state 4 respiration while it increases the RCR of NS-mito from healthy rats. Oxygen consumption assay was performed on NS-mito (350 µg/ml protein) from healthy rats suspended in respiration buffer containing KCl (135 mM), $MgCl_2$ (2 mM), K_2HPO_4 (5mM), HEPES (20 mM) and BSA free fatty acid (0.1%, w/v) with pH at 7.2, titrated with KOH. (A) Om reduces state 4 respiration (B) Om increases the RCR.

3.2.3 Effect of epilepsy on the resting respiratory rate of NS-mito

To determine overall metabolic alterations in NS-mito$_{EP}$, I compared the resting state (expressed in nmolO_2/min/mg protein) of NS-mito$_{EP}$ with the resting state of NS-mito$_{HE}$. Here, I showed a reduction of the resting state in NS-mito$_{EP}$ ($P<0.05$, HE: 13.5±2.0, n=18 *vs*. EP: 9.3±0.7, n=18) (Fig. 3-5).

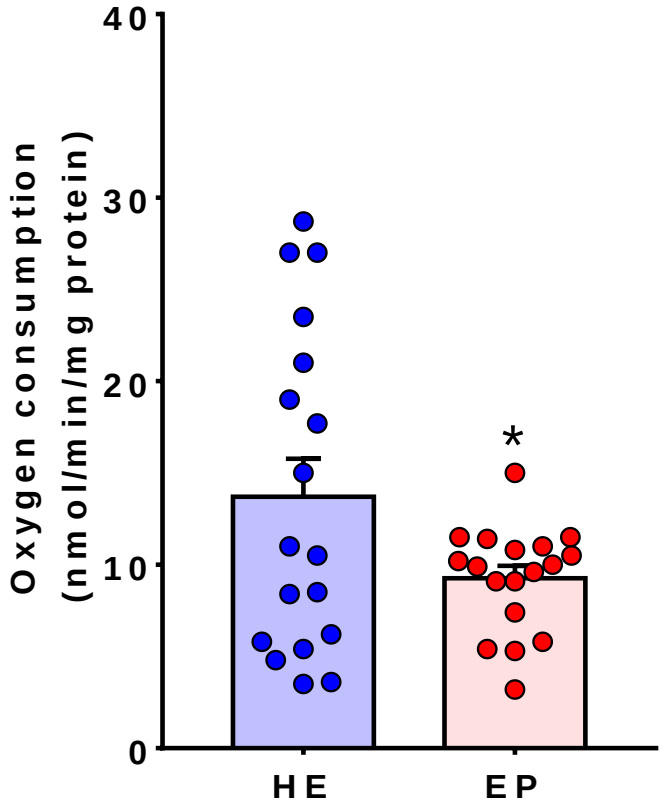

Figure 3-5. Reduction of resting respiratory rate in NS-mito from epileptic rats. Resting respiratory rate was assessed in NS-mito (350 µg/ml protein) from healthy (HE) and epileptic (EP) rats suspended in a buffer containing KCl (125 mM), K2HPO4 (5 mM), HEPES (20 mM), EGTA (1 mM) and BSA free fatty acid (0.1%, w/v) with pH at 7.2, titrated with KOH. Individual data points were obtained from five rats per group. Results are presented as mean ± SEM. NS-mito from EP rats exhibit a decreased resting respiratory rate compare to that of HE rats (*$P<0.05$, Student's t-test).

3.2.4 S18 DOES NOT ALTER PARAMETERS OF OXPHOS IN NS-MITO$_{HE}$ FOLLOWING SUC-INDUCED RESPIRATION AND ADDITION OF HIGH CONCENTRATION OF ADP^{3-}

The effect of S18 on OXPHOS was investigated in rat NS-mito (350 µg protein). In these experiments, state 3 respiration was induced with ADP (268 µM). First, NS-mito$_{HE}$ were energised with SUC, then treated with either Veh1 (see section 2.5.4) or the VDAC blocker S18 (3 µM) before adding ADP^{3-}. To prevent H^+ slip through the ATP^{4-} synthase after state 3 respiration (resulting in the increase of state 4 respiration), I added the ATP^{4-} synthase inhibitor Om (10 µM) to achieve state 4 respiration. State 3 respiration (expressed in nmol O_2/min/mg protein) induced with 268 µM ADP (P>0.05, Veh1: 170±14.2, N=5 *vs*. S18: 171±11.1, N=5) as well as state 4 respiration (expressed in nmol O_2/min/mg protein) (P>0.05, Veh1: 61±4.8, N=5 *vs*. S18: 58±5.2, N=5) in NS-mito$_{HE}$ were not affected by S18 treatment (Fig. 3-6A, 3-6B & 3-6C). In addition, S18 treatment did not alter the P:O ratio (P>0.05, Veh1: 1.5±0.0, N=5 *vs*. S18: 1.5±0.0, N=5) as well as the RCR (P>0.05, Veh1: 2.8±0.2 *vs*. S18: 3.0±0.1, N=5) (Fig. 3-7A & 3-7B). Finally, the length of state 3 respiration (expressed in s) was not altered by S18 treatment (P>0.05, Veh1: 103±8.8, N=5 *vs*. S18: 102±9.7, N=5) (Fig. 3-8).

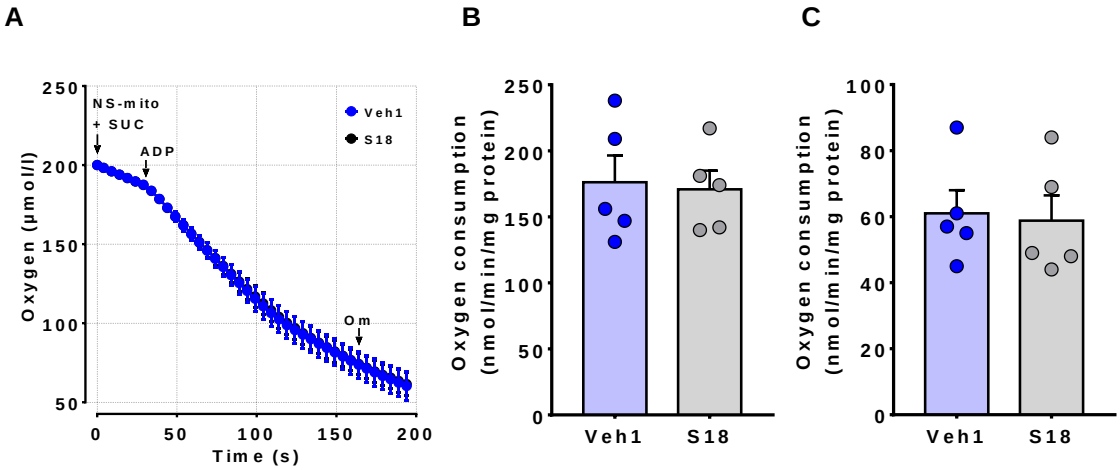

Figure 3-6. S18 exhibits no effect on state 3 and state 4 respiration of NS-mito from healthy rats under a high ADP^{3-} condition. NS-mito (350 µg/ml protein) from healthy rats were energised with 5 mM succinate (SUC). While S18 (3 µM) was added 1 min 30 subsequently to SUC-induced respiration, ADP^{3-} (268 µM) was added 1 min following S18 or vehicle (Veh1) to stimulate state 3 respiration. State 4 respiration was achieved by adding Om (10 µM). (A) Plotted traces illustrating oxygen consumption in NS-mito from healthy rat treated either with Veh1 or S18. (B) S18 shows no effect on state 3 respiration ($P>0.05$, Student's t-test). (C) S18 shows no effect on state 4 respiration ($P>0.05$, Student's t-test). Each data point was obtained from individual rat. Results are expressed as mean ± SEM.

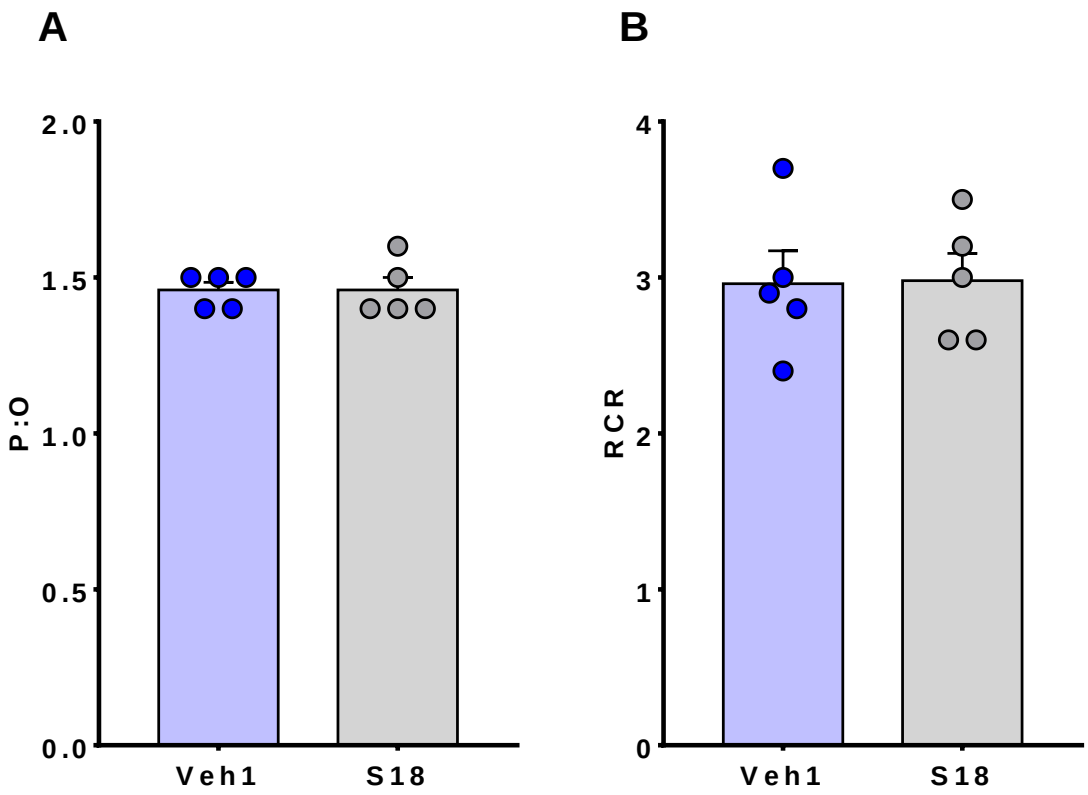

Figure 3-7. S18 exhibits no effect on the P:O ratio and the RCR of NS-mito from of healthy rats under a high ADP^{3-} condition. NS-mito (350 µg/ml protein) from healthy rats were energised with 5 mM succinate (SUC). While S18 (3 µM) was added 1 min 30 subsequently to SUC-induced respiration, ADP^{3-} (268 µM) was added 1 min following S18 or vehicle (Veh1) to stimulate state 3 respiration. State 4 respiration was achieved by adding Om (10 µM). (A) S18 shows no effect on P:O ratio ($P>0.05$, Student's t-test). (B) S18 shows no effect on RCR ($P>0.05$, Student's t-test). Each data point was obtained from individual rat. Results are expressed as mean ± SEM.

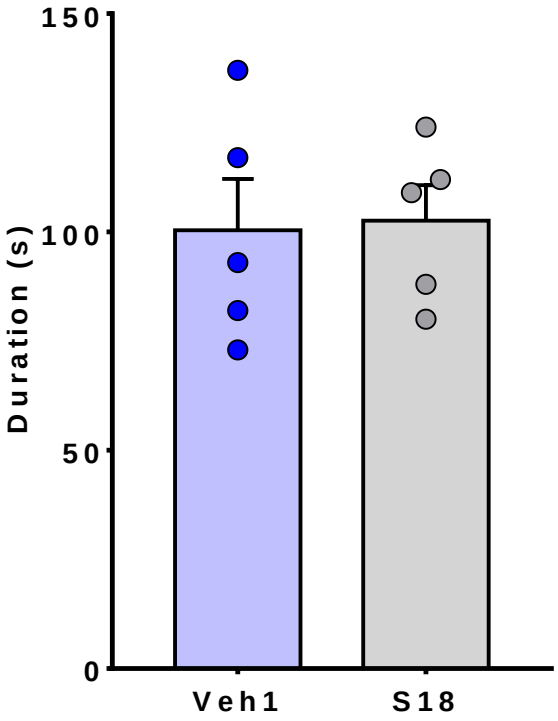

Figure 3-8. S18 does not affect the duration of state 3 respiration of NS-mito from of healthy rats under a high ADP^{3-} condition. NS-mito (350 µg/ml protein) from healthy rats were energised with 5 mM succinate (SUC). While S18 (3 µM) was added 1 min 30 subsequently to SUC-induced respiration, ADP^{3-} (268 µM) was added 1 min following S18 or vehicle (Veh1) to stimulate state 3 respiration. State 4 respiration was achieved by adding Om (10 µM). S18 shows no effect on the duration state 3 respiration ($P>0.05$, Student's t-test). Each data point was obtained from individual rat. Results are expressed as mean ± SEM.

3.2.5 Effect of CBD, CBDV and S18 on OXPHOS in NS-mito$_{HE}$ and NS-mito$_{EP}$ following addition of SUC and low concentration ADP^{3-}

Both NS-mito$_{HE}$ and NS-mito$_{EP}$ (350 µg protein/group) were energised with SUC. The effect of CBD (10 µM), CBDV (10 µM) or S18 (3 µM) upon OXPHOS were assessed in the presence of a low concentration of ADP^{3-} (80 µM). Veh1, CBD, CBDV or S18 were added prior to state 3 respiration. State 4 respiration was achieved by adding Om (10 µM) as previously described (see section 2.5.4).

3.2.5.1 State 3 respiration stimulated with low concentration of ADP^{3-} in NS-mito$_{HE}$ and NS-mito$_{EP}$: effect of CBD, CBDV and S18 treatment

To address the question of whether CBD, CBDV or S18 exert any effect on ATP synthase or the RC, I determined their effect on state 3 respiration (expressed in O_2/min/mg protein) induced with low ADP concentration (80 µM). NS-mito$_{EP}$ did not exhibit any alteration of state 3 respiration (Q>0.05, HE-Veh1 178±9.7, N=5 *vs*. EP-Veh1 175±9.9, N=5) (Fig. 3-9A, 3-9B & 3-9C). Treatment of NS-mito$_{HE}$ with CBD (Q>0.05, HE-Veh1: 178±9.7 *vs*. HE-CBD: 167±13.6, N=5), CBDV (Q>0.05, HE-Veh1: 178±9.7, N=5 *vs*. HE-CBDV: 159±11.3, N=3) and S18 (Q>0.05, HE-Veh1: 178±9.7 *vs*. HE-S18: 167.4±13.6, N=5) did not alter the respiratory rate of state 3 (Fig. 3-9A, 3-9B & 3-9C). Furthermore, this data showed that neither the VDAC blocker S18 (Q>0.05, Veh1: 175±9.9, N=4 *vs*. S18: 175±13.8, N=4) nor the phytocannabinoids CBD (Q>0.05, Veh1: 175±9.9, N=5 *vs*. CBD: 171±14.4, N=5) and CBDV (Q>0.05, Veh1: 175±9.9, N=5 *vs*. CBDV: 193±13.8, N=4) affected state 3 respiration in NS-mito$_{EP}$ (Fig. 3-9A, 3-9B & 3-9C). Given that inhibitors of the RC or the ATP synthase reduce state 3 respiration, and that the contribution of complex I is negligible under SUC-induced respiration, these results showed that CBD, CBDV or S18 directly inhibited neither the ATP synthase nor complexes II, III and IV of the RC.

3.2.5.2 Effect of CBD, CBDV and S18 on state 4 respiration in NS-mito$_{HE}$ and NS-mito$_{EP}$ following state 3 respiration induced with low concentration of ADP^{3-}

As previously shown (section 3.2.5.1), CBD, CBDV or S18 directly inhibited neither the RC (II, III and IV) and the ATP synthase, I then determined if they could inhibit the RC via a mediator or could induce H^+ leak by measuring their effect on state 4 respiration (expressed in O_2/min/mg protein). While state 4 respiration in NS-mito$_{HE}$ was not affected by CBD (Q>0.05, HE-Veh1: 63.4±4.4, N=5 *vs*. HE-CBD: 64.6±4.7, N=5) and CBDV treatment (Q>0.05, HE-Veh1: 63.4±4.4, N=5 *vs*. HE-CBDV: 61.7±1.9, N=3), blockade of VDAC with S18 reduced state 4 respiratory rate in NS-mito$_{HE}$ (Q<0.05, HE-Veh1: 63.4±4.4, N=5 *vs*. HE-S18: 55.0±3.3, N=5) (Fig. 3-9A, 3-9B & 3-9D). In all pharmacological conditions, NS-mito$_{EP}$ exhibited higher state 4 respiration compared to that of Veh1-treated NS-mito$_{HE}$. NS-mito$_{EP}$ treated with Veh1 (Q<0.05, HE-Veh1: 63.4±4.4 *vs*. EP-Veh1: 81.9±2.6, N=5), CBD (Q<0.05, HE-Veh1: 63.4±4.4 vs. EP-CBD: 91.0±2.6, N=5), CBDV (Q<0.05, HE-Veh1: 63.4±4.4, N=4 vs. EP-CBDV: 81.0±0.1, N=4) or S18 (Q<0.05, HE-Veh1: 63.4±4.4, N=4 vs. EP-S18: 79.5±1.4, N=4) exhibited higher state 4 respiration compare to that of Veh1-treated NS-mito$_{HE}$ (Fig. 3-9A, 3-9B & 3-9D). I then examined whether there was a difference between state 4 respiration in Veh1-treated NS-mito$_{EP}$ and that of CBD, S18 and CBDV-treated NS-mito$_{EP}$. While S18 (Q>0.05, EP-Veh1: 81.9±2.6, N=5 *vs*. EP-CBDV: 81.0±0.1, N=4) and CBDV (Q>0.05, EP-Veh1: 81.9±2.6, N=5 *vs*. EP-CBDV: 81.0±0.1, N=4) did not alter state 4 respiration in NS-mito$_{EP}$, CBD-treated NS-mito$_{EP}$ exhibited an increased state 4 respiration compared to that of NS-mito$_{EP}$ treated with Veh1 (Q<0.05, Veh1: 81.9±2.6 vs. CBD: 91.0±2.6, N=5), CBDV (Q<0.05, CBDV: 81.0±0.1, N=4 vs. CBD: 91.0±2.6, N=5) or S18 (Q<0.05, S18: 79.5±1.4, N=4 vs. CBD: 91.0±2.6, N=5) (Fig. 3-9A, 3-9B & 3-9D). In conclusion, CBD induced a small H^+ leak (as state 4 respiration was increased) in NS-mito$_{EP}$ but had no effect on state 4 respiration in NS-mito$_{HE}$. Conversely, S18 did not affect

state 4 respiration in NS-mito$_{EP}$ but did inhibit state 4 respiration in NS-mito$_{HE}$, most likely via mediator, as S18 did not alter state 3 respiration in NS-mito$_{HE}$.

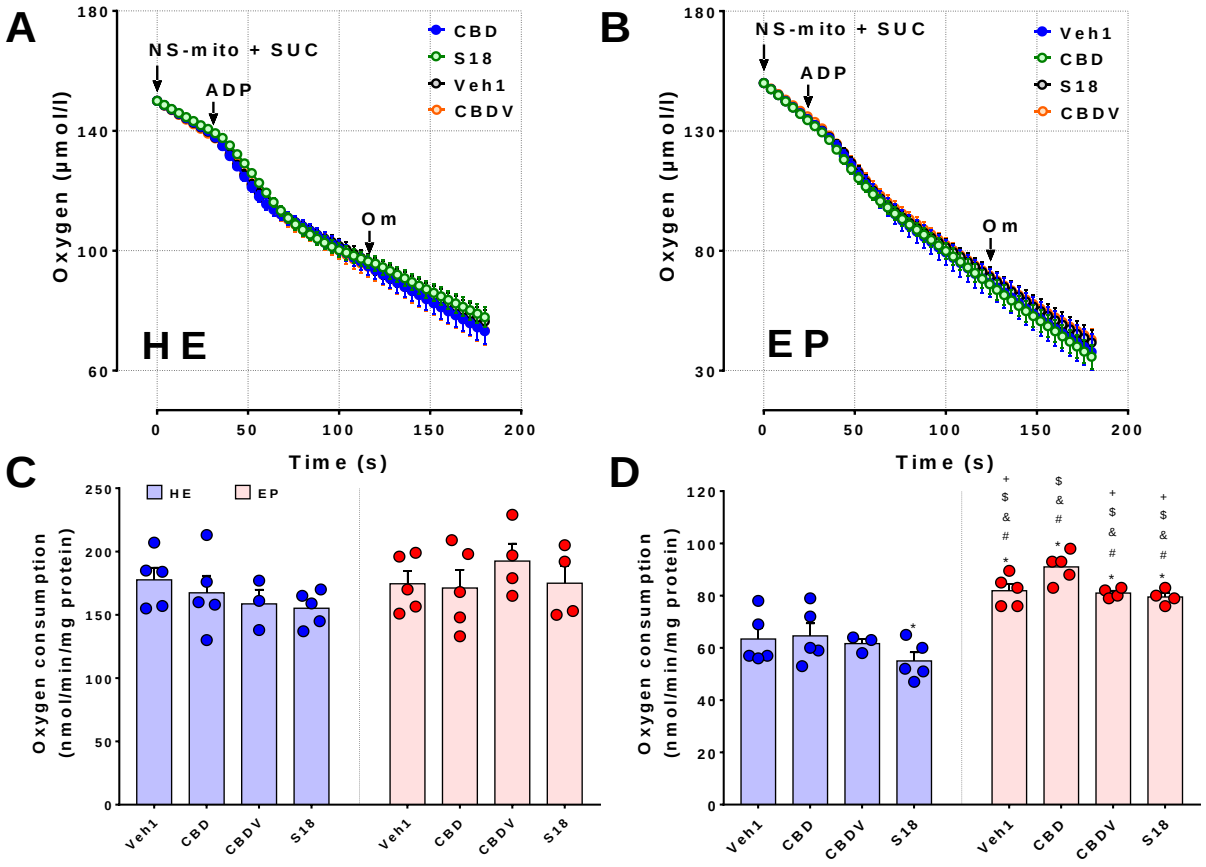

Figure 3-9. S18 reduces State 4 respiration in non-synaptic mitochondria from hippocampi (NS-mito) of healthy rats but CBD increases state 4 respiration in NS-mito from epileptic rats under a low ADP^{3-} condition. NS-mito (350 µg/ml protein) from healthy (HE) and epileptic (EP) rats were energised with 5 mM succinate (SUC). While Veh1 (0.03 % DMSO), S18 (3 µM), CBD (10 µM) or CBDV (10 µM) were added 1 min 30 subsequently to SUC-induced respiration, ADP^{3-} (80 µM) was added 1 min following addition of Veh1/CBD/S18/CBDV to stimulate state 3 respiration. State 4 respiration was achieved by adding the ATP synthase inhibitor Om (10 µM). Traces plotted to illustrate the effect of CBD, S18 and CBDV on OXPHOS in NS-mito from (A) HE and (B) EP. (C) Effect of CBD, S18 and CBDV on state 3 respiration. (D) Effect of CBD, S18 and CBDV on state 4 respiration. Individual measurements were obtained from different rats. Results are expressed as mean ± SEM. Upon statistical difference using two-way ANOVA ($P<0.05$), multiple comparisons were performed using the two-stage linear step-up procedure of BKY. Discovery of statistical difference with Veh1-treated NS-mito from HE rats (*), CBD-treated NS-mito from HE rats (#), CBDV-treated NS-mito from HE rats (&), S18-treated NS-mito from HE rats ($) or CBD-treated NS-mito from EP rats was determined with the Q-value ($Q<0.05$).

3.2.5.3 Effect of CBD, CBDV and S18 on the P:O ratio in both NS-mito$_{HE}$ and NS-mito$_{EP}$ following state 3 respiration induced with a low concentration of ADP^{3-}

The production of ATP by the ATP synthase requires an influx of H^+ through the enzyme and the presence of ADP and Pi in mitochondrial matrix. To investigate the effect of the VDAC blocker S18, CBD and CBDV on the "efficiency" of ATP synthesis in NS-mito$_{HE}$ and NS-mito$_{EP}$, I determined the effect of these drugs on the P:O ratio. The P:O ratio of NS-mito$_{EP}$ was reduced compared to NS-mito$_{HE}$ (Q<0.05, HE-Veh1: 1.6±0.1, N=5 *vs*. EP-Veh1: 1.4±0.1, N=5) (Fig. 3-10A). CBD did not affect the P:O ratio in both NS-mito$_{HE}$ (Q>0.05, HE-Veh1: 1.6±0.1, N=5 *vs*. HE-CBD: 1.7±0.1, N=5) (Fig. 3-10A). CBD-treated NS-mito$_{EP}$ exhibited a decreased P:O ratio compared to that of Veh1-treated NS-mito$_{HE}$ (Q<0.05, HE-Veh1: 1.6±0.1, N=5, N=5 *vs*. EP-CBD: 1.2±0.1, N=5) (Fig. 3-10A). CBDV-treated NS-mito$_{HE}$ did not exhibit any difference compared to Veh1-treated NS-mito$_{HE}$ (Q>0.05, HE-Veh1: 1.6±0.1, N=5 vs. HE-CBDV: 1.5±0.1, N=3) (Fig. 3-10A). However, CBDV-treated NS-mito$_{EP}$ exhibited a lower P:O ratio compared to that of Veh1-treated NS-mitoEP (Q<0.05, HE-Veh1: 1.6±0.1, N=5 *vs*. EP-CBDV: 1.3±0.1, N=4) (Fig. 8A). NS-mito$_{HE}$ treated with S18 exhibited lower P:O ratio than Veh1-treated NS-mito$_{HE}$ (Q<0.05, HE-Veh1: 1.6±0.1, N=5 *vs*. HE-S18: 1.3±0.1, N=5) (Fig. 3-10A). Conversely, the treatment of NS-mito$_{EP}$ with S18 showed no difference from Veh1 treatment (Q>0.05, EP-Veh1: 1.4±0.1, N=5 *vs*. EP-S18: 1.3±0.0, N=4) (Fig. 3-10A). While there is no difference between the P:O ratio of CBD-treated NS-mito$_{HE}$ to that of CBDV-treated NS-mito$_{HE}$ (Q>0.05, HE-CBD: 1.7±0.1, N=5 *vs*. HE-CBDV: 1.5±0.1, N=3) (Fig. 8A), NS-mito$_{HE}$ treated with CBD exhibited a reduced P:O ratio compared to that of S18-treated NS-mito$_{HE}$ (Q<0.05, HE-CBD: 1.7±0.1, N=5 vs. HE-S18: 1.3±0.1, N=5) (Fig. 3-10A). Subsequently, comparing the P:O ratio of CBD-treated NS-mito$_{EP}$ and that of Veh1-treated NS-mito$_{EP}$ exhibited no differences (Q>0.05, EP-Veh1: 1.4±0.1, N=5 *vs.* EP-CBD: 1.2±0.1, N=5) (Fig. 3-10A). Treatment of NS-mito$_{EP}$ with CBDV-treated did not

affect the P:O ratio (Q>0.05, EP-Veh1: 1.4±0.1, N=5 *vs.* EP-CBDV: 1.3±0.1, N=4) (Fig. 3-10A). In addition, S18-treated NS-mito$_{EP}$ did not vary from Veh1-treated NS-mito$_{EP}$ (Q>0.05, EP-Veh1: 1.4±0.1, N=5 *vs*. EP-S18: 1.3±0.0, N=4) (Fig. 3-10A). NS-mito$_{EP}$ treated with CBD exhibited no change of P:O compared to that of CBDV-treated NS-mito$_{EP}$ (Q>0.05, EP-CBD: 1.2±0.1, N=5 *vs*. EP-CBDV: 1.3±0.1, N=4) (Fig. 3-10A). The P:O ratio of CBD-treated NS-mito$_{EP}$ did not differ from that of S18-treated NS-mito$_{EP}$ (Q>0.05, EP-CBD: 1.2±0.1, N=5 *vs*. EP-S18: 1.3±0.0, N=4) (Fig. 3-10A). In summary, S18 reduced the P:O ratio only in NS-mito$_{HE}$ while CBD and CBDV exerted no effect on the P:O ratio of both NS-mito$_{HE}$ and NS-mito$_{EP}$.

3.2.5.4 Effect of CBD, CBDV and S18 on the RCR in NS-mito$_{HE}$ and NS-mito$_{EP}$ following state 3 respiration induced with low concentration of ADP^{3-}

The effects of CBD, CBDV and S18 on the tightness of OXPHOS coupling in NS-mito$_{HE}$ and NS-mito$_{EP}$ are unknown. Therefore, these drugs were investigated whether they exerted a strong uncoupling effect (by reducing the RCR) in both NS-mito$_{HE}$ and NS-mito$_{EP}$. The RCR was reduced in NS-mito$_{EP}$ compared to that of NS-mito$_{HE}$ (Q<0.05, HE-Veh1: 2.8±0.1, N=5 *vs.* EP-Veh1: 2.2±0.1, N=5) (Fig. 3-10B). As previously reported, S18 treatment exhibited an effect on state 4 respiration and on the P:O ratio in NS-mito$_{HE}$ (see section 3.2.5.2 & section 5.2.5.3), I also determined whether these compounds changed the RCR in both NS-mito$_{HE}$ and NS-mito$_{EP}$. My results showed that S18 does not affect RCR in NS-mito$_{HE}$, as they were not exhibiting any difference with NS-mito$_{HE}$ treated with Veh1 (Q>0.05, HE-Veh1: 2.8±0.1, N=5 *vs*. HE-S18: 2.9±0.1, N=5) (Fig. 3-10B). The RCR of NS-mito$_{EP}$ was not affected by S18 treatment (Q>0.05, EP-Veh1: 2.2±0.1, N=5 *vs*. EP-S18: 2.2±0.2, N=4) (Fig. 3-10B). Treatment of NS-mito$_{HE}$ with CBD did not change RCR (Q>0.05, HE-Veh1: 2.8±0.1, N=5 vs. HE-CBD: 2.6±0.1, N=5) (Fig. 3-10B). Despite the increase of state 4 respiration in CBD-treated NS-mito$_{EP}$ (see section 3.2.5.2), CBD did not alter the RCR of NS-mito$_{EP}$ (Q>0.05, EP-Veh1: 2.2±0.1, N=5 *vs*. EP-CBD:

1.9±0.2, N=5) (Fig. 3-10B). CBDV had no effect on the RCR of NS-mito$_{HE}$ compared to Veh1-treated NS-mito$_{HE}$ (Q>0.05, HE-Veh1: 2.7±0.1, N=5 vs. HE-CBDV: 2.9±0.1, N=3) (Fig. 3-10B). CBDV's effect on the RCR in NS-mito$_{EP}$ showed no difference compared to Veh1-treated NS-mito$_{EP}$ (Q>0.05, EP-Veh1: 2.2±0.1, N=5 vs. EP-CBDV: 2.4±0.2, N=4) (Fig. 3-10B). In conclusion, the RCR is reduced in NS-mito$_{EP}$ and treatment of NS-mito$_{EP}$ with CBD, CBDV and S18 did not alter it.

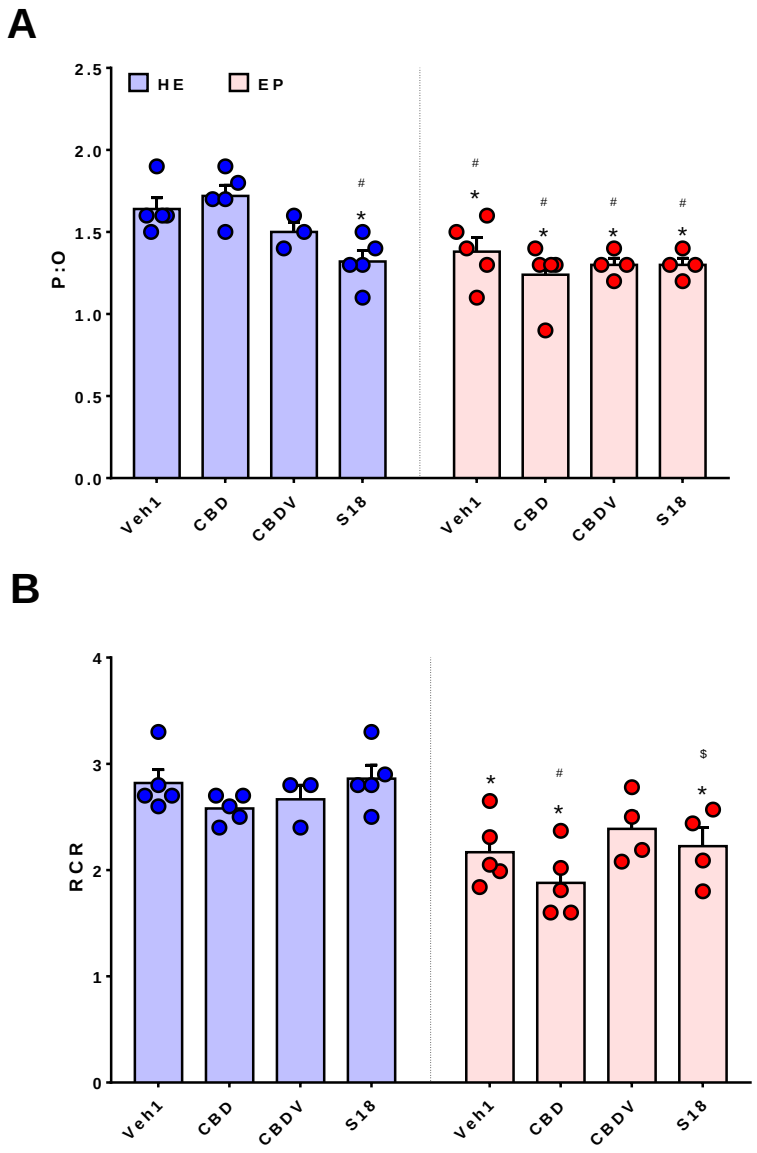

Figure 3-10. S18 induces reduction of P:O ratio in NS-mito from HE rats under a low ADP^{3-} condition. Effect of CBD, S18 and CBDV on (A) the P:O ratio and (B) RCR (State 3/state 4) following induction of state 3 respiration with ADP^{3-} (80µM) in NS-mito (350 µg/ml protein) from HE and EP rats. Individual measurements were obtained from different rats. Results are presented as mean ± SEM. Upon statistical difference using two-way ANOVA ($P<0.05$), multiple comparisons were performed using the two-stage linear step-up procedure of BKY. Discovery of statistical difference with Veh1-treated NS-mito from HE rats (*), CBD-treated NS-mito from HE rats (#) or S18-treated NS-mito from HE rats ($) was determined with the Q-value ($Q<0.05$).

3.2.5.5 Effect of CBD, CBDV and S18 on the duration of state 3 respiration in NS-mito$_{HE}$ and NS-mito$_{EP}$ following state 3 respiration induced with low concentration ADP^{3-}

Measuring the duration of state 3 respiration (expressed in s) allows to determine the length of time it takes to all ADP molecules to be converted into ATP. We showed that this duration was altered in our rat model of TLE, since Veh1 treated NS-mito$_{HE}$ exhibited no difference in this duration from Veh1 treated NS-mito$_{HE}$ ($Q>0.05$, HE-Veh1: 26.6±1.3, N=5 *vs*. EP-Veh1: 34.4±2.7, N=5) (Fig. 3-11). Subsequently, the effects of CBD, CBDV and S18 on the duration of state 3 respiration were examined in both NS-mito$_{HE}$ and NS-mito$_{EP}$. Two-way ANOVA performed on the duration of state 3 showed a main effect of drug ($P<0.05$, $F(3, 28) = 2.98$), but fails to demonstrate any main effect of disease ($P=0.28$, $F(1, 28) = 1.34$) or interaction ($P=0.13$, $F(3, 28) = 2.45$). In contrast, although this study showed a main effect of drug treatment, subsequent multiple comparisons could not identify a drug which altered the duration of state 3 respiration in both NS-mito$_{HE}$ and NS-mito$_{EP}$ (Fig. 3-11).

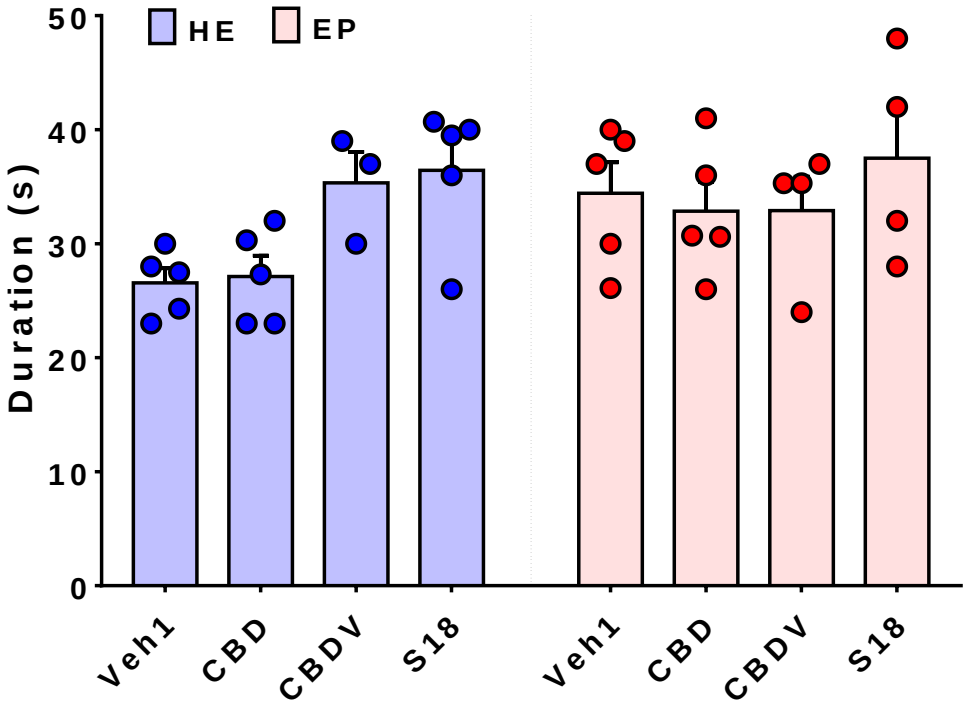

Figure 3-11. No effect of CBD, S18 and CBDV on the duration of state 3 respiration in NS-mito from HE and EP rats under a low ADP^{3-} condition. Effect of CBD, CBDV and S18 on duration of state 3 respiration was assessed following stimulation of state 3 respiration with ADP^{3-} (80 µM) in NS-mito (350 µg/ml protein) from HE and EP rats. Results are presented as mean ± SEM. Individual measurements presented here were obtained from different rats. Two-way ANOVA showed main effect of drug treatment ($P<0.05$) but multiple comparisons using the two-stage linear step-up procedure of BKY show no differences between groups ($Q>0.05$).

3.2.6 Alterations in the relationship between OXPHOS parameters in NS-mito$_{EP}$

I then designed a scatterplot matrix to assess whether the relations among pairs of OXPHOS parameters were affected by epilepsy. Parameters of OXPHOS that were selected for correlation analysis were state 3 respiration, state 4 respiration, P:O ratio and duration of state 3 of NS-mito$_{HE}$ and NS-mito$_{EP}$.

In NS-mito$_{HE}$, the relationship between state 3 and state 4 was linear (Fig. 3-12). This was supported by the linear fit between state 3 and state 4 which explains 67% of the variability of state 3 in addition to the scatterplot (Table 3-2 & Fig. 3-12). Also, there was a very strong and positive correlation between state 3 and state 4 (Table 3-3). The R^2 values between state 3 and duration and between P:O and duration were greater than 0.4, which suggests that in both cases the relationship is linear (Table 3-2 & Fig. 3-12). Furthermore, there was a strong and negative correlation between state 3 and duration and between P:O and duration (Table 3-2). In spite of the relatively strong and negative relationship (-0.56) between state 4 and the duration of state 3 respiration, it seems unlikely that the nature of the relationship between both variables is linear, because the linear model fit only explained 31% of the of the relationship (Table 3-2) and the scatterplot did not illustrate any form of linear pattern (Fig. 3-12). Finally, linear dependencies were not observed between state 3 and P:O or between state 4 and P:O (Table 3-2).

In NS-mito$_{EP}$, there was no linear correlation between state 3 and state 4 respiration (Table 3-2). Conversely, the increase of the duration of state 3 respiration was correlated to the decrease of state 3 respiration (Table 3-3 & Fig. 3-12). The linear fit between these latter parameters of OXPHOS, showed that changes in the duration of state 3 respiration explained 45% of the variability of state 3 respiration. This is also confirmed by the scatterplot matrix

(Fig. 3-12). Analysis of the relationship between state 3 respiration and the P:O ratio as well as between state 4 respiration and duration of state 3, revealed no correlations among these OXPHOS parameters (Table 3-3). In addition, no dependencies were found between state 4 respiration and the P:O ratio, as well as between the P:O ratio and the duration of state 3 respiration.

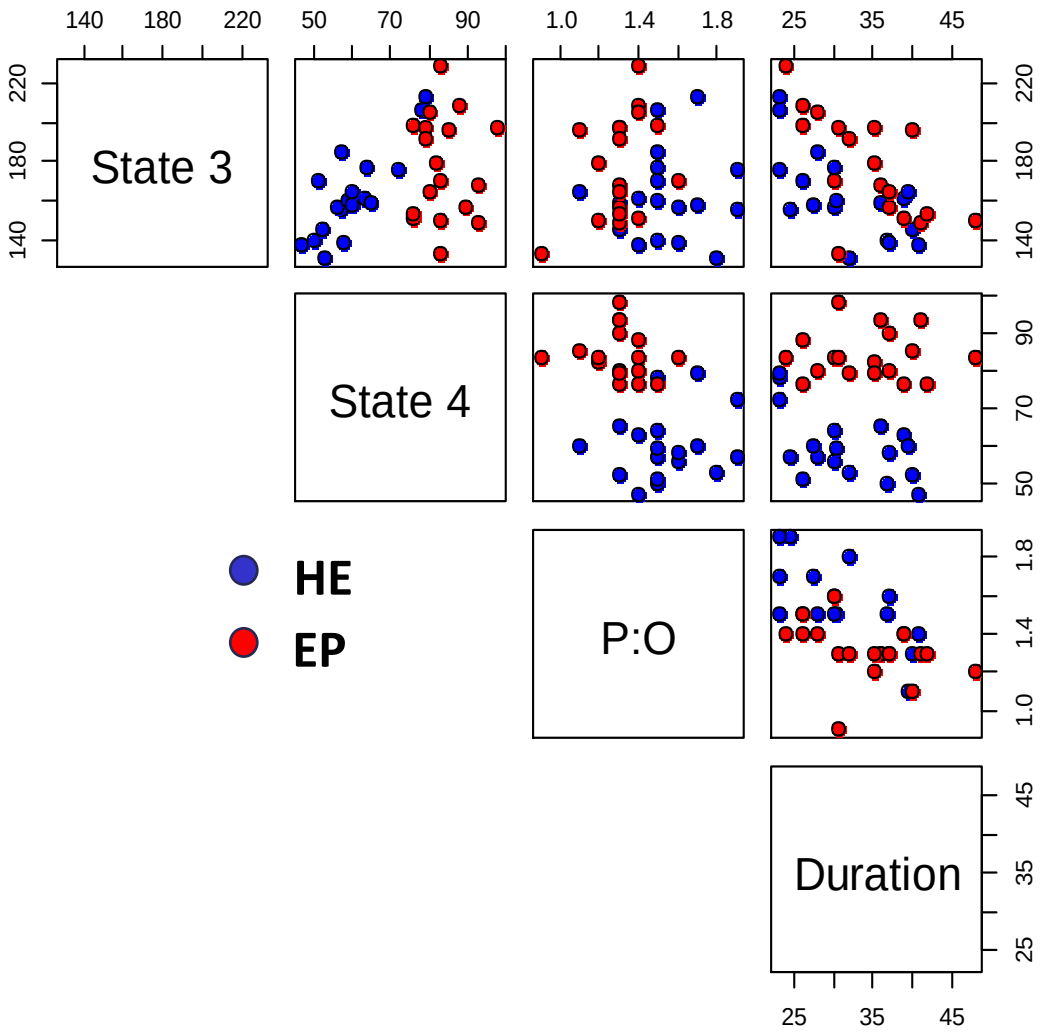

Figure 3-12. Scatterplot matrix illustrating impairment of dependency between OXPHOS parameters in NS-mito from epileptic rats. These results show a loss of linear relation between state 3 - state 4, P:O – duration and state 4 – duration in NS-mito isolated rats with epilepsy.

Table 3-2. Relations between OXPHOS parameters in NS-mito from healthy rats.

Pairs of correlation	N	df	r (Pearson)	R^2	p-value
State 3 - State 4	18	16	0.82	0.67	< 0.01
State 3 - P:O	18	16	0.06	0.00	0.83
State 3 - Duration	18	16	-0.67	0.45	< 0.01
State 4 - P:O	18	16	0.2	0.04	0.44
State 4 - Duration	18	16	-0.56	0.31	0.02
P:O - Duration	18	16	-0.69	0.48	< 0.01

Table 3-3. Relations between OXPHOS parameters in NS-mito from epileptic rats.

Pairs of correlation	N	df	r (Pearson)	R^2	p-value
State 3 - State 4	18	16	0.00	0.00	1.00
State 3 - P:O	18	16	0.40	0.16	0.10
State 3 - Duration	18	16	-0.67	0.45	< 0.01
State 4 - P:O	18	16	-0.14	0.02	0.58
State 4 - Duration	18	16	0.00	0.00	0.99
P:O - Duration	18	16	-0.37	0.14	0.13

3.3 DISCUSSION

Using NS-mito$_{HE}$ and NS-mito$_{EP}$, I demonstrated for the first time that the mechanism of action of CBD (10 µM) on OXPHOS differs from that of the VDAC blocker S18 (3 µM). Furthermore, my findings demonstrate that CBD acts only under epileptic condition since it uncouples NS-mito$_{EP}$ by inducing a weak H^+ leak from the intermembrane space. CBD's effect on NS-mito OXPHOS is dependent on the length of its lateral aliphatic chain, since treatment of NS-mito$_{EP}$ with 10 µM CBDV (which possesses a shorter lateral chain) did not altered their OXPHOS. The mechanism by which the mode of action of CBD accounts for its anti-epileptic effect will be discuss in details the sections below.

3.3.1 METABOLIC IMPAIRMENT OF OXPHOS IN NS-MITO$_{EP}$

In this study, the P:O ratio was used as an indicator of the efficiency of ATP^{4-} production under SUC-induced respiration. Three H^+ are required to influx through the ATP^{4-} synthase in order to allow the synthesis of one molecule of ATP^{4-} (Hinkle, 2005). Therefore, it is considered that the H^+:ATP^{4-} ratio is three (Hinkle, 2005). It was assumed for a long time that the P:O ratio generated with SUC-induced respiration was two because six H^+ are released into the intermembrane space by the RC subsequently to one succinate/$FADH_2$ oxidation (Ferguson, 2010; Hinkle, 2005). Hinkle and Ferguson convincingly argued in their respective reviews, based on observations in several laboratories and on thermodynamic grounds, that the P:O ratio of SUC-induced respiration could not be integer, but rather lower than 2 (Ferguson, 2010; Hinkle, 2005). Consistent with the literature, the P:O ratio of SUC-induced respiration in NS-mito$_{HE}$ showed a value of 1.6 or 1.5 depending on whether state 3 respiration was either induced with 80 µM and 268 µM ADP^{3-}, respectively. Under this experimental conditions, which includes the temperature at 30°C, the presence of EGTA (1

mM) and BSA (1 mg/ml), the P:O ratio in this study is expected to be affected by the influx of H^+ and metabolite (ATP^{4-}/ADP^{3-} and Pi^{3-}) into the matrix as well as the structure of the ATP^{4-} synthase (Canton et al., 1995; Ferguson, 2010; Hinkle, 2005).

In this model of TLE, the P:O ratio of NS-mito is reduced, thus indicating that oxidisation of SUC results in a reduced production of ATP^{4-}, compared to healthy. Consistent with this, the intracellular ATP^{4-} levels have been shown to decrease in neurons during seizures (Kovac et al., 2012). This depleted production of ATP^{4-} by mitochondria may serve as an adaptive mechanism to reduce susceptibility to seizures. In recent years, there has been growing evidence showing that increasing the level of extracellular ATP^{4-} renders the brain more susceptible to seizures (Collins et al., 1970; Kumaria et al., 2008). In the Coriaria lactone kindling model of epilepsy, the inhibition of the ATP^{4-} receptor $P2X_7$ ($P2X_7R$) reduced the occurrence of severe seizures while its activation increased it (Huang et al., 2017). This suggests that activation of $P2X_7R$ with ATP^{4-} could be implicated in the proconvulsive effect of ATP^{4-}. As $P2X_7R$ is upregulated in the hippocampi of rodent model of TLE (Doná et al., 2009; Vianna et al., 2002), it is plausible that higher extracellular levels of ATP^{4-} increases susceptibility to seizures in this model.

The observed reduction of the P:O ratio in this model of TLE could be caused by either altered transport of Pi and ADP/ATP or increased H^+ leak (which causes uncoupling of OXPHOS). This study showed that there is indeed an increase of H^+ leak in NS-$mito_{EP}$, as state 4 respiration is increased and the RCR is reduced. Several systems are likely to be involved in the process of uncoupling NS-mito. Uncoupling protein 2 (UCP2), as well as other mitochondrial uncoupling proteins (UCPs), are expressed in the inner membrane of mitochondria and are known to transport H^+ from the intermembrane space to mitochondrial

matrix. UCP2 is upregulated in the hippocampus of rodents following seizures (Chuang et al., 2012). The physiological function of UCPs in the brain is not well understood. Unlike uncoupling protein 1 (UCP1) that is preferentially expressed in brown adipose tissue, UCP2 is expressed in the brain and does not appear to be implicated in thermogenesis (Kim-Han and Dugan, 2005; Richard et al., 1998; Varela et al., 2016). Instead, UCP2 appears to exert antioxidant effects, synaptic remodelling, as well as protecting against cell death, particularly following seizures (Bechmann et al., 2002; Shin et al., 2011; Varela et al., 2016). Increasing OXPHOS uncoupling in genetic model of TLE exerts anti-seizure effects (Simeone et al., 2014). Interestingly, uncoupling of mitochondria in this rodent model of TLE may explain why there is reduced cell death in this model (Modebadze et al., 2016). Taken together, it could be argued that UCP2 may be upregulated in the rat model of epilepsy used in this study.

3.3.2 THE INTEGRITY OF VDAC FUNCTION MAY BE COMPROMISED IN NS-MITO$_{EP}$

In this section, I will refer to VDAC as a combination of all three isoforms (VDAC1, VDAC2 and VDAC3). Currently, there is no known pharmacological agent with clear selectivity to any of the VDAC isoforms.

VDAC blockade with S18 in NS-mito$_{HE}$ exhibited no effect on state 3 respiration induced with low concentration ADP^{3-} (80 μM) but diminished the P:O ratio and state 4 respiration. Although S18 reduced ATP^{4-} synthesis (as indicated by the reduction of the P:O ratio) under low levels of ADP^{3-}, my findings suggest that it does not directly inhibit the RC (complex II, III and IV) or the ATP^{4-} synthase, as state 3 respiration was not affected by S18 treatment. Given that S18 reduced state 4 without affecting state 3 respiration, one could hypothesise that S18 induces the formation of a mediator which in turn inhibits the RC. It is plausible that this mediator is a free radical, since treatment of mitochondria with Om is

known to generate ROS (A Shchepina et al., 2002), while POL were found to inhibit efflux of free radicals through VDAC (Tikunov et al., 2010). As S18 does not cause H^+ leak in NS-mito$_{HE}$, it is very likely that the reduction of the P:O ratio induced by S18 treatment is due to a reduction of ADP^{3-} or Pi^{3-} uptake, because both metabolites are required simultaneously in mitochondrial matrix for ATP^{4-} synthesis. At its physiological opened state, VDAC can transport ATP^{4-}, ADP^{3-} and Pi^{3-} (either in the form of $H_2PO_4^-$ or HPO_4^{2-}) (Colombini, 2004; Hodge and Colombini, 1997; Rostovtseva and Bezrukov, 1998; Rostovtseva and Colombini, 1996, 1997; Rostovtseva et al., 2002a, 2002b; Tan et al., 2007a). Uptake of ADP^{3-} in mitochondria through VDAC appears to require ATP^{4-} efflux (Rostovtseva et al., 2002a; Tan et al., 2007a), while the influx of Pi^{3-} through VDAC does not require any additional ion transport (Hodge and Colombini, 1997). My findings are in conflict with Tan et al. results, since they demonstrated that blockade of VDAC with G3139 (another POL like S18) induced a strong uncoupling of OXPHOS in liver mitochondria (Stein and Colombini, 2008; Tan et al., 2007b, 2007a). Given that I used mitochondria from a different tissue, it is plausible that the function of VDAC may differ depending on the tissue. Alternatively, S18 inhibits VDAC by binding in a different site from G3139 binding site. If the second hypothesis is incorrect, this would suggest that in NS-mito$_{HE}$, VDAC's constitutive activity (which would involve flickering between closed and opened state) may not be required to maintain the coupling of OXPHOS.

Furthermore, I investigated whether higher concentration of ADP^{3-} (268 µM) could change the effect of S18 on the P:O ratio and state 4 respiration. Interestingly, my results showed that S18 had no effect on any parameters of OXPHOS under high ADP^{3-} condition, suggesting that high concentration of ADP^{3-}/ATP^{4-} (resulting from the synthesis of ATP^{4-} synthase) may exert antagonistic effect to POL. This finding is consistent with work of Tan et

al. (Tan et al., 2007a), has they also demonstrated that treatment of liver mitochondria with G3139 caused no change on OXPHOS when state 3 respiration was induced with high concentration of ADP^{3-}. Given the fact that compounds like S18 or G3139 occlude the VDAC pore (Tan et al., 2007b), it is plausible that S18 also binds to the binding site of ADP^{3-}/ATP^{4-} on VDAC. Therefore, high concentrations of ADP^{3-}/ATP^{4-} may displace S18 from its binding site on VDAC. It is important to note that this effect may not occur *in vivo*, because intracellular concentrations of ADP^{3-} or ATP^{4-} do not exceed 100 µM (Kirby et al., 2014; Tian et al., 1997; Williams et al., 1993).

The VDAC blocker S18 affects OXPHOS in NS-$mito_{HE}$ but did not alter OXPHOS in NS-$mito_{EP}$. This may suggest that the molecular integrity (expression or conformation) of VDAC may be compromised in rats with TLE. Consistent with this, the reduced P:O ratio observed in NS-$mito_{EP}$ could also be caused by these changes in VDAC structure, which may affect the binding of ADP^{3-}/ATP^{4-} leading to a reduction of ADP^{3-} uptake. This modulation of VDAC conformation could be caused either by changes in expression of proteins interacting with VDAC (including oligomerisation) or by internal damage to VDAC. VDAC can bind to other VDAC to form oligomers (Ben-Hail and Shoshan-Barmatz, 2016; Maldonado et al., 2013). As reviewed by Shoshan-Barmatz et al., the level of VDAC oligomers (particularly VDAC1-oligomers) appears to increase proportionally with the increase of the monomeric form of VDAC (here VDAC1) (Shoshan-Barmatz et al., 2017). Therefore, the observed changes of VDAC expression in some rodent models of seizures/epilepsy may suggest change of conformation or configuration of VDAC (Jiang et al., 2007; Liu et al., 2008). Alternatively, alteration of VDAC structure can be caused by reactive oxygen species (ROS) released during seizures in epilepsy. As reviewed by Waldbaum and Patel, many proteins have been shown to be oxidised during

seizures (Waldbaum and Patel, 2010). All isoforms of VDAC possess cysteine residues, which will render them more susceptible to react with free radicals (De Pinto et al., 2016; Naghdi and Hajnóczky, 2016; Sampson et al., 1997). VDAC isoforms could suffer from oxidative damages since one of their function (particularly VDAC1) implicates transport of free radicals (Tikunov et al., 2010).

3.3.3 Mechanism of action of CBD

In 2013, Rimmerman et al. demonstrated that CBD (20 µM) can bind and inhibit the activity of an isoform of VDAC (namely VDAC1) reconstituted in an artificial bilayer membrane (Rimmerman et al., 2013). The expression of three isoforms of VDAC have been observed in the brain (Cesar and Wilson, 2004). These isoforms are highly conserved across mammalian species. Sequence alignment analysis demonstrate more than 90% homology between VDAC1 and VDAC2 while all three isoforms of VDAC exhibit more than 70% homology (Messina et al., 2012; Naghdi and Hajnóczky, 2016). Given the high conservation of sequence between VDAC1 and VDAC2, it is very likely that VDAC2 may be targeted by CBD, assuming the latter targets VDAC1. In support this hypothesis, 4'-diisothiocyanatostilbene-2,2'-disulphonate (DIDS) a drug known to inhibit VDAC1 also blocks VDAC2 (Li et al., 2012; Shoshan-Barmatz et al., 2017).

In this study, CBD was used at 10 µM, since this concentration is consistent with the therapeutic window of CBD in rodent model of epilepsy (Deiana et al., 2012; Jones et al., 2010, 2012; Kaplan et al., 2017). Despite the presence of VDAC1 in both NS-mito$_{HE}$ and NS-mito$_{EP}$, my findings demonstrated that CBD only acts on OXPHOS in NS-mito$_{EP}$ by increasing state 4 respiration, while the VDAC blocker S18 only acts on OXPHOS in NS-mito$_{HE}$ by reducing state 4 respiration and the P:O ratio. Given that the RCR was not changed but that state 4 respiration was increased in CBD-treated NS-mito$_{EP}$, this indicates that the uncoupling effect

(or H^+ leak) of CBD is weak. Interestingly, the induction of weak mitochondrial uncoupling (H^+ leak) with fatty acids or ketones bodies is known to exert anti-epileptic effect (Rogovik and Goldman, 2010; Simeone et al., 2014; Sullivan et al., 2004). Taken together, this study appears to indicate that the mechanism underlying the effect of CBD on OXPHOS (of NS-mito) is independent from VDAC. Furthermore, although this data shows that CBD induces a weak H^+ leak, the question on whether CBD activates H^+ transport through the inner-membrane or the outer-membrane remains undetermined. Since the effect of CBD is not consistent with that of the VDAC blocker S18, it is plausible that the target of CBD is localised in the inner-membrane of NS-mito$_{EP}$. A number of mitochondrial inner-membrane proteins could be implicated in CBD-induced H^+ leak. This H^+ leak induced by CBD in NS-mito$_{EP}$ could result from the activation of UCPs (e.g. UCP2 as described in section 3.3.1), Cation/H^+ exchangers (e.g. Na^+/H^+ exchanger) or Pi^{3-}/H^+ symporter which allows mitochondrial uptake of both H^+ and Pi^{3-} (Brand and Lehninger, 1977; Santo-Domingo and Demaurex, 2012).

CBDV (10 µM) does not affect OXPHOS in both NS-mito$_{HE}$ and NS-mito$_{EP}$. The chemical structures of CBD and CBDV differ from one another by the length of their lateral aliphatic chain. In fact, CBD possesses two more carbons in their lateral aliphatic chain compared to that of CBDV. Since CBDV did not affect OXPHOS in neither NS-mitoHE or NS-mitoEP while CBD exhibited an effect in NS-mitoEP, it is plausible that the direct effect of CBD on OXPHOS in NS-mito is due to its longer lateral aliphatic chain.

3.4 CONCLUSION

In summary, using a Li-pilo rat model of TLE, this study demonstrated alterations of OXPHOS in NS-mito resulting from the pathophysiology of epilepsy. My findings show that

the effect CBD differs from the effect of the VDAC blocker S18 on OXPHOS in NS-mito which raises the question whether CBD is acting through VDAC. I showed that CBD act a weak uncoupler on OXPHOS in NS-mito$_{EP}$ which may account for its anti-epileptic. This study also established that complexes II, III and IV, as well as the ATP synthase are not targeted by CBD in both NS-mito$_{HE}$ and NS-mito$_{EP}$.

CHAPTER 4 – EFFECT OF CANNABIDIOL ON Ca^{2+}-INDUCED PERMEABILITY TRANSITION IN NON-SYNAPTIC MITOCHONDRIA ISOLATED FROM HIPPOCAMPI OF HEALTHY AND EPILEPTIC RATS

4 EFFECT OF CANNABIDIOL ON Ca^{2+}-INDUCED PERMEABILITY TRANSITION IN NON-SYNAPTIC MITOCHONDRIA ISOLATED FROM HIPPOCAMPI HEALTHY AND EPILEPTIC RATS

4.1 INTRODUCTION

In the previous chapter (chapter 3), I demonstrated that CBD induces a weak H^+ leak in non-synaptic mitochondria isolated from epileptic rat. Here I will be addressing the question on whether CBD may be activating H^+ transport through the inner-membrane or the outer-membrane.

Nearly a decade ago, Ryan et al. showed that CBD regulates intracellular Ca^{2+} oscillations in neurons during epileptiform activity (Ryan et al., 2009). Furthermore, these authors demonstrated that CBD modulates mitochondrial homeostasis of Ca^{2+} (Ryan et al., 2009). It is still unclear whether this modulation of mitochondrial Ca^{2+} results from a direct interaction between CBD and mitochondria or whether CBD may act through other non-mitochondrial processes. Recently, Rimmerman et *al.* demonstrated that CBD can directly bind to reconstituted voltage-dependent anion-selective channel 1 (VDAC1), a protein known to regulate the transport of ions/metabolites (e.g. HPO_4^-, Cl^-, Na^+ or Ca^{2+}, ATP^{4-}) in mitochondria (Rimmerman et al., 2013). However, it remains uncertain whether this direct interaction between CBD and VDAC1 could account for CBD's effect on mitochondrial Ca^{2+} homeostasis. Since CBD (20 µM) was shown to reduce the conductance of VDAC1 reconstituted in an artificial bilayer membrane in the presence of NaCl (buffered with a Tris medium), it remains uncertain whether CBD exerts a pharmacological effect on the native form of VDAC1 embedded within mitochondrial membrane (Rimmerman et al., 2013).

Furthermore, it is plausible that CBD may act on other VDAC isoforms such as VDAC2 or VDAC3 given their structural similarity to VDAC1 (Messina et al., 2012; Raghavan et al., 2012).

The global role of VDAC as well as the individual function of its isoforms in brain mitochondria are poorly understood. This is due to small number of studies performed on brain VDAC since there are no known compounds with demonstrable selectivity limited to an isoform of VDAC. Conversely, the function of VDAC has extensively been studied *in vitro* using VDAC reconstituted in artificial bilayer membranes. In these studies, VDAC has been shown to be permeable to Na^+, Cl^-, Ca^{2+} and metabolites such as ATP^{4-} or ADP^{3-} (Liobikas et al., 2001; Tan and Colombini, 2007; Tan et al., 2007a). Furthermore, blockade of VDAC with phosphorothioate oligonucleotides (POL) such as S18 randomer (S18) or G3139 has been shown to alter Ca^{2+}-mediated mitochondrial swelling as well as the transport of ADP in liver mitochondria (Tan et al., 2007a; Tikunov et al., 2010).

Measuring mitochondrial swelling by absorbance is a method commonly used to investigate the opening of the mitochondrial permeability transition pore (mPTP), an inner membrane mega channel (Wong et al., 2012). During Ca^{2+}-induced swelling, Ca^{2+} accumulates in the matrix and triggers opening of the mPTP, which in turn induces water uptake causing mitochondrial swelling (Halestrap, 2009). Another consequence of mPTP opening, is the release into the cytosol of mitochondrial proteins triggering apoptosis such as cytochrome C (Grancara et al., 2012; Kobayashi et al., 2003; Tan, 2012). Despite extensive studies, the molecular identity of mPTP remains poorly defined. Pharmacological studies in liver mitochondria suggest that mitochondrial VDAC may act as a regulator of mitochondrial permeability transition (mPT) (Tikunov et al., 2010). However, there are no pharmacological studies that investigated the role VDAC on the opening of mPTP in brain mitochondria.

Since CBD inhibits the conductance of reconstructed VDAC on artificial bilayer membranes and that VDAC inhibitors/blockers (e.g. POL) exhibit the same effect on reconstructed VDAC, I hypothesised that the effect of CBD should be consistent with that of VDAC blocker on both Ca^{2+}-induced mitochondrial swelling and Ca^{2+}-induced cytochrome C release. In the present study, I aim to determine the role of VDAC in the regulation of mPT in non-synaptic mitochondria (NS-mito) using the VDAC blocker S18. Furthermore, I investigate biochemical changes in NS-mito caused by epilepsy. Finally, I investigate whether the effect of CBD is consistent with that of S18 on Ca^{2+}-induced mitochondrial swelling and cytochrome C (Cyt C) release in both NS-mito isolated from healthy (NS-$mito_{HE}$) and epileptic (NS-$mito_{EP}$) rats.

4.2 RESULTS

4.2.1 CBD INCREASES Ca^{2+}-MEDIATED MITOCHONDRIAL SWELLING IN NS-$MITO_{EP}$

To address the question whether CBD (10 µM) or S18 (3 µM) are exerting any effect on Ca^{2+}-mediated mitochondrial permeability transition (mPT) in NS-mito from healthy (NS-$mito_{HE}$) or epileptic rats (NS-$mito_{EP}$), their effects were assessed on Ca^{2+}-mediated mitochondrial swelling. Mitochondrial swelling increased in both NS-$mito_{HE}$ and NS-$mito_{EP}$ as $CaCl_2$ (200 µM) is added (Fig. 4-1A & 4-1B). However, these results show that NS-$mito_{EP}$ exhibited lesser level of swelling than NS-$mito_{HE}$ ($Q<0.05$, HE-Veh2: 35±1.9, N=12 *vs*. EP-Veh2: 26±2.8, N=13) (Fig. 4-1C). Treatment of NS-$mito_{HE}$ with the mPTP inhibitor CsA (9.5 µM) causes partial reduction of mitochondrial swelling ($Q<0.05$, HE-Veh2: 35±1.9, N=12 *vs*. HE-CsA: 13±3.3, N=12) (Fig. 4-1A & 4-1C). Conversely, CsA exerted no effect on NS-$mito_{EP}$ ($Q>0.05$, EP-Veh2: 26±2.8, N=13 *vs*. EP-CsA: 21±2.4, N=11) (Fig. 4-1B & 4-1C). Comparison between CsA-treated NS-$mito_{HE}$ and CsA-treated NS-$mito_{EP}$ showed no significant difference

(Q>0.05, HE-CsA: 13±3.3, N=12 *vs*. EP-CsA: 21±2.4, N=11) (Fig. 4-1C). Blockade of VDAC with S18 (3 µM) exacerbated Ca^{2+}-induced swelling in both NS-mito$_{HE}$ (Q<0.05, HE-Veh2: 35±1.9, N=12 *vs*. HE-S18: 60±5.4, N=13) and NS-mito$_{EP}$ (Q<0.05, EP-Veh2: 26±2.8, N=13 *vs*. EP-S18: 49±4.0, N=11) (Fig. 4-1C). Furthermore, Ca^{2+}-induced mitochondrial swelling was decreased in NS-mito$_{EP}$ compared to that of NS-mito$_{HE}$ (Q<0.05, HE-S18: 60±5.4, N=13 *vs*. EP-S18: 49±4.0, N=11) (Fig. 4-1C). Treatment of NS-mito$_{HE}$ with CBD (10 µM) did not affect Ca^{2+} mediated swelling (Q>0.05, HE-Veh2: 35±1.9, N=12 *vs*. HE-CBD: 31±3.6, N=12) (Fig. 4-1C), although CBD increased Ca^{2+}-induced swelling in NS-mito$_{EP}$ (Q<0.05, EP-Veh2: 26±2.8, N=13 *vs*. EP-CBD: 36±3.2, N=13) (Fig. 4-1C). NS-mito$_{EP}$ treated with CBD exhibited lesser swelling than NS-mito$_{EP}$ treated with S18 (Q<0.05, EP-CBD: 36±3.2, N=13 *vs*. EP-S18: 49±4.0, N=13) and NS-mito$_{HE}$ treated with S18 (Q<0.05, EP-CBD: 36±3.2, N=13 *vs*. HE-S18: 60±5.4, N=13) but showed no differences with veh2 treated NS-mito$_{HE}$ (Q<0.05, HE-Veh2: 35±1.9, N=12 *vs*. EP-CBD: 36±3.2, N=13) (Fig. 4-1C). In conclusion, CBD increased Ca^{2+}-induced mitochondrial swelling in NS-mito$_{EP}$ but exhibited no effect on NS-mito$_{HE}$. Conversely, blockade of VDAC with S18 exacerbated mitochondrial swelling in both NS-mito$_{HE}$ and NS-mito$_{EP}$ although the magnitude of Ca^{2+}-mediated swelling was reduced in NS-mito$_{EP}$.

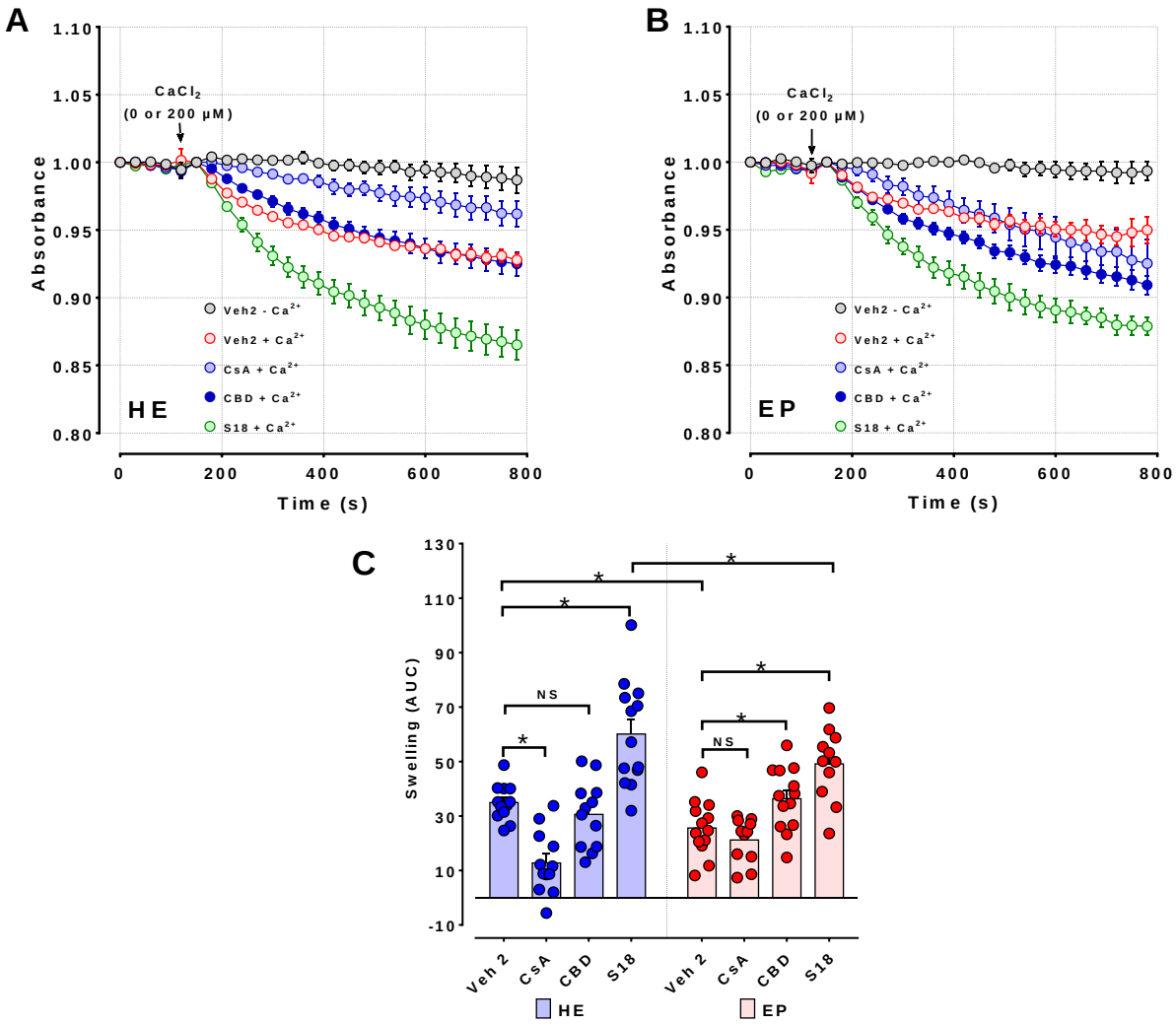

Figure 4-1. CBD as well as S18 increase $CaCl_2$-induced mitochondrial swelling in non-synaptic mitochondria from hippocampi (NS-mito) of epileptic rats while NS-mito from healthy rats are not affected by CBD treatment. NS-mito (800 µg/ml protein) from healthy (HE) and epileptic (EP) rats were energised with 5 mM succinate and pre-treated (7-10 min) with either vehicle (Veh2; 0.03% DMSO), CsA (9.5 µM), CBD (10 µM) or S18 (3 µM). Mitochondrial swelling was determined by measuring decrease in absorbance following addition of $CaCl_2$ (200 µM). Plot of traces illustrating mitochondrial swelling in NS-mito from (A) HE and (B) EP. (C) The effect of different drug treatments in both NS-mito from HE and EP on the magnitude of mitochondrial swelling. (C) Each measurement (data point) was obtained from individual rat. Results are expressed as mean ± SEM. Upon statistical difference using two-way ANOVA ($P<0.05$), multiple comparisons were performed using BKY pairwise comparisons. Discovery of statistical difference was determined with the Q-value (*$Q<0.05$). Only essential

comparisons are presented on the bar graph (see appendix for more details). NS, non-significant.

4.2.2 CBD EXHIBITS NO ADDITIVE EFFECT TO S18 TREATMENT ON Ca^{2+}-INDUCED MITOCHONDRIAL SWELLING IN NS-$MITO_{EP}$

Our previous results showed that CBD exhibited a weaker effect on Ca^{2+}-mediated swelling compared to S18. Given the possibility that CBD may target at least one of VDAC isoforms, namely VDAC1 (Rimmerman et al., 2013), I investigated whether the combined treatment of S18 and CBD exhibited a similar effect on mitochondrial swelling in NS-$mito_{EP}$ as that of S18 alone. Since it has been reported by Tan el al., that 20 µM of POL is required to reduce 60% of VDAC's probability of opening, while 3 µM of POL would decrease only 20% of VDAC's probability of opening (Tan et al., 2007a), expected high concentration of S18 (high-S18; 20 µM) to exhibit a greater level of Ca^{2+}-induced swelling than that of low concentration S18 (low-S18; 3 µM). Consequently, Ca^{2+}-mediated swelling induced by low-S18 was not expected to reach maximal swelling allowing the possibility for CBD to exert an additive effect to low-S18 if CBD was not acting through VDAC. Here the effect of both high-S18 and low-S18 on Ca^{2+}-mediated mitochondrial swelling were assessed in the presence or absence of CBD treatment (10 µM) (Fig. 4-2A & 4-2B). This work shows that treatments with high-S18 ($Q>0.05$, EP-Veh2: 27±4.4, N=8 *vs.* EP-highS18: 42±5.1, N=7) or with a combination of high-S18 and CBD (10 µM) (high-S18/CBD) ($Q>0.05$, EP-Veh2: 27±4.4, N=8 *vs.* EP-highS18/CBD: 38±3.8, N=8) had no significant effect on the overall Ca^{2+} mediated mitochondrial swelling in NS-$mito_{EP}$ (Fig. 4-2B). However, treatments with low-S18 ($Q<0.05$, EP-Veh2: 27±4.4, N=8 *vs.* EP-lowS18: 48±3.2, N=8) or with the combined treatment of low-S18 and CBD (10 µM) (low-S18/CBD) ($Q<0.05$, EP-Veh2: 27±4.4, N=8 *vs.* EP-lowS18/CBD: 51±7.5, N=8) enhanced the overall magnitude of Ca^{2+} mediated swelling(Fig. 4-2B). The addition of CBD to either low-S18

or high-S18 did not alter their effect on Ca^{2+}-induced mitochondrial swelling in NS-mito$_{EP}$ (Fig. 4-2A & 4-2B). Pre-treatment of NS-mito$_{EP}$ with low-S18 and with low-S18/CBD resulted in enhanced mitochondrial swelling at 270 and 300 s following onset mPT with Ca^{2+} (Fig. 4-2A, 4-2C & 4-2D). Conversely, Ca^{2+}-induced mitochondrial swelling increases with a greater latency (at 360 s) after mPT in NS-mito$_{EP}$ treated with either high-S18 high-S18/CBD (Fig. 4-2A, 4-2E & 4-2F). Although the overall swelling (determined by the area under the curve) induced by both high-S18 and high-S18/CBD are not significantly different from that of Veh2 treatment, I showed that swelling is increased in both high-S18 and high-S18/CBD compared to Veh2 treatment only at later stages after onset of mPT with Ca^{2+}. In summary, CBD modulates the effect of neither low-S18 nor high-S18 on Ca^{2+}-induced mitochondrial swelling in NS-mito$_{EP}$. It is plausible that even low-S18 treated NS-mito$_{EP}$ have reached a maximal level of swelling although 3 µM of S18 is supposed to inhibit only 20 % of VDAC activity.

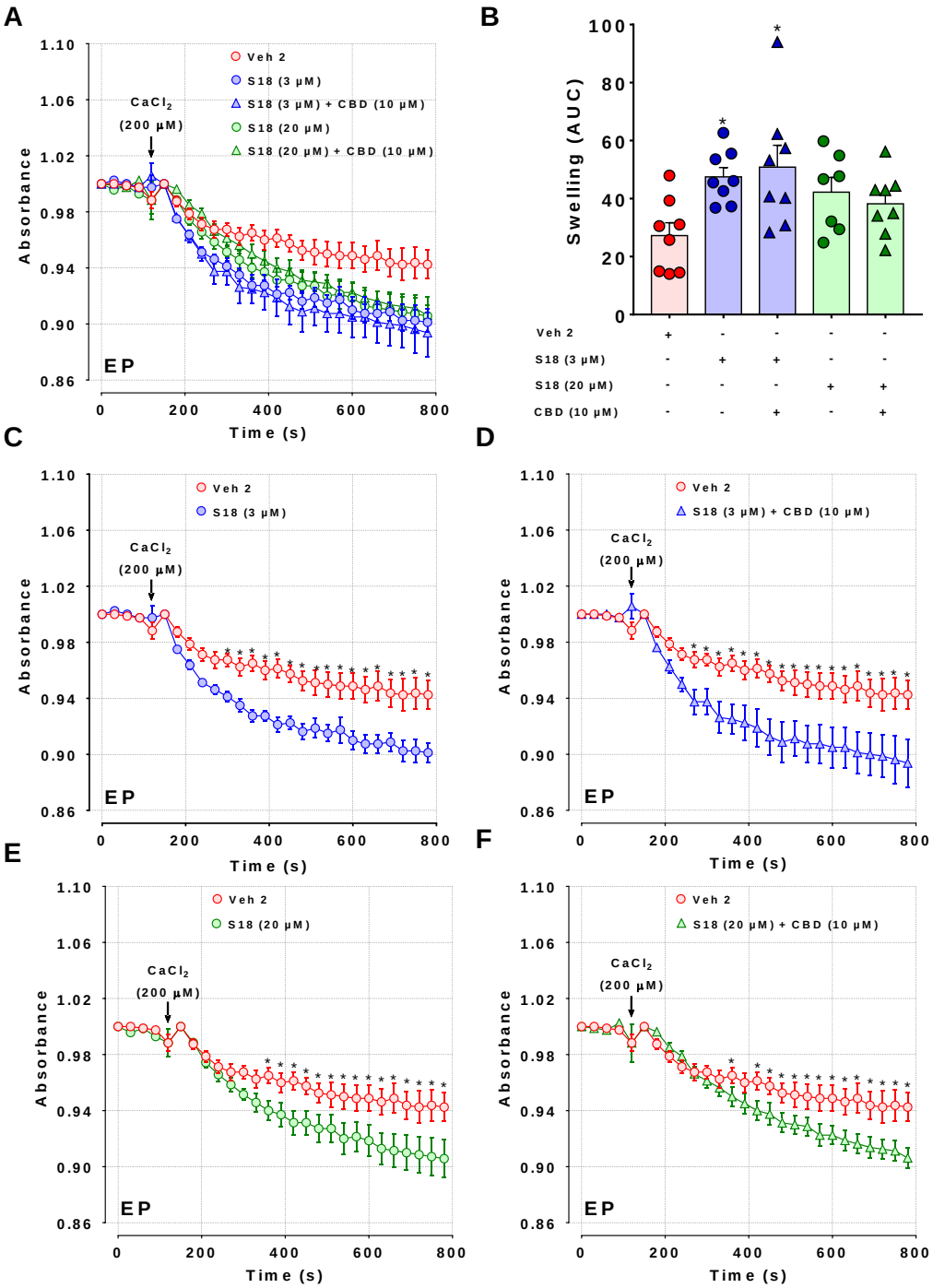

Figure 4-2. Ca^{2+}-induced swelling in NS-mito$_{EP}$ treated with a combination of CBD and S18 does not differ from that of NS-mito$_{EP}$ treated with S18 alone. NS-mito (800 µg/ml protein) from epileptic (EP) rats were energised with 5 mM succinate and pre-treated (7-10 min) with either S18 alone or with both S18 and CBD. Mitochondrial swelling was determined by measuring decrease in absorbance following addition of $CaCl_2$ (200 µM). (A) Plot of traces showing the decrease in absorbance following Ca^{2+}-induced mitochondrial swelling in the presence of different combination of drugs treatment. (B) The effect of drug treatment on

the magnitude of mitochondrial swelling in NS-mito$_{EP}$. (B) Each measurement (data point) was obtained from individual rat. (C) Plot of traces showing the effect of S18 (3 μM) compared to Veh2. (D) Plot of traces showing the combine effect of S18 (3 μM) and CBD (10 μM) compared to Veh2. (E) Plot of traces showing the effect of S18 (20 μM) compared to Veh2. (F) Plot of traces showing the combine effect of S18 (20 μM) and CBD (10 μM) compared to Veh2. Upon statistical difference using one-way or two-way ANOVA ($P<0.05$), multiple comparisons were performed using BKY pairwise comparisons. Discovery of statistical difference from Veh2 treatment was determined with the Q-value (*$Q<0.05$). Results are presented as mean ± SEM.

4.2.3 PROTEIN EXPRESSION IN HIPPOCAMPI OF EPILEPTIC RATS

In this study, immunoreactions of all proteins of interest were normalised to that of NDUFS1, as I demonstrated that the latter was a more reliable (with minimal variability across samples) loading control compared to COX-IV (Table 2-2 & Fig. 2-6).

4.2.3.1 EXPRESSION OF VDAC1

To assess whether the effect of CBD can be associated with potential changes of VDAC1 expression in the RISE-SRS model of TLE, I assessed VDAC1 expression in hippocampal tissue, NS-mito and synaptosomes (SYN) using western blot. VDAC1 expression remains unchanged (P>0.05, HE: 100±8.2, N=6 *vs.* EP: 93±12.6, N=7) in the hippocampal tissue of epileptic rats (Fig. 4-3A & 4-3B). Analysis of VDAC1 expression in NS-mito also showed no change in NS-mito$_{EP}$ compared to NS-mito$_{HE}$ (P>0.05, HE: 100±8.1, N=7 vs. EP: 103±8.3, N=7) (Fig. 4-5A & 4-5B). Furthermore, VDAC1 expression in hippocampal SYN from healthy rats does not differ from that of epileptic rats (P>0.05, HE: 100±7.8, N=4 vs. EP: 116.5±29, N=4) (Fig. 4-6A & 4-6B).

4.2.3.2 EXPRESSION OF NADH-UBIQUINONE OXIDOREDUCTASE CHAIN 4

NADH-ubiquinone oxidoreductase chain 4 (ND4) is a protein of complex I that is synthesised from mitochondrial genome. To evaluate a potential dysfunction of OXPHOS due to abnormal translation in mitochondria from rat with TLE, I investigated the change of ND4 expression in the RISE-SRS model of TLE. The overall expression of ND4 in hippocampi of epileptic rats did not differ from that of healthy rats (P>0.05, HE: 100±5.1, N=4 vs. EP: 100±5.5, N=4) (Fig. 4-4A & 4-4B). However, the expression of ND4 was significantly reduced in both NS-mito$_{EP}$ (P>0.05, HE: 100±5.9, N=7 vs. EP: 40±11.4, N=7) and SYN of epileptic rats (P>0.05, HE: 100±5.9, N=4 vs. EP: 40±11.4, N=4) (Fig. 4-5 & Fig. 4-6).

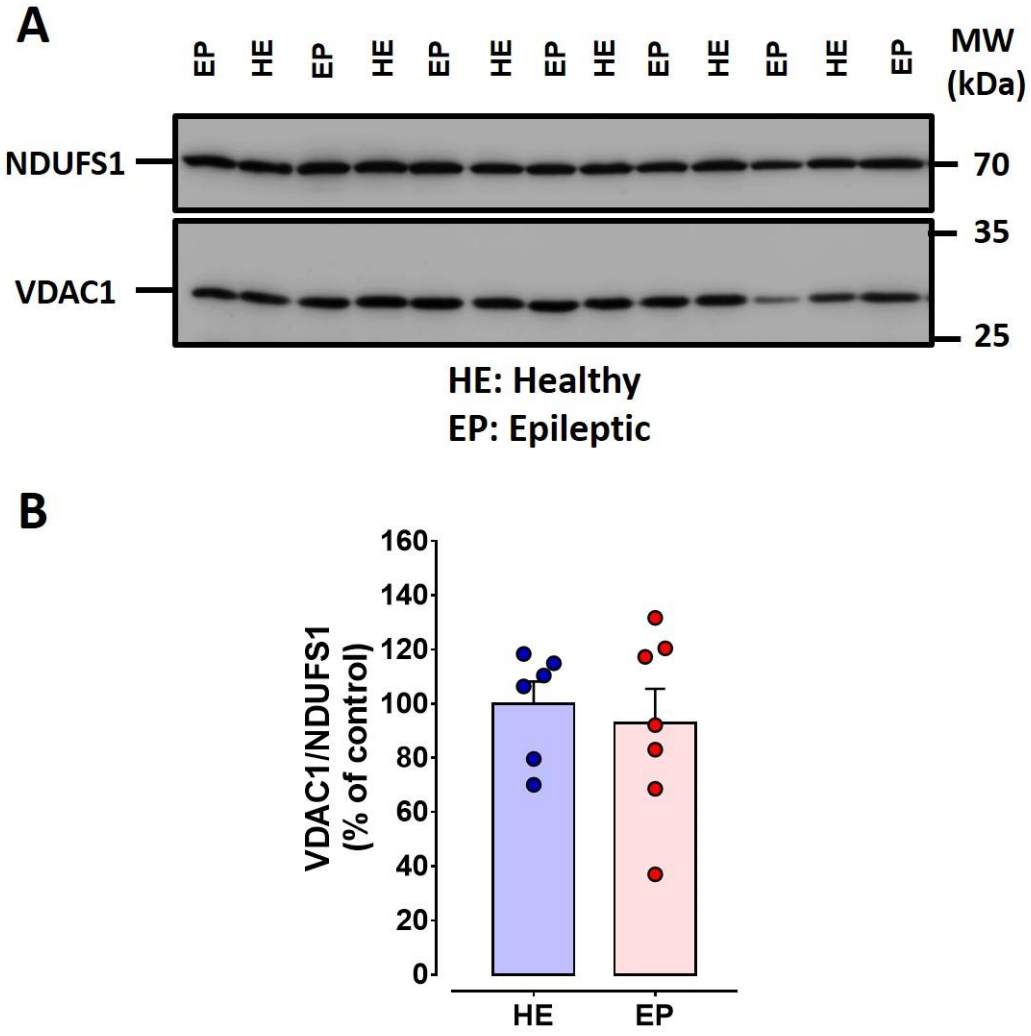

Figure 4-3. No change in VDAC1 expression in hippocampal tissue from epileptic rat. Proteins Lysates (50 µg) were denatured and reduced at 95°C for 3 min with SDS (2%) and β-mercaptoethanol (2.5%), respectively. NDUFS1 was used loading as control. (A) Immunodetection of NDUFS1 (75 kDa) and VDAC1 (31 kDa) in tissue from healthy (HE) and epileptic (EP) rats. Intensities of immunoreactions were determined by densitometry. (B) No change of VDAC1 expression in hippocampal tissue from EP rats. Statistical difference was determined using Mann-Whitney test (*P<0.05). Each measurement (data point) was obtained from individual rat. Results are presented as mean ± SEM.

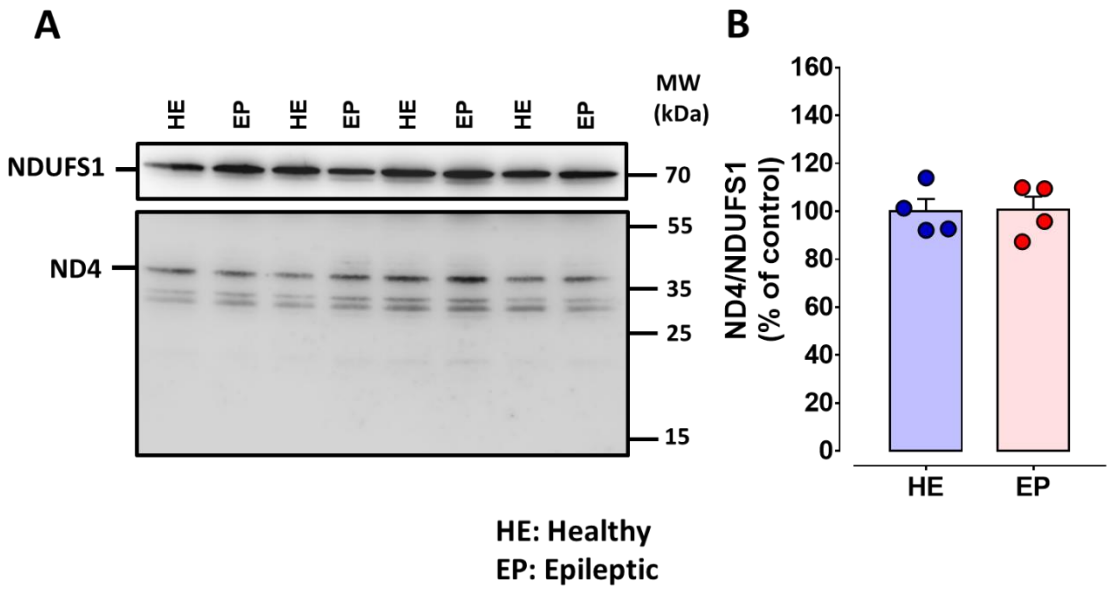

Figure 4-4. No change in ND4 expression in hippocampal tissue from epileptic rat. Proteins from tissue lysate (50 µg) were denatured and reduced at 95℃ for 3 min with SDS (2%) and β-mercaptoethanol (2.5%), respectively. NDUFS1 was used as loading control. (A) Immunodetection of NDUFS1 (75 kDa) and ND4 (55 kDa, but ~40 kDa in 12% polyacrylamide gel) in tissue from healthy (HE) and epileptic (EP) rats. Intensities of immunoreactions were determined by densitometry. (B) No change of ND4 expression in hippocampal tissue from EP rats. Statistical difference was determined using Mann-Whitney test (*P<0.05). Each measurement (data point) was obtained from individual rat. Results are presented as mean ± SEM.

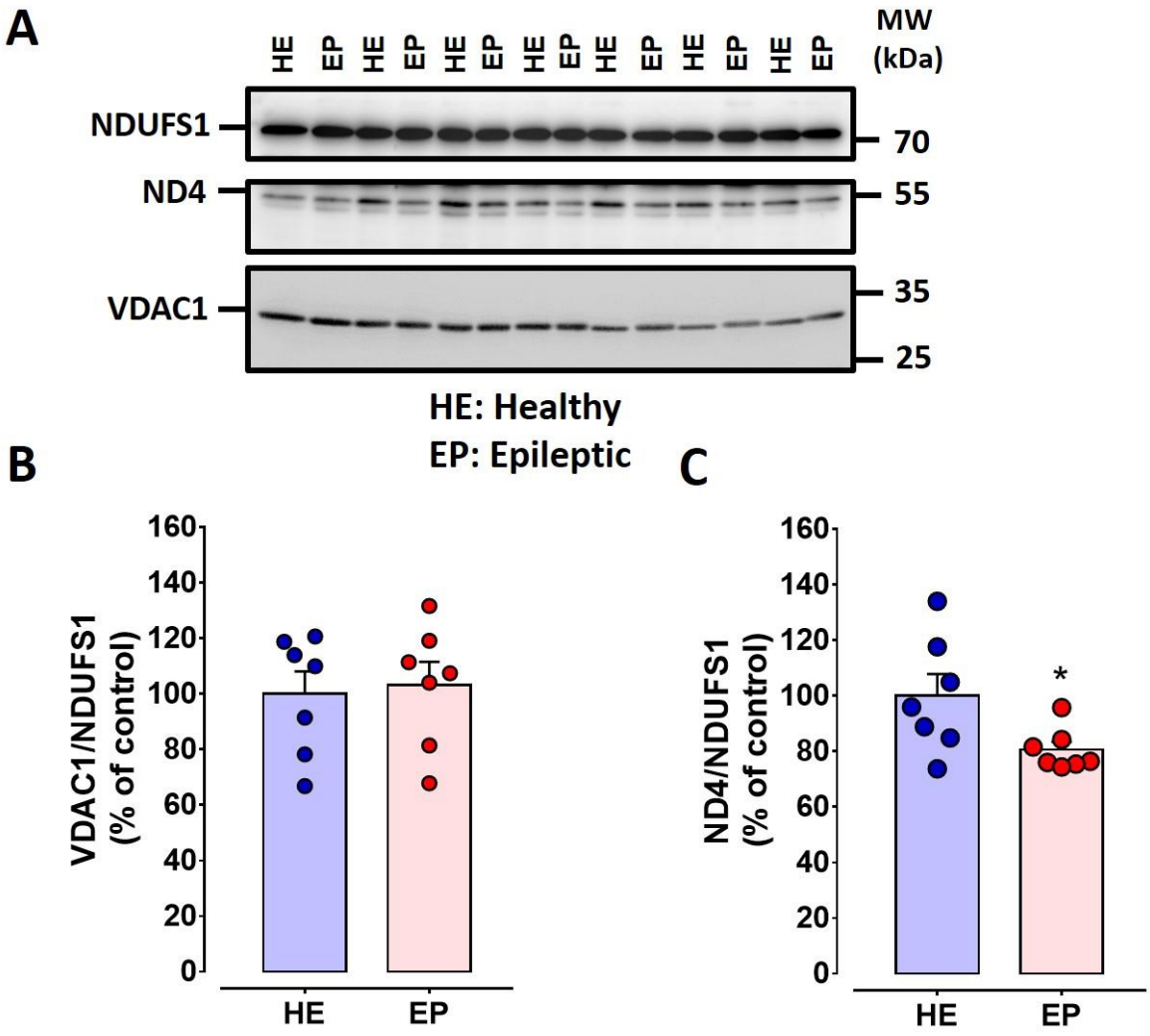

Figure 4-5. Reduction of ND4 expression but no change in VDAC1 expression in hippocampal non-synaptic mitochondria (NS-mito) from epileptic rat. Proteins from NS-mito lysate (20 µg) were denatured and reduced at 95℃ for 3 min with SDS (2%) and β-mercaptoethanol (2.5%), respectively. NDUFS1 was used as loading control. (A) Immunodetection of NDUFS1 (75 kDa), VDAC1 (31 kDa) and ND4 (55 kDa) in NS-mito from healthy (HE) and epileptic (EP) rats. Intensities of immunoreactions were determined by densitometry. (B) No change of VDAC1 expression in NS-mito$_{EP}$. (C) Decrease of ND4 expression in NS-mito$_{EP}$. Statistical difference was determined using Mann-Whitney test (*P<0.05). Each measurement (data point) was obtained from individual rat. Results are presented as mean ± SEM.

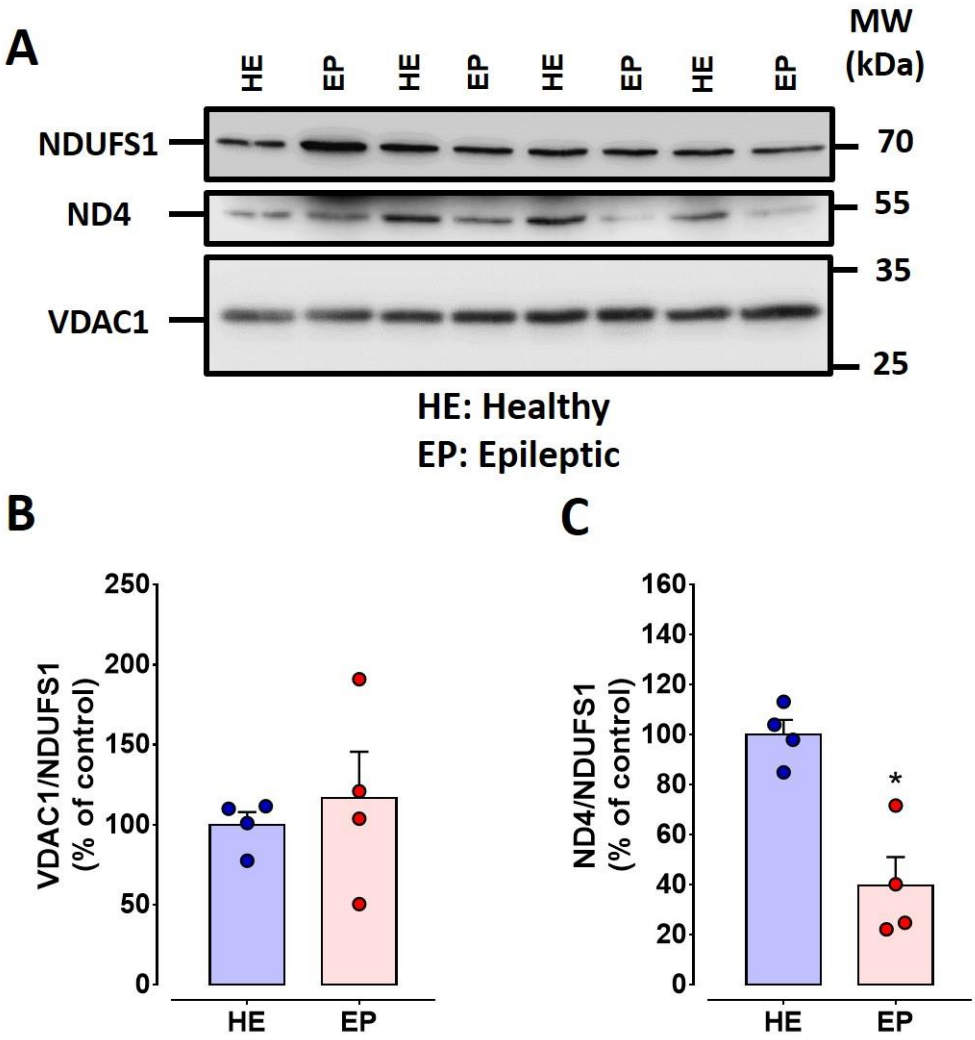

Figure 4-6. Reduction of ND4 expression but no change in VDAC1 expression in hippocampal synaptopsomes from epileptic rat. Synaptosomal proteins (SYN) (30 µg) were denatured and reduced at 95℃ for 3 min with SDS (2%) and β-mercaptoethanol (2.5%), respectively. NDUFS1 was used as loading control. (A) Immunodetection of NDUFS1 (75 kDa), VDAC1 (31 kDa) and ND4 (55 kDa) in SYN from healthy (HE) and epileptic (EP) rats. Intensities of immunoreactions were determined by densitometry. (B) VDAC1 expression was not changed in NS-mito$_{EP}$. (C) Decreased ND4 expression in the synaptosomes of EP rats. Statistical difference was determined using Mann-Whitney test (*P<0.05). Each measurement (data point) was obtained from individual rat. Results are presented as mean ± SEM.

4.2.4 CYTOCHROME C RELEASE FOLLOWING INDUCTION OF MPT IN NS-MITO$_{EP}$

Subsequently, I determined the effect of CBD (10 µM), CBDV (10 µM) and S18 (3 µM) on cytochrome C (Cyt C) release from NS-mito$_{EP}$ following induction of mPT with 200 µM Ca^{2+}. Treatment of NS-mito$_{EP}$ with CBD ($P>0.05$, EP-Veh2: 100±5.9, N=4 vs. EP-CBD: 40±11.4, N=4) or CBDV ($P>0.05$, EP-Veh2: 100±5.9, N=4 vs. EP-CBDV: 40±11.4, N=4) does not affect Cyt C release (compared to Veh2 treatment) (Fig. 4-7A & 4-7B). Conversely, closure/blockade of VDAC in NS-mito$_{EP}$ with S18 (3 µM) exacerbated Cyt C release (compared to Veh2 treatment) ($P>0.05$, EP-Veh2: 100±5.9, N=4 vs. EP-S18: 40±11.4, N=4) (Fig. 4-7A & 4-7B).

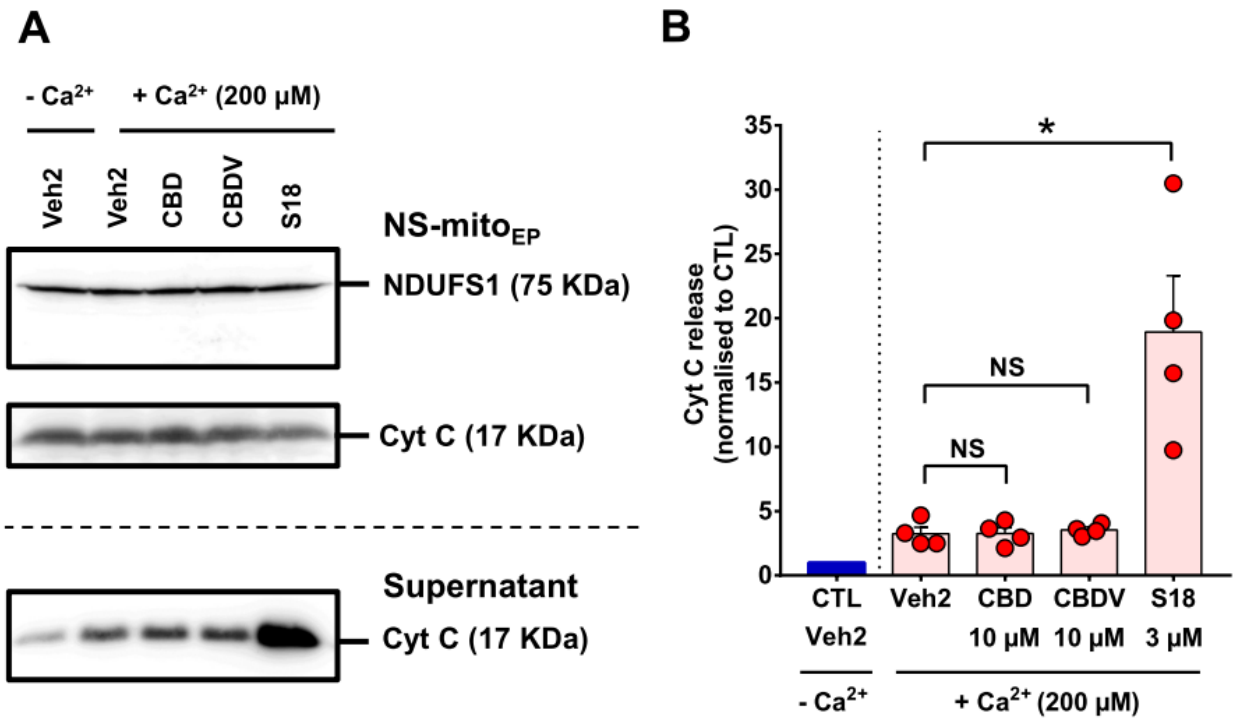

Figure 4-7. Blockade of VDAC with S18 increases cytochrome C release in NS-mito$_{EP}$ following induction of mPT with Ca^{2+}. NS-mito (800 µg/ml protein) from epileptic (EP) rats were energised with 5 mM succinate and pre-treated (10 min) with either vehicle (Veh2; 0.03% DMSO), CBD (10 µM), CBDV (10 µM) or S18 (3 µM). $CaCl_2$ (200 µM) was then added to mitochondrial suspension and were allowed to incubate for another 10 min. The supernatant was separated from NS-mito$_{EP}$ by centrifugation (14,000 *g*, 10 min). Proteins in the supernatant (40 µl/well) were denatured and reduced at 95°C for 3 min with SDS (2%) and β-mercaptoethanol (2.5%). (A) Immunodetection of NDUFS1 (in NS-mito$_{EP}$) and Cyt C (in NS-mito$_{EP}$ and supernatant). (B) Level of cyt C in the supernatant following induction of mPT in NS-mito$_{EP}$ the presence of different drug treatment. The intensity of Cyt C immunoreaction was determined by densitometry. Upon statistical difference using Kruskal-Wallis ($P<0.05$), pairwise comparisons were performed using Dunn's multiple comparisons test. Differences from Veh2 treatment were determined with the P-value (*$P<0.05$). Each measurement was obtained from individual rat. Results are presented as mean ± SEM. The control group (CTL) was not treated with Ca^{2+} and served to normalised Cyt C release in other groups treated with Ca^{2+}. NS, non-significant.

4.3 DISCUSSION

Using NS-mito isolated from RISE-SRS rats, I demonstrated for the first time that Ca^{2+}-mediated mitochondrial swelling is reduced in NS-mito$_{EP}$ compared to NS-mito$_{HE}$ while VDAC expression is unaffected by epilepsy. As CBD (10 µM) is directly applied to NS-mito$_{EP}$, it allows Ca^{2+}-induced swelling to return to a normal level (Veh2-treated NS-mito$_{HE}$). Given that CBD exhibits no effect on Ca^{2+}-induced swelling in NS-mito$_{HE}$ and that its effect on Ca^{2+}-mediated Cyt C release differs from that of the VDAC blocker S18, it appears that CBD may not be acting though VDAC. Finally, I report here that CBDV doesn't exhibit any effect on Ca^{2+}-mediated Cyt C release in NS-mito$_{EP}$.

4.3.1 MITOCHONDRIAL SWELLING MEDIATED BY Ca^{2+} IN NS-MITO FROM RATS

4.3.1.1 Ca^{2+}-INDUCED SWELLING IN NS-MITO

For a long time, it was known that exposure of mitochondria to high levels of Ca^{2+} induces mitochondrial swelling, but it is only in the early 90's that the mechanism was shown to involve opening of the mPTP (Lehninger, 1962; Szabó and Zoratti, 1991, 1992; Szabó et al., 1992). Effectively, overload of Ca^{2+} in mitochondrial matrix does not only renders the matrix hypertonic, but it also triggers the opening of mPTP which together subsequently result in water uptake (as matrix become hypertonic), thus causing mitochondria to swell (Lehninger, 1962; Szabó and Zoratti, 1991, 1992; Szabó et al., 1992). Although mPTP inhibition with CsA does not prevent Ca^{2+} uptake in mitochondria, it significantly reduces swelling thus demonstrating that the route of water uptake is mPTP (Hansson et al., 2011). The degree of swelling mediated by Ca^{2+} in NS-mito is consistent with that of brain mitochondria observed in other laboratories (Brustovetsky et al., 2002, 2003; Galindo et al., 2003; Kobayashi et al., 2003; Naga and Geddes, 2011). In the presence of Ca^{2+}, mitochondria isolated from the brain

exhibit a reduced amplitude of swelling compared to mitochondria isolated from other tissues (Brustovetsky et al., 2002, 2003; Galindo et al., 2003; Kobayashi et al., 2003; Naga and Geddes, 2011). Swelling mediated by Ca^{2+} can be increased in brain mitochondria when the latter are exposed to channel-forming peptide such as alamethicin (Brustovetsky et al., 2002; Kobayashi et al., 2003). This demonstrates that "rupturing" the outer-membrane cause brain mitochondria to reach maximal swelling following Ca^{2+}-mediated mPTP opening (Brustovetsky et al., 2002; Kobayashi et al., 2003). Similarly, in my study I demonstrated that blockade of VDAC in NS-mito$_{HE}$ increased Ca^{2+}-mediated swelling. Given the low magnitude of swelling in these NS-mito$_{HE}$, it is plausible that these mitochondria accumulate a limited amount of water following the induction of mPTP opening because small quantities of ions accumulate in the matrix.

4.3.1.2 Ca^{2+}-INDUCED APOPTOSIS IN NS-MITO

MPT can induced mitochondrial release of cytochrome C (Cyt C) into the cytosol which in turn activates the intrinsic pathway of apoptosis. Given that mPTP opening is activated with high Ca^{2+}, it is essential that brain mitochondria should be more resistant to Ca^{2+}-induced mPT as there is regular need of high cytosolic Ca^{2+} to allow neurotransmission and synaptic plasticity. Interestingly, at equal amount of Ca^{2+}, brain mitochondria release less Cyt C than liver mitochondria (Kobayashi et al., 2003), suggesting that mitochondria from brain tissue may be less susceptible to Ca^{2+}-mediated apoptosis. Although the mechanism underlying the resistance of brain mitochondria to apoptosis remains undetermined, it is likely that their high-threshold susceptibility to swell may play a critical role (Kobayashi et al., 2003).

4.3.1.3 *Cyclophilin D and regulation of rat NS-mito mPTP*

The molecular composition of the mPTP in NS-mito may differ from mitochondria of other tissue type. In liver mitochondria, low levels (1 µM) of the cyclophilin D (CypD) inhibitor cyclosporin A (CsA) are sufficient to completely repress Ca^{2+} induced mitochondrial swelling (Basso et al., 2005; Kanno et al., 2004; Kim et al., 2015; Szabó and Zoratti, 1991). In this study, I use a high concentration of CsA (9.5 µM) which was required to achieve only partial inhibition of mitochondrial swelling in NS-mito$_{HE}$. This result is consistent with other studies performed on brain mitochondria, which demonstrated that even at high concentrations (5-10 µM), CsA only partially inhibits mitochondrial swelling mediated by Ca^{2+} (100-250 µM) (Brustovetsky et al., 2002; Hansson et al., 2011; Kim et al., 2015; Kobayashi et al., 2003; Naga and Geddes, 2011). Given that CsA treatment is less effective in inhibiting mitochondrial swelling in brain mitochondria, it is plausible that CypD may not play a significant role in the regulation of brain mPTP closure compared to non-brain mPTP.

4.3.2 Metabolic impairment of mitochondria in epilepsy

My study demonstrated a metabolic dysfunction in both synaptic mitochondria (S-mito) and NS-mito$_{EP}$. The expression of NADH-ubiquinone oxidoreductase chain 4 (ND4), a component of complex I, was significantly reduced in S-mito and NS-mito of rats with TLE. ND4 is encoded by mitochondrial DNA, thus any alteration of its expression suggests an impairment of complex I function as well as a dysfunction of translation (protein synthesis) in mitochondria. Mutation and loss of function of the *ND4* gene causes epilepsy (Finsterer and Zarrouk Mahjoub, 2012; Guerriero et al., 2011; Wang et al., 2017). My finding suggests that alteration of ND4 expression may contribute to the pathophysiology of TLE. Therefore, it is plausible that ND4 may be an important target for future pharmacotherapies of epilepsy.

4.3.3 IMPAIRMENT OF MITOCHONDRIAL SWELLING IN EPILEPSY

This work demonstrates that mPT is inducible in NS-mito$_{EP}$ (with high concentration of Ca^{2+}) but the amplitude of Ca^{2+}-induced mitochondrial swelling was reduced in NS-mito$_{EP}$ compared to that of NS-mito$_{HE}$. In the sections below, I will be discussing potential mechanisms which could explain the difference between mPT in NS-mito$_{EP}$ and that of NS-mito$_{HE}$.

4.3.3.1 MITOCHONDRIAL SWELLING AND MEMBRANE ELASTICITY

Biochemical alterations in NS-mito$_{EP}$ may alter mechanical (biophysical) proprieties of mitochondrial membrane by reducing their elasticity (Frolov et al., 2011; Harayama and Riezman, 2018; Heimburg, 2009; Lee, 1975). Consequently, this may lead to reduced swelling in NS-mito$_{EP}$. Consistent with this hypothesis, lipid composition alterations in brain mitochondria membrane have been observed in another model of epilepsy, namely the picrotoxin kindling model of epilepsy (Acharya and Katyare, 2005). This hypothesis remains speculative because similar studies have not been performed in models of TLE. In addition, there are no studies (to my knowledge) which explored the link between mitochondrial membrane elasticity and lipid composition (Frolov et al., 2011; Harayama and Riezman, 2018; Heimburg, 2009; Lee, 1975).

4.3.3.2 ALTERATIONS OF Ca^{2+}-INDUCED SWELLING MAY BE CAUSED BY IN SITU SWELLING OF MITOCHONDRIA IN EPILEPSY

Using electron microscopy, a variety of swollen mitochondria have been identified in the hippocampi of both kainic acid (KA) and pilocarpine rodent models of TLE (Chuang et al., 2004; Gao et al., 2007). My investigation demonstrated that the magnitude of Ca^{2+}-mediated swelling is reduced in NS-mito$_{EP}$. While in the hippocampus, it is plausible that NS-mito$_{EP}$ may

already be swollen, thus limiting the magnitude by which these mitochondria could swell further even in the presence of Ca^{2+}. The work of Kobayashi et al. showed that a second bolus Ca^{2+} could not further increase mitochondrial swelling (Kobayashi et al., 2003). Taken together, this is consistent with the hypothesis that Ca^{2+} is not very effective in inducing mitochondrial swelling when the latter are already swollen before isolation from brain tissue (*in situ*).

4.3.4 Impairment of mPTP in epilepsy

To examine the integrity of NS-mito$_{EP}$ mPTP, I investigated the effect of the mPTP inhibitor CsA on Ca^{2+}-induced swelling. Although CsA partially inhibits mitochondrial swelling in NS-mito$_{HE}$, I demonstrated that CsA treatment is unable to inhibit mitochondrial swelling in NS-mito$_{EP}$. Other investigators have demonstrated the key role of CypD in regulating the threshold of the opening of mPTP in liver and brain mitochondria using CypD deficient *(ppif* $^{-/-}$) mice (Hansson et al., 2011). Given that CsA targets CypD to inhibit the opening of mPTP, this study provides evidence for the first time that CypD function in regulating the mPTP is impaired in NS-mito$_{EP}$ in this model of TLE (Basso et al., 2005; Kanno et al., 2004; Kim et al., 2015; Szabó and Zoratti, 1991). Recently, it has been established that NIM811 (an analogue of CsA) reduces the number of daily seizures in kcna1 deficient (*kcna1*$^{-/-}$) mice (Kim et al., 2015), indicating that inhibition of mPTP has anti-convulsant effects. Consistent with this, it has been demonstrated that the anti-convulsant effect of ketogenic diet in *kcna1*$^{-/-}$ mice is mediated through inhibition mPTP by targeting CypD (Kim et al., 2015).

Patients with epilepsy can exhibit cognitive impairments including memory deficit (Blake et al., 2000; Butler and Zeman, 2008; Helmstaedter and Kurthen, 2001; Mataró-Serrat and Junqué-Plaja, 1997; Zhao et al., 2014). Similarly, alterations of memory and long term

potentiation (LTP), have also been reported in various animal models of epilepsy such as in *kcna1*$^{-/-}$ mice and Li-pilo-induced TLE rats (Fares et al., 2013; Kim et al., 2015). The role of mPTP in synaptic plasticity remains uncertain. Some studies have demonstrated that targeting mPTP improves synaptic plasticity and memory in neurological diseases (e.g. dementia and epilepsy) (Du et al., 2008; Kim et al., 2015). Inhibition of mPTP with NIM811 or ketone bodies (e.g. β-hydroxybutyrate) reversed the decline of hippocampal LTP in *kcna1*$^{-/-}$ mice model of epilepsy (Kim et al., 2015). However, high concentration of CsA (10 µM) reduced the amplitude of fEPSP following LTP induction (Weeber et al., 2002), while lower concentrations (1 µM) alleviated the decline of LTP induced by amyloid-β in a CypD dependent manner (Du et al., 2008). It is not clear whether this controversial effect of CsA is due to its non-selective action, since CsA is also known to inhibit calcineurin, a phosphatase implicated in the activation of nuclear factor of activated T-cells (Erdmann et al., 2010).

4.3.5 Mitochondrial swelling and VDAC

I assessed whether the role of VDAC on mPTP was altered in NS-mito$_{EP}$ by investigating the effect of the VDAC blocker S18 on mitochondrial swelling mediated by Ca^{2+}. To date, aside from VDAC, there are no other channels in mitochondrial outer-membrane that has been implicated in mitochondrial Ca^{2+} uptake. Given that the initial step of mPT requires activation of mPTP with Ca^{2+} from its matrix side in the mitochondrial inner membrane (Szabó et al., 1992), blockade of VDAC with S18 was expected to inhibit Ca^{2+} mediated mitochondrial swelling. However, this study showed that blockade of VDAC increases Ca^{2+}-mediated mitochondrial swelling by more than two-fold in both NS-mito$_{HE}$ and NS-mito$_{EP}$. Several mechanisms could explain this result. First, the VDAC blocker S18 may not inhibit all isoforms of VDAC. In this scenario, Ca^{2+} uptake into mitochondrial matrix can be performed by VDAC

isoforms which are not inhibited. Secondly, it is possible that outer-membrane mitochondrial Ca^{2+} uptake may depend on non-VDAC route. Finally, whilst POL (e.g. S18) are known to induce VDAC closure, regardless of the membrane potential (Tan and Colombini, 2007; Tan et al., 2007a, 2007b), Ca^{2+} flux may occur during these VDAC closed states; as VDAC conducts Ca^{2+} currents at membrane voltages below -20 mV and above 20 mV (Tan and Colombini, 2007). Although my results demonstrated that S18 increase mitochondrial swelling in NS-mito, the work of Tikunov et al. showed that treatment of liver mitochondria with G3139 (another POL) decreased the threshold of the onset of Ca^{2+}-induced mPTP opening while the amplitude of mitochondrial swelling remained unaffected (Tikunov et al., 2010). Interestingly, Tikunov et al. demonstrated that Ca^{2+} uptake was not prevented in liver mitochondria treated with G3139 (Tikunov et al., 2010).

4.3.6 VDAC1 EXPRESSION IN EPILEPSY

In this study, I showed that VDAC1 expression was not affected in this model TLE. This result is in conflicts with Jian et al.'s observation who showed that the expression of VDAC1 was reduced in a mouse kindling model of pharmacoresistant seizures (Jiang et al., 2007). This suggests that there may be pathophysiological differences between this model of TLE and that their kindling model. While the expression of VDAC1 does not change in NS-mito$_{EP}$, I showed that the effect of VDAC blockade (with S18) on Ca^{2+}-mediated swelling was reduced in NS-mito$_{EP}$ compared to that of S18-treated NS-mito$_{HE}$. The significance of the function of hippocampal VDAC1 in comparison to that of VDAC2 and VDAC3 remains uncertain. While it has been established that VDAC1 is involved in mitochondrial transport of metabolites (e.g. ATP^{4-} or ADP^{3-}) (Anflous et al., 2001; Choudhary et al., 2014), studies performed on VDAC1-deficient mice suggest that VDAC2 and VDAC3 can compensate for the lack of VDAC1

(Anflous-Pharayra et al., 2011; J Sampson et al., 2001; Messina et al., 2012). Furthermore, long term potentiation in hippocampal CA1 pyramidal neuron is not impaired in mice lacking VDAC1 or VDAC3 (Weeber et al., 2002). However, it appears that VDAC2 may play a more essential role compared to VDAC1 or VDAC3 since its absence is lethal *in utero* (Cheng et al., 2003). The difference of mitochondrial swelling between S18-treated NS-mito$_{EP}$ and S18-treated NS-mito$_{HE}$ could be due to a change in expression of either VDAC2 or VDAC3 in NS-mito$_{EP}$. Consistent with this, it has been demonstrated that VDAC2 is upregulated in the hippocampi of rodent model of TLE (Liu et al., 2008).

4.3.7 Mechanism of action of CBD

In my previous chapter (chapter 3), I demonstrated that CBD induces weak uncoupling of NS-mito$_{EP}$. Here, I report that CBD increases Ca^{2+}-induced swelling in NS-mito$_{EP}$ (to normal level) but does not affect Ca^{2+}-mediated mitochondrial swelling in NS-mito$_{HE}$. It appears that CBD may act on NS-mito$_{EP}$ independently from VDAC as its effect on Ca^{2+}-mediated swelling and Ca^{2+}-mediated Cyt C release in NS-mito$_{EP}$ differs from that of the VDAC blocker S18. In addition, CBD could not alter the effect of S18 on Ca^{2+}-induced swelling in NS-mito$_{EP}$ because maximal mitochondrial swelling may have been triggered with 3 µM S18 although this concentration is known to inhibit only 20% of the opening probability of VDAC (Tan et al., 2007a).

The mechanism by which S18 exacerbates Ca^{2+}-mediated mitochondrial swelling may be due to the "rupture" of the outer-membrane and accumulation of free radicals (e.g. superoxide ion) in mitochondria. I report here that S18 induces an increased permeability ("rupture") in the outer-membrane of NS-mito$_{EP}$ since Cyt C was excessively released under this condition. Furthermore, VDAC inhibition was shown to cause accumulation of superoxide

ion in mitochondria which in turn could contribute to exacerbate of mitochondrial swelling (Tikunov et al., 2010).

CBD does not prevent Ca^{2+} uptake in either NS-mito$_{HE}$ or NS-mito$_{EP}$ as extra-mitochondrial Ca^{2+} is required to be transported in the matrix to induced mPT (Lehninger, 1962; Szabó and Zoratti, 1991, 1992; Szabó et al., 1992). While CBD increases Ca^{2+}-mediated mitochondrial swelling in NS-mito$_{EP}$, it does not appear to "rupture" the outer-membrane since the level of Cyt C release was not affected. The mechanism by which CBD induces the increase of mitochondrial swelling in NS-mito$_{EP}$ may be due to its effect on H^+ leak (see chapter 3) as uncoupling agents also induce mitochondrial swelling (Kowaltowski et al., 1996; Mellors et al., 1967; Schönfeld et al., 2000). It is plausible that the increase of Ca^{2+}-mediated mitochondrial swelling in CBD-treated NS-mito$_{EP}$ could be caused by accumulation of H^+ in the matrix. CBD could target one of several inner-membrane H^+ transporters/channels which could result in CBD-induced H^+ uptake. For example, uncoupling proteins (UCPs), inorganic phosphate carrier symporter (PiC) or H^+ antiporters such as Ca^{2+}/H^+ exchanger (CHX), Na^+/H^+ exchanger (NHX), K^+/H^+ exchanger (KHX) are localised in the inner-membrane of mitochondria and are known to induce H^+ uptake (Santo-Domingo and Demaurex, 2012). In neurons and glia cells, CBD was shown to promote a slow rate mitochondrial Ca^{2+} efflux which suppresses cytosolic Ca^{2+} oscillation during seizures (Ryan et al., 2009). The effect of CBD on neuronal Ca^{2+} efflux can be supressed with the inhibition Na^+/Ca^{2+} exchanger (NCX) using GCP37157 (Ryan et al., 2009). My study suggest that CBD may not require to act directly on NCX to induce the Ca^{2+} efflux (NCX). Given that NCX is a Ca^{2+} transporter, I could not expect CBD to act in the absence of Ca^{2+}. However, in my previous work (chapter 3), CBD was shown to induce H^+ leak in the absence of Ca^{2+}. Taken together, I propose NHX as a possible target of CBD. As NHX

allows the uptake of H^+, Na^+ efflux into the intermembrane space. The increase of the concentration of Na^+ in the intermembrane space may subsequently drive Ca^{2+} efflux through NCX. This could explain why NCX inhibition prevented the effect CBD-induced Ca^{2+} efflux (Ryan et al., 2009).

4.4 CONCLUSION

In conclusion, CBD increased Ca^{2+}-induced mitochondrial swelling in NS-mito$_{EP}$. Here I demonstrated that the mode of action of CBD differs from that of the VDAC blocker S18 suggesting that CBD may not act through VDAC. Based on my results and the current literature, it is plausible that CBD may be targeting NHX.

CHAPTER 5 – EFFECT OF CANNABIDIOL ON VOLTAGE-EVOKED CURRENTS IN HEK293 CELLS OVEREXPRESSING RAT VDAC2 AT THE PLASMA MEMBRANE

5 EFFECT OF CANNABIDIOL ON VOLTAGE-EVOKED CURRENTS IN HEK293 CELLS OVEREXPRESSING RAT VDAC2 AT THE PLASMA MEMBRANE

5.1 INTRODUCTION

As previously demonstrated (see section 3.2.5 & 4.2.1), CBD does not appear to require VDAC1 to induced weak uncoupling or increase of Ca^{2+}-induced swelling in non-synaptic mitochondria (NS-mito) from rat with temporal lobe epilepsy (NS-$mito_{EP}$).

5.1.1 THE EFFECT OF CBD DIFFERS FROM VDAC INHIBITORS

In my previous chapter (chapter 4), I investigated whether changes of VDAC1 expression in NS-$mito_{EP}$ could be link to epilepsy-dependent effect of CBD, given that CBD only alters the function of NS-$mito_{EP}$ and not NS-mito isolated from healthy rats. My findings demonstrated that VDAC1 expression was not affected in rats with temporal lobe epilepsy. This could suggest that VDAC1 oligomerisation may not be affected in this model of epilepsy. Since, upregulation of VDAC1 expression is associated with VDAC1 oligomerisation and cytochrome C (cyt C) release induction (Keinan et al., 2013; Shimizu and Tsujimoto, 2000; Shoshan-Barmatz et al., 2015). Taken together, CBD's effect on mitochondria does not require VDAC1. Consistent with this, compounds inhibiting VDAC1 such as 4,4'-diisothiocyanatostilbene-2,2'-disulphonate (DIDS) or antibodies directed against VDAC1 induced apoptosis via mitochondrial accumulation of the superoxide anion (O_2^-•) accompanied by Cyt C release (Madesh and Hajnóczky, 2001). Similarly, G3139, an oligonucleotide like S18, has previously been demonstrated to inhibit VDAC in liver mitochondria (Tan, 2012; Tan et al., 2007a; Tikunov et al., 2010). In turn, this activates Cyt C release due to mitochondrial accumulation of O_2^-• (Tan, 2012; Tan et al., 2007a; Tikunov et al., 2010). My results on NS-mito were also consistent with these studies, since the use of the

VDAC blocker S18 dramatically increased Cyt C release from NS-mito$_{EP}$ following Ca^{2+}-induced mitochondrial permeability transition.

Conversely, CBD does not exhibit VDAC1 inhibitors-like proprieties as it does not induce cyt C release. My findings clearly conflict with the study of Rimmerman et al., since they showed that CBD's effect on mitochondria is consistent with inhibitors VDAC1 (such as G3139, aspirin or DIDS) using BV-2 microglial cells (Rimmerman et al., 2013).

5.1.2 Role of VDAC2 in epilepsy

The three isoforms of VDAC are expressed in the brain (Baines et al., Shinohara et al., 2000, Naghdi 2017). Although VDAC1 is clearly involved in the transport of ions and metabolites such as ADP^{3-}/ATP^{4-} (Anflous et al., 2001; Choudhary et al., 2014), mice lacking VDAC1 are viable and do not exhibit altered synaptic plasticity (Weeber et al., 2002). Furthermore, the mortality rate due to genetic deletion of both VDAC1 and VDAC3 is not 100%. Moreover, mice lacking both VDAC1 and VDAC3 exhibit minor adverse effects on synaptic plasticity. Currently, there are no mice model lacking VDAC2 because a deletion of both *vdac2* alleles is lethal *in utero* (Cheng et al., 2003). This clearly highlight the importance of VDAC2, despite its homology with other isoforms of VDAC, VDAC2 could be more susceptible to oxidation (particularly from ROS) compared to other isoforms of VDAC given its high number of cysteine residues (9 or 11 depending on the species) (De Pinto et al., 2016; Naghdi and Hajnóczky, 2016; Sampson et al., 1997). In addition, VDAC2 possesses a longer sequence at its N-terminus which could confer functions to VDAC2 that are different from that of other VDAC isoforms (Naghdi and Hajnóczky, 2016). Based on the mRNA levels of VDAC isoforms in the brain, VDAC1 is the most abundant then followed by VDAC2 (Naghdi and Hajnóczky, 2016; Sampson et al., 1997; Shinohara et al., 2000). VDAC2 is involved in OXPHOS

as well as VDAC1. In contrast, to VDAC1 and despite the high homology with VDAC1 (>90%), VDAC2 plays a critical role during development and the mechanism by which VDAC2 regulates apoptosis and OXPHOS differs from VDAC1 (Maurya and Mahalakshmi, 2017; Naghdi and Hajnóczky, 2016).

5.1.3 HYPOTHESIS AND AIM

Given the peculiar function of rat VDAC2 compared to VDAC1, I hypothesis that if CBD targets an isoform of VDAC, perhaps it could be VDAC2. Given that other investigators have suggested that the expression of VDAC2 was altered in some models of epilepsy and seizures (Jiang et al., 2007). I could not determine any change of VDAC2 expression, as all commercial anti-VDAC2 antibodies I used in this study failed to detect VDAC2 as it will be shown in this chapter. Using whole-cell patch-clamp, the main aim of this section is to assess the pharmacological effect of CBD on voltage-evoked currents in two stable cell lines. One with the empty vector (VC-HEK293 cells) and the other overexpresses rat VDAC2 (Igκ:HA-rVDAC2-HEK293 cells). The VC-HEK293 cells were graciously provided by Graeme Cottrell, while I generated and characterised Igκ:HA-rVDAC2-HEK293 cells. Furthermore, commercial anti-VDAC2 antibodies were assessed for detection of rat VDAC2. In this study, the VDAC2 inhibitor DIDS was used to examine the electrophysiological function of VDAC2 in Igκ:HA-rVDAC2-HEK293 cells in addition to the VDAC inhibitor S18 (Li et al., 2012; Shoshan-Barmatz et al., 2017). Different concentrations of CBD (1, 5 and 10 μM) were also assessed.

5.2 RESULTS

5.2.1 TRANSFECTION OF HEK293 WITH pcDNA5/FRT/Igκ:HA-rVDAC2

Initially, rVDAC2 cDNA was cloned into a pcDNA5/FRT plasmid to synthesised pcDNA5/FRT:rVDAC2. Subsequently, competent *E. coli* transformed with pcDNA5/FRT:rVDAC2 were cultured on agar containing ampicillin (100 μg/ml). Colonies resistant to ampicillin were screened using colony PCR to determine the presence or absence of DNA fragment of similar length to rVDAC2 (Fig. 5-1A & 5-1B). As shown in Fig. 5-1B, the length of the PCR product in colonies resistant to antibiotic treatment was ~ 950 bp. Digestion of plasmid DNA from these colonies with *BamHI* and *XhoI* yield fragments with expected lengths (Fig. 5-1B). Finally, DNA sequencing was used to confirm the integrity of the sequence of the insert.

To generate a pcDNA5/FRT plasmid with Igκ:HA-rVDAC2 (pcDNA5/FRT/Igκ:HA-rVDAC2), pcDNA5/FRT:rVDAC2 was used to subcloned HA-rVDAC2 into the pcDNA5/FRT/Igκ plasmid (with Igκ at the downstream of the CMV promoter). *E. coli* transformed with pcDNA5/FRT/Igκ:HA-rVDAC2 were then seeded on agar containing ampicillin (100 μg/ml). Initially, colonies exhibiting resistance to the antibiotic treatment were screened for the presence of Igκ:HA-rVDAC2 using colony PCR (Fig. 5-2A & 5-2B). A colony which yield a PCR product of comparable size to Igκ:HA-rVDAC2 (~ 1050 bp) was identified (Fig. 5-2B). The digestion of the plasmid DNA of this colony with *AgeI* and *XhoI* produced DNA fragments with expected length (Fig. 5-2B). DNA sequencing was used to confirm the integrity of the sequence of the insert.

After DNA sequence assessment of the DNA plasmid, HEK293 cells were transfected with pcDNA5/FRT/Igκ:HA-rVDAC2 to generate stable cell lines. Subsequently to transfection

of HEK293 cells with pcDNA5/FRT/Igκ:HA-rVDAC2, I demonstrated that Igκ:HA-rVDAC2 is overexpressed in these cells using an antibody raised in mouse and directed against the HA tag (Fig. 5-3A). Two commercial anti-VDAC2 antibodies raised in rabbit (polyclonal) and in mouse (monoclonal) were not effective in detecting Igκ:HA-rVDAC2 (Fig. 5-3B & 5-3C). Western blotting and plasma membrane biotinylation assay showed respectively an increase of overall Igκ:HA-rVDAC2 expression in Igκ:HA-rVDAC2-HEK293 cells and increase of Igκ:HA-rVDAC2 expression at the plasma membrane (Fig. 5-4A- Fig. 5-4B).

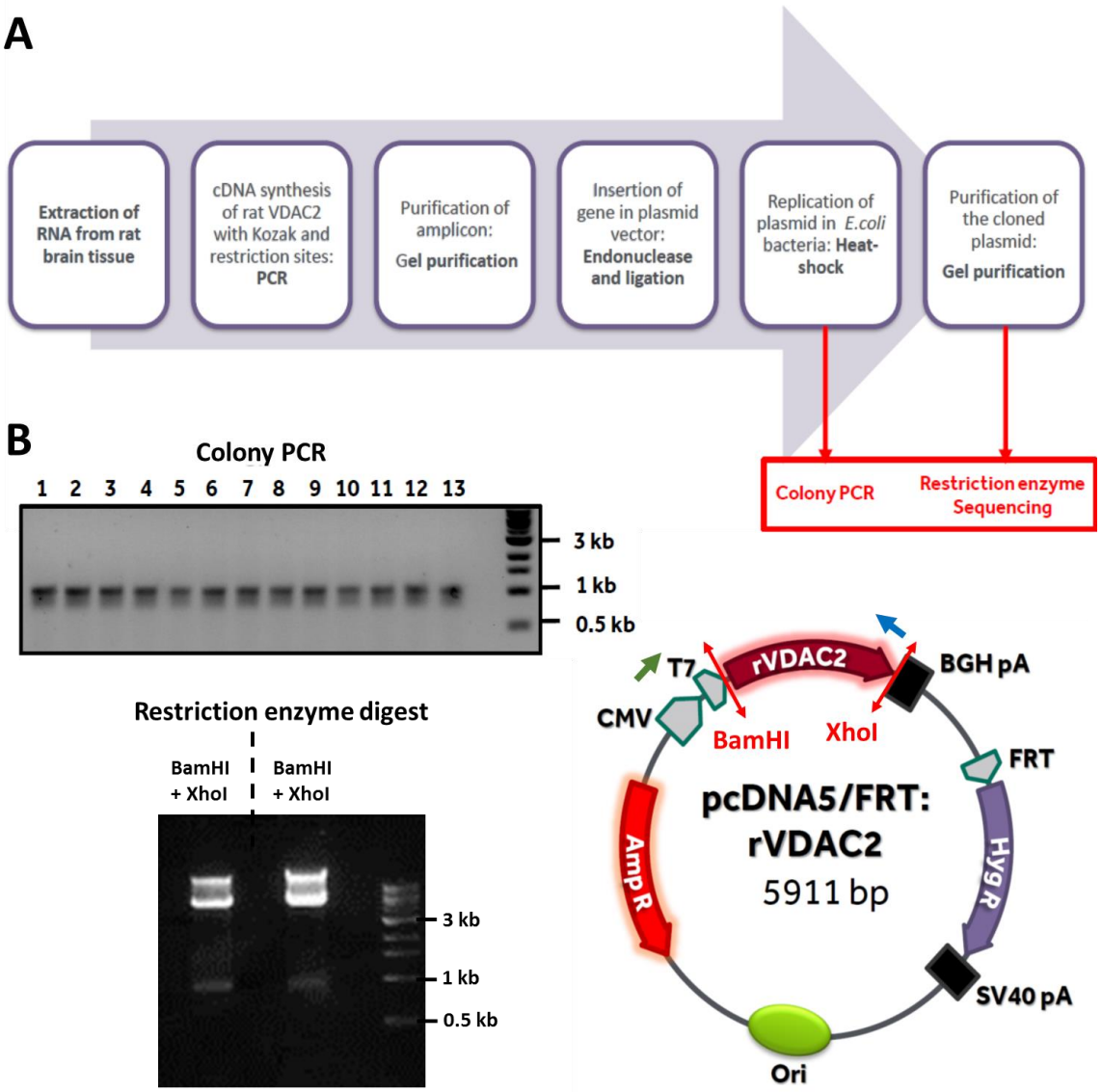

Figure 5-1. Characterisation of the pcDNA5/FRT/rVDAC2 construct. (A) Procedure to create pcDNA5/FRT/rVDAC2 from mRNA rVDAC2. (B) Screening for bacterial transformation with colony PCR shows that all 13 colonies were positive. Restriction digest of plasmid DNA (2h) using both *BamHI* and *XhoI* shows fragments at predicted size. Green arrows, forward primer for colony PCR. Blue, arrow reverse primers for colony PCR. Red arrow, site of activity of restriction enzymes.

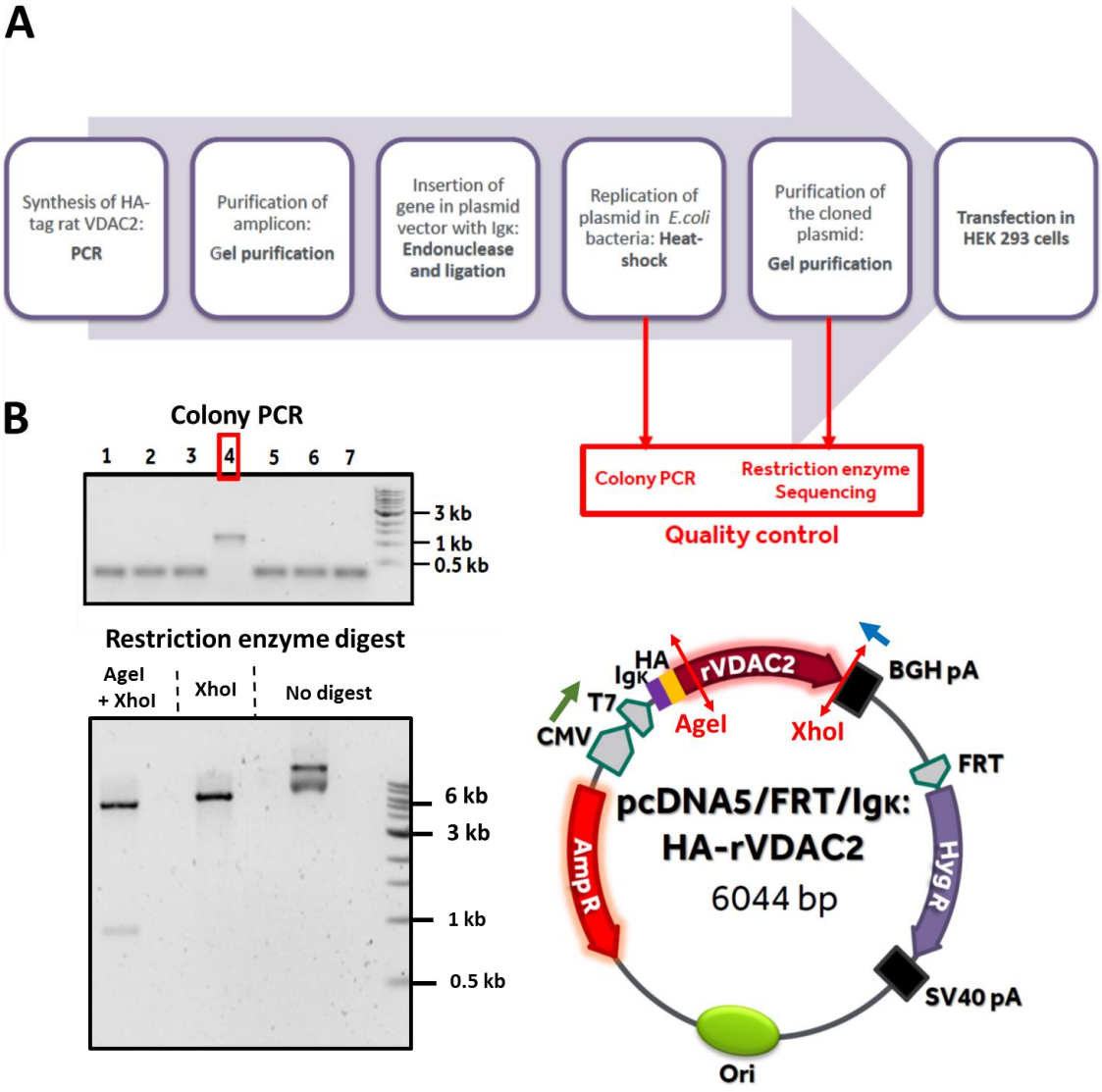

Figure 5-2. Characterisation of the pcDNA5/FRT/Igκ:HA-rVDAC2 construct. (A) Procedure to create pcDNA5/FRT/Igκ:HA-rVDAC2 from pcDNA5/FRT:rVDAC2. (B) Screening for bacterial transformation with colony PCR shows only positive colony. Overnight plasmid DNA digest using both *AgeI* and *XhoI* shows fragments at predicted size. Green arrows, forward primer for colony PCR. Blue, arrow reverse primers for colony PCR. Red arrow, site of activity of restriction enzymes.

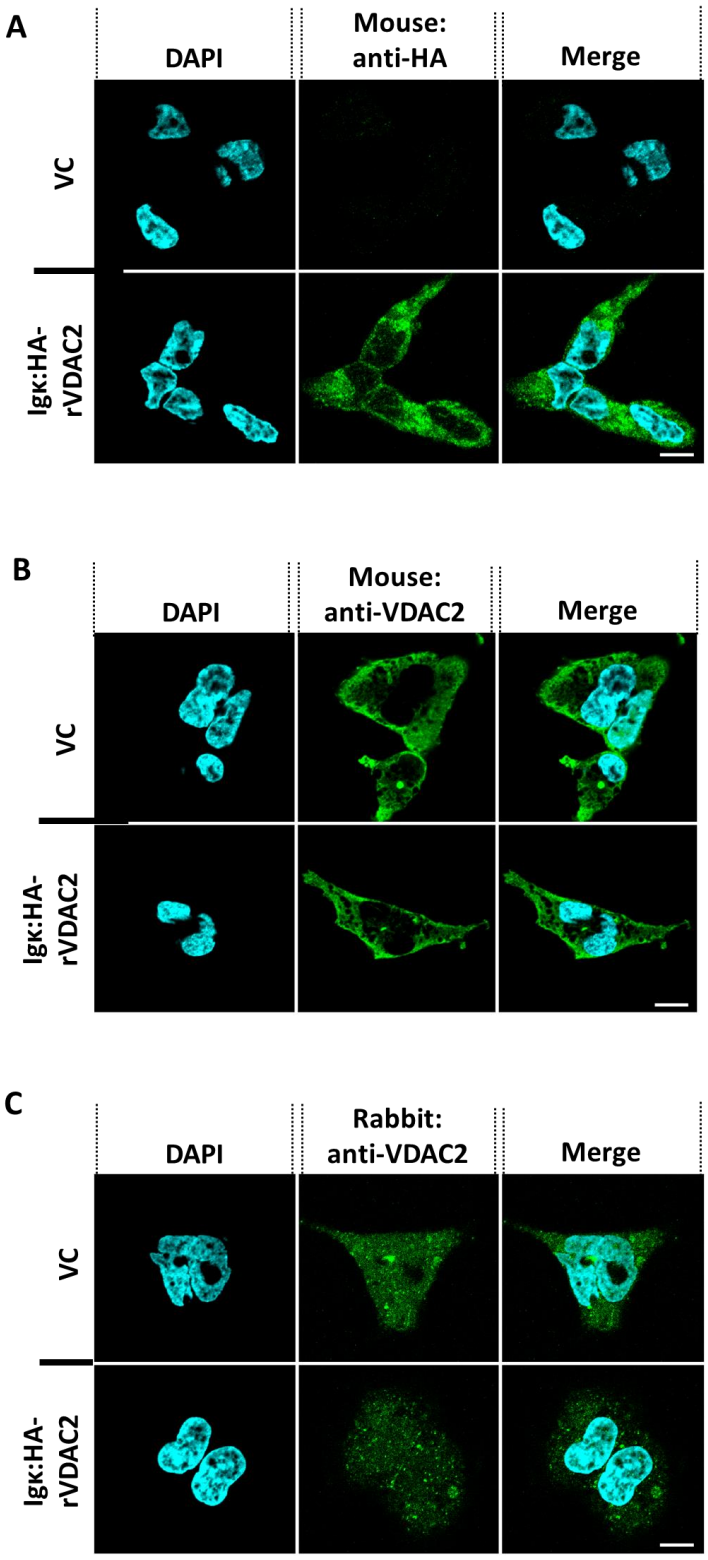

Figure 5-3. Immunofluorescence detection of Igκ:HA-rVDAC2 protein in in Igκ:HA-rVDAC2-HEK293 cells. (A) the anti-HAtag antibody raised in mouse detected Igκ:HA-rVDAC2. Commercial anti-VDAC2 raised in (B) mouse and (C) rabbit did not detect Igκ:HA-rVDAC2. Scale bars = 10 µm. Antibodies used in study are catalogued in the appendix.

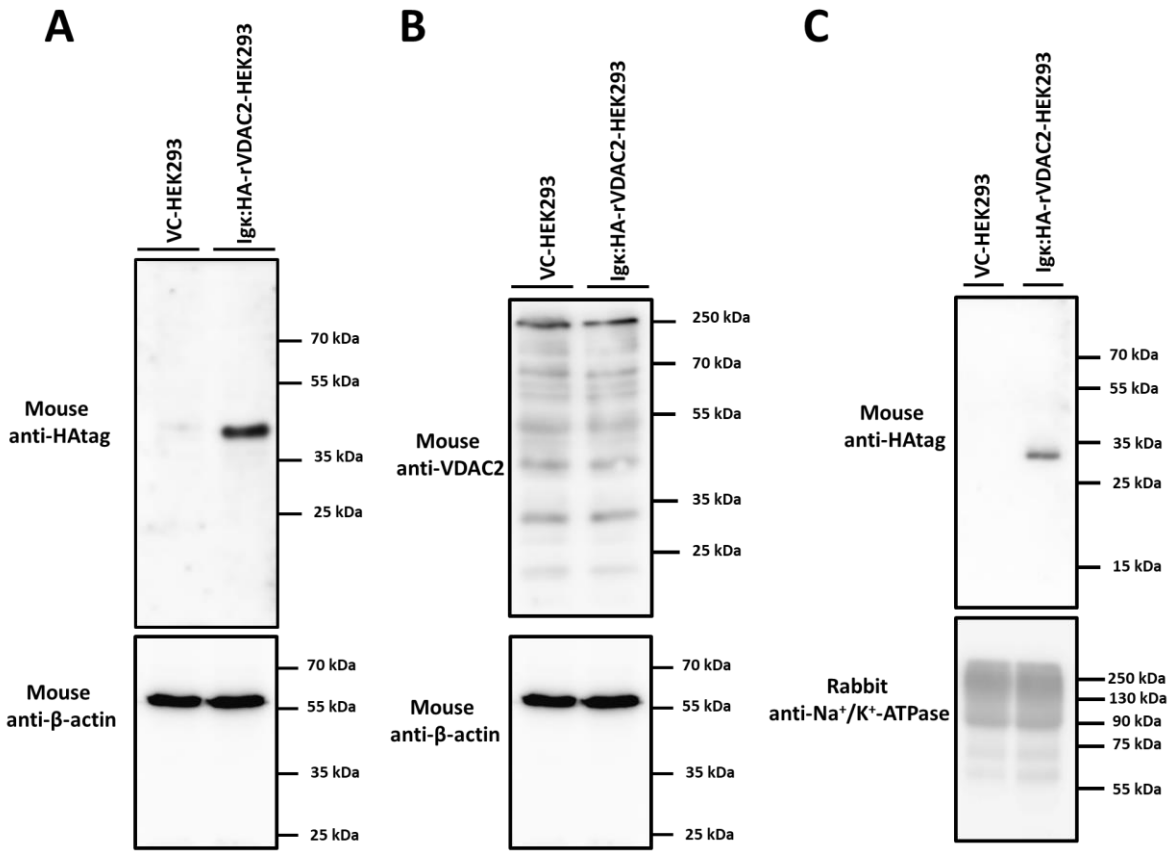

Figure 5-4. Expression of Igκ:HA-rVDAC2 in Igκ:HA-rVDAC2-HEK293 cells. Western blotting showing increased Igκ:HA-rVDAC2 expression in cell lysate of Igκ:HA-rVDAC2-HEK293 cell. (A) Detection of Igκ:HA-rVDAC2 using an anti-HA-tag antibody (B) Igκ:HA-rVDAC2 is not detected by commercial anti-VDAC2 antibody (C) Biotinylation assay shows increased level Igκ:HA-rVDAC2 protein expression at the plasma membrane of Igκ:HA-rVDAC2-HEK293 cells. Antibodies used in study are catalogued in the appendix.

5.2.2 Effect of the vehicle on current flux in both VC-HEK293 cells and Igκ:HA-rVDAC2-HEK293 cells

The vehicle used to dilute 10 µM CBD (Veh3; 0.03% DMSO diluted in extracellular medium) was investigated to determine whether it presents any effect on voltage-evoked currents in both VC-HEK293 cells and Igκ:HA-rVDAC2 cells. As expected, this study showed that Veh3 exhibits no effect on voltage-evoked currents in both cell lines (Fig. 5-4).

5.2.3 Effect of VDAC inhibition on current flux in both VC-HEK293 cells and Igκ:HA-rVDAC2-HEK293 cells

The effect of VDAC inhibition was then assessed in both VC-HEK293 and Igκ:HA-rVDAC2-HEK293 cells. Given that the inhibitory effect of S18 (3 µM) on VDAC2 is still unknown, the effect of DIDS (10 µM) was also assessed. This study showed no effect of DIDS (10 µM) as well as S18 (3 µM) on voltage-evoke currents in both VC-HEK293 and Igκ:HA-rVDAC2-HEK293 cells (Fig. 5-5 & 5-6).

5.2.4 Effect of CBD on current flux in both VC-HEK293 cells and Igκ:HA-rVDAC2-HEK293 cells

Although Veh3, S18 (3 µM) and DIDS (10 µM) did not affect current flux in both VC-HEK cells and Igκ:HA-rVDAC2-HEK293 cells, the effect of three concentrations (1, 5, 10 µM) of CBD on these cell lines were subsequently determined. High concentration of CBD (10 µM) reduced significantly current flux in both VC-HEK cells and Igκ:HA-rVDAC2-HEK293 cells (Fig. 5-7). However, 5 µM CBD decreased the current flux only in VC-HEK293 cells (Fig. 5-8). At low concentration, CBD (1 µM) exerted no effect on voltage-evoked currents in both VC-HEK cells and Igκ:HA-rVDAC2-HEK293 cells (Fig. 5-9).

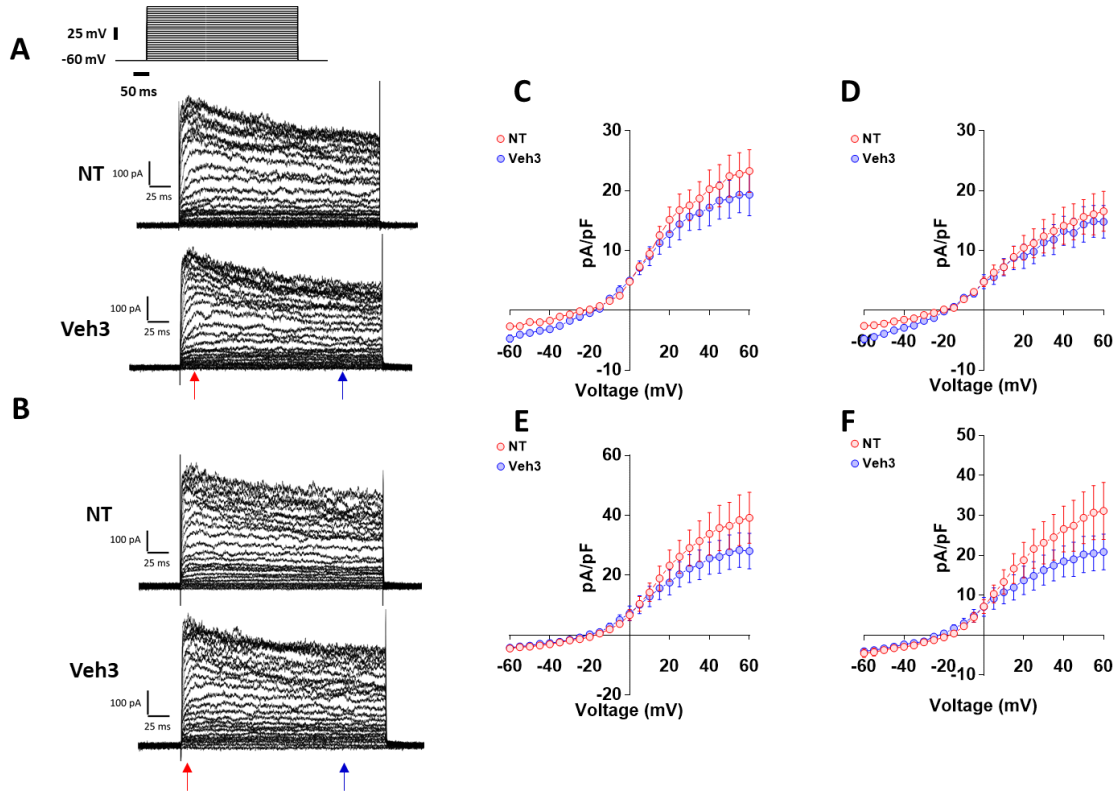

Figure 5-4. Veh3 treatment does not affect current flux in neither VC-HEK293 and Igκ:HA-rVDAC2-HEK293 cells. Representative traces showing effect of Veh3 (10 µM) on voltage-evoked currents, in both (A) VC-HEK293 and (B) Igκ:HA-rVDAC2-HEK293 cells. Current responses were evoked at different steps of voltage (-60 mV and +60 mV; 500ms), with 5 mV increment. Red arrow indicates that data was acquired at 30 ms and blue arrow indicates that data was acquired at 400 ms. (C) Plot of the effect of Veh3 at 30 ms after voltage stimulation in VC-HEK293 cells. (D) Plot of the effect of Veh3 at 400 ms after voltage stimulation in VC-HEK293 cells. (E) Plot of the effect of Veh3 at 30 ms after voltage stimulation in Igκ:HA-rVDAC2-HEK293 (F) Plot of the effect of Veh3 at 400 ms after voltage stimulation in Igκ:HA-rVDAC2-HEK293 cells. Data are expressed in mean ± SEM. N = 4 for VC-HEK293 cells, N = 8 for Igκ:HA-rVDAC2-HEK293 cells. Two-way ANOVA showed no statistical difference (P>0.05). NT, non-treated. Veh3, vehicle.

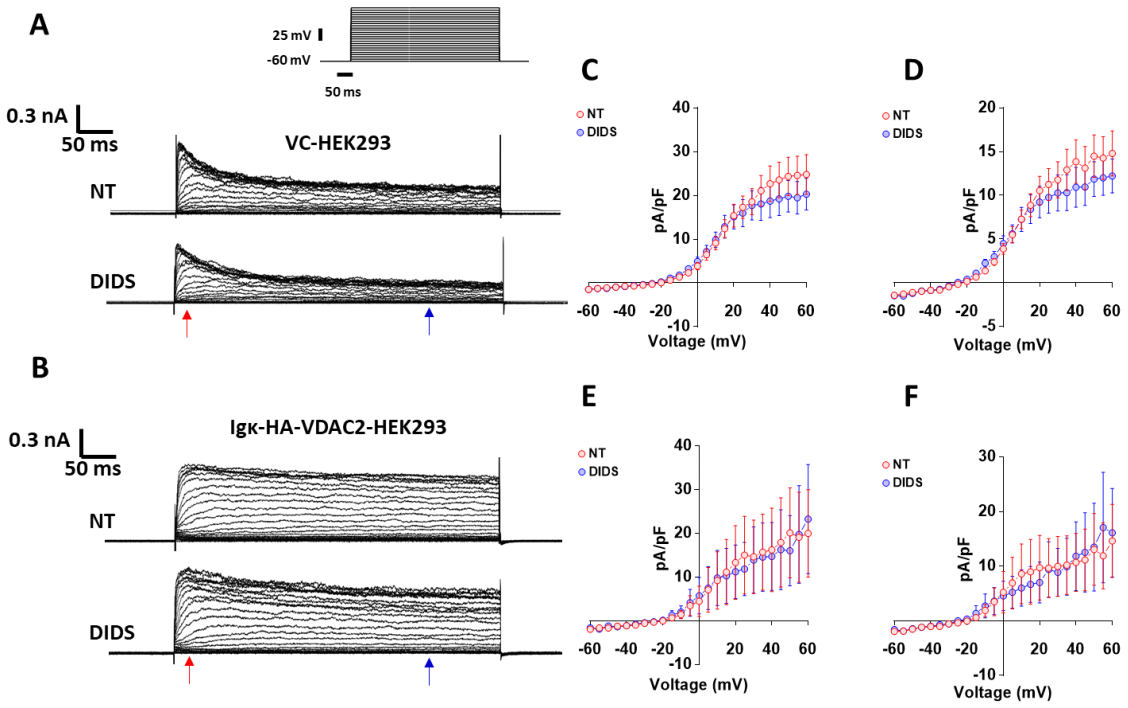

Figure 5-5. DIDS treatment does not affect current flux in neither VC-HEK293 and Igκ:HA-rVDAC2-HEK293 cells. Representative traces showing effect of DIDS (10 µM) on voltage-evoked currents, in both (A) VC-HEK293 and (B) Igκ:HA-rVDAC2-HEK293 cells. Current responses were evoked at different steps of voltage (-60 mV and +60 mV; 500ms), with 5 mV increment. Red arrow indicates that data was acquired at 30 ms and blue arrow indicates that data was acquired at 400 ms. (C) Plot of the effect of DIDS at 30 ms after voltage stimulation in VC-HEK293 cells. (D) Plot of effect of DIDS at 400 ms after voltage stimulation in VC-HEK293 cells. (E) Plot of the effect of DIDS at 30 ms after voltage stimulation in Igκ:HA-rVDAC2-HEK293 cells. (F) The effect of DIDS at 400 ms after voltage stimulation in Igκ:HA-rVDAC2-HEK293 cells. Data are expressed in mean ± SEM. N = 9 for VC-HEK293 cells, N = 4 for Igκ:HA-rVDAC2-HEK293 cells. Two-way ANOVA showed no statistical difference (P>0.05). NT, non-treated. DIDS, 4,4'-diisothiocyanatostilbene-2,2'-disulphonate.

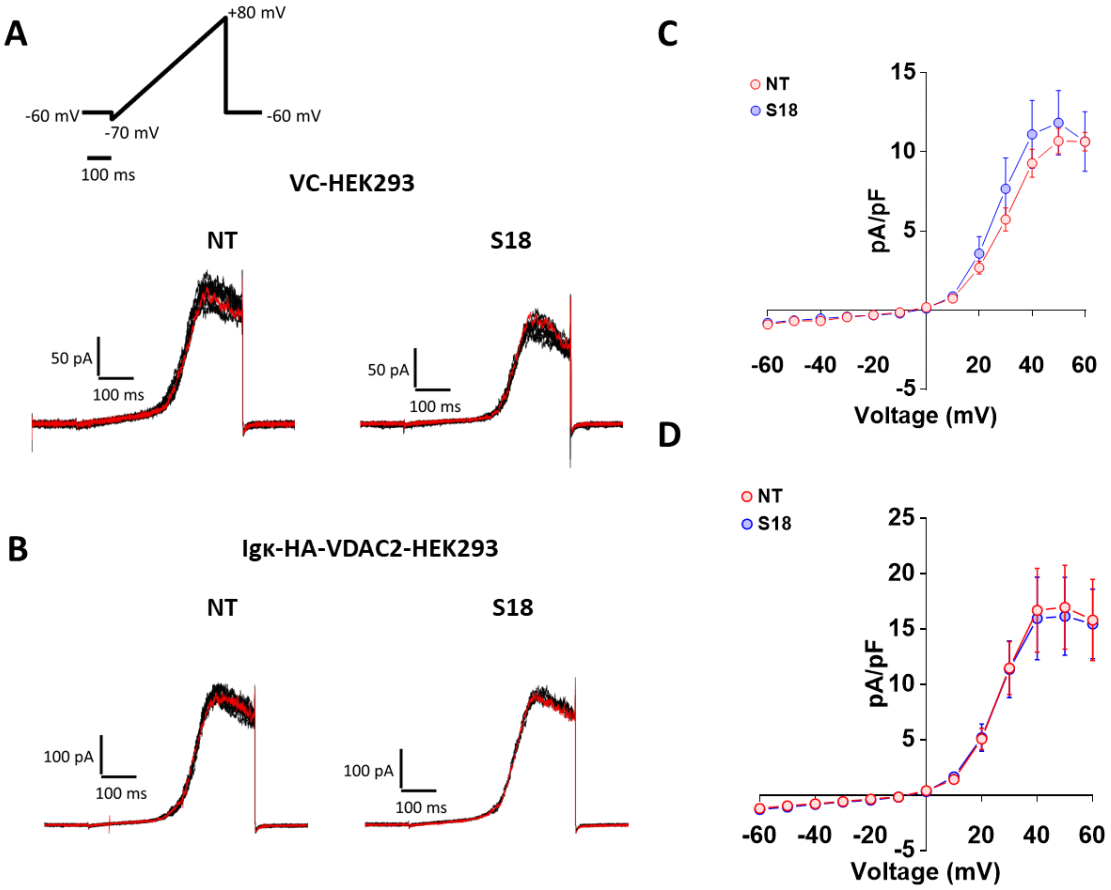

Figure 5-6. S18 treatment does not affect current flux in neither VC-HEK293 and Igκ:HA-rVDAC2-HEK293 cells. Superimposed traces showing effect of S18 (3 µM) on voltage-evoked currents, in both (A) VC-HEK293 and (B) Igκ:HA-rVDAC2-HEK293 cells. Current responses were evoked using a voltage ramp (-70 mV and +80 mV; 500 ms). (C) Plot of the effect of S18 on voltage-evoked current in VC-HEK293 cells. (D) Plot of the effect of S18 on voltage-evoked current in Igκ:HA-rVDAC2-HEK293. Data are expressed in mean ± SEM. N = 3 for VC-HEK293 cells, N = 3 for Igκ:HA-rVDAC2-HEK293 cells. Two-way ANOVA showed no statistical difference (P>0.05). NT, non-treated. S18, S18 randomer.

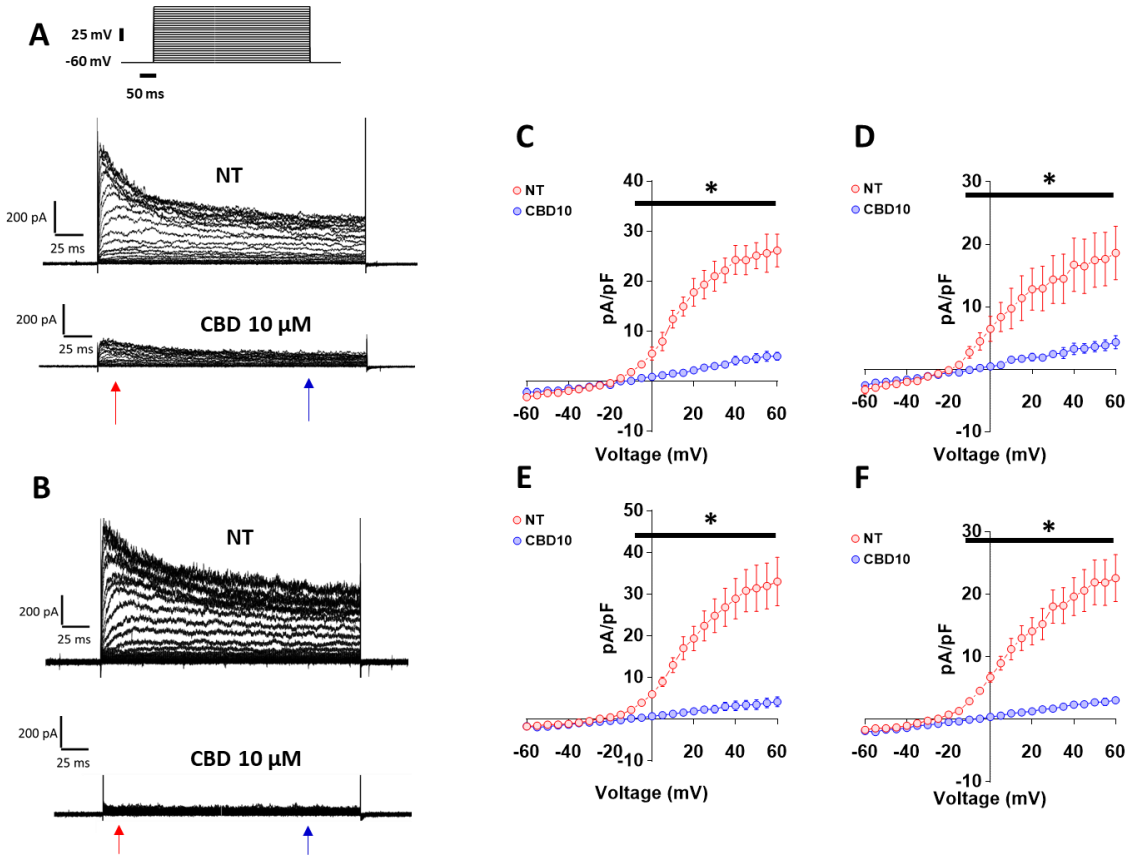

Figure 5-7. High concentration CBD treatment reduced current flux in VC-HEK293 and Igκ:HA-rVDAC2-HEK293 cells. Representative traces showing effect of CBD (10 µM) on voltage-evoked currents, in both (A) VC-HEK293 and (B) Igκ:HA-rVDAC2-HEK293 cells. Current responses were evoked at different steps of voltage (-60 mV and +60 mV; 500ms), with 5 mV increment. Red arrow indicates that data was acquired at 30 ms and blue arrow indicates that data was acquired at 400 ms. (C) Plot of the effect of CBD at 30 ms after voltage stimulation in VC-HEK293 cells. (D) Plot of the effect of CBD at 400 ms after voltage stimulation in VC-HEK293 cells. (E) Plot of the effect of CBD at 30 ms after voltage stimulation in Igκ:HA-rVDAC2-HEK293 (F) The effect of CBD at 400 ms after voltage stimulation in Igκ:HA-rVDAC2-HEK293 cells. Data are expressed in mean ± SEM. N = 4 for VC-HEK293 cells, N = 6 for Igκ:HA-rVDAC2-HEK293 cells. Two-way ANOVA showed statistical difference ($P<0.05$). Pairwise comparison was performed using BKY procedure (*$Q<0.05$). NT, non-treated. CBD, cannabidiol.

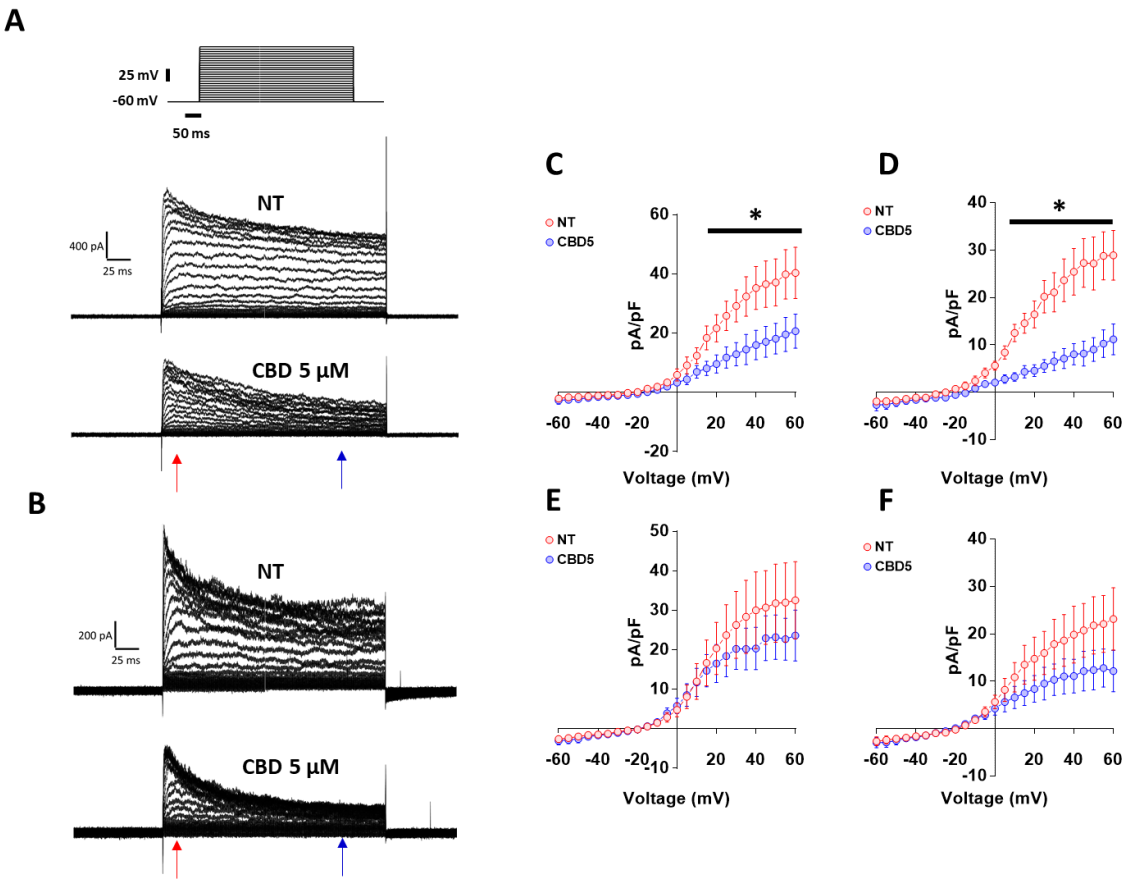

Figure 5-8. Intermediate concentration CBD treatment affects current flux in VC-HEK293 but exhibits no effect on Igκ:HA-rVDAC2-HEK293 cells. Representative traces showing effect of CBD (5 µM) on voltage-evoked currents, in both (A) VC-HEK293 and (B) Igκ:HA-rVDAC2-HEK293 cells. Current responses were evoked at different steps of voltage (-60 mV and +60 mV; 500ms), with 5 mV increment. Red arrow indicates that data was acquired at 30 ms and blue arrow indicates that data was acquired at 400 ms. (C) Plot of the effect of CBD at 30 ms after voltage stimulation in VC-HEK293 cells. (D) Plot of the effect of CBD at 400 ms after voltage stimulation in VC-HEK293 cells. (E) Plot of the effect of CBD at 30 ms after voltage stimulation in Igκ:HA-rVDAC2-HEK293 (F) The effect of CBD at 400 ms after voltage stimulation in Igκ:HA-rVDAC2-HEK293 cells. Data are expressed in mean ± SEM. N = 4 for VC-HEK293 cells, N = 5 for Igκ/HA-rVDAC2-HEK293 cells. Two-way ANOVA showed statistical difference ($P<0.05$). Pairwise comparison was performed using BKY procedure (*$Q<0.05$). NT, non-treated. CBD, cannabidiol.

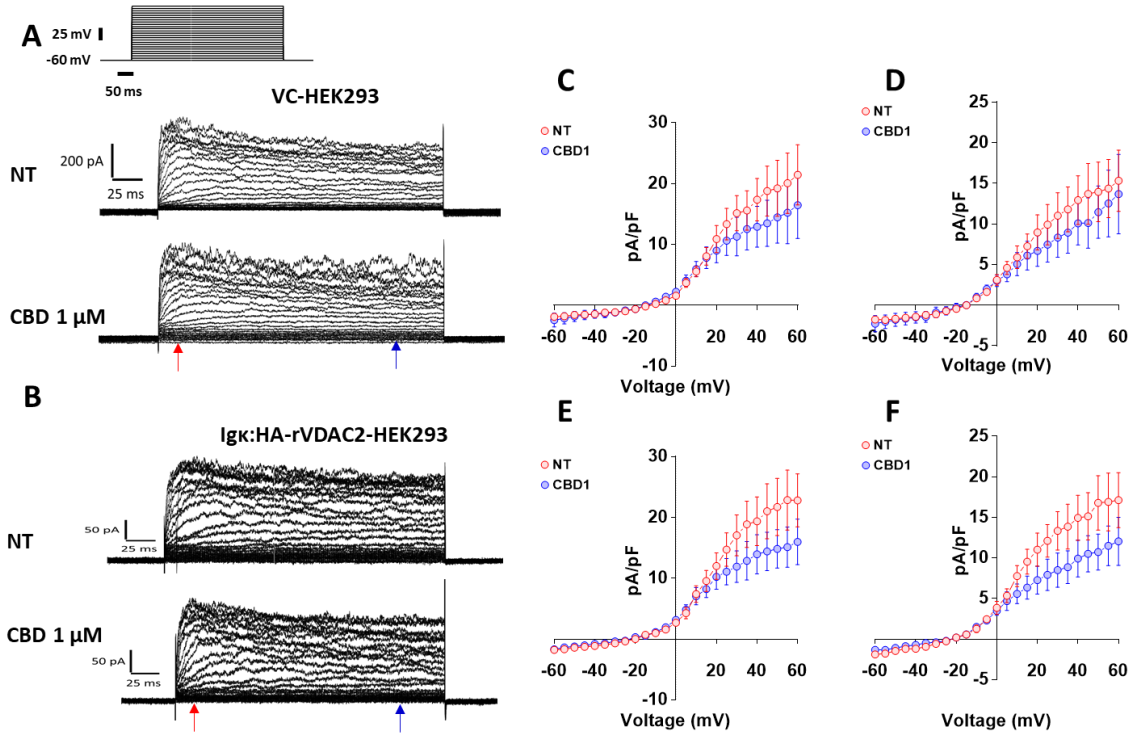

Figure 5-9. Low concentration CBD treatment affects current flux in neither VC-HEK293 nor Igκ:HA-rVDAC2-HEK293 cells. Representative traces showing effect of CBD (1 µM) on voltage-evoked currents, in both (A) VC-HEK293 and (B) Igκ:HA-rVDAC2-HEK293 cells. Current responses were evoked at different steps of voltage (-60 mV and +60 mV; 500ms), with 5 mV increment. Red arrow indicates that data was acquired at 30 ms and blue arrow indicates that data was acquired at 400 ms. (C) Plot of the effect of CBD at 30 ms after voltage stimulation in VC-HEK293 cells. (D) Plot of the effect of CBD at 400 ms after voltage stimulation in VC-HEK293 cells. (E) Plot of the effect of CBD at 30 ms after voltage stimulation in Igκ:HA-rVDAC2-HEK293 (F) The effect of CBD at 400 ms after voltage stimulation in Igκ:HA-rVDAC2-HEK293 cells. Data are expressed in mean ± SEM. N = 4 for VC-HEK293 cells, N = 6 for Igκ:HA-rVDAC2-HEK293 cells. Two-way ANOVA showed no statistical difference (P>0.05). NT, non-treated. CBD, cannabidiol.

5.3 DISCUSSION

This study does not lead to a conclusive answer on whether CBD targets rVDAC2 as I could not established whether Igκ:HA-rVDAC2-HEK293 cells expressed functional rVDAC2. Igκ:HA-rVDAC2-HEK293 cells exhibited high variability of voltage-evoked currents compared to VC-HEK293 cells. Inhibition of VDAC with DIDS or S18 did not alter voltage-evoked currents in both Igκ:HA-rVDAC2-HEK293 cells and VC-HEK293 cells. Taken together, this suggests that Igκ:HA-rVDAC2 may not be functional. The inhibitory effect of CBD on voltage-evoked currents in both Igκ:HA-rVDAC2-HEK293 cells and VC-HEK293 cells could not be related to VDAC2 as CBD was acting only at 10 µM in both cell lines.

The presence of Igκ:HA at rVDAC2 N-terminus may have affected the electrophysiological proprieties of rVDAC2. Designing a new DNA plasmid construct with Igκ:HA at the C-terminus of rVDAC2 may resolve this problem. Alternatively, the variability of current flux (evoked with voltage stimuli) in Igκ:HA-rVDAC2-HEK293 cells may be explained by a possible variability of Igκ:HA-rVDAC2 density at the plasma membrane. For example, low expression of Igκ:HA-rVDAC2 at the plasma membrane could result in reduced voltage-evoked currents. This study showed that the overall expression of Igκ:HA-rVDAC2 was increased in Igκ:HA-rVDAC2-HEK293 cells (using an anti-HA-tag antibody for detection), however Igκ:HA-VDAC2 may be localised mainly in mitochondria which would explain the very low expression of Igκ:HA-rVDAC2 at the cell surface of Igκ:HA-rVDAC2-HEK293 cells (Maurya and Mahalakshmi, 2017; Naghdi and Hajnóczky, 2016).

Lastly, the variability of current flux in Igκ:HA-rVDAC2-HEK293 cells could be due to a loss/change of activity of Igκ:HA-rVDAC2 during its translocation into the plasma membrane. For example, some Igκ:HA-rVDAC2 may be oriented in a manner that allows the efflux of an

ion while others may be oriented in opposite direction which allows the influx of the same ion.

GENERAL DISCUSSION AND CONCLUSION

6 GENERAL DISCUSSION

The discovery of new targets and AEDs has become necessity. The difficulty of treating epilepsy with pharmacological agents remains present despite more than a 160 years of AED discovery. Given the complexity of symptoms (e.g. comorbidities) and cellular/molecular changes surrounding epilepsy, it is no longer possible to reduce epilepsy to a simple synaptic dysfunction. For example, while phasic inhibition of pyramidal cells discharges mediated by fast-spiking GABAergic interneurons produce gamma waves (Fuchs et al., 2007). Growing evidence suggests that metabolic changes (e.g. apoptosis, sodium channel dysfunction or mitochondrial dysfunction) in these GABAergic interneurons leading to their functional impairment may contribute to epileptogenic networks formation (Cheah et al., 2012; de Lanerolle et al., 1989; Ma et al., 2012; Sloviter, 1987; Whittaker et al., 2011; Yu et al., 2006). Furthermore, metabolic changes affecting $GABA_A$ receptors or the transport of Cl^- (e.g. reduction of KCC2 expression) could lead to dyfunctional $GABA_A$ receptor signalling and pharmacoresistance (Bethmann et al., 2008; Deisz et al., 2011; Huberfeld et al., 2007; Wolf et al., 1994).

Cannabidiol (CBD) has recently been approved by the FDA for treatment of seizures in Lennox-Gastaut syndrome and Dravet syndrome patients (Commissioner, 2018). Although, mechanisms underlying its anti-epileptic effect remain uncertain, it is plausible that it may be mediated through the regulation of mitochondrial Ca^{2+} (Ryan et al., 2009). As there is no clear evidence that CBD acts directly on mitochondria, in this project I investigated whether CBD's anti-epileptic effect could involve a direct modulation of the function of non-synaptic mitochondria isolated from the hippocampi of healthy ($NS\text{-}mito_{HE}$) and epileptic ($NS\text{-}mito_{EP}$) rats.

My main finding demonstrated that CBD regulates oxidative phosphorylation (OXPHOS) and Ca^{2+}-induced mitochondrial permeability transition (mPT) only in NS-mito$_{EP}$ via a mechanism independent from VDAC inhibition. Under my experimental design, the effect of CBD on OXPHOS was determined in the presence of a Ca^{2+} chelator (EGTA; 1mM) in the extramitochondrial medium. EGTA can inhibit the inner-membrane Ca^{2+} uniporter, a major contributor of mitochondrial Ca^{2+} influx (Igbavboa and Pfeiffer, 1988). Thus, all OXPHOS experiments were performed without the influence of Ca^{2+}. At 10 µM, CBD induced a weak H^+ leak in NS-mito$_{EP}$ given that CBD increased state 4 respiration but affected neither state 3 respiration and the respiratory control ratio. In contrast, CBD does not exhibit any effect on OXPHOS in NS-mito$_{HE}$. Subsequently, I demonstrated that CBD does not affect Ca^{2+}-induced swelling in NS-mito$_{HE}$ while it normalises mitochondrial swelling in NS-mito$_{EP}$. The effect of CBD on NS-mito$_{EP}$ cannot be associated with a potential change of VDAC1 expression in rats with temporal lobe epilepsy (TLE), since its expression is not altered in NS-mito$_{EP}$. CBD's effect on OXPHOS differs from that of the VDAC blocker S18 randomer (S18). Taken together, CBD appears to target CBD a non-VDAC H^+ channel/transporter in NS-mito$_{EP}$. These results contradict the finding of Rimmerman et al. who showed that CBD inhibits at least one of VDAC isoforms (namely VDAC1) reconstructed in an artificial bilayer membrane (Rimmerman et al., 2013). It is likely that this reconstituted form of VDAC1 may differ from native VDAC1 (embedded in mitochondria). Although CBD did not increase Ca^{2+}-induced swelling in S18-treated NS-mito$_{EP}$, it likely that even low concentration S18 (3 µM) causes maximal swelling.

To investigate whether CBD's effect on NS-mito$_{EP}$ could be mediated by VDAC2, I use HEK293 cells overexpressing rat VDAC2 tag with HA (Igκ:HA-rVDAC2-HEK293 cells). This study showed that the effect of CBD was similar in both Igκ:HA-rVDAC2-HEK293 cells and control

HEK293 cells. In contrast, Igκ:HA-rVDAC2-HEK293 cells did respond to inhibitors of VDAC such as S18 (3 μM) and 4,4'-diisothiocyanatostilbene-2,2'-disulphonate (DIDS; 10 μM), perhaps because the density of the channel on the plasma membrane was not consistent in all cells that were investigated using whole-cell patch-clamp. Nonetheless, it would seem unlikely that VDAC2 is targeted by CBD. If that was the case, CBD treatment should have caused a reduction of the P:O ratio since VDAC2 also transport metabolites (e.g. ADP^{3-}) involved in OXPHOS (Maurya and Mahalakshmi, 2017; Naghdi and Hajnóczky, 2016).

CBD does not prevent Ca^{2+} uptake in either NS-$mito_{HE}$ or NS-$mito_{EP}$ as high extra-mitochondrial Ca^{2+} could still induce mPT. The increase of mitochondrial swelling induced with high Ca^{2+} in NS-$mito_{EP}$ may be caused by accumulation of ions in mitochondrial matrix. Since CBD induces H^+ leak (increases of state 4 respiration) in NS-$mito_{EP}$, it is very likely that this leak is caused by the activation of H^+ uptake in the matrix of mitochondria. ATP^{4-}synthase is not targeted by CBD. However, CBD-induced H^+ leak in NS-$mito_{EP}$ may be mediated through activation of another inner-membrane H^+ channel/transporter. Potential candidates of inner-membrane H^+ channels/transporters may include: uncoupling proteins (UCPs), inorganic phosphate carrier symporter (PiC) or H^+ antiporters such as Ca^{2+}/H^+ exchanger (CHX), Na^+/H^+ exchanger (NHX), K^+/H^+ exchanger (KHX) (Santo-Domingo and Demaurex, 2012).

In neurons and glia cells, CBD induces a slow rate mitochondrial Ca^{2+} efflux which suppresses cytosolic Ca^{2+} oscillation during seizures (Ryan et al., 2009). Furthermore, these authors showed that GCP37157 (an inhibitor of Na^+/Ca^{2+} exchanger (NCX)) supresses CBD-induced Ca^{2+} efflux under the same conditions. Initially, this was interpreted as CBD may be acting directly through NCX (Ryan et al., 2009). Conversely, my study demonstrated that Ca^{2+} is not required to drive H^+ leak mediated by CBD as my OXPHOS experiments were performed

in a condition devoid of Ca^{2+}. Therefore, CBD may interact directly with neither CHX nor NCX but rather NHX. Consequently, NHX activation with CBD would increase H^+ uptake as well as Na^+ efflux in intermembrane space. As the concentration of Na^+ increases in the intermembrane space, this would allow NCX to use Na^+ influx to drive Ca^{2+} efflux (Ryan et al., 2009). This may be the mechanism by which CBD mediates its anti-epileptic effect.

Since CBD does not appear to act on Ca^{2+}-induced swelling and OXPHOS of NS-mito$_{HE}$, my data suggest that the coupling between NHX and NCX may be altered in epilepsy. The coupled function of NHX-NCX allows a net H^+ influx and Ca^{2+} efflux, a function similar to that of CHX (Palty et al., 2012; Santo-Domingo and Demaurex, 2012). Mitochondrial NCX is encoded by leucine zipper-EF-hand containing transmembrane protein 1 *(Letm1)* (Tsai et al., 2014). Wolf–Hirschhorn syndrome is caused by the deletion of *Letm1* which leads to a haploinsufficiency of LETM1 (Battaglia et al., 2015; Hart et al., 2014). Interestingly, patients with Wolf–Hirschhorn syndrome (WHS) also suffer from epilepsy (Battaglia et al., 2015; Hart et al., 2014). Therefore, it is plausible that impairment of mitochondrial Ca^{2+} efflux could be implicated in WHS-epilepsy. Given that mitochondrial Ca^{2+} efflux may be altered in TLE as suggested by my work, it is plausible that CBD could also be indicated for patients with WHS.

Induction of cytochrome C (Cyt C) release from mitochondria activates the intrinsic pathway of apoptosis (Ott et al., 2002). To determine whether the increase of Ca^{2+}-induced swelling mediated by CBD could be associated with an increase permeability ("rupture") of the outer-membrane, I investigated the effect of CBD on Cyt C release following Ca^{2+}-induced mPT (Ott et al., 2002). Unlike the VDAC blocker S18, CBD did not promote Cyt C release (or "rupture" of the outer-membrane) in NS-mito$_{EP}$ following Ca^{2+}-mediated mPT. This suggests that CBD does not trigger the intrinsic pathway of apoptosis in NS-mito$_{EP}$. This finding is

consistent with the work of Do Val-da Silva et al. who showed that CBD does not induce neuronal death but rather exert a neuroprotective effect (Do Val-da Silva et al., 2017; Ryan et al., 2009). The mechanism underlying the neuroprotective of CBD may involve its action on NHX-NCX. The effect of CBD on NS-mito$_{EP}$ clearly depends on the length of its lateral aliphatic chain. In comparison with CBD, CBDV only lacks an ethyl-group at its lateral aliphatic chain. This small difference between both molecules appears to affect the interaction of CBDV with mitochondria as it altered neither OXPHOS nor Ca^{2+}-induced mPT in both NS-mito$_{HE}$ and NS-mito$_{EP}$.

Finally, my findings showed that blockade of VDAC should not be used as therapeutic approach to treat epilepsy as S18 treatment causes a dramatic increase of Cyt C release from NS-mito$_{EP}$. In this study, NS-mito$_{EP}$ contained mitochondria of neuronal soma in addition to that of microglia cells and astrocytes. This suggests that the effect of S18 may not be limited to one cell type. Similarly, VDAC blockers such as 4,4'-diisothiocyanatostilbene-2,2'-disulphonate (DIDS), G3139 or aspirin have been shown to increase the production of reactive oxidative species (ROS) as well as inducing apoptosis in neurons and liver cells (Han et al., 2003; Pamenter et al., 2013; Tan, 2012; Tewari et al., 2017). This is consistent with the effect of endogenous inhibitors of VDAC such as BCL2 Associated X (Bax) and BH3 interacting-domain (Bid), since both induce ROS production and apoptosis mediated by mitochondria (Banerjee and Ghosh, 2004; Jürgensmeier et al., 1998; Kim et al., 2000; Rostovtseva et al., 2004). Taken together, it appears that blockade of VDAC (whether with pharmacological compounds or proteins produced endogenously) leads to the activation of the intrinsic pathway of apoptosis.

7 GENERAL CONCLUSION

The function of hippocampal non-synaptic mitochondria (NS-mito) is impaired in rats with temporal lobe epilepsy. In this work, I demonstrated a downregulation of ND4 (a component of complex I), a reduction of the P:O ratio and an uncoupling of oxidative phosphorylation (OXPHOS) in NS-mito isolated from rats with TLE. Furthermore, I showed that the magnitude of mitochondrial swelling was reduced in NS-mito$_{EP}$ following Ca^{2+}-induced mitochondrial permeability transition (mPT). A direct treatment of NS-mito$_{EP}$ with cannabidiol (CBD; 10 µM) normalised the magnitude of swelling, while a treatment of NS-mito$_{HE}$ with CBD affected neither OXPHOS nor Ca^{2+}-induced swelling. Furthermore, it is very likely that CBD-induced H^+ leak in NS-mito$_{EP}$ may cause the increase of Ca^{2+}-induced swelling observed in these mitochondria. Based upon the current literature of how CBD may affect mitochondrial Ca^{2+} efflux, as well as my findings, here I speculate that CBD may target the inner-membrane Na^+/H^+ exchanger (NHX) rather than mitochondrial voltage-dependent anion-selective channel (VDAC). This study also indicates that CBD's effect on mitochondrial function depends on the length of its lateral aliphatic chain, as cannabidivarin, which possesses a shorter lateral aliphatic chain (by an ethyl-group) did not exhibit a comparable effect to CBD.

CBD did not affect Cyt C release following Ca^{2+}-induced mPT In NS-mito$_{EP}$, thus suggesting that CBD may not activate the intrinsic pathway of apoptosis. The absence of CBD's effect on Cyt C release substantially differs from that of the VDAC blocker S18 as it causes both an exacerbation of mitochondrial swelling as well as a dramatic increase of Cyt C release after Ca^{2+}-induced mPT. Further investigation into the effect of VDAC blockade on OXPHOS indicates that S18's effect differs from that of CBD. VDAC blockade did not induce mitochondrial uncoupling in NS-mito$_{EP}$, but it reduced both state 4 respiration and the P:O

ratio. In contrast, VDAC blockade did not exhibit any effect on OXPHOS in NS-mito$_{HE}$. CBD does not directly act upon complex II, III, IV or ATP^{4-} synthase as VDAC blockade affected state 3 respiration in neither NS-mito$_{HE}$ nor NS-mito$_{EP}$. However, given its effect on the P:O ratio, blockade of VDAC may appear to reduce the transport of ADP^{3-}/ATP^{4-}.

8 FUTURE WORK

To study whether CBD acts on the inner-membrane, mitoplasts isolated from NS-mito$_{HE}$ and NS-mito$_{EP}$ will be used to investigate its effect (Costa and Krieger, 2009). The effect of CBD treatment on the conductance of mitoplasts will be determined with whole-cell patch-clamp since mitoplasts are relatively large (3-6 µm) (Keller and Hedrich, 1992). Keller and Hedrich recommended that the resistance of the pipette should be 5-18 MΩ, and during the cell-attach mode, seals should be formed with a resistance >10GΩ (Keller and Hedrich, 1992). As CBD increases H^+ leak in NS-mito$_{EP}$, mitoplasts from NS-mito$_{EP}$ are expected to exhibit a greater CBD-mediated conductance compared to that of NS-mito$_{HE}$.

After establishing the effect of CBD on the conductance of mitoplasts isolated from NS-mito$_{EP}$, the mechanism of action by which CBD alters the conductance of mitoplasts will be investigated. To determine what H^+ transporters/channels are activated by CBD, specific inhibitors of inorganic phosphate carrier (PiC), uncoupling proteins (UCPs), Na^+/H^+ exchanger (NHX), Ca^{2+}/H^+ exchanger (CHX), and Na^+/Ca^{2+} exchanger (NCX) will be investigated for alteration of CBD's effect. Subsequently, proteins targeted by CBD could then be investigated for changes in expression in epilepsy using western blotting using lysates from NS-mito and hippocampal tissue.

Next, oxygen consumption assay and mitochondrial swelling assays will be used to assess the contribution of proteins targeted by CBD on oxidative phosphorylation and Ca^{2+}-induced swelling in NS-mito$_{EP}$, respectively. Here, the combination of CBD and the inhibitors mentioned above will also be used to determine how the function of these inner-membrane transporters/channels are affected in NS-mito$_{EP}$.

Abnormal hypersynchronised neuronal activity of hyperexcitable epileptogenic networks are responsible for the recurrence of seizures in epilepsy (Bertram et al., 1998; Esclapez et al., 1999). Epileptogenic neurons contribute to hyperexcitability and hyper-synchronicity in neural network in the hippocampi of patients and animals with TLE (Deisz et al., 2011). Consequently, CBD's effect on mitochondria could be investigated for regulation of excitability of interneurons (inhibitory neurons) and pyramidal neurons (excitatory neurons) in the CA1 region of both healthy and epileptic rats using whole-cell patch-clamp electrophysiology on hippocampal slices.

Each spontaneous miniature excitatory postsynaptic potential or current (mEPSP or mEPSC) is generated by individual synaptic vesicle containing discrete amounts of neurotransmitter (here glutamate) since mEPSP/C is caused by a quantal release of excitatory neurotransmitter into the synaptic cleft (Bykhovskaia, 2008). As a result, the rate of spontaneous firing of pre-synaptic neurons (here glutamatergic neurons) can be determined by measuring the frequency of mEPSPs (or mEPSCs). Conversely, the excitability of post-synaptic neurons to glutamate can be assessed by measuring the amplitude of mEPSPs (or mEPSCs). For example, the amplitude of mEPSPs (or mEPSCs) will be greater in hyperexcitable post-synaptic neurons compared to that of control neurons. Alternatively, neuronal excitability can be assessed using the current-voltage (I-V) relationship protocol which measures neuronal adaptation, plasma membrane conductance and the threshold at which post-synaptic neurons fire action potentials.

In a future study, the effect of CBD on glutamatergic synaptic transmission could be assessed on the amplitude and frequency of mEPSPs. Its effect on neuronal excitability could also be determined using the I-V relationship protocol. Furthermore, inhibitors of proteins

targeted by CBD will be used to investigate whether the anti-epileptic effect of CBD (in neurons from epileptic rats) is dependent on the activation of mitochondrial inner-membrane H^+ transporters/channels (previously determined as targets of CBD).

The anti-epileptic effect of CBD could be mediated through modulation of Ca^{2+} homeostasis in NS-mito$_{EP}$. Its effect on intracellular Ca^{2+} could be investigated in CA1 neurons in slices from rat with TLE following activation of N-methyl-D-aspartate. Furthermore, the effect of inhibitors (affecting CBD's effect in previous experiments) of inner-membrane channels or transporters can be assessed for alteration of CBD's effect on Ca^{2+} handling under epileptic conditions. Protocols and procedures in these brain slices would be similar to that of Ryan et al. (Ryan et al., 2009). Here, the mechanism by which CBD exerts its effect on mitochondrial Ca^{2+} efflux through NCX could be studied by determining whether the function of NCX is affected by the inhibition of H^+ transporters/channels targeted by CBD. After performing all the above experiments on brain slices from rat with TLE, brain tissues resected from pharmacoresistant patients with epilepsy could subsequently be used to investigate whether this mechanism underlying the anti-epileptic effect of CBD is also present in human epilepsy.

As previously described in literature review (see section 1.1.3), anti-epileptic drugs have been developed to control seizures, although comorbidities associated with epilepsy also affect significantly the quality of life of patients with epilepsy (Baca et al., 2011; Keezer et al., 2016; Modi et al., 2009). Therefore, investigating targets which could control some of these comorbidities is essential. Given the association between impairment of memory and epilepsy, it would be critical to investigate the implication of the previously determined mitochondrial target (or targets) of CBD on synaptic plasticity in hippocampal slices of rats

with TLE. These experiments can either be assessed at a network level using a multi-electrode array (MEA) system or on single neurons using whole-cell patch-clamp. MEA possesses the advantage over whole-cell patch-clamp when it comes to investigate plasticity (e.g. long-term potentiation (LTP)). In addition, LTP protocols are more likely to fail when using whole-cell patch-clamp compared to MEA. Thus, this indicates that experiments performed on patch-clamp may require more trials.

Finally, as my current data suggests that CBD may act through NHX (see general discussion), the potential anti-convulsant or anti-comorbidity effect of CBD could be assessed in mice with Wolf–Hirschhorn syndrome (Zhang et al., 2014). If CBD exhibited any effect on these mice, all *in vitro* assays will be performed as described above.

9 APPENDIX

Table 9-1. Classification of behavioural seizures according to Racine, 1972.

Score	***Behaviour***
1	*Oro-facial movements (e.g. blinking eyes, salivation, mouth clonus)*
2	*Head nodding*
3	*Unilateral clonus of one anterior limb*
4	*Bilateral clonus of both anterior limb with rearing*
5	*Generalised tonic-clonic seizures with rearing and loss of balance*

Table 9-2. List of antibodies used in this study.

Target (Clone)	Description	Host	Conjugation	Supplier	Catalogue N°/ #Lot N°
β-actin (AC-15)	Polyclonal	Mouse	None	Sigma Aldrich	A5441
COX-IV (D-20)	Polyclonal	Goat	None	Insight Biotech	Sc-69359/ #D2115
Cyt C (37BA11)	Polyclonal	Goat	None	Abcam	ab110325/ #GR289719-6
Na^+/K^+-ATPase (EP1845Y)	Polyclonal	Rabbit	None	Abcam	ab76020/ #YH022206
ND4 (A-16)	Polyclonal	Rabbit	None	Insight Biotech	Sc-20499/ #B0514
NDUFS1	Polyclonal	Rabbit	None	Insight Biotech	GTX105270/ #39827
HA-tag	Monoclonal	Mouse	None	Source Bioscience	AB-10110
VDAC1 (N152B/23)	Monoclonal	Mouse	None	Millipore	MABN504/ #2780173
VDAC2 (3D2)	Monoclonal	Mouse	None	Sigma Aldrich	SAB1402389-100UG/ #D8251-3D2
VDAC2	Polyclonal	Rabbit	None	New England Biolabs	9412S/ 04.2015#1
Rabbit-IgG	Polyclonal	Goat	HRP	Abcam	ab205718
Mouse-IgG	Polyclonal	Goat	HRP	Abcam	ab6728
Goat-IgG	Polyclonal	Donkey	HRP	Insight Biotech	Sc2020/ #A2216
Rabbit-IgG	Polyclonal	Goat	Alexa - 488	Abcam	ab150077
Mouse-IgG	Polyclonal	Goat	Alexa - 488	Abcam	ab150113

Table 9-3. Effect of CsA, CBD and S18 on Ca^{2+}-induced mitochondrial swelling in both NS-$mito_{HE}$ and NS-$mito_{EP}$

Groups	Mean, N	Adjusted P-value (Q<0.05)
HE-Veh2 *vs* EP-Veh2	35±1.9, N=12 *vs* 26±2.8, N=13	Yes
HE-Veh2 *vs* HE-CsA	35±1.9, N=12 *vs* 13±3.3, N=12	Yes
HE-CsA *vs* EP-CsA	13±3.3, N=12 *vs* 21±2.4, N=11	No
HE-Veh2 *vs* HE-S18	35±1.9, N=12 *vs* 60±5.4, N=13	Yes
EP-Veh2 *vs* EP-S18	26±2.8, N=13 *vs* 49±4.0, N=11	Yes
HE-S18 *vs* EP-S18	60±5.4, N=13 *vs* 49±4.0, N=11	Yes
HE-Veh2 *vs* HE-CBD	35±1.9, N=12 *vs* 31±3.6, N=12	No
EP-Veh2 *vs* EP-CBD	26±2.8, N=13 *vs* 36±3.2, N=13	Yes
EP-CBD *vs* EP-S18	36±3.2, N=13 *vs* 49±4.0, N=13	Yes
EP-CBD *vs* HE-S18	36±3.2, N=13 *vs* 60±5.4, N=13	Yes
HE-Veh2 *vs* EP-CBD	35±1.9, N=12 *vs* 36±3.2, N=13	Yes

Table 9-4. Expression of NDUFS1 normalised to COX-IV.

Types of lysate	NDUFS1/COX-IV (N = number of animals per group)	Mann-Whitney test (P<0.05)?
Tissue: HE *vs* EP	100 ± 55.7 (N = 6) *vs* 55.2 ± 14.1 (N = 7)	No
NS-mito: HE *vs* EP	100 ± 15.9 (N = 7) *vs* 136.5 ± 30.0 (N = 7)	No
SYN: HE *vs* EP	100 ± 17.4 (N = 4) *vs* 111 ± 27.1 (N = 4)	No

REFERENCES

10 REFERENCES

A Shchepina, L., Pletjushkina, O., V Avetisyan, A., E Bakeeva, L., Fetisova, E., S Izyumov, D., B Saprunova, V., Vyssokikh or Vysokikh, M., Chernyak, B., and Skulachev, V. (2002). Oligomycin, inhibitor of the F-0 part of H+-ATP-synthase, suppresses the TNF-induced apoptosis. Oncogene *21*, 8149–8157.

Abraham, J., Fox, P.D., Condello, C., Bartolini, A., and Koh, S. (2012). Minocycline attenuates microglia activation and blocks the long-term epileptogenic effects of early-life seizures. Neurobiol. Dis. *46*, 425–430.

Acharya, M.M., and Katyare, S.S. (2005). Structural and functional alterations in mitochondrial membrane in picrotoxin-induced epileptic rat brain. Exp. Neurol. *192*, 79–88.

Adrain, C., Creagh, E.M., and Martin, S.J. (2001). Apoptosis-associated release of Smac/DIABLO from mitochondria requires active caspases and is blocked by Bcl-2. EMBO J. *20*, 6627–6636.

Ahrens, J., Demir, R., Leuwer, M., Roche, J. de la, Krampfl, K., Foadi, N., Karst, M., and Haeseler, G. (2009). The Nonpsychotropic Cannabinoid Cannabidiol Modulates and Directly Activates Alpha-1 and Alpha-1-Beta Glycine Receptor Function. Pharmacology *83*, 217–222.

Alves, M., Gomez-Villafuertes, R., Delanty, N., Farrell, M.A., O'Brien, D.F., Miras-Portugal, M.T., Hernandez, M.D., Henshall, D.C., and Engel, T. (2017). Expression and function of the metabotropic purinergic P2Y receptor family in experimental seizure models and patients with drug-refractory epilepsy. Epilepsia *58*, 1603–1614.

Amidfar, M., Colic, L., Walter, M., and Kim, Y.-K. (2018). Complex Role of the Serotonin Receptors in Depression: Implications for Treatment. In Understanding Depression, (Springer, Singapore), pp. 83–95.

Amorim, B.O., Hamani, C., Ferreira, E., Miranda, M.F., Fernandes, M.J.S., Rodrigues, A.M., de Almeida, A.-C.G., and Covolan, L. (2016). Effects of A1 receptor agonist/antagonist on spontaneous seizures in pilocarpine-induced epileptic rats. Epilepsy Behav. EB *61*, 168–173.

Anflous, K., Armstrong, D.D., and Craigen, W.J. (2001). Altered Mitochondrial Sensitivity for ADP and Maintenance of Creatine-stimulated Respiration in Oxidative Striated Muscles from VDAC1-deficient Mice. J. Biol. Chem. *276*, 1954–1960.

Anflous-Pharayra, K., Lee, N., Armstrong, D.L., and Craigen, W.J. (2011). VDAC3 has differing mitochondrial functions in two types of striated muscles. Biochim. Biophys. Acta BBA - Bioenerg. *1807*, 150–156.

Angelatou, F., Pagonopoulou, O., Maraziotis, T., Olivier, A., Villemeure, J.G., Avoli, M., and Kostopoulos, G. (1993). Upregulation of A1 adenosine receptors in human temporal lobe epilepsy: a quantitative autoradiographic study. Neurosci. Lett. *163*, 11–14.

Aroniadou-Anderjaska, V., Fritsch, B., Qashu, F., and Braga, M.F.M. (2008). Pathology and Pathophysiology of the Amygdala in Epileptogenesis and Epilepsy. Epilepsy Res. *78*, 102–116.

Austgen, J.R., and Kline, D.D. (2013). Endocannabinoids blunt the augmentation of synaptic transmission by serotonin 2A receptors in the nucleus tractus solitarii (nTS). Brain Res. *1537*, 27–36.

Baca, C.B., Vickrey, B.G., Caplan, R., Vassar, S.D., and Berg, A.T. (2011). Psychiatric and Medical Comorbidity and Quality of Life Outcomes in Childhood-Onset Epilepsy. Pediatrics *128*, e1532–e1543.

Bakas, T., van Nieuwenhuijzen, P.S., Devenish, S.O., McGregor, I.S., Arnold, J.C., and Chebib, M. (2017). The direct actions of cannabidiol and 2-arachidonoyl glycerol at GABAA receptors. Pharmacol. Res. *119*, 358–370.

Balosso, S., Maroso, M., Sanchez-Alavez, M., Ravizza, T., Frasca, A., Bartfai, T., and Vezzani, A. (2008). A novel non-transcriptional pathway mediates the proconvulsive effects of interleukin-1beta. Brain J. Neurol. *131*, 3256–3265.

Banerjee, J., and Ghosh, S. (2004). Bax increases the pore size of rat brain mitochondrial voltage-dependent anion channel in the presence of tBid. Biochem. Biophys. Res. Commun. *323*, 310–314.

Barker-Haliski, M., and White, H.S. (2015). Glutamatergic Mechanisms Associated with Seizures and Epilepsy. Cold Spring Harb. Perspect. Med. *5*.

Barrell, B.G., Bankier, A.T., and Drouin, J. (1979). A different genetic code in human mitochondria. Nature *282*, 189–194.

Barros-Barbosa, A.R., Ferreirinha, F., Oliveira, Â., Mendes, M., Lobo, M.G., Santos, A., Rangel, R., Pelletier, J., Sévigny, J., Cordeiro, J.M., et al. (2016). Adenosine A2A receptor and ecto-5'-nucleotidase/CD73 are upregulated in hippocampal astrocytes of human patients with mesial temporal lobe epilepsy (MTLE). Purinergic Signal. *12*, 719–734.

Basheer, R., Strecker, R.E., Thakkar, M.M., and McCarley, R.W. (2004). Adenosine and sleep-wake regulation. Prog. Neurobiol. *73*, 379–396.

Basso, E., Fante, L., Fowlkes, J., Petronilli, V., Forte, M.A., and Bernardi, P. (2005). Properties of the Permeability Transition Pore in Mitochondria Devoid of Cyclophilin D. J. Biol. Chem. *280*, 18558–18561.

Batandier, C., Poulet, L., Hininger, I., Couturier, K., Fontaine, E., Roussel, A.-M., and Canini, F. (2014). Acute stress delays brain mitochondrial permeability transition pore opening. J. Neurochem. *131*, 314–322.

Bàthori, G., Parolini, I., Tombola, F., Szabò, I., Messina, A., Oliva, M., Pinto, V.D., Lisanti, M., Sargiacomo, M., and Zoratti, M. (1999). Porin Is Present in the Plasma Membrane Where It Is Concentrated in Caveolae and Caveolae-related Domains. J. Biol. Chem. *274*, 29607–29612.

Báthori, G., Parolini, I., Szabó, I., Tombola, F., Messina, A., Oliva, M., Sargiacomo, M., De Pinto, V., and Zoratti, M. (2000). Extramitochondrial porin: facts and hypotheses. J. Bioenerg. Biomembr. *32*, 79–89.

Battaglia, A., Carey, J.C., and South, S.T. (2015). Wolf–Hirschhorn syndrome: A review and update. Am. J. Med. Genet. C Semin. Med. Genet. *169*, 216–223.

Baulac, M., de Boer, H., Elger, C., Glynn, M., Kälviäinen, R., Little, A., Mifsud, J., Perucca, E., Pitkänen, A., and Ryvlin, P. (2015). Epilepsy priorities in Europe: A report of the ILAE-IBE Epilepsy Advocacy Europe Task Force. Epilepsia *56*, 1687–1695.

Bazán, N.G., Liberti, S.A.M. de, and Turco, E.B.R. de (1982). Arachidonic acid and arachidonoyldiglycerols increase in rat cerebrum during bicuculline-induced status epilepticus. Neurochem. Res. *7*, 839–843.

Bazán, N.G., Rodríguez, E. de T., and Morelli, S. de L. (1983). Free arachidonic acid and membrane lipids in the central nervous system during bicuculline-induced status epilepticus. Adv. Neurol. *34*, 305–310.

Beach, T.G., Woodhurst, W.B., MacDonald, D.B., and Jones, M.W. (1995). Reactive microglia in hippocampal sclerosis associated with human temporal lobe epilepsy. Neurosci. Lett. *191*, 27–30.

Bechmann, I., Diano, S., Warden, C.H., Bartfai, T., Nitsch, R., and Horvath, T.L. (2002). Brain mitochondrial uncoupling protein 2 (UCP2): a protective stress signal in neuronal injury. Biochem. Pharmacol. *64*, 363–367.

Benani, A., Barquissau, V., Carneiro, L., Salin, B., Colombani, A.-L., Leloup, C., Casteilla, L., Rigoulet, M., and Pénicaud, L. (2009). Method for functional study of mitochondria in rat hypothalamus. J. Neurosci. Methods *178*, 301–307.

Ben-Hail, D., and Shoshan-Barmatz, V. (2016). VDAC1-interacting anion transport inhibitors inhibit VDAC1 oligomerization and apoptosis. Biochim. Biophys. Acta BBA - Mol. Cell Res. *1863*, 1612–1623.

Benjamini, Y., Krieger, A.M., and Yekutieli, D. (2006). Adaptive linear step-up procedures that control the false discovery rate. Biometrika *93*, 491–507.

Bertram, E.H., Zhang, D.X., Mangan, P., Fountain, N., and Rempe, D. (1998). Functional anatomy of limbic epilepsy: a proposal for central synchronization of a diffusely hyperexcitable network. Epilepsy Res. *32*, 194–205.

Bethmann, K., Fritschy, J.-M., Brandt, C., and Löscher, W. (2008). Antiepileptic drug resistant rats differ from drug responsive rats in GABAA receptor subunit expression in a model of temporal lobe epilepsy. Neurobiol. Dis. *31*, 169–187.

Bezençon, O., Heidmann, B., Siegrist, R., Stamm, S., Richard, S., Pozzi, D., Corminboeuf, O., Roch, C., Kessler, M., Ertel, E.A., et al. (2017). Discovery of a Potent, Selective T-type Calcium Channel Blocker as a Drug Candidate for the Treatment of Generalized Epilepsies.

Bhaskaran, M.D., and Smith, B.N. (2010). Effects of TRPV1 activation on synaptic excitation in the dentate gyrus of a mouse model of temporal lobe epilepsy. Exp. Neurol. *223*, 529–536.

Bialer, M., and White, H.S. (2010). Key factors in the discovery and development of new antiepileptic drugs. Nat. Rev. Drug Discov. *9*, 68–82.

Biber, K., Lubrich, B., Fiebich, B.L., Boddeke, H.W., and van Calker, D. (2001). Interleukin-6 enhances expression of adenosine A(1) receptor mRNA and signaling in cultured rat cortical astrocytes and brain slices. Neuropsychopharmacol. Off. Publ. Am. Coll. Neuropsychopharmacol. *24*, 86–96.

Biber, K., Pinto-Duarte, A., Wittendorp, M.C., Dolga, A.M., Fernandes, C.C., Von Frijtag Drabbe Künzel, J., Keijser, J.N., de Vries, R., Ijzerman, A.P., Ribeiro, J.A., et al. (2008). Interleukin-6 upregulates neuronal adenosine A1 receptors: implications for neuromodulation and neuroprotection. Neuropsychopharmacol. Off. Publ. Am. Coll. Neuropsychopharmacol. *33*, 2237–2250.

Billeter, A.T., Hellmann, J.L., Bhatnagar, A., and Polk, H.C. (2014). Transient receptor potential ion channels: powerful regulators of cell function. Ann. Surg. *259*, 229–235.

Bisogno, T., Hanus, L., De Petrocellis, L., Tchilibon, S., Ponde, D.E., Brandi, I., Moriello, A.S., Davis, J.B., Mechoulam, R., and Di Marzo, V. (2001). Molecular targets for cannabidiol and its synthetic analogues: effect on vanilloid VR1 receptors and on the cellular uptake and enzymatic hydrolysis of anandamide. Br. J. Pharmacol. *134*, 845–852.

Blake, R.V., Wroe, S.J., Breen, E.K., and McCarthy, R.A. (2000). Accelerated forgetting in patients with epilepsy evidence for an impairment in memory consolidation. Brain *123*, 472–483.

Blanchard, M.G., Willemsen, M.H., Walker, J.B., Dib-Hajj, S.D., Waxman, S.G., Jongmans, M.C.J., Kleefstra, T., van de Warrenburg, B.P., Praamstra, P., Nicolai, J., et al. (2015). De novo gain-of-function and loss-of-function mutations of SCN8A in patients with intellectual disabilities and epilepsy. J. Med. Genet. *52*, 330–337.

Boison, D. (2012). Adenosine dysfunction in epilepsy. Glia *60*, 1234–1243.

Boro, A., and Haut, S. (2003). Medical comorbidities in the treatment of epilepsy. Epilepsy Behav. *4*, 2–12.

Borst, P., Evers, R., Kool, M., and Wijnholds, J. (2000). A Family of Drug Transporters: the Multidrug Resistance-Associated Proteins. JNCI J. Natl. Cancer Inst. *92*, 1295–1302.

Bradford, H.F. (1995). Glutamate, GABA and epilepsy. Prog. Neurobiol. *47*, 477–511.

Bradley, C.A., Taghibiglou, C., Collingridge, G.L., and Wang, Y.T. (2008). Mechanisms Involved in the Reduction of GABAA Receptor α1-Subunit Expression Caused by the Epilepsy Mutation A322D in the Trafficking-competent Receptor. J. Biol. Chem. *283*, 22043–22050.

Brand, M.D., and Lehninger, A.L. (1977). H+/ATP ratio during ATP hydrolysis by mitochondria: modification of the chemiosmotic theory. Proc. Natl. Acad. Sci. U. S. A. *74*, 1955–1959.

Brodie, M.J. (2010). Antiepileptic drug therapy the story so far. Seizure *19*, 650–655.

Brodie, M.J., and Sills, G.J. (2011). Combining antiepileptic drugs--rational polytherapy? Seizure *20*, 369–375.

Brunner, T.F. (1973). Marijuana in ancient greece and rome? The literary evidence. Bull. Hist. Med. *47*, 344–355.

Brustovetsky, N., Brustovetsky, T., Jemmerson, R., and Dubinsky, J.M. (2002). Calcium-induced Cytochrome c release from CNS mitochondria is associated with the permeability transition and rupture of the outer membrane. J. Neurochem. *80*, 207–218.

Brustovetsky, N., Brustovetsky, T., Purl, K.J., Capano, M., Crompton, M., and Dubinsky, J.M. (2003). Increased Susceptibility of Striatal Mitochondria to Calcium-Induced Permeability Transition. J. Neurosci. *23*, 4858–4867.

Butler, C.R., and Zeman, A.Z. (2008). Recent insights into the impairment of memory in epilepsy: transient epileptic amnesia, accelerated long-term forgetting and remote memory impairment. Brain *131*, 2243–2263.

Bykhovskaia, M. (2008). Making Quantal Analysis more Convenient, Fast, and Accurate: User Friendly Software Quantan. J. Neurosci. Methods *168*, 500–513.

Calder, P.C. (2010). Omega-3 Fatty Acids and Inflammatory Processes. Nutrients *2*, 355–374.

Canton, M., Luvisetto, S., Schmehl, I., and Azzone, G.F. (1995). The nature of mitochondrial respiration and discrimination between membrane and pump properties. Biochem. J. *310*, 477–481.

Carlini, E.A., and Cunha, J.M. (1981). Hypnotic and antiepileptic effects of cannabidiol. J. Clin. Pharmacol. *21*, 417S-427S.

Carrier, E.J., Auchampach, J.A., and Hillard, C.J. (2006). Inhibition of an equilibrative nucleoside transporter by cannabidiol: a mechanism of cannabinoid immunosuppression. Proc. Natl. Acad. Sci. U. S. A. *103*, 7895–7900.

Carvill, G.L., Regan, B.M., Yendle, S.C., O'Roak, B.J., Lozovaya, N., Bruneau, N., Burnashev, N., Khan, A., Cook, J., Geraghty, E., et al. (2013). GRIN2A mutations cause epilepsy-aphasia spectrum disorders. Nat. Genet. *45*, 1073–1076.

Catterall, W.A. (2011). Voltage-Gated Calcium Channels. Cold Spring Harb. Perspect. Biol. *3*.

Cesar, M. de C., and Wilson, J.E. (2004). All three isoforms of the voltage-dependent anion channel (VDAC1, VDAC2, and VDAC3) are present in mitochondria from bovine, rabbit, and rat brain. Arch. Biochem. Biophys. *422*, 191–196.

Ceulemans, B., Boel, M., Leyssens, K., Van Rossem, C., Neels, P., Jorens, P.G., and Lagae, L. (2012). Successful use of fenfluramine as an add-on treatment for Dravet syndrome. Epilepsia *53*, 1131–1139.

Chalfant, C.E., and Spiegel, S. (2005). Sphingosine 1-phosphate and ceramide 1-phosphate: expanding roles in cell signaling. J. Cell Sci. *118*, 4605–4612.

Chapp, A.D., Schum, S., Behnke, J.E., Hahka, T., Huber, M.J., Jiang, E., Larson, R.A., Shan, Z., and Chen, Q. (2018). Measurement of cations, anions, and acetate in serum, urine, cerebrospinal fluid, and tissue by ion chromatography. Physiol. Rep. *6*.

Chatenoud, L., and Bach, J.-F. (2012). Immunologie - 6e édition (Lavoisier).

Cheah, C.S., Yu, F.H., Westenbroek, R.E., Kalume, F.K., Oakley, J.C., Potter, G.B., Rubenstein, J.L., and Catterall, W.A. (2012). Specific deletion of NaV1.1 sodium channels in inhibitory interneurons causes seizures and premature death in a mouse model of Dravet syndrome. Proc. Natl. Acad. Sci. U. S. A. *109*, 14646–14651.

Chemel, B.R., Roth, B.L., Armbruster, B., Watts, V.J., and Nichols, D.E. (2006). WAY-100635 is a potent dopamine D4 receptor agonist. Psychopharmacology (Berl.) *188*, 244–251.

Cheng, E.H.-Y., Sheiko, T.V., Fisher, J.K., Craigen, W.J., and Korsmeyer, S.J. (2003). VDAC2 Inhibits BAK Activation and Mitochondrial Apoptosis. Science *301*, 513–517.

Cheong, E., and Shin, H.-S. (2013). T-type Ca^{2+} channels in absence epilepsy. Biochim. Biophys. Acta *1828*, 1560–1571.

Choi, H., Sell, R.L., Lenert, L., Muennig, P., Goodman, R.R., Gilliam, F.G., and Wong, J.B. (2008). Epilepsy surgery for pharmacoresistant temporal lobe epilepsy: a decision analysis. JAMA *300*, 2497–2505.

Choudhary, O.P., Paz, A., Adelman, J.L., Colletier, J.-P., Abramson, J., and Grabe, M. (2014). Structure-guided simulations illuminate the mechanism of ATP transport through VDAC1. Nat. Struct. Mol. Biol. *21*, 626–632.

Chuang, Y.-C., Chang, A.Y.W., Lin, J.-W., Hsu, S.-P., and Chan, S.H.H. (2004). Mitochondrial Dysfunction and Ultrastructural Damage in the Hippocampus during Kainic Acid–induced Status Epilepticus in the Rat. Epilepsia *45*, 1202–1209.

Chuang, Y.-C., Chen, S.-D., Lin, T.-K., Chang, W.-N., Lu, C.-H., Liou, C.-W., Chan, S.H.H., and Chang, A.Y.W. (2010). Transcriptional upregulation of nitric oxide synthase II by nuclear factor-kappaB promotes apoptotic neuronal cell death in the hippocampus following experimental status epilepticus. J. Neurosci. Res. *88*, 1898–1907.

Chuang, Y.-C., Lin, T.-K., Huang, H.-Y., Chang, W.-N., Liou, C.-W., Chen, S.-D., Chang, A.Y., and Chan, S.H. (2012). Peroxisome proliferator-activated receptors γ/mitochondrial uncoupling protein 2 signaling protects against seizure-induced neuronal cell death in the hippocampus following experimental status epilepticus. J. Neuroinflammation *9*, 184.

Citraro, R., Leo, A., Marra, R., De Sarro, G., and Russo, E. (2015). Antiepileptogenic effects of the selective COX-2 inhibitor etoricoxib, on the development of spontaneous absence seizures in WAG/Rij rats. Brain Res. Bull. *113*, 1–7.

Clark, L.C., Wolf, R., Granger, D., and Taylor, Z. (1953). Continuous recording of blood oxygen tensions by polarography. J. Appl. Physiol. *6*, 189–193.

Collins, R.C., Plum, F., Posner, J., Sanders, A.P., Kramer, R.S., Woodhall, B., and Currie, W.D. (1970). Energy and Epilepsy. Science *170*, 1430–1431.

Colombini, M. (1979). A candidate for the permeability pathway of the outer mitochondrial membrane. Nature *279*, 643–645.

Colombini, M. (1983). Purification of VDAC (voltage-dependent anion-selective channel) from rat liver mitochondria. J. Membr. Biol. *74*, 115–121.

Colombini, M. (2004). VDAC: the channel at the interface between mitochondria and the cytosol. Mol. Cell. Biochem. *256–257*, 107–115.

Colombini, M., Blachly-Dyson, E., and Forte, M. (1996). VDAC, a channel in the outer mitochondrial membrane. Ion Channels *4*, 169–202.

Commissioner, O. of the (2018). Press Announcements - FDA approves first drug comprised of an active ingredient derived from marijuana to treat rare, severe forms of epilepsy.

Conrad, J., Pawlowski, M., Dogan, M., Kovac, S., Ritter, M.A., and Evers, S. (2013). Seizures after cerebrovascular events: Risk factors and clinical features. Seizure *22*, 275–282.

Consroe, P., Benedito, M.A., Leite, J.R., Carlini, E.A., and Mechoulam, R. (1982). Effects of cannabidiol on behavioral seizures caused by convulsant drugs or current in mice. Eur. J. Pharmacol. *83*, 293–298.

Costa, A.D.T., and Krieger, M.A. (2009). Evidence for an ATP-sensitive K+ channel in mitoplasts isolated from Trypanosoma cruzi and Crithidia fasciculata. Int. J. Parasitol. *39*, 955–961.

Cottrell, G.S., Amadesi, S., Grady, E.F., and Bunnett, N.W. (2004). Trypsin IV, a novel agonist of protease-activated receptors 2 and 4. J. Biol. Chem. *279*, 13532–13539.

Covolan, L., Ribeiro, L.T., Longo, B.M., and Mello, L.E. (2000). Cell damage and neurogenesis in the dentate granule cell layer of adult rats after pilocarpine- or kainate-induced status epilepticus. Hippocampus *10*, 169–180.

Cserép, C., Pósfai, B., Schwarcz, A.D., and Dénes, Á. (2018). Mitochondrial Ultrastructure Is Coupled to Synaptic Performance at Axonal Release Sites. ENeuro *5*, ENEURO.0390-17.2018.

Cunha, J.M., Carlini, E.A., Pereira, A.E., Ramos, O.L., Pimentel, C., Gagliardi, R., Sanvito, W.L., Lander, N., and Mechoulam, R. (1980). Chronic administration of cannabidiol to healthy volunteers and epileptic patients. Pharmacology *21*, 175–185.

Curia, G., Longo, D., Biagini, G., Jones, R.S.G., and Avoli, M. (2008). The pilocarpine model of temporal lobe epilepsy. J. Neurosci. Methods *172*, 143–157.

Dan Dunn, J., Alvarez, L.A., Zhang, X., and Soldati, T. (2015). Reactive oxygen species and mitochondria: A nexus of cellular homeostasis. Redox Biol. *6*, 472–485.

Dark, P. (2000). The Environment of Britain in the First Millennium AD (Bloomsbury Academic).

De Petrocellis, L., Vellani, V., Schiano-Moriello, A., Marini, P., Magherini, P.C., Orlando, P., and Di Marzo, V. (2008). Plant-derived cannabinoids modulate the activity of transient receptor potential channels of ankyrin type-1 and melastatin type-8. J. Pharmacol. Exp. Ther. *325*, 1007–1015.

De Petrocellis, L., Ligresti, A., Moriello, A.S., Allarà, M., Bisogno, T., Petrosino, S., Stott, C.G., and Di Marzo, V. (2011). Effects of cannabinoids and cannabinoid-enriched Cannabis extracts on TRP channels and endocannabinoid metabolic enzymes. Br. J. Pharmacol. *163*, 1479–1494.

De Petrocellis, L., Orlando, P., Moriello, A.S., Aviello, G., Stott, C., Izzo, A.A., and Di Marzo, V. (2012). Cannabinoid actions at TRPV channels: effects on TRPV3 and TRPV4 and their potential relevance to gastrointestinal inflammation. Acta Physiol. Oxf. Engl. *204*, 255–266.

De Pinto, V., Guarino, F., Guarnera, A., Messina, A., Reina, S., Tomasello, F.M., Palermo, V., and Mazzoni, C. (2010). Characterization of human VDAC isoforms: A peculiar function for VDAC3? Biochim. Biophys. Acta BBA - Bioenerg. *1797*, 1268–1275.

De Pinto, V., Reina, S., Gupta, A., Messina, A., and Mahalakshmi, R. (2016). Role of cysteines in mammalian VDAC isoforms' function. Biochim. Biophys. Acta BBA - Bioenerg. *1857*, 1219–1227.

Deiana, S., Watanabe, A., Yamasaki, Y., Amada, N., Arthur, M., Fleming, S., Woodcock, H., Dorward, P., Pigliacampo, B., Close, S., et al. (2012). Plasma and brain pharmacokinetic profile of cannabidiol (CBD), cannabidivarine (CBDV), Δ^9-tetrahydrocannabivarin (THCV) and cannabigerol (CBG) in rats and mice following oral and intraperitoneal administration and CBD action on obsessive-compulsive behaviour. Psychopharmacology (Berl.) *219*, 859–873.

Deisz, R.A., Lehmann, T.-N., Horn, P., Dehnicke, C., and Nitsch, R. (2011). Components of neuronal chloride transport in rat and human neocortex. J. Physiol. *589*, 1317–1347.

Deshpande, L.S., Lou, J.K., Mian, A., Blair, R.E., Sombati, S., Attkisson, E., and DeLorenzo, R.J. (2008). Time course and mechanism of hippocampal neuronal death in an in vitro model of status epilepticus: Role of NMDA receptor activation and NMDA dependent calcium entry. Eur. J. Pharmacol. *583*, 73–83.

Do Val-da Silva, R.A., Peixoto-Santos, J.E., Kandratavicius, L., De Ross, J.B., Esteves, I., De Martinis, B.S., Alves, M.N.R., Scandiuzzi, R.C., Hallak, J.E.C., Zuardi, A.W., et al. (2017). Protective Effects of Cannabidiol against Seizures and Neuronal Death in a Rat Model of Mesial Temporal Lobe Epilepsy. Front. Pharmacol. *8*, 131.

Dollery, C.M., and Libby, P. (2006). Atherosclerosis and proteinase activation. Cardiovasc. Res. *69*, 625–635.

Doná, F., Ulrich, H., Persike, D.S., Conceição, I.M., Blini, J.P., Cavalheiro, E.A., and Fernandes, M.J.S. (2009). Alteration of purinergic P2X4 and P2X7 receptor expression in rats with temporal-lobe epilepsy induced by pilocarpine. Epilepsy Res. *83*, 157–167.

Doná, F., Conceição, I.M., Ulrich, H., Ribeiro, E.B., Freitas, T.A., Nencioni, A.L.A., and da Silva Fernandes, M.J. (2016). Variations of ATP and its metabolites in the hippocampus of rats subjected to pilocarpine-induced temporal lobe epilepsy. Purinergic Signal. *12*, 295–302.

Du, H., Guo, L., Fang, F., Chen, D., Sosunov, A.A., McKhann, G.M., Yan, Y., Wang, C., Zhang, H., Molkentin, J.D., et al. (2008). Cyclophilin D deficiency attenuates mitochondrial and neuronal perturbation and ameliorates learning and memory in Alzheimer's disease. Nat. Med. *14*, 1097–1105.

Dubey, D., McRae, P.A., Rankin-Gee, E.K., Baranov, E., Wandrey, L., Rogers, S., and Porter, B.E. (2017). Increased metalloproteinase activity in the hippocampus following status epilepticus. Epilepsy Res. *132*, 50–58.

Duncan, J.S., Sander, J.W., Sisodiya, S.M., and Walker, M.C. (2006). Adult epilepsy. The Lancet *367*, 1087–1100.

Dutertre, S., Becker, C.-M., and Betz, H. (2012). Inhibitory Glycine Receptors: An Update. J. Biol. Chem. *287*, 40216–40223.

Dwivedi, R., Ramanujam, B., Chandra, P.S., Sapra, S., Gulati, S., Kalaivani, M., Garg, A., Bal, C.S., Tripathi, M., Dwivedi, S.N., et al. (2017). Surgery for Drug-Resistant Epilepsy in Children. N. Engl. J. Med. *377*, 1639–1647.

Ehrlich, P. (1885). Das sauerstufbudurfnis des organismus. Eine Farbenanalytische Studie. Hirschwald Berl. 167.

Eichler, S.A., Kirischuk, S., Jüttner, R., Schafermeier, P.K., Legendre, P., Lehmann, T.-N., Gloveli, T., Grantyn, R., and Meier, J.C. (2008). Glycinergic tonic inhibition of hippocampal neurons with depolarizing GABAergic transmission elicits histopathological signs of temporal lobe epilepsy. J. Cell. Mol. Med. *12*, 2848–2866.

El Yacoubi, M., Ledent, C., Parmentier, M., Costentin, J., and Vaugeois, J.-M. (2008). Evidence for the involvement of the adenosine A(2A) receptor in the lowered susceptibility to pentylenetetrazol-induced seizures produced in mice by long-term treatment with caffeine. Neuropharmacology *55*, 35–40.

El Yacoubi, M., Ledent, C., Parmentier, M., Costentin, J., and Vaugeois, J.-M. (2009). Adenosine A2A receptor deficient mice are partially resistant to limbic seizures. Naunyn. Schmiedebergs Arch. Pharmacol. *380*, 223–232.

Engel, J., McDermott, M.P., Wiebe, S., Langfitt, J.T., Stern, J.M., Dewar, S., Sperling, M.R., Gardiner, I., Erba, G., Fried, I., et al. (2012). Early surgical therapy for drug-resistant temporal lobe epilepsy: a randomized trial. JAMA *307*, 922–930.

Erdmann, F., Weiwad, M., Kilka, S., Karanik, M., Pätzel, M., Baumgrass, R., Liebscher, J., and Fischer, G. (2010). The Novel Calcineurin Inhibitor CN585 Has Potent Immunosuppressive Properties in Stimulated Human T Cells. J. Biol. Chem. *285*, 1888–1898.

Esclapez, M., Hirsch, J.C., Ben-Ari, Y., and Bernard, C. (1999). Newly formed excitatory pathways provide a substrate for hyperexcitability in experimental temporal lobe epilepsy. J. Comp. Neurol. *408*, 449–460.

Fabene, P.F., Mora, G.N., Martinello, M., Rossi, B., Merigo, F., Ottoboni, L., Bach, S., Angiari, S., Benati, D., Chakir, A., et al. (2008). A role for leukocyte-endothelial adhesion mechanisms in epilepsy. Nat. Med. *14*, 1377–1383.

Fares, R.P., Belmeguenai, A., Sanchez, P.E., Kouchi, H.Y., Bodennec, J., Morales, A., Georges, B., Bonnet, C., Bouvard, S., Sloviter, R.S., et al. (2013). Standardized Environmental Enrichment Supports Enhanced Brain Plasticity in Healthy Rats and Prevents Cognitive Impairment in Epileptic Rats. PLOS ONE *8*, e53888.

Fearnley, I.M., and Walker, J.E. (1987). Initiation codons in mammalian mitochondria: differences in genetic code in the organelle. Biochemistry (Mosc.) *26*, 8247–8251.

Ferguson, S.J. (2010). ATP synthase: From sequence to ring size to the P/O ratio. Proc. Natl. Acad. Sci. *107*, 16755–16756.

Finsterer, J., and Zarrouk Mahjoub, S. (2012). Epilepsy in mitochondrial disorders. Seizure *21*, 316–321.

Fišar, Z., Singh, N., and Hroudová, J. (2014). Cannabinoid-induced changes in respiration of brain mitochondria. Toxicol. Lett. *231*, 62–71.

Folbergrová, J., and Kunz, W.S. (2012). Mitochondrial dysfunction in epilepsy. Mitochondrion *12*, 35–40.

Folbergrová, J., Ješina, P., Haugvicová, R., Lisý, V., and Houštěk, J. (2010). Sustained deficiency of mitochondrial complex I activity during long periods of survival after seizures induced in immature rats by homocysteic acid. Neurochem. Int. *56*, 394–403.

Foresti, M.L., Arisi, G.M., Katki, K., Montañez, A., Sanchez, R.M., and Shapiro, L.A. (2009). Chemokine CCL2 and its receptor CCR2 are increased in the hippocampus following pilocarpine-induced status epilepticus. J. Neuroinflammation *6*, 40.

Fornal, C.A., Metzler, C.W., Gallegos, R.A., Veasey, S.C., McCreary, A.C., and Jacobs, B.L. (1996). WAY-100635, a potent and selective 5-hydroxytryptamine1A antagonist, increases serotonergic neuronal activity in behaving cats: comparison with (S)-WAY-100135. J. Pharmacol. Exp. Ther. *278*, 752–762.

Forte, M., Adelsberger-Mangan, D., and Colombini, M. (1987). Purification and characterization of the voltage-dependent anion channel from the outer mitochondrial membrane of yeast. J. Membr. Biol. *99*, 65–72.

Fountain, N.B. (2000). Status epilepticus: risk factors and complications. Epilepsia *41 Suppl 2*, S23-30.

Frolov, V.A., Shnyrova, A.V., and Zimmerberg, J. (2011). Lipid Polymorphisms and Membrane Shape. Cold Spring Harb. Perspect. Biol. *3*.

Fuchs, E.C., Zivkovic, A.R., Cunningham, M.O., Middleton, S., LeBeau, F.E.N., Bannerman, D.M., Rozov, A., Whittington, M.A., Traub, R.D., Rawlins, J.N.P., et al. (2007). Recruitment of

Parvalbumin-Positive Interneurons Determines Hippocampal Function and Associated Behavior. Neuron *53*, 591–604.

Fukuda, M., Suzuki, Y., Hino, H., Morimoto, T., and Ishii, E. (2011). Activation of central adenosine A(2A) receptors lowers the seizure threshold of hyperthermia-induced seizure in childhood rats. Seizure *20*, 156–159.

Galindo, M.F., Jordán, J., González-García, C., and Ceña, V. (2003). Reactive oxygen species induce swelling and cytochrome c release but not transmembrane depolarization in isolated rat brain mitochondria. Br. J. Pharmacol. *139*, 797–804.

Gao, J., Chi, Z.-F., Liu, X.-W., Shan, P.-Y., and Wang, R. (2007). Mitochondrial dysfunction and ultrastructural damage in the hippocampus of pilocarpine-induced epileptic rat. Neurosci. Lett. *411*, 152–157.

Gent, J.P., Bentley, M., Feely, M., and Haigh, J.R. (1986). Benzodiazepine cross-tolerance in mice extends to sodium valproate. Eur. J. Pharmacol. *128*, 9–15.

Gil Borlado, M.C., Moreno Lastres, D., Gonzalez Hoyuela, M., Moran, M., Blazquez, A., Pello, R., Marin Buera, L., Gabaldon, T., Garcia Peñas, J.J., Martín, M.A., et al. (2010). Impact of the Mitochondrial Genetic Background in Complex III Deficiency. PLoS ONE *5*.

Gilliam, F. (2002). Optimizing health outcomes in active epilepsy. Neurology *58*, S9-20.

Gilmer, L.K., Ansari, M.A., Roberts, K.N., and Scheff, S.W. (2010). Age-related Changes in Mitochondrial Respiration and Oxidative Damage in the Cerebral Cortex of the Fischer 344 Rat. Mech. Ageing Dev. *131*, 133–143.

Goldmann, E.E. (1913). Vitalfarbung am zentralnervensystem. Abhandl Konigl Preuss Akad Wiss *1*, 1–60.

Gomora, J.C., Daud, A.N., Weiergräber, M., and Perez-Reyes, E. (2001). Block of cloned human T-type calcium channels by succinimide antiepileptic drugs. Mol. Pharmacol. *60*, 1121–1132.

Gonzalez-Reyes, L.E., Ladas, T.P., Chiang, C.-C., and Durand, D.M. (2013). TRPV1 antagonist capsazepine suppresses 4-AP-induced epileptiform activity in vitro and electrographic seizures in vivo. Exp. Neurol. *250*, 321–332.

Gotterer, G.S., Thompson, T.E., and Lehninger, A.L. (1961). Angular light-scattering studies on isolated mitochondria. J. Biophys. Biochem. Cytol. *10*, 15–21.

Governo, R.J.M., Deuchars, J., Baldwin, S.A., and King, A.E. (2005). Localization of the NBMPR-sensitive equilibrative nucleoside transporter, ENT1, in the rat dorsal root ganglion and lumbar spinal cord. Brain Res. *1059*, 129–138.

Gower, A.J., Falter, U., and Lamberty, Y. (2003). Anxiolytic effects of the novel anti-epileptic drug levetiracetam in the elevated plus-maze test in the rat. Eur. J. Pharmacol. *481*, 67–74.

Grancara, S., Battaglia, V., Martinis, P., Viceconte, N., Agostinelli, E., Toninello, A., and Deana, R. (2012). Mitochondrial oxidative stress induced by Ca2+ and monoamines: different behaviour of liver and brain mitochondria in undergoing permeability transition. Amino Acids *42*, 751–759.

Guerriero, S., Vetrugno, M., Ciracì, L., Artuso, L., Dell'Aglio, R., and Petruzzella, V. (2011). Bilateral Progressive Visual Loss in an Epileptic, Mentally Retarded Boy. Middle East Afr. J. Ophthalmol. *18*, 67–70.

Guo, F., Nimmanapalli, R., Paranawithana, S., Wittman, S., Griffin, D., Bali, P., O'Bryan, E., Fumero, C., Wang, H.G., and Bhalla, K. (2002). Ectopic overexpression of second mitochondria-derived activator of caspases (Smac/DIABLO) or cotreatment with N-terminus of Smac/DIABLO peptide potentiates epothilone B derivative-(BMS 247550) and Apo-2L/TRAIL-induced apoptosis. Blood *99*, 3419–3426.

GW Pharma (2015). GWPharma - GW Pharmaceuticals Provides Update on Epidiolex® Program in Treatment-Resistant Childhood Epilepsies.

GW Pharma (2016). GW Announces New Epidiolex® (CBD) Positive Phase 3 Data in Dravet Syndrome and Lennox-Gastaut Syndrome.

Halestrap, A.P. (2009). What is the mitochondrial permeability transition pore? J. Mol. Cell. Cardiol. *46*, 821–831.

Han, D., Antunes, F., Canali, R., Rettori, D., and Cadenas, E. (2003). Voltage-dependent Anion Channels Control the Release of the Superoxide Anion from Mitochondria to Cytosol. J. Biol. Chem. *278*, 5557–5563.

Hansson, M.J., Morota, S., Chen, L., Matsuyama, N., Suzuki, Y., Nakajima, S., Tanoue, T., Omi, A., Shibasaki, F., Shimazu, M., et al. (2011). Cyclophilin D-Sensitive Mitochondrial Permeability Transition in Adult Human Brain and Liver Mitochondria. J. Neurotrauma *28*, 143–153.

Harayama, T., and Riezman, H. (2018). Understanding the diversity of membrane lipid composition. Nat. Rev. Mol. Cell Biol. *19*, 281.

Hardingham, G.E., and Bading, H. (2010). Synaptic versus extrasynaptic NMDA receptor signalling: implications for neurodegenerative disorders. Nat. Rev. Neurosci. *11*, 682–696.

Hart, L., Rauch, A., Carr, A.M., Vermeesch, J.R., and O'Driscoll, M. (2014). LETM1 haploinsufficiency causes mitochondrial defects in cells from humans with Wolf-Hirschhorn syndrome: implications for dissecting the underlying pathomechanisms in this condition. Dis. Model. Mech. *7*, 535–545.

Heimburg, T. (2009). Physical Properties of Biological Membranes. ArXiv09022454 Phys.

Helmstaedter, C., and Kurthen, M. (2001). Memory and epilepsy: characteristics, course, and influence of drugs and surgery. Curr. Opin. Neurol. *14*, 211.

Hill, A.J., Mercier, M.S., Hill, T.D.M., Glyn, S.E., Jones, N.A., Yamasaki, Y., Futamura, T., Duncan, M., Stott, C.G., Stephens, G.J., et al. (2012). Cannabidivarin is anticonvulsant in mouse and rat. Br. J. Pharmacol. *167*, 1629–1642.

Hill, A.J., Jones, N.A., Smith, I., Hill, C.L., Williams, C.M., Stephens, G.J., and Whalley, B.J. (2014). Voltage-gated sodium (NaV) channel blockade by plant cannabinoids does not confer anticonvulsant effects per se. Neurosci. Lett. *566*, 269–274.

Hillard, C.J., Harris, R.A., and Bloom, A.S. (1985). Effects of the cannabinoids on physical properties of brain membranes and phospholipid vesicles: fluorescence studies. J. Pharmacol. Exp. Ther. *232*, 579–588.

Hinkle, P.C. (2005). P/O ratios of mitochondrial oxidative phosphorylation. Biochim. Biophys. Acta BBA - Bioenerg. *1706*, 1–11.

Hodge, T., and Colombini, M. (1997). Regulation of metabolite flux through voltage-gating of VDAC channels. J. Membr. Biol. *157*, 271–279.

Holtman, L., van Vliet, E.A., van Schaik, R., Queiroz, C.M., Aronica, E., and Gorter, J.A. (2009). Effects of SC58236, a selective COX-2 inhibitor, on epileptogenesis and spontaneous seizures in a rat model for temporal lobe epilepsy. Epilepsy Res. *84*, 56–66.

Holtman, L., van Vliet, E.A., Edelbroek, P.M., Aronica, E., and Gorter, J.A. (2010). Cox-2 inhibition can lead to adverse effects in a rat model for temporal lobe epilepsy. Epilepsy Res. *91*, 49–56.

Houser, C.R., and Esclapez, M. (2003). Downregulation of the α5 subunit of the GABAA receptor in the pilocarpine model of temporal lobe epilepsy. Hippocampus *13*, 633–645.

Huang, C.-W., and Kuo, C.-C. (2015). Flow- and voltage-dependent blocking effect of ethosuximide on the inward rectifier K^+ (Kir2.1) channel. Pflugers Arch. *467*, 1733–1746.

Huang, C., Chi, X., Li, R., Hu, X., Xu, H., Li, J., and Zhou, D. (2017). Inhibition of P2X7 Receptor Ameliorates Nuclear Factor-Kappa B Mediated Neuroinflammation Induced by Status Epilepticus in Rat Hippocampus. J. Mol. Neurosci. *63*, 173–184.

Huang, W.-X., Yu, F., Sanchez, R.M., Liu, Y.-Q., Min, J.-W., Hu, J.-J., Bsoul, N.B., Han, S., Yin, J., Liu, W.-H., et al. (2015). TRPV1 promotes repetitive febrile seizures by pro-inflammatory cytokines in immature brain. Brain. Behav. Immun. *48*, 68–77.

Huberfeld, G., Wittner, L., Clemenceau, S., Baulac, M., Kaila, K., Miles, R., and Rivera, C. (2007). Perturbed Chloride Homeostasis and GABAergic Signaling in Human Temporal Lobe Epilepsy. J. Neurosci. *27*, 9866–9873.

Huguenard, J.R. (2004). T-Channel Defects in Patients with Childhood Absence Epilepsy. Epilepsy Curr. *4*, 7–8.

Hunt, R.F., Hortopan, G.A., Gillespie, A., and Baraban, S.C. (2012). A novel zebrafish model of hyperthermia-induced seizures reveals a role for TRPV4 channels and NMDA-type glutamate receptors. Exp. Neurol. *237*, 199–206.

Hunter, D.R., Haworth, R.A., and Southard, J.H. (1976). Relationship between configuration, function, and permeability in calcium-treated mitochondria. J. Biol. Chem. *251*, 5069–5077.

Iannotti, F.A., Hill, C.L., Leo, A., Alhusaini, A., Soubrane, C., Mazzarella, E., Russo, E., Whalley, B.J., Di Marzo, V., and Stephens, G.J. (2014). Nonpsychotropic plant cannabinoids, cannabidivarin (CBDV) and cannabidiol (CBD), activate and desensitize transient receptor potential vanilloid 1 (TRPV1) channels in vitro: potential for the treatment of neuronal hyperexcitability. ACS Chem. Neurosci. *5*, 1131–1141.

Ibeas Bih, C., Chen, T., Nunn, A.V.W., Bazelot, M., Dallas, M., and Whalley, B.J. (2015). Molecular Targets of Cannabidiol in Neurological Disorders. Neurotherapeutics *12*, 699–730.

Igbavboa, U., and Pfeiffer, D.R. (1988). EGTA inhibits reverse uniport-dependent Ca2+ release from uncoupled mitochondria. Possible regulation of the Ca2+ uniporter by a Ca2+ binding site on the cytoplasmic side of the inner membrane. J. Biol. Chem. *263*, 1405–1412.

ILAE (2003). The History and Stigma of Epilepsy. Epilepsia *44*, 12–14.

Inoue, H., Nojima, H., and Okayama, H. (1990). High efficiency transformation of Escherichia coli with plasmids. Gene *96*, 23–28.

J Sampson, M., Decker, W., Beaudet, A., Ruitenbeek, W., Armstrong, D., Hicks, J., and J Craigen, W. (2001). Immotile Sperm and Infertility in Mice Lacking Mitochondrial Voltage-dependent Anion Channel Type 3. J. Biol. Chem. *276*, 39206–39212.

Jacobs, M.D., and Harrison, S.C. (1998). Structure of an IkappaBalpha/NF-kappaB complex. Cell *95*, 749–758.

Jacoby, A., and Austin, J.K. (2007). Social stigma for adults and children with epilepsy. Epilepsia *48*, 6–9.

Janneh, O., Jones, E., Chandler, B., Owen, A., and Khoo, S.H. (2007). Inhibition of P-glycoprotein and multidrug resistance-associated proteins modulates the intracellular concentration of lopinavir in cultured CD4 T cells and primary human lymphocytes. J. Antimicrob. Chemother. *60*, 987–993.

Jiang, W., Du, B., Chi, Z., Ma, L., Wang, S., Zhang, X., Wu, W., Wang, X., Xu, G., and Guo, C. (2007). Preliminary explorations of the role of mitochondrial proteins in refractory epilepsy: some findings from comparative proteomics. J. Neurosci. Res. *85*, 3160–3170.

Jimenez-Pacheco, A., Diaz-Hernandez, M., Arribas-Blázquez, M., Sanz-Rodriguez, A., Olivos-Oré, L.A., Artalejo, A.R., Alves, M., Letavic, M., Miras-Portugal, M.T., Conroy, R.M., et al. (2016). Transient P2X7 Receptor Antagonism Produces Lasting Reductions in Spontaneous Seizures and Gliosis in Experimental Temporal Lobe Epilepsy. J. Neurosci. Off. J. Soc. Neurosci. *36*, 5920–5932.

Jobst, B.C., and Cascino, G.D. (2015). Resective epilepsy surgery for drug-resistant focal epilepsy: a review. JAMA *313*, 285–293.

Jones, N.A., Hill, A.J., Smith, I., Bevan, S.A., Williams, C.M., Whalley, B.J., and Stephens, G.J. (2010). Cannabidiol displays antiepileptiform and antiseizure properties in vitro and in vivo. J. Pharmacol. Exp. Ther. *332*, 569–577.

Jones, N.A., Glyn, S.E., Akiyama, S., Hill, T.D.M., Hill, A.J., Weston, S.E., Burnett, M.D.A., Yamasaki, Y., Stephens, G.J., Whalley, B.J., et al. (2012). Cannabidiol exerts anti-convulsant effects in animal models of temporal lobe and partial seizures. Seizure *21*, 344–352.

Jürgensmeier, J.M., Xie, Z., Deveraux, Q., Ellerby, L., Bredesen, D., and Reed, J.C. (1998). Bax directly induces release of cytochrome c from isolated mitochondria. Proc. Natl. Acad. Sci. U. S. A. *95*, 4997–5002.

Kaebisch, C., Schipper, D., Babczyk, P., and Tobiasch, E. (2015). The role of purinergic receptors in stem cell differentiation. Comput. Struct. Biotechnol. J. *13*, 75–84.

Kang, H.-C., Lee, Y.-M., Kim, H.D., Lee, J.S., and Slama, A. (2007). Safe and Effective Use of the Ketogenic Diet in Children with Epilepsy and Mitochondrial Respiratory Chain Complex Defects. Epilepsia *48*, 82–88.

Kann, O., and Kovács, R. (2007). Mitochondria and neuronal activity. Am. J. Physiol. Cell Physiol. *292*, C641-657.

Kanno, T., Yorimitsu, M., Muranaka, S., Sato, E.F., Nagano, M., Inoue, A., Inoue, M., and Utsumi, K. (2004). Vitamin E Role of α-Tocopherol in the Regulation of Mitochondrial Membrane Permeability Transition. J. Clin. Biochem. Nutr. *35*, 7–15.

Kaplan, J.S., Stella, N., Catterall, W.A., and Westenbroek, R.E. (2017). Cannabidiol attenuates seizures and social deficits in a mouse model of Dravet syndrome. Proc. Natl. Acad. Sci. *114*, 11229–11234.

Karin, M. (1999). How NF-kappaB is activated: the role of the IkappaB kinase (IKK) complex. Oncogene *18*, 6867–6874.

Karler, R., Cely, W., and Turkanis, S.A. (1973). The anticonvulsant activity of cannabidiol and cannabinol. Life Sci. *13*, 1527–1531.

Kaskow, B.J., and Baecher-Allan, C. (2018). Effector T Cells in Multiple Sclerosis. Cold Spring Harb. Perspect. Med. *8*.

Katyal, J., Kumar, H., and Gupta, Y.K. (2015). Anticonvulsant activity of the cyclooxygenase-2 (COX-2) inhibitor etoricoxib in pentylenetetrazole-kindled rats is associated with memory impairment. Epilepsy Behav. EB *44*, 98–103.

Keezer, M.R., Sisodiya, S.M., and Sander, J.W. (2016). Comorbidities of epilepsy: current concepts and future perspectives. Lancet Neurol. *15*, 106–115.

Keinan, N., Pahima, H., Ben-Hail, D., and Shoshan-Barmatz, V. (2013). The role of calcium in VDAC1 oligomerization and mitochondria-mediated apoptosis. Biochim. Biophys. Acta *1833*, 1745–1754.

Keller, B.U., and Hedrich, R. (1992). [46] Patch clamp techniques to study ion channels from organelles. In Methods in Enzymology, (Academic Press), pp. 673–681.

Kim, J.-E., and Kang, T.-C. (2011). The P2X7 receptor–pannexin-1 complex decreases muscarinic acetylcholine receptor–mediated seizure susceptibility in mice. J. Clin. Invest. *121*, 2037–2047.

Kim, D.Y., Simeone, K.A., Simeone, T.A., Pandya, J.D., Wilke, J.C., Ahn, Y., Geddes, J.W., Sullivan, P.G., and Rho, J.M. (2015). Ketone Bodies Mediate Anti-Seizure Effects Through Mitochondrial Permeability Transition. Ann. Neurol. *78*, 77–87.

Kim, H.-J., Chung, J.-I., Lee, S.H., Jung, Y.-S., Moon, C.-H., and Baik, E.J. (2008). Involvement of endogenous prostaglandin F2alpha on kainic acid-induced seizure activity through FP receptor: the mechanism of proconvulsant effects of COX-2 inhibitors. Brain Res. *1193*, 153–161.

Kim, J.-E., Ryu, H.J., Yeo, S.-I., and Kang, T.-C. (2010). P2X7 receptor regulates leukocyte infiltrations in rat frontoparietal cortex following status epilepticus. J. Neuroinflammation *7*, 65.

Kim, J.-E., Kim, D.-S., Ryu, H.J., Kim, W.I., Kim, M.-J., Kim, D.W., Choi, S.Y., and Kang, T.-C. (2013). The effect of P2X7 receptor activation on nuclear factor-kappa B phosphorylation induced by status epilepticus in the rat hippocampus. Hippocampus *23*, 500–514.

Kim, T.H., Zhao, Y., Barber, M.J., Kuharsky, D.K., and Yin, X.M. (2000). Bid-induced cytochrome c release is mediated by a pathway independent of mitochondrial permeability transition pore and Bax. J. Biol. Chem. *275*, 39474–39481.

Kim-Han, J.S., and Dugan, L.L. (2005). Mitochondrial Uncoupling Proteins in the Central Nervous System. Antioxid. Redox Signal. *7*, 1173–1181.

Kirby, B.S., Hanna, G., Hendargo, H.C., and McMahon, T.J. (2014). Restoration of intracellular ATP production in banked red blood cells improves inducible ATP export and suppresses RBC-endothelial adhesion. Am. J. Physiol. - Heart Circ. Physiol. *307*, H1737–H1744.

Kobayashi, T., Kuroda, S., Tada, M., Houkin, K., Iwasaki, Y., and Abe, H. (2003). Calcium-induced mitochondrial swelling and cytochrome c release in the brain: its biochemical characteristics and implication in ischemic neuronal injury. Brain Res. *960*, 62–70.

Kovac, S., Domijan, A.-M., Walker, M.C., and Abramov, A.Y. (2012). Prolonged seizure activity impairs mitochondrial bioenergetics and induces cell death. J. Cell Sci. *125*, 1796–1806.

Kowaltowski, A.J., Castilho, R.F., and Vercesi, A.E. (1996). Opening of the mitochondrial permeability transition pore by uncoupling or inorganic phosphate in the presence of Ca2+ is dependent on mitochondrial-generated reactive oxygen species. FEBS Lett. *378*, 150–152.

Kreuzer, F. (1957). A new polarographic procedure for measuring the blood oxygen tension in vitro. Experientia *13*, 300.

Kumari, R., Lakhan, R., Kalita, J., Misra, U.K., and Mittal, B. (2010). Association of alpha subunit of GABAA receptor subtype gene polymorphisms with epilepsy susceptibility and drug resistance in north Indian population. Seizure *19*, 237–241.

Kumaria, A., Tolias, C.M., and Burnstock, G. (2008). ATP signalling in epilepsy. Purinergic Signal. *4*, 339–346.

Kunz, W.S., Kudin, A.P., Vielhaber, S., Blümcke, I., Zuschratter, W., Schramm, J., Beck, H., and Elger, C.E. (2000). Mitochondrial complex I deficiency in the epileptic focus of patients with temporal lobe epilepsy. Ann. Neurol. *48*, 766–773.

de Lanerolle, N.C., Kim, J.H., Robbins, R.J., and Spencer, D.D. (1989). Hippocampal interneuron loss and plasticity in human temporal lobe epilepsy. Brain Res. *495*, 387–395.

Laun, A.S., and Song, Z.-H. (2017). GPR3 and GPR6, novel molecular targets for cannabidiol. Biochem. Biophys. Res. Commun. *490*, 17–21.

Laun, A.S., Shrader, S.H., Brown, K.J., and Song, Z.-H. (2018). GPR3, GPR6, and GPR12 as novel molecular targets: their biological functions and interaction with cannabidiol. Acta Pharmacol. Sin.

Laurén, H.B., Pitkänen, A., Nissinen, J., Soini, S.L., Korpi, E.R., and Holopainen, I.E. (2003). Selective changes in gamma-aminobutyric acid type A receptor subunits in the hippocampus in spontaneously seizing rats with chronic temporal lobe epilepsy. Neurosci. Lett. *349*, 58–62.

Le Duc, D., Schulz, A., Lede, V., Schulze, A., Thor, D., Brüser, A., and Schöneberg, T. (2017). P2Y Receptors in Immune Response and Inflammation. Adv. Immunol. *136*, 85–121.

Lee, A.G. (1975). Functional properties of biological membranes: a physical-chemical approach. Prog. Biophys. Mol. Biol. *29*, 3–56.

Lee, C.-Y., Chen, C.-C., and Liou, H.-H. (2009). Levetiracetam inhibits glutamate transmission through presynaptic P/Q-type calcium channels on the granule cells of the dentate gyrus. Br. J. Pharmacol. *158*, 1753–1762.

Lee, K.-M., Kang, B.-S., Lee, H.-L., Son, S.-J., Hwang, S.-H., Kim, D.-S., Park, J.-S., and Cho, H.-J. (2004). Spinal NF-kB activation induces COX-2 upregulation and contributes to inflammatory pain hypersensitivity. Eur. J. Neurosci. *19*, 3375–3381.

Lehninger, A.L. (1962). Water uptake and extrusion by mitochondria in relation to oxidative phosphorylation. Physiol. Rev. *42*, 467–517.

Li, H.-L. (1974). An Archaeological and Historical Account of Cannabis in China. Econ. Bot. *28*, 437–448.

Li, Z., Wang, Y., Xue, Y., Li, X., Cao, H., and Zheng, S.J. (2012). Critical Role for Voltage-Dependent Anion Channel 2 in Infectious Bursal Disease Virus-Induced Apoptosis in Host Cells via Interaction with VP5. J. Virol. *86*, 1328–1338.

Liao, C.W., and Lien, C.C. (2009). Estimating intracellular Ca2+ concentrations and buffering in a dendritic inhibitory hippocampal interneuron. Neuroscience *164*, 1701–1711.

Liobikas, J., Kopustinskiene, D.M., and Toleikis, A. (2001). What controls the outer mitochondrial membrane permeability for ADP: facts for and against the role of oncotic pressure. Biochim. Biophys. Acta BBA - Bioenerg. *1505*, 220–225.

Liu, X.-Y., Yang, J.-L., Chen, L.-J., Zhang, Y., Yang, M.-L., Wu, Y.-Y., Li, F.-Q., Tang, M.-H., Liang, S.-F., and Wei, Y.-Q. (2008). Comparative proteomics and correlated signaling network of rat hippocampus in the pilocarpine model of temporal lobe epilepsy. PROTEOMICS *8*, 582–603.

Lobão-Soares, B., Bianchin, M.M., Linhares, M.N., Carqueja, C.L., Tasca, C.I., Souza, M., Marques, W., Brentani, R., Martins, V.R., Sakamoto, A.C., et al. (2005). Normal brain mitochondrial respiration in adult mice lacking cellular prion protein. Neurosci. Lett. *375*, 203–206.

Lodish, H., Berk, A., Zipursky, S.L., Matsudaira, P., Baltimore, D., and Darnell, J. (2000). Oxidation of Glucose and Fatty Acids to CO2. Mol. Cell Biol. 4th Ed.

Löscher, W. (2011). Critical review of current animal models of seizures and epilepsy used in the discovery and development of new antiepileptic drugs. Seizure *20*, 359–368.

Löscher, W., and Potschka, H. (2002). Role of Multidrug Transporters in Pharmacoresistance to Antiepileptic Drugs. J. Pharmacol. Exp. Ther. *301*, 7–14.

Löscher, W., and Schmidt, D. (2006). Experimental and clinical evidence for loss of effect (tolerance) during prolonged treatment with antiepileptic drugs. Epilepsia *47*, 1253–1284.

Luan, G., Wang, X., Gao, Q., Guan, Y., Wang, J., Deng, J., Zhai, F., Chen, Y., and Li, T. (2017). Upregulation of Neuronal Adenosine A1 Receptor in Human Rasmussen Encephalitis. J. Neuropathol. Exp. Neurol. *76*, 720–731.

Luna-Tortós, C., Fedrowitz, M., and Löscher, W. (2010). Evaluation of transport of common antiepileptic drugs by human multidrug resistance-associated proteins (MRP1, 2 and 5) that are overexpressed in pharmacoresistant epilepsy. Neuropharmacology *58*, 1019–1032.

Lynch, J.W. (2004). Molecular Structure and Function of the Glycine Receptor Chloride Channel. Physiol. Rev. *84*, 1051–1095.

Ma, L., Cui, X.-L., Wang, Y., Li, X.-W., Yang, F., Wei, D., and Jiang, W. (2012). Aspirin attenuates spontaneous recurrent seizures and inhibits hippocampal neuronal loss, mossy fiber sprouting and aberrant neurogenesis following pilocarpine-induced status epilepticus in rats. Brain Res. *1469*, 103–113.

Madesh, M., and Hajnóczky, G. (2001). VDAC-dependent permeabilization of the outer mitochondrial membrane by superoxide induces rapid and massive cytochrome c release. J. Cell Biol. *155*, 1003–1015.

Maldonado, E.N., Sheldon, K.L., DeHart, D.N., Patnaik, J., Manevich, Y., Townsend, D.M., Bezrukov, S.M., Rostovtseva, T.K., and Lemasters, J.J. (2013). Voltage-dependent Anion Channels Modulate Mitochondrial Metabolism in Cancer Cells Regulation by free Tubulin and Erastin. J. Biol. Chem. *288*, 11920–11929.

Manley, N.C., Bertrand, A.A., Kinney, K.S., Hing, T.C., and Sapolsky, R.M. (2007). Characterization of monocyte chemoattractant protein-1 expression following a kainate model of status epilepticus. Brain Res. *1182*, 138–143.

Manna, S.S.S., and Umathe, S.N. (2012). Involvement of transient receptor potential vanilloid type 1 channels in the pro-convulsant effect of anandamide in pentylenetetrazole-induced seizures. Epilepsy Res. *100*, 113–124.

Mannella, C.A., and Bonner, W.D. (1975). Biochemical characteristics of the outer membranes of plant mitochondria. Biochim. Biophys. Acta BBA - Biomembr. *413*, 213–225.

Mannella, C.A., Colombini, M., and Frank, J. (1983). Structural and functional evidence for multiple channel complexes in the outer membrane of Neurospora crassa mitochondria. Proc. Natl. Acad. Sci. U. S. A. *80*, 2243–2247.

Manniche, L. (1989). An Ancient Egyptian Herbal (British Museum Press).

Maschio, M. (2012). Brain Tumor-Related Epilepsy. Curr. Neuropharmacol. *10*, 124–133.

Mataró-Serrat, M., and Junqué-Plaja, C. (1997). Memory and epilepsy. Rev. Neurol. *25*, 1241–1245.

Mathre, M.L. (1997). Cannabis in Medical Practice: A Legal, Historical and Pharmacological Overview of the Therapeutic Use of Marijuana (McFarland).

Mattson, M.P., and Camandola, S. (2001). NF-kappaB in neuronal plasticity and neurodegenerative disorders. J. Clin. Invest. *107*, 247–254.

Maurya, S.R., and Mahalakshmi, R. (2017). Mitochondrial VDAC2 and cell homeostasis: highlighting hidden structural features and unique functionalities. Biol. Rev. *92*, 1843–1858.

Meador, K.J. (2006). Cognitive and memory effects of the new antiepileptic drugs. Epilepsy Res. *68*, 63–67.

Mehmedic, Z., Chandra, S., Slade, D., Denham, H., Foster, S., Patel, A.S., Ross, S.A., Khan, I.A., and ElSohly, M.A. (2010). Potency Trends of Δ9-THC and Other Cannabinoids in Confiscated Cannabis Preparations from 1993 to 2008*. J. Forensic Sci. *55*, 1209–1217.

Mellors, A., Tappel, A.L., Sawant, P.L., and Desai, I.D. (1967). Mitochondrial swelling and uncoupling of oxidative phosphorylation by lysosomes. Biochim. Biophys. Acta BBA - Bioenerg. *143*, 299–309.

Messina, A., Reina, S., Guarino, F., and De Pinto, V. (2012). VDAC isoforms in mammals. Biochim. Biophys. Acta BBA - Biomembr. *1818*, 1466–1476.

Mikuriya, T.H. (1969). Marijuana in medicine: past, present and future. Calif. Med. *110*, 34–40.

Mizoguchi, H., and Yamada, K. (2013). Roles of matrix metalloproteinases and their targets in epileptogenesis and seizures. Clin. Psychopharmacol. Neurosci. Off. Sci. J. Korean Coll. Neuropsychopharmacol. *11*, 45–52.

Modebadze, T., Morgan, N.H., Pérès, I.A.A., Hadid, R.D., Amada, N., Hill, C., Williams, C., Stanford, I.M., Morris, C.M., Jones, R.S.G., et al. (2016). A Low Mortality, High Morbidity Reduced Intensity Status Epilepticus (RISE) Model of Epilepsy and Epileptogenesis in the Rat. PLOS ONE *11*, e0147265.

Modi, A.C., King, A.S., Monahan, S.R., Koumoutsos, J.E., Morita, D.A., and Glauser, T.A. (2009). Even a single seizure negatively impacts pediatric health-related quality of life. Epilepsia *50*, 2110–2116.

Mohd Sairazi, N.S., Sirajudeen, K.N.S., Muzaimi, M., Mummedy, S., Asari, M.A., and Sulaiman, S.A. (2018). Tualang Honey Reduced Neuroinflammation and Caspase-3 Activity in Rat Brain after Kainic Acid-Induced Status Epilepticus. Evid.-Based Complement. Altern. Med. ECAM *2018*, 7287820.

Morales-Aza, B.M., Chillingworth, N.L., Payne, J.A., and Donaldson, L.F. (2004). Inflammation alters cation chloride cotransporter expression in sensory neurons. Neurobiol. Dis. *17*, 62–69.

Morgan, M.J., and Liu, Z. (2011). Crosstalk of reactive oxygen species and NF-κB signaling. Cell Res. *21*, 103–115.

Morningstar, P.J. (1985). Thandai and chilam: traditional Hindu beliefs about the proper uses of Cannabis. J. Psychoactive Drugs *17*, 141–165.

Moser, V.C., McCormick, J.P., Creason, J.P., and MacPhail, R.C. (1988). Comparison of chlordimeform and carbaryl using a functional observational battery. Fundam. Appl. Toxicol. *11*, 189–206.

Motamedi, G.K., and Meador, K.J. (2004). Antiepileptic drugs and memory. Epilepsy Behav. *5*, 435–439.

Mula, M. (2016). Using anxiolytics in epilepsy: neurobiological, neuropharmacological and clinical aspects. Epileptic. Disord. *18*, 217–227.

Murphy, M.P. (2009). How mitochondria produce reactive oxygen species. Biochem. J. *417*, 1–13.

Murray, R., Granner, D., Mayes, P., and Rodwell, V. (2003). Harper's Illustrated Biochemistry (McGraw Hill Professional).

Musto, A.E., Gjorstrup, P., and Bazan, N.G. (2011). The omega-3 fatty acid-derived neuroprotectin D1 limits hippocampal hyperexcitability and seizure susceptibility in kindling epileptogenesis. Epilepsia *52*, 1601–1608.

Nabissi, M., Morelli, M.B., Santoni, M., and Santoni, G. (2013). Triggering of the TRPV2 channel by cannabidiol sensitizes glioblastoma cells to cytotoxic chemotherapeutic agents. Carcinogenesis *34*, 48–57.

Naga, K.K., and Geddes, J.W. (2011). Dimebon Inhibits Calcium-Induced Swelling of Rat Brain Mitochondria But Does Not Alter Calcium Retention or Cytochrome C Release. Neuromolecular Med. *13*, 31–36.

Naghdi, S., and Hajnóczky, G. (2016). VDAC2-specific cellular functions and the underlying structure. Biochim. Biophys. Acta *1863*, 2503–2514.

Namvar, S., Mirnajafi-Zadeh, J., Fathollahi, Y., and Zeraati, M. (2008). The role of piriform cortex adenosine A1 receptors on hippocampal kindling. Can. J. Neurol. Sci. J. Can. Sci. Neurol. *35*, 226–231.

Negi, N., and Das, B.K. (2018). CNS: Not an immunoprivilaged site anymore but a virtual secondary lymphoid organ. Int. Rev. Immunol. *37*, 57–68.

O'Brien, J.E., and Meisler, M.H. (2013). Sodium channel SCN8A (Nav1.6): properties and de novo mutations in epileptic encephalopathy and intellectual disability. Front. Genet. *4*, 213.

Oka, M., Itoh, Y., Wada, M., Yamamoto, A., and Fujita, T. (2003). Gabapentin blocks L-type and P/Q-type Ca2+ channels involved in depolarization-stimulated nitric oxide synthase activity in primary cultures of neurons from mouse cerebral cortex. Pharm. Res. *20*, 897–899.

Oliveira, M.S., Furian, A.F., Royes, L.F.F., Fighera, M.R., Fiorenza, N.G., Castelli, M., Machado, P., Bohrer, D., Veiga, M., Ferreira, J., et al. (2008). Cyclooxygenase-2/PGE2 pathway facilitates pentylenetetrazol-induced seizures. Epilepsy Res. *79*, 14–21.

Ott, M., Robertson, J.D., Gogvadze, V., Zhivotovsky, B., and Orrenius, S. (2002). Cytochrome c release from mitochondria proceeds by a two-step process. Proc. Natl. Acad. Sci. U. S. A. *99*, 1259–1263.

Palty, R., Hershfinkel, M., and Sekler, I. (2012). Molecular Identity and Functional Properties of the Mitochondrial Na+/Ca2+ Exchanger. J. Biol. Chem. *287*, 31650–31657.

Pamenter, M.E., Perkins, G.A., Gu, X.Q., Ellisman, M.H., and Haddad, G.G. (2013). DIDS (4,4-diisothiocyanatostilbenedisulphonic acid) induces apoptotic cell death in a hippocampal neuronal cell line and is not neuroprotective against ischemic stress. PloS One *8*, e60804.

Pandya, J.D., Nukala, V.N., and Sullivan, P.G. (2013). Concentration dependent effect of calcium on brain mitochondrial bioenergetics and oxidative stress parameters. Front. Neuroenergetics *5*.

Parent, J.M., and Lowenstein, D.H. (2002). Seizure-induced neurogenesis: are more new neurons good for an adult brain? Prog. Brain Res. *135*, 121–131.

Parihar, R., and Ganesh, S. (2013). The SCN1A gene variants and epileptic encephalopathies. J. Hum. Genet. *58*, 573–580.

Patel, R.R., Barbosa, C., Brustovetsky, T., Brustovetsky, N., and Cummins, T.R. (2016). Aberrant epilepsy-associated mutant Nav1.6 sodium channel activity can be targeted with cannabidiol. Brain J. Neurol. *139*, 2164–2181.

Patsalos, P.N. (1999). The mechanism of action of topiramate. REV CONTEMP Pharm. *10*, 147–153.

Peng, L., Huang, R., Yu, A.C.H., Fung, K.Y., Rathbone, M.P., and Hertz, L. (2005). Nucleoside transporter expression and function in cultured mouse astrocytes. Glia *52*, 25–35.

Pepicelli, O., Fedele, E., Bonanno, G., Raiteri, M., Ajmone-Cat, M.A., Greco, A., Levi, G., and Minghetti, L. (2002). In vivo activation of N-methyl-d-aspartate receptors in the rat hippocampus increases prostaglandin E2 extracellular levels and triggers lipid peroxidation through cyclooxygenase-mediated mechanisms. J. Neurochem. *81*, 1028–1034.

Pertwee, R.G. (2014). Handbook of Cannabis (Oxford University Press).

Perucca, E., French, J., and Bialer, M. (2007). Development of new antiepileptic drugs: challenges, incentives, and recent advances. Lancet Neurol. *6*, 793–804.

Picot, M.-C., Baldy-Moulinier, M., Daurès, J.-P., Dujols, P., and Crespel, A. (2008). The prevalence of epilepsy and pharmacoresistant epilepsy in adults: A population-based study in a Western European country. Epilepsia *49*, 1230–1238.

Pisani, A., Bonsi, P., Martella, G., De Persis, C., Costa, C., Pisani, F., Bernardi, G., and Calabresi, P. (2004). Intracellular calcium increase in epileptiform activity: modulation by levetiracetam and lamotrigine. Epilepsia *45*, 719–728.

Polascheck, N., Bankstahl, M., and Löscher, W. (2010). The COX-2 inhibitor parecoxib is neuroprotective but not antiepileptogenic in the pilocarpine model of temporal lobe epilepsy. Exp. Neurol. *224*, 219–233.

Pollington, S. (2008). Leechcraft: Early English Charms, Plant Lore, and Healing (Anglo-Saxon Books).

Qin, N., Neeper, M.P., Liu, Y., Hutchinson, T.L., Lubin, M.L., and Flores, C.M. (2008). TRPV2 is activated by cannabidiol and mediates CGRP release in cultured rat dorsal root ganglion neurons. J. Neurosci. Off. J. Soc. Neurosci. *28*, 6231–6238.

Qiu, X., Cao, L., Yang, X., Zhao, X., Liu, X., Han, Y., Xue, Y., Jiang, H., and Chi, Z. (2013). Role of mitochondrial fission in neuronal injury in pilocarpine-induced epileptic rats. Neuroscience *245*, 157–165.

Racine, R.J. (1972). Modification of seizure activity by electrical stimulation. II. Motor seizure. Electroencephalogr. Clin. Neurophysiol. *32*, 281–294.

Raghavan, A., Sheiko, T., Graham, B.H., and Craigen, W.J. (2012). Voltage-dependant anion channels: Novel insights into isoform function through genetic models. Biochim. Biophys. Acta *1818*, 1477–1485.

Rajapakse, N., Shimizu, K., Payne, M., and Busija, D. (2001). Isolation and characterization of intact mitochondria from neonatal rat brain. Brain Res. Protoc. *8*, 176–183.

Raza, M., Pal, S., Rafiq, A., and DeLorenzo, R.J. (2001). Long-term alteration of calcium homeostatic mechanisms in the pilocarpine model of temporal lobe epilepsy. Brain Res. *903*, 1–12.

Raza, M., Blair, R.E., Sombati, S., Carter, D.S., Deshpande, L.S., and DeLorenzo, R.J. (2004). Evidence that injury-induced changes in hippocampal neuronal calcium dynamics during epileptogenesis cause acquired epilepsy. Proc. Natl. Acad. Sci. U. S. A. *101*, 17522–17527.

Rice, A., Rafiq, A., Shapiro, S.M., Jakoi, E.R., Coulter, D.A., and DeLorenzo, R.J. (1996). Long-lasting reduction of inhibitory function and gamma-aminobutyric acid type A receptor subunit mRNA expression in a model of temporal lobe epilepsy. Proc. Natl. Acad. Sci. U. S. A. *93*, 9665–9669.

Richard, D., Rivest, R., Huang, Q., Bouillaud, F., Sanchis, D., Champigny, O., and Ricquier, D. (1998). Distribution of the uncoupling protein 2 mRNA in the mouse brain. J. Comp. Neurol. *397*, 549–560.

Richerson, G.B., and Buchanan, G.F. (2011). The serotonin axis: Shared mechanisms in seizures, depression and SUDEP. Epilepsia *52*, 28–38.

Rimmerman, N., Ben-Hail, D., Porat, Z., Juknat, A., Kozela, E., Daniels, M.P., Connelly, P.S., Leishman, E., Bradshaw, H.B., Shoshan-Barmatz, V., et al. (2013). Direct modulation of the outer mitochondrial membrane channel, voltage-dependent anion channel 1 (VDAC1) by cannabidiol: a novel mechanism for cannabinoid-induced cell death. Cell Death Dis. *4*, e949.

Rogawski, M.A., and Löscher, W. (2004). The neurobiology of antiepileptic drugs for the treatment of nonepileptic conditions. Nat. Med. *10*, 685–692.

Rogovik, A.L., and Goldman, R.D. (2010). Ketogenic diet for treatment of epilepsy. Can. Fam. Physician *56*, 540–542.

Rojas, A., Jiang, J., Ganesh, T., Yang, M.-S., Lelutiu, N., Gueorguieva, P., and Dingledine, R. (2014). Cyclooxygenase-2 in epilepsy. Epilepsia *55*, 17–25.

Ross, H.R., Napier, I., and Connor, M. (2008). Inhibition of recombinant human T-type calcium channels by Delta9-tetrahydrocannabinol and cannabidiol. J. Biol. Chem. *283*, 16124–16134.

Rossi, L., Salvestrini, V., Ferrari, D., Virgilio, F.D., and Lemoli, R.M. (2012). The sixth sense: hematopoietic stem cells detect danger through purinergic signaling. Blood *120*, 2365–2375.

Rostovtseva, T., and Colombini, M. (1996). ATP Flux Is Controlled by a Voltage-gated Channel from the Mitochondrial Outer Membrane. J. Biol. Chem. *271*, 28006–28008.

Rostovtseva, T., and Colombini, M. (1997). VDAC channels mediate and gate the flow of ATP: implications for the regulation of mitochondrial function. Biophys. J. *72*, 1954–1962.

Rostovtseva, T.K., and Bezrukov, S.M. (1998). ATP transport through a single mitochondrial channel, VDAC, studied by current fluctuation analysis. Biophys. J. *74*, 2365–2373.

Rostovtseva, T.K., Komarov, A., Bezrukov, S.M., and Colombini, M. (2002a). Dynamics of nucleotides in VDAC channels: structure-specific noise generation. Biophys. J. *82*, 193–205.

Rostovtseva, T.K., Komarov, A., Bezrukov, S.M., and Colombini, M. (2002b). VDAC Channels Differentiate between Natural Metabolites and Synthetic Molecules. J. Membr. Biol. *187*, 147–156.

Rostovtseva, T.K., Antonsson, B., Suzuki, M., Youle, R.J., Colombini, M., and Bezrukov, S.M. (2004). Bid, but Not Bax, Regulates VDAC Channels. J. Biol. Chem. *279*, 13575–13583.

Ruiz, A., Alberdi, E., and Matute, C. (2014). CGP37157, an inhibitor of the mitochondrial Na+/Ca2+ exchanger, protects neurons from excitotoxicity by blocking voltage-gated Ca2+ channels. Cell Death Dis. *5*, e1156.

Russo, E.B., Burnett, A., Hall, B., and Parker, K.K. (2005). Agonistic properties of cannabidiol at 5-HT1a receptors. Neurochem. Res. *30*, 1037–1043.

Ryan, D., Drysdale, A.J., Lafourcade, C., Pertwee, R.G., and Platt, B. (2009). Cannabidiol targets mitochondria to regulate intracellular Ca2+ levels. J. Neurosci. Off. J. Soc. Neurosci. *29*, 2053–2063.

Ryberg, E., Larsson, N., Sjögren, S., Hjorth, S., Hermansson, N.-O., Leonova, J., Elebring, T., Nilsson, K., Drmota, T., and Greasley, P.J. (2007). The orphan receptor GPR55 is a novel cannabinoid receptor. Br. J. Pharmacol. *152*, 1092–1101.

Saffarzadeh, F., Eslamizade, M.J., Ghadiri, T., Modarres Mousavi, S.M., Hadjighassem, M., and Gorji, A. (2015). Effects of TRPV1 on the hippocampal synaptic plasticity in the epileptic rat brain. Synap. N. Y. N *69*, 375–383.

Saffarzadeh, F., Eslamizade, M.J., Mousavi, S.M.M., Abraki, S.B., Hadjighassem, M.R., and Gorji, A. (2016). TRPV1 receptors augment basal synaptic transmission in CA1 and CA3 pyramidal neurons in epilepsy. Neuroscience *314*, 170–178.

Saigal, N., Bajwa, A.K., Faheem, S.S., Coleman, R.A., Pandey, S.K., Constantinescu, C.C., Fong, V., and Mukherjee, J. (2013). Evaluation of Serotonin 5-HT1A Receptors in Rodent Models using [18F]Mefway PET. Synap. N. Y. N *67*, 596–608.

Salvadori, M.G.S.S., Banderó, C.R.R., Jesse, A.C., Gomes, A.T., Rambo, L.M., Bueno, L.M., Bortoluzzi, V.T., Oliveira, M.S., and Mello, C.F. (2012). Prostaglandin E(2) potentiates methylmalonate-induced seizures. Epilepsia *53*, 189–198.

Sampson, M.J., Lovell, R.S., and Craigen, W.J. (1997). The Murine Voltage-dependent Anion Channel Gene Family Conserved Stucture and Function. J. Biol. Chem. *272*, 18966–18973.

Santiago, M.F., Veliskova, J., Patel, N.K., Lutz, S.E., Caille, D., Charollais, A., Meda, P., and Scemes, E. (2011). Targeting Pannexin1 Improves Seizure Outcome. PLOS ONE *6*, e25178.

Santo-Domingo, J., and Demaurex, N. (2012). The renaissance of mitochondrial pH. J. Gen. Physiol. *139*, 415–423.

Sato, M., and Sato, K. (2013). Maternal inheritance of mitochondrial DNA by diverse mechanisms to eliminate paternal mitochondrial DNA. Biochim. Biophys. Acta BBA - Mol. Cell Res. *1833*, 1979–1984.

Saunders, N.R., Dreifuss, J.-J., Dziegielewska, K.M., Johansson, P.A., Habgood, M.D., Møllgård, K., and Bauer, H.-C. (2014). The rights and wrongs of blood-brain barrier permeability studies: a walk through 100 years of history. Front. Neurosci. *8*.

Schein, S.J., Colombini, M., and Finkelstein, A. (1976). Reconstitution in planar lipid bilayers of a voltage-dependent anion-selective channel obtained from paramecium mitochondria. J. Membr. Biol. *30*, 99–120.

Schmidt, D., and Schachter, S.C. (2014). Drug treatment of epilepsy in adults. BMJ *348*, g254.

Schönfeld, P., Więckowski, M.R., and Wojtczak, L. (2000). Long-chain fatty acid-promoted swelling of mitochondria: further evidence for the protonophoric effect of fatty acids in the inner mitochondrial membrane. FEBS Lett. *471*, 108–112.

Schwartz, M., and Vissing, J. (2002). Paternal inheritance of mitochondrial DNA. N. Engl. J. Med. *347*, 576–580.

Schwarzer, C., Tsunashima, K., Wanzenböck, C., Fuchs, K., Sieghart, W., and Sperk, G. (1997). GABAA receptor subunits in the rat hippocampus II: Altered distribution in kainic acid-induced temporal lobe epilepsy. Neuroscience *80*, 1001–1017.

Semple, B.D., O'Brien, T.J., Gimlin, K., Wright, D.K., Kim, S.E., Casillas-Espinosa, P.M., Webster, K.M., Petrou, S., and Noble-Haeusslein, L.J. (2017). Interleukin-1 Receptor in Seizure Susceptibility after Traumatic Injury to the Pediatric Brain. J. Neurosci. Off. J. Soc. Neurosci. *37*, 7864–7877.

Severson, C., and Hafler, D.A. (2010). T-cells in multiple sclerosis. Results Probl. Cell Differ. *51*, 75–98.

Shibasaki, K., Murayama, N., Ono, K., Ishizaki, Y., and Tominaga, M. (2010). TRPV2 Enhances Axon Outgrowth through Its Activation by Membrane Stretch in Developing Sensory and Motor Neurons. J. Neurosci. *30*, 4601–4612.

Shibasaki, K., Ishizaki, Y., and Mandadi, S. (2013). Astrocytes express functional TRPV2 ion channels. Biochem. Biophys. Res. Commun. *441*, 327–332.

Shimizu, S., and Tsujimoto, Y. (2000). Proapoptotic BH3-only Bcl-2 family members induce cytochrome c release, but not mitochondrial membrane potential loss, and do not directly modulate voltage-dependent anion channel activity. Proc. Natl. Acad. Sci. U. S. A. *97*, 577–582.

Shin, E.-J., Jeong, J.H., Chung, Y.H., Kim, W.-K., Ko, K.-H., Bach, J.-H., Hong, J.-S., Yoneda, Y., and Kim, H.-C. (2011). Role of oxidative stress in epileptic seizures. Neurochem. Int. *59*, 122–137.

Shinohara, Y., Ishida, T., Hino, M., Yamazaki, N., Baba, Y., and Terada, H. (2000). Characterization of porin isoforms expressed in tumor cells. Eur. J. Biochem. *267*, 6067–6073.

Shorvon, S.D. (2011). The etiologic classification of epilepsy. Epilepsia *52*, 1052–1057.

Shoshan-Barmatz, V., Ben-Hail, D., Admoni, L., Krelin, Y., and Tripathi, S.S. (2015). The mitochondrial voltage-dependent anion channel 1 in tumor cells. Biochim. Biophys. Acta BBA - Biomembr. *1848*, 2547–2575.

Shoshan-Barmatz, V., Maldonado, E.N., and Krelin, Y. (2017). VDAC1 at the crossroads of cell metabolism, apoptosis and cell stress. Cell Stress *1*, 11–36.

de Silva, M., MacArdle, B., McGowan, M., Hughes, E., Stewart, J., Neville, B.G., Johnson, A.L., and Reynolds, E.H. (1996). Randomised comparative monotherapy trial of phenobarbitone, phenytoin, carbamazepine, or sodium valproate for newly diagnosed childhood epilepsy. Lancet Lond. Engl. *347*, 709–713.

Simeone, K.A., Matthews, S.A., Samson, K.K., and Simeone, T.A. (2014). Targeting deficiencies in mitochondrial respiratory complex I and functional uncoupling exerts anti-seizure effects in a genetic model of temporal lobe epilepsy and in a model of acute temporal lobe seizures. Exp. Neurol. *251*, 84–90.

Sims, N.R., and Anderson, M.F. (2008). Isolation of mitochondria from rat brain using Percoll density gradient centrifugation. Nat. Protoc. *3*, 1228–1239.

Siomek, A. (2012). NF-κB signaling pathway and free radical impact. Acta Biochim. Pol. *59*, 323–331.

Sloviter, R.S. (1987). Decreased hippocampal inhibition and a selective loss of interneurons in experimental epilepsy. Science *235*, 73–76.

Soares, V. de P., Campos, A.C., Bortoli, V.C. de, Zangrossi, H., Guimarães, F.S., and Zuardi, A.W. (2010). Intra-dorsal periaqueductal gray administration of cannabidiol blocks panic-like response by activating 5-HT1A receptors. Behav. Brain Res. *213*, 225–229.

Socała, K., Nieoczym, D., Pieróg, M., and Wlaź, P. (2015). α-Spinasterol, a TRPV1 receptor antagonist, elevates the seizure threshold in three acute seizure tests in mice. J. Neural Transm. Vienna Austria 1996 *122*, 1239–1247.

Sondossi, K., Majdzadeh, M., Ghaeli, P., Ghahremani, M.H., Shafaroodi, H., Paknejad, B., and Ostad, S.N. (2014). Analysis of the antiepileptic, ethosuximide impacts on neurogenesis of rat forebrain stem cells. Fundam. Clin. Pharmacol. *28*, 512–518.

Sproule, B.J., Miller, W.F., Cushing, I.E., and Chapman, C.B. (1957). An improved polarographic method for measuring oxygen tension in whole blood. J. Appl. Physiol. *11*, 365–370.

Squire, L.R. (2009). The Legacy of Patient H.M. for Neuroscience. Neuron *61*, 6–9.

Stark, D.T., and Bazán, N.G. (2011). Synaptic and extrasynaptic NMDA receptors differentially modulate neuronal COX-2 function, lipid peroxidation, and neuroprotection. J. Neurosci. Off. J. Soc. Neurosci. *31*, 13710–13721.

Stein, C.A., and Colombini, M. (2008). Specific VDAC inhibitors: phosphorothioate oligonucleotides. J. Bioenerg. Biomembr. *40*, 157–162.

Steinhoff, B.J., and Staack, A.M. (2018). Is there a place for surgical treatment of nonpharmacoresistant epilepsy? Epilepsy Behav.

Stretton, J., and Thompson, P.J. (2012). Frontal lobe function in temporal lobe epilepsy. Epilepsy Res. *98*, 1–13.

Sullivan, P.G., Rippy, N.A., Dorenbos, K., Concepcion, R.C., Agarwal, A.K., and Rho, J.M. (2004). The ketogenic diet increases mitochondrial uncoupling protein levels and activity. Ann. Neurol. *55*, 576–580.

Sun, D.A., Sombati, S., Blair, R.E., and DeLorenzo, R.J. (2002). Calcium-dependent Epileptogenesis in an In Vitro Model of Stroke-induced “Epilepsy.” Epilepsia *43*, 1296–1305.

Sylantyev, S., Jensen, T.P., Ross, R.A., and Rusakov, D.A. (2013). Cannabinoid- and lysophosphatidylinositol-sensitive receptor GPR55 boosts neurotransmitter release at central synapses. Proc. Natl. Acad. Sci. U. S. A. *110*, 5193–5198.

Szabó, I., and Zoratti, M. (1991). The giant channel of the inner mitochondrial membrane is inhibited by cyclosporin A. J. Biol. Chem. *266*, 3376–3379.

Szabó, I., and Zoratti, M. (1992). The mitochondrial megachannel is the permeability transition pore. J. Bioenerg. Biomembr. *24*, 111–117.

Szabó, I., Bernardi, P., and Zoratti, M. (1992). Modulation of the mitochondrial megachannel by divalent cations and protons. J. Biol. Chem. *267*, 2940–2946.

Taanman, J.-W. (1999). The mitochondrial genome: structure, transcription, translation and replication. Biochim. Biophys. Acta BBA - Bioenerg. *1410*, 103–123.

Takács, E., Nyilas, R., Szepesi, Z., Baracskay, P., Karlsen, B., Røsvold, T., Bjørkum, A.A., Czurkó, A., Kovács, Z., Kékesi, A.K., et al. (2010). Matrix metalloproteinase-9 activity increased by two different types of epileptic seizures that do not induce neuronal death: a possible role in homeostatic synaptic plasticity. Neurochem. Int. *56*, 799–809.

Tan, W. (2012). VDAC blockage by phosphorothioate oligonucleotides and its implication in apoptosis. Biochim. Biophys. Acta BBA - Biomembr. *1818*, 1555–1561.

Tan, W., and Colombini, M. (2007). VDAC closure increases calcium ion flux. Biochim. Biophys. Acta *1768*, 2510–2515.

Tan, W., Lai, J.C., Miller, P., Stein, C.A., and Colombini, M. (2007a). Phosphorothioate oligonucleotides reduce mitochondrial outer membrane permeability to ADP. Am. J. Physiol. Cell Physiol. *292*, C1388-1397.

Tan, W., Loke, Y.-H., Stein, C.A., Miller, P., and Colombini, M. (2007b). Phosphorothioate oligonucleotides block the VDAC channel. Biophys. J. *93*, 1184–1191.

Tan, W., Lai, J.C., Miller, P., Stein, C.A., and Colombini, M. (2007c). Phosphorothioate oligonucleotides reduce mitochondrial outer membrane permeability to ADP. Am. J. Physiol. - Cell Physiol. *292*, C1388–C1397.

Tewari, D., Majumdar, D., Vallabhaneni, S., and Bera, A.K. (2017). Aspirin induces cell death by directly modulating mitochondrial voltage-dependent anion channel (VDAC). Sci. Rep. *7*, 45184.

Theodore, W.H., Hasler, G., Giovacchini, G., Kelley, K., Reeves-Tyer, P., Herscovitch, P., and Drevets, W. (2007). Reduced hippocampal 5HT1A PET receptor binding and depression in temporal lobe epilepsy. Epilepsia *48*, 1526–1530.

Thompson, R.J., Jackson, M.F., Olah, M.E., Rungta, R.L., Hines, D.J., Beazely, M.A., MacDonald, J.F., and MacVicar, B.A. (2008). Activation of pannexin-1 hemichannels augments aberrant bursting in the hippocampus. Science *322*, 1555–1559.

Tian, R., Nascimben, L., Ingwall, J.S., and Lorell, B.H. (1997). Failure to maintain a low ADP concentration impairs diastolic function in hypertrophied rat hearts. Circulation *96*, 1313–1319.

Tian, Z., Dong, C., Zhang, K., Chang, L., and Hashimoto, K. (2018). Lack of antidepressant effects of low-voltage-sensitive T-type calcium channel blocker ethosuximide in a chronic social defeat stress model: Comparison with (R)-ketamine. Int. J. Neuropsychopharmacol.

Tikunov, A., Johnson, C.B., Pediaditakis, P., Markevich, N., Macdonald, J.M., Lemasters, J.J., and Holmuhamedov, E. (2010). Closure of VDAC Causes Oxidative Stress and Accelerates the Ca2+-induced Mitochondrial Permeability Transition in Rat Liver Mitochondria. Arch. Biochem. Biophys. *495*, 174–181.

Tonin, A.M., Ferreira, G.C., Grings, M., Viegas, C.M., Busanello, E.N., Amaral, A.U., Zanatta, A., Schuck, P.F., and Wajner, M. (2010). Disturbance of mitochondrial energy homeostasis caused by the metabolites accumulating in LCHAD and MTP deficiencies in rat brain. Life Sci. *86*, 825–831.

Touw, M. (1981). The religious and medicinal uses of Cannabis in China, India and Tibet. J. Psychoactive Drugs *13*, 23–34.

Tsai, M.-F., Jiang, D., Zhao, L., Clapham, D., and Miller, C. (2014). Functional reconstitution of the mitochondrial Ca2+/H+ antiporter Letm1. J. Gen. Physiol. *143*, 67–73.

Tsunashima, K., Schwarzer, C., Kirchmair, E., Sieghart, W., and Sperk, G. (1997). GABAA receptor subunits in the rat hippocampus III: altered messenger RNA expression in kainic acid-induced epilepsy. Neuroscience *80*, 1019–1032.

Ude, C., and Ambegaonkar, G. (2016). Glycine receptor antibody-associated epilepsy in a boy aged 4 years. BMJ Case Rep. *2016*.

Uusi-Oukari, M., and Korpi, E.R. (2010). Regulation of GABAA Receptor Subunit Expression by Pharmacological Agents. Pharmacol. Rev. *62*, 97–135.

Valvassori, S.S., Bavaresco, D.V., Scaini, G., Varela, R.B., Streck, E.L., Chagas, M.H., Hallak, J.E.C., Zuardi, A.W., Crippa, J.A., and Quevedo, J. (2013). Acute and chronic administration of cannabidiol increases mitochondrial complex and creatine kinase activity in the rat brain. Rev. Bras. Psiquiatr. Sao Paulo Braz. 1999 *35*, 380–386.

Varela, L., Schwartz, M.L., and Horvath, T.L. (2016). Mitochondria controlled by UCP2 determine hypoxia-induced synaptic remodeling in the cortex and hippocampus. Neurobiol. Dis. *90*, 68–74.

Vazquez, J.F., Clement, H.-W., Sommer, O., Schulz, E., and van Calker, D. (2008). Local stimulation of the adenosine A2B receptors induces an increased release of IL-6 in mouse striatum: an in vivo microdialysis study. J. Neurochem. *105*, 904–909.

Veeramah, K.R., O'Brien, J.E., Meisler, M.H., Cheng, X., Dib-Hajj, S.D., Waxman, S.G., Talwar, D., Girirajan, S., Eichler, E.E., Restifo, L.L., et al. (2012). De novo pathogenic SCN8A mutation identified by whole-genome sequencing of a family quartet affected by infantile epileptic encephalopathy and SUDEP. Am. J. Hum. Genet. *90*, 502–510.

Vezzani, A., and Granata, T. (2005). Brain inflammation in epilepsy: experimental and clinical evidence. Epilepsia *46*, 1724–1743.

Vianna, E.P.M., Ferreira, A.T., Naffah-Mazzacoratti, M.G., Sanabria, E.R.G., Funke, M., Cavalheiro, E.A., and Fernandes, M.J.S. (2002). Evidence That ATP Participates in the Pathophysiology of Pilocarpine-Induced Temporal Lobe Epilepsy: A Fluorimetric, Immunohistochemical, and Western Blot Studies. Epilepsia *43*, 227–229.

Vianna, E.P.M., Ferreira, A.T., Doná, F., Cavalheiro, E.A., and da Silva Fernandes, M.J. (2005). Modulation of seizures and synaptic plasticity by adenosinergic receptors in an experimental model of temporal lobe epilepsy induced by pilocarpine in rats. Epilepsia *46 Suppl 5*, 166–173.

Villinger, S., Giller, K., Bayrhuber, M., Lange, A., Griesinger, C., Becker, S., and Zweckstetter, M. (2014). Nucleotide Interactions of the Human Voltage-dependent Anion Channel. J. Biol. Chem. *289*, 13397–13406.

Viviani, B., Bartesaghi, S., Gardoni, F., Vezzani, A., Behrens, M.M., Bartfai, T., Binaglia, M., Corsini, E., Di Luca, M., Galli, C.L., et al. (2003). Interleukin-1beta enhances NMDA receptor-mediated intracellular calcium increase through activation of the Src family of kinases. J. Neurosci. Off. J. Soc. Neurosci. *23*, 8692–8700.

Wake, H., Watanabe, M., Moorhouse, A.J., Kanematsu, T., Horibe, S., Matsukawa, N., Asai, K., Ojika, K., Hirata, M., and Nabekura, J. (2007). Early changes in KCC2 phosphorylation in response to neuronal stress result in functional downregulation. J. Neurosci. Off. J. Soc. Neurosci. *27*, 1642–1650.

Waldbaum, S., and Patel, M. (2010). Mitochondria, oxidative stress, and temporal lobe epilepsy. Epilepsy Res. *88*, 23–45.

Wallace, R.H., Marini, C., Petrou, S., Harkin, L.A., Bowser, D.N., Panchal, R.G., Williams, D.A., Sutherland, G.R., Mulley, J.C., Scheffer, I.E., et al. (2001). Mutant GABAA receptor γ2-subunit in childhood absence epilepsy and febrile seizures. Nat. Genet. *28*, 49–52.

Wang, J., Lin, Z.-J., Liu, L., Xu, H.-Q., Shi, Y.-W., Yi, Y.-H., He, N., and Liao, W.-P. (2017). Epilepsy-associated genes. Seizure *44*, 11–20.

Watanabe, K., and Yokobori, S. (2011). tRNA Modification and Genetic Code Variations in Animal Mitochondria.

Weeber, E.J., Levy, M., Sampson, M.J., Anflous, K., Armstrong, D.L., Brown, S.E., Sweatt, J.D., and Craigen, W.J. (2002). The role of mitochondrial porins and the permeability transition pore in learning and synaptic plasticity. J Biol Chem *277*, 18891–18897.

Wekerle, H. (2017). B cells in multiple sclerosis. Autoimmunity *50*, 57–60.

Whittaker, R.G., Turnbull, D.M., Whittington, M.A., and Cunningham, M.O. (2011). Impaired mitochondrial function abolishes gamma oscillations in the hippocampus through an effect on fast-spiking interneurons. Brain *134*, e180.

WHO (2017). Dementia. http://www.who.int/news-room/fact-sheets/detail/dementia.

WHO (2018). Epilepsy. http://www.who.int/news-room/fact-sheets/detail/epilepsy.

Whyte, L.S., Ryberg, E., Sims, N.A., Ridge, S.A., Mackie, K., Greasley, P.J., Ross, R.A., and Rogers, M.J. (2009). The putative cannabinoid receptor GPR55 affects osteoclast function in vitro and bone mass in vivo. Proc. Natl. Acad. Sci. U. S. A. *106*, 16511–16516.

Wiebe, S., Blume, W.T., Girvin, J.P., Eliasziw, M., and Effectiveness and Efficiency of Surgery for Temporal Lobe Epilepsy Study Group (2001). A randomized, controlled trial of surgery for temporal-lobe epilepsy. N. Engl. J. Med. *345*, 311–318.

Williams, G.S.B., Boyman, L., Chikando, A.C., Khairallah, R.J., and Lederer, W.J. (2013). Mitochondrial calcium uptake. Proc. Natl. Acad. Sci. U. S. A. *110*, 10479–10486.

Williams, S.P., Fulton, A.M., and Brindle, K.M. (1993). Estimation of the intracellular free ADP concentration by 19F NMR studies of fluorine-labeled yeast phosphoglycerate kinase in vivo. Biochemistry (Mosc.) *32*, 4895–4902.

Wolf, H.K., Spänle, M., Müller, M.B., Elger, C.E., Schramm, J., and Wiestler, O.D. (1994). Hippocampal loss of the GABAA receptor α1 subunit in patients with chronic pharmacoresistant epilepsies. Acta Neuropathol. (Berl.) *88*, 313–319.

Wong, R., Steenbergen, C., and Murphy, E. (2012). Mitochondrial permeability transition pore and calcium handling. Methods Mol. Biol. Clifton NJ *810*, 235–242.

Wuerfel, E., Bien, C.G., Vincent, A., Woodhall, M., and Brockmann, K. (2014). Glycine receptor antibodies in a boy with focal epilepsy and episodic behavioral disorder. J. Neurol. Sci. *343*, 180–182.

Xiong, W., Cui, T., Cheng, K., Yang, F., Chen, S.-R., Willenbring, D., Guan, Y., Pan, H.-L., Ren, K., Xu, Y., et al. (2012). Cannabinoids suppress inflammatory and neuropathic pain by targeting α3 glycine receptors. J. Exp. Med. *209*, 1121–1134.

Yamamoto, Y., and Gaynor, R.B. (2004). IkappaB kinases: key regulators of the NF-kappaB pathway. Trends Biochem. Sci. *29*, 72–79.

Yamamoto, T., Kuniki, K., Takekuma, Y., Hirano, T., Iseki, K., and Sugawara, M. (2007). Ribavirin uptake by cultured human choriocarcinoma (BeWo) cells and Xenopus laevis oocytes expressing recombinant plasma membrane human nucleoside transporters. Eur. J. Pharmacol. *557*, 1–8.

Yu, F.H., Mantegazza, M., Westenbroek, R.E., Robbins, C.A., Kalume, F., Burton, K.A., Spain, W.J., McKnight, G.S., Scheuer, T., and Catterall, W.A. (2006). Reduced sodium current in GABAergic interneurons in a mouse model of severe myoclonic epilepsy in infancy. Nat. Neurosci. *9*, 1142.

Zattoni, M., Mura, M.L., Deprez, F., Schwendener, R.A., Engelhardt, B., Frei, K., and Fritschy, J.-M. (2011). Brain infiltration of leukocytes contributes to the pathophysiology of temporal lobe epilepsy. J. Neurosci. Off. J. Soc. Neurosci. *31*, 4037–4050.

Zeraati, M., Mirnajafi-Zadeh, J., Fathollahi, Y., Namvar, S., and Rezvani, M.E. (2006). Adenosine A1 and A2A receptors of hippocampal CA1 region have opposite effects on piriform cortex kindled seizures in rats. Seizure *15*, 41–48.

Zhang, X., Chen, G., Lu, Y., Liu, J., Fang, M., Luo, J., Cao, Q., and Wang, X. (2014). Association of mitochondrial letm1 with epileptic seizures. Cereb. Cortex N. Y. N 1991 *24*, 2533–2540.

Zhao, F., Kang, H., You, Li., Rastogi, P., Venkatesh, D., and Chandra, M. (2014). Neuropsychological deficits in temporal lobe epilepsy: A comprehensive review. Ann. Indian Acad. Neurol. *17*, 374–382.

Zhen, J., Qu, Z., Fang, H., Fu, L., Wu, Y., Wang, H., Zang, H., and Wang, W. (2014). Effects of grape seed proanthocyanidin extract on pentylenetetrazole-induced kindling and associated cognitive impairment in rats. Int. J. Mol. Med. *34*, 391–398.

Zuliani, L., Ferlazzo, E., Andrigo, C., Casano, A., Cianci, V., Zoccarato, M., Leite, M.I., Waters, P., Woodhall, M., Della Mora, E., et al. (2014). Glycine receptor antibodies in 2 cases of new, adult-onset epilepsy. Neurol. Neuroimmunol. Neuroinflammation *1*.